

University of Alberta

**SEDIMENTARY CHARACTERISTICS OF THE SPRAY
RIVER GROUP OF WEST-CENTRAL ALBERTA**

by

David Campbell Nordheimer

A thesis submitted to the Faculty of Graduate Studies and Research
in partial fulfillment of the requirements for the degree of

Master of Science

Department of Earth and Atmospheric Sciences

©David Campbell Nordheimer

Spring, 2012
Edmonton, Alberta

Permission is hereby granted to the University of Alberta Libraries to reproduce single copies of this thesis and to lend or sell such copies for private, scholarly or scientific research purposes only. Where the thesis is converted to, or otherwise made available in digital form, the University of Alberta will advise potential users of the thesis of these terms.

The author reserves all other publication and other rights in association with the copyright in the thesis and, except as herein before provided, neither the thesis nor any substantial portion thereof may be printed or otherwise reproduced in any material form whatsoever without the author's prior written permission.

Dedication

To my family past, present, future, and my daughter
Alyssa Marie Nordheimer

Abstract

Triassic lithologies in west-central Alberta are divided into the Sulphur Mountain Formation and Whitehorse Formation of the Spray River Group. The Sulphur Mountain Formation is subdivided into three members: the Vega-Phroso Siltstone, Whistler, and Llama members. The Whitehorse Formation is subdivided into three members: the Starlight Evaporite, Brewster Limestone, and Winnifred members. Analysis of six outcrops in the Willmore Wilderness Park for this study suggests that the Whitehorse Formation was emplaced in an overall progradational system with occasional regressive transgressive deposition.

From outcrop analysis five facies associations (1, 2, 3, 4 and 5) were developed based on fifteen identified facies. The five associations relate to offshore deposits (1), offshore to shoreface (2), ephemeral/lacustrine supratidal (3), aeolian sabkha depositional environments (4), and offshore turbidite deposits (5). Ichnological, biostratigraphic, and chemostratigraphic analyses of outcrop samples were used in delineating the Sulphur Mountain Formation and Whitehorse Formation of the Spray River Group.

Acknowledgements

First and foremost, I would like to address the acknowledgements to my supervisors Dr. George Pemberton, Dr. Murray Gingras, and Dr. J-P Zonneveld. Their wealth of knowledge, support, and endless stories have made my experience unforgettable. Special thanks committee member Dr. Mirko van der Baan. Support and guidance of this thesis was generously given from Talisman Energy Inc. and BP Canada Energy Company. Logistical support was provided by George Kelley Outfitters.

I'd like to thank my field assistants Luke McHugh and Kelsey Soldan for all of there hard work, keen insights, and fantastic stories. I would also like to thank Rares Bistran for his assistance with the Chemostratigraphy and Mike Orchard for the microfossil analyses.

My family and friends played a huge roll in encouraging me to continue my education. Thank you all so very much for your support. Special thanks to my parents David and Debbie Nordheimer and my sister and brother Nancy and Barry.

TABLE OF CONTENTS

CHAPTER ONE	1
1.1 INTRODUCTION	1
1.2 PREVIOUS WORK.....	6
1.3 STUDY AREA	10
1.4 METHODS	11
1.5 STRATIGRAPHIC FRAMEWORK.....	22
1.6 TECTONIC AND GEOLOGIC SETTING.....	27
1.7 PALEOLATITUDE.....	32
1.8 PALEOCLIMATE.....	35
1.9 PALEO-SEA LEVEL	37
1.10 PALEONTOLOGY AND BIOSTRATIGRAPHY	38
CHAPTER TWO	42
2.1 INTRODUCTION	42
2.2 OUTCROP DESCRIPTIONS.....	46
2.3 FACIES DESCRIPTIONS AND INTERPRETATIONS.....	47
2.3.1 FACIES A: DOLOMITIC SILTSTONE.....	47
2.3.2 FACIES B: INTERBEDDED VF DOLOMITIC SILTY SANDSTONE AND DOLOMITIC SILTSTONE	51
2.3.3 FACIES C: BLACK SHALE	56
2.3.4 FACIES D: MUDDY SILTSTONE	60
2.3.5 FACIES E: VF DOLOMITIC SILTY SANDSTONE	62
2.3.6 FACIES F: VF CALCAREOUS SANDSTONE.....	64
2.3.7 FACIES G: INTERBEDDED VF TO F SANDSTONE AND SANDY MUDSTONE	67
2.3.8 FACIES H: F TO C PLANAR TABULAR TO TROUGH CROSS- STRATIFIED SANDSTONE AND F TO M PLANAR LAMINATED SANDSTONE.....	70
2.3.9 FACIES I: BINDSTONE LAMINATE.....	74
2.3.10: FACIES J BRECCIA.....	77
2.3.11 FACIES K: VF TO F CALCAREOUS SANDSTONE.....	80
2.3.12 FACIES L: HIGH-ANGLE CROSS-STRATIFIED SANDSTONE	82
2.3.13 FACIES M: DOLOMITIC SILTY MUDSTONE	85
2.3.14 FACIES N CONTORTED SANDSTONE.....	88
2.3.15 FACIES O: CALCAREOUS BIOCLASTIC WACKESTONE/PACKSTONE	91

2.4 FACIES ASSOCIATIONS	94
2.4.1 FACIES ASSOCIATION 1	95
2.4.2 FACIES ASSOCIATION 2	96
2.4.3 FACIES ASSOCIATION 3	99
2.4.4 FACIES ASSOCIATION 4	101
2.4.5 FACIES ASSOCIATION 5	103
2.5 DISCUSSION	103
CHAPTER THREE	108
3.1 INTRODUCTION	108
3.2 BIOSTRATIGRAPHY RESULTS	108
3.3 BIOSTRATIGRAPHY INTERPRETATIONS	108
3.4 CHEMOSTRATIGRAPHY RESULTS	115
3.5 CHEMOSTRATIGRAPHY INTERPRETATIONS	127
3.6 LOG CORRELATION	130
3.7 STRATIGRAPHIC FRAMEWORK	131
3.8 TECTONIC AND EUSTATIC IMPLICATIONS	138
CHAPTER FOUR	139
4.1.0 Conclusion and Summary	139
REFERENCES	143
APENDIX A: OUTCROP LOGS	165
APENDIX B: RAW GEOCHEMISTRY DATA	182
APENDIX C: GEOCHEMISTRY DATA NORMALIZED TO ZIRCON	205
APENDIX D: GEOCHEMISTRY GRAPHS, BISTRAN 2009	228

LIST OF TABLES

Table 2-1: Facies descriptions A.....	43
Table 2-2: Facies descriptions B.....	44
Table 2-3: Facies descriptions C.....	45
Table 2-4: Outcrop descriptions.....	48
Table 3-1: Biostratigraphy results A.....	109
Table 3-2: Biostratigraphy results B.....	110
Table 3-3: Stratigraphic profile A.....	134
Table 3-4: Stratigraphic profile B.....	135

LIST OF FIGURES

Figure 1-1: Triassic stratigraphy chart.....	2
Figure 1-2: Location map of the Willmore Wilderness Park.....	3
Figure 1-3: Outcrop location map within the Willmore Wilderness Park.....	5
Figure 1-4: Poupanee outcrop.....	12
Figure 1-5: East 53 outcrop.....	13
Figure 1-6: Cody Found Horse outcrop.....	14
Figure 1-7: Monaghan Creek outcrop.....	15
Figure 1-8: Blue Grouse South outcrop.....	16
Figure 1-9: Blue Grouse Brewster outcrop.....	17
Figure 1-10: Position of Pangea during the Triassic.....	33
Figure 1-11: Triassic paleogeography.....	34
Figure 2-1: Facies A Dolomitic Siltstone.....	49
Figure 2-2: Facies B Interbedded VF Dolomitic Silty Sandstone and Dolomitic Siltstone.....	53
Figure 2-3: Photo: Satellite image of African dust plume.....	55
Figure 2-4: Facies C: Black Shale.....	57
Figure 2-5: Facies D: Muddy Siltstone.....	61
Figure 2-6: Facies E: VF Dolomitic Silty Sandstone.....	63
Figure 2-7: Facies F: VF Calcareous Sandstone.....	65
Figure 2-8: Facies G: Interbedded VF to F Sandstone and Sandy Mudstone.....	68
Figure 2-9: Facies H: F to C Planar Tabular to Trough Cross-stratified Sandstone and F to M Planar Laminated Sandstone.....	71
Figure 2-10: Facies H: F to C Planar Tabular to Trough Cross-stratified Sandstone and F to M Planar Laminated Sandstone.....	73

Figure 2-11: Facies I: Bindstone Laminate.....	75
Figure 2-12: Facies J: Breccia.....	78
Figure 2-13: Facies K: Calcareous Sandstone.....	81
Figure 2-14: Facies L: High-angle Cross-stratified Sandstone.....	84
Figure 2-15: Facies M: Dolomitic Silty Mudstone.....	87
Figure 2-16: Facies N: Contorted Sandstone.....	89
Figure 2-17: Facies O: Calcareous Bioclastic Wackestone/Packstone.....	92
Figure 2-18: Schematic of Lateral Facies Distribution.....	105
Figure 3-1: Elements Li, Be, Mg, Al, Si, P, K, Ca, Ti, V, Cr, Mn, and Fe geochemical profiles for the study interval from the East 53 outcrop.....	116
Figure 3-2: Elements Co, Cu, Zn, Ga, Ge, As, Rb, Sr, Y, Nb, Mo, Ru, and Pd geochemical profiles for the study interval from the East 53 outcrop.....	117
Figure 3-3: Elements Ag, Sn, Sb, Cs, Ba, La, Ce, Pr, Nd, Sm, Eu, Gd, and Dy geochemical profiles for the study interval from the East 53 outcrop.....	118
Figure 3-4: Elements Ho, Er, Tm, Yb, Hf, Ta, Au, Tl, Pb, Th, and U geochemical profiles for the study interval from the East 53 outcrop.....	119
Figure 3-5: Elements Li, Be, Mg, Al, Si, P, K, Ca, Ti, V, Cr, Mn, and Fe geochemical profiles for the study interval from the Monaghan Creek outcrop.....	120
Figure 3-6: Elements Co, Cu, Zn, Ga, Ge, As, Rb, Sr, Y, Nb, Mo, Ru, and Pd geochemical profiles for the study interval from the Monaghan Creek outcrop.....	121
Figure 3-7: Elements Ag, Sn, Sb, Cs, Ba, La, Ce, Pr, Nd, Sm, Eu, Gd, and Dy geochemical profiles for the study interval from the Monaghan Creek outcrop.....	122
Figure 3-8: Elements Ho, Er, Tm, Yb, Hf, Ta, Au, Tl, Pb, Th, and U geochemical profiles for the study interval from the Monaghan Creek outcrop.....	123
Figure 3-9: Immobile Element Correlation.....	125
Figure 3-10: Outcrop Log Correlation.....	132

CHAPTER ONE

1.1 INTRODUCTION

This study examines the sedimentologic, stratigraphic, and depositional characteristics of the Whitehorse Formation, based upon outcrop analyses in the Willmore Wilderness Park of west-central Alberta. A detailed analysis of the sedimentology and ichnology of the Triassic (Carnian) Whitehorse Formation (Figure 1-1) has not previously been undertaken.

This study addresses: 1) characterization and interpretation of the depositional facies of the Whitehorse Formation through integrated ichnology and sedimentology, 2) establishment of the relationship of the Whitehorse Formation stratigraphy to lateral and positionally equivalent units in the subsurface to the east, such as the Doig, Halfway, and Charlie Lake formations to the east and northeast, 3) establishment of a geological database from selected outcrops in the Willmore area of the Western Canadian Sedimentary Basin (WCSB), and 4) establishment of a stratigraphic framework and proposal of a set of depositional models for the Whitehorse Formation. Results of this study are relevant to the understanding of producing reservoirs in subsurface equivalents to the east and northeast as well as regional Triassic depositional models in western Canada.

The Whitehorse Formation is a mixed siliciclastic carbonate unit cropping out primarily in the Front Ranges of the Willmore Wilderness Park (Figure 1-2). Common lithologies of the Whitehorse Formation include: dolomite, limestone,

PERIOD / EPOCH / AGE		FOOTHILLS / FRONT RANGES		PLAINS	
		SIKANNI CHIEF PINE RIVERS	SUKUNKA BOW RIVERS	PEACE RIVER SUBSURFACE	
JURASSIC		FERNIE FM.	FERNIE FM.	FERNIE FM.	
TRIASSIC	LATE	RHAETIAN	BOCOCK FM.		
		NORIAN	PARDONET FM.	PARDONET FM.	
		CARNIAN	BALDONNEL FM.	BALDONNEL FM.	
	MIDDLE	LADINIAN	CHARLIE LAKE FM.	CHARLIE LAKE FM.	
		ANISIAN	LIARD FM.	HALFWAY FM.	
		SPATHIAN	TOAD FM.	DOIG FM.	
		SMITHIAN			
	EARLY	DIENERIAN	GRAYLING FM.	MONTNEY FM.	
		GRIESBACHIAN			
PERM.	LATE	TATARIAN	ISHBEL GROUP	ISHBEL GROUP	ISHBEL GROUP

* MACKENZIE
DOLOMITE LENTIL

Figure 1-1. Triassic stratigraphy, including the Whitehorse Formation of this study within the Sukunka-Bow Rivers region and lateral equivalent units. Modified after Davies (1997a), Gibson and Barclay (1989).

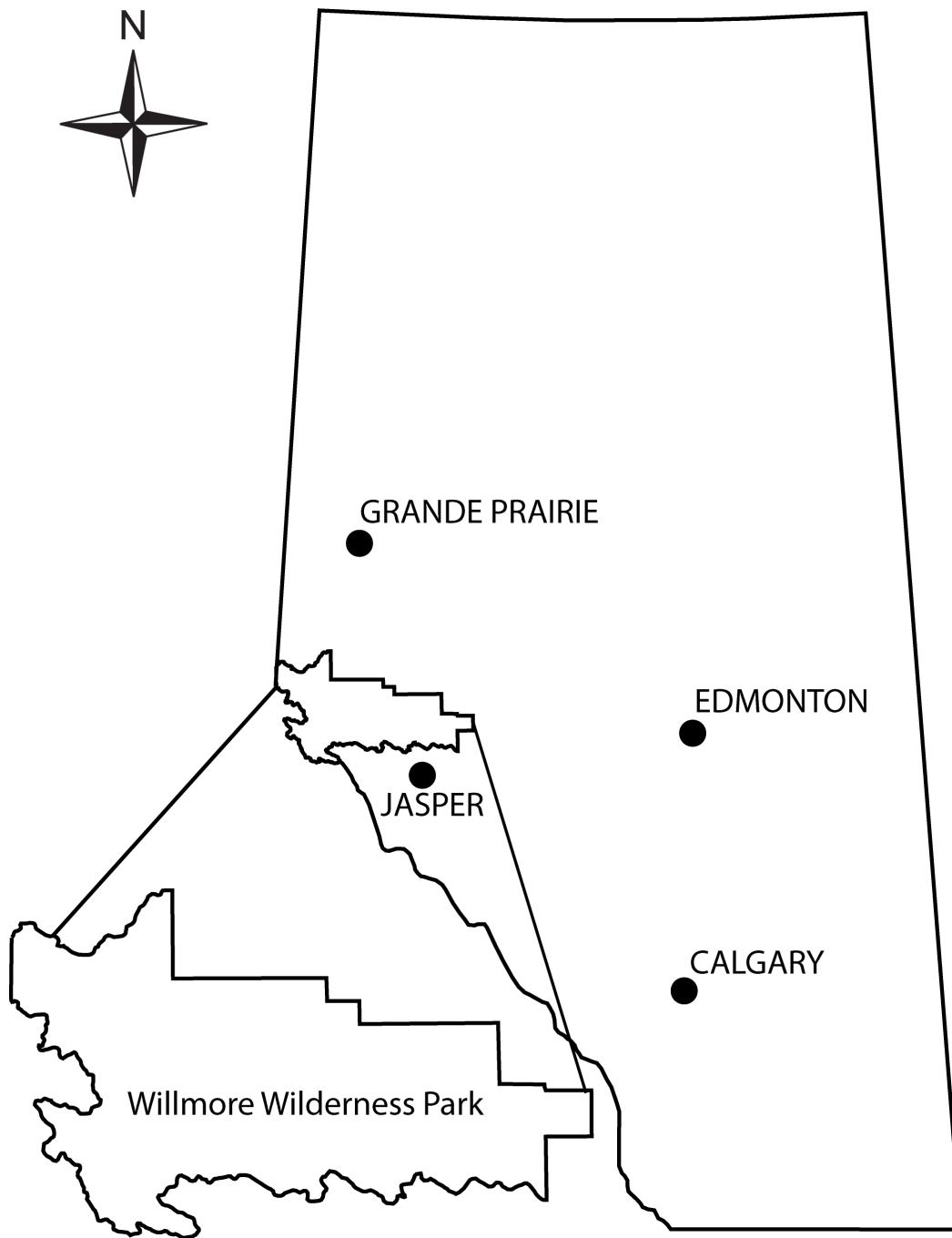


Figure 1-2. Location Map of the Willmore Wilderness Park in west-central Alberta. Central coordinates 53° 41'09" N, 119° 25'10"W (NTS).

mudstone, siltstone, sandstone, breccia, and evaporite. The most extensively exposed Triassic rocks in the Willmore Wilderness Park are located on the Starlight and Persimmon ranges. As this is the case, outcrop analysis focused on exposures within this study area (Figure 1-3). Structural deformation, weathering, covered intervals, and erosive processes have resulted in incomplete sections in the study area (Gibson, 1974). As the fieldwork proceeded in this study, additionally prospective outcrops were identified for inclusion in this, and future, studies.

Initial research on Triassic lithostratigraphy in the study area was completed in the 1960's by D.W. Gibson (Gibson, 1968a). Gibson's research was used to establishing the stratigraphy of the area, however, it did not address the sedimentologic variability within the Willmore Wilderness Park as it relates to Triassic stratigraphy. In addition, no studies have incorporated the ichnology of the deposits.

Results of this study extend the work of Gibson by adding sedimentologic and ichnological analyses. This chapter provides a background to the ensuing topics explored in later chapters including: observed facies, facies associations, depositional interpretations, chemostratigraphy, biostratigraphy, and stratigraphic framework. This chapter addresses the tectonic and geologic setting, stratigraphic framework, paleoclimate, paleo-oceanography, paleo-sea level, paleontology, and paleolatitude of the Triassic Whitehorse Formation.

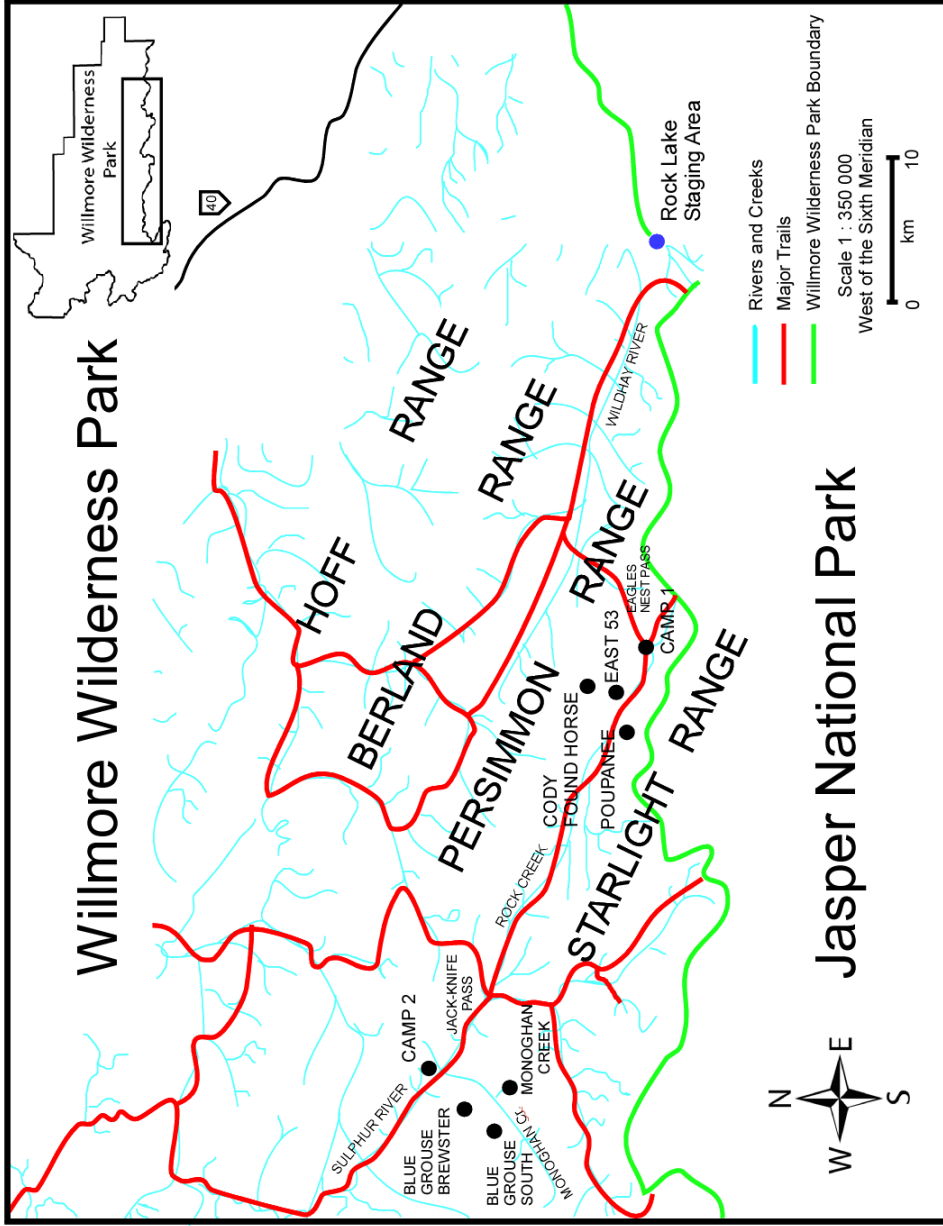


Figure 1-3. Outcrop location map, major trails, and staging area within the Willmore Wilderness Park.

1.2 PREVIOUS WORK

In the late 1800's, preliminary studies on Triassic stratigraphy in western Canada were conducted northeast and south of Willmore Wilderness Park. Triassic outcrop exposures were first described in the Peace River Foothills of northeastern British Columbia by A.R.C Selwyn in 1875 (Selwyn, 1877). Subsequently Dawson (1881) described Triassic lithologies in the Pine River Valley. McConnell (1887) worked on Triassic rocks in the Bow Valley area and later in the Liard River Valley in 1891 (McConnell, 1891). McConnell grouped both the Rocky Mountain Formation and successions we now know to be Triassic in the Carboniferous, designating the sequence the Upper Banff shale (McConnell, 1887).

The Athabasca-Bow Rivers region described by McConnell in 1887 was later visited by Dowling (1907), who suggested a Permian-Triassic age be assigned to the succession. The published work of Lambe (1916), based upon fossil evidence collected by E. M. Kindle, L. D. Burling, and H.W. Shimer, allocated a Triassic age to the Upper Banff shale. Kindle (1924) formally named the Triassic succession as the Spray River Formation and designated the Spray River Gorge as the type section. The efforts of McLearn and Kindle spanning the early to mid 1900's, enabled the establishment of a foundational stratigraphic framework for the Triassic of the WCSB, summarized in a Geological Survey of Canada report (McLearn and Kindle, 1950).

P.S. Warren (1927) completed additional paleontological and stratigraphic descriptions in the Spray River gorge. Following this, Triassic studies in west-central Alberta continued including Parejas and Collet (1931) in Jasper National Park and Allan (1934) on Triassic gypsum at Mowich Creek. P.S. Warren (1945) divided the Spray River Formation into two members, the Lower Sulphur Mountain Member and the Middle Whitehorse Member, based upon identified lithologies and faunas. P.S. Warren designated the Spray River gorge as the type section for the Sulphur Mountain Member (Warren, 1945). The Whitehorse Member did not receive a designated type section at this time.

Triassic outcrop sections near the Willmore Wilderness Park were not described until Laudon et al., (1949) described exposures while studying Devonian and Mississippian stratigraphy northeast of the study area in the Wapiti Lake region. Irish (1951), mapped a section of Triassic stratigraphy near the current northern boundaries of the Willmore Wilderness Park at Llama Mountain and continued work in 1954 at Kvass Flats. In 1958, the type section for the Whitehorse Member was described and designated by Best at Whitehorse Creek Alberta (Best, 1958). In his doctorate thesis of the Miette area, Mountjoy (1960) raised the Spray River Formation to group status and upgraded the Whitehorse and Sulphur Mountain Members to formation status.

The identification of Triassic rocks as hydrocarbon bearing resources during the 1950's resulted in numerous studies surrounding the Willmore Wilderness Park.

Manko (1960) published a field guide book outlining the lithostratigraphy of the Triassic in the Rock Lake region from data provided by Imperial Oil Limited. Subsurface research outlining Triassic stratigraphy was conducted by Hunt and Ratcliffe (1959), Clark (1961), and Armitage (1962). Brass et al., (1964) completed the first edition of the Western Canadian Sedimentary Basin Atlas including a summary of Triassic stratigraphy. Pelletier (1960, 1961, 1963, 1964, 1965) and Tozer (1961, 1962, 1963, 1965, 1967, 1982a, b, 1984) completed works on Triassic stratigraphy, paleocurrent, primary sedimentary structure, and fauna. Research on Triassic biostratigraphy using ammonoids, conodonts, and fish fossils was completed by Tozer (1961, 1962, 1963, 1965, 1967, 1982a, b, 1984, 1994), Silberling and Tozer (1968), Schaeffer and Mangus (1976), Callaway and Brinkman (1989), and Orchard and Tozer (1997). Additional Triassic studies were completed during the 1960's and 1970's including Irish (1970), and Price and Ollerenshaw (1971), however, few Triassic studies were completed within the current Willmore Wilderness Park area.

Gibson (1968a) conducted early lithostratigraphic research within the Willmore Wilderness Park. The three members of the Whitehorse Formation designated by Gibson in 1968 include: the Starlight Evaporite Member, the Brewster Member, and the Winnifred Member. Gibson completed research on Triassic stratigraphy ranging from the Bow River-Crowsnest Pass, Smokey River (this study), Pine Pass, and the southern Trutch region of northeastern British Columbia (Gibson 1965, 1968a, b, 1969, 1970, 1971a, 1972, 1974, 1975). The purpose of Gibson's work from the late 1960's to the mid 1970's was to describe the distribution, age,

and stratigraphic relationships of Triassic rocks in the study area and relate it to comparable stratigraphy, both to the north in the Pine Pass region and to the south to Crowsnest Pass (Gibson 1975).

Later studies completed by Gibson addressing Triassic stratigraphy and depositional models in western Canada include works by Gibson and Barclay (1989), Gibson and Edwards (1990a, b), Gibson (1993), and Embry and Gibson (1995). Other research addressing Triassic depositional models of equivalent Triassic stratigraphy to the Whitehorse Formation in the WCSB include: Cant (1986), Campbell and Hassler (1989), Campbell et al., (1989), Wittenberg and Moslow (1991), Wittenberg (1992, 1993), Arnold (1994), Evoy (1995, 1997), Evoy and Moslow (1995), Davies (1997a, b), Dixon (1999, 2001a, b, 2002a, b, c, d, 2003, 2004, 2005, 2007, 2008), Harris and Bustin (2000), and Rahman and Henderson (2005). Applicable aspects of Triassic stratigraphy and depositional models presented in these papers as related to Whitehorse Formation of this study are discussed in following sections.

Research that has addressed ichnology and biostratigraphy of equivalent Triassic Whitehorse Formation stratigraphy includes: Arnold (1994), Zonneveld et al., (1997a, b), Zonneveld (1999), Zonneveld (2001), Zonneveld et al., (2001), Zonneveld and Orchard (2002), Zonneveld and Pemberton (2003), Buatois et al. (2004), Zonneveld et al., (2004), Beatty and Pemberton (2005), Zonneveld et al., (2007a, b), and Lamothe (2008). Pertinent features of Triassic ichnology and biostratigraphy as related to the Whitehorse Formation of this study identified in these research papers are discussed in subsequent sections.

1.3 STUDY AREA

The Willmore Wilderness Park is situated north of Jasper National Park in the elbow of the western edge of central Alberta. The park encompasses 4,600 square kilometers with overall topography displaying increasing relief westward towards the provincial boundary of Alberta and British Columbia. The study area occurs within the Mount Robson topographic map area 1: 250,000 scale, 83E NTS.

Rock Lake, the staging area used for access into the Willmore Wilderness Park for this study, is approximately one and a half hours north of Hinton by vehicle (Figure 1-3). An eight-hour horseback ride enables access to the first camp (Eagles Nest) (Figure 1-3). An additional ten-hour ride from Eagles Nest is required to access the second camp (Monaghan Creek) (Figure 1-3).

Outcrop sections within the study area extend south from Twp. 53 to Twp. 52 and west from Range 4 to Range 7 W of 6 (83E NTS). The outcrops studied occur on both the Persimmon and Starlight Ranges of the gradually dipping northwest-trending slopes of the Front Ranges (Figure 1-3). As motorized vehicles are prohibited within the park, the outcrops are accessed by horseback and hiking. Daily access into each of the six outcrop sections required an average of one hour of horseback riding and one hour of hiking.

In total six outcrop sections were examined: Poupanee Chute (PC), East 53 (E53), Cody Found Horse (CFH), Monaghan Creek (MC), Blue Grouse Brewster (BGB),

and Blue Grouse South (BGS) (Figure 1-4 to 1-9). The three outcrops studied from the Eagles Nest camp include: PC on the Starlight Range, as well as E53 and CFH on the Persimmon Range (Figure 1-3). Outcrops studied from the Monaghan Creek camp include: MC, BGB, and BGS, all of which are located on the Starlight Range (Figure 1-3).

1.4 METHODS

Of the six outcrop sections, three, PC, CFH, and E53 were visited in the summer of 2007. These locations were selected on the basis of accessibility and vertical extent. During the summer of 2008, all six outcrops were visited and described. Sedimentological strip logs were created for each outcrop section. Data compiled in each strip log include: lithology, facies relationships/contacts, lithological accessories, physical sedimentary structures, biogenic sedimentary structures, and fossils. Ichnological observations concentrated on the identification of ichnogenera, assessing the intensity of bioturbation, and the distribution of ichnofossils and ichnofossil assemblages. The size of the trace fossils and their physical interrelationships (such as interpenetrating or isolated occurrences) were also noted. To account for variability within exposed sections lateral variability was integrated into the outcrop descriptions. Lithologies of the Whitehorse Formation in outcrop were sampled, photographed and subjected to hand held gamma ray analysis. Rock samples were collected for later petrographic, geochemical, and conodont analyses.

Lithological samples were analyzed by thin section analysis to assess depositional



Figure 1-4. Photo of Poupanee outcrop as indicate by the white arrow. This outcrop is located on the Star Light Range and consists of 130m of measured section height. This photo was taken from the E53 outcrop on the Persimmon Range. Elevation at the base of the Poupanee section is 2134m with a GPS accuracy of ± 10 m.



Figure 1-5. In this photo the East 53 outcrop can be seen as indicated by the white arrow. This outcrop is located on the Persimmon Range and provided 89m of measurable section. The elevation at the base of the section accurate to within $\pm 3\text{m}$ is 1955m based on GPS.



Figure 1-6. This photo displays the overturned and extensively covered by overburden Cody Found Horse outcrop. This outcrop is located on the Persimmon Range. The section was measured to be 102m from the base of the outcrop, located at an elevation of 2224m with ± 3 m accuracy based on GPS.



Figure 1-7. The Monaghan Creek outcrop section is located on the Starlight Range. This outcrop is within close proximity to Monaghan Creek (not observed in this photo) and was originally described by Gibson in 1968. The measured section height of this outcrop is 261.5m from the base at an elevation of 1767m with an accuracy of ± 20 m based on GPS. The creek in this photo remains unnamed. Both the base and top of the outcrop are not observed in this photo.



Figure 1-8. The white arrow in this photo indicates the base (0m) of the Blue Grouse South outcrop located on the Starlight Range. The base of the measured section is at an elevation of 2198m with an accuracy of $\pm 5\text{m}$ based on GPS.



Figure 1-9. This photo is of a resistive cliff at the Blue Grouse Brewster outcrop is located on the Starlight Range. The Jacob staff in the photo is parallel to bedding. The elevation at the base of the section is 2251m with an accuracy of $\pm 2\text{m}$ based on GPS.

microfacies for chemostratigraphic analysis. Sample processing and interpretations were conducted at the University of Alberta. A digital database of photographs was created of all thin sections. Lithological analyses, characterization of trace fossils, and interpretation of results were aided by the database. Photos were taken under both plane-polarized light (PPL) and cross-polarized light (XPL), under magnifications of 10X and 60X. Only the most significant features, which were deemed the most likely to contribute to the interpretation of the data, are discussed herein.

Each of the six outcrop locations studied were analyzed with the aid of the RS-125 Super-Spec hand-held radiation spectrometer. The RS-125 Super-Spec uses a Sodium-Iodide crystal to collect total count spectra data and assay results to permit line profiles. The data collected was sampled in 120 second increments to ensure good quality data and fast sampling to get the maximum data for an area in a reasonable period of time. Assay results include: potassium (K) data shown in percent, uranium (U) and thorium (Th) data in parts/million (ppm), and total count spectral data in dose units to give an indication of the overall radiation intensity. Data was collected at regular intervals of 75 centimeters (cm) beginning at the base of each section to the top of each logged interval. Measured sections and associated gamma analysis assay numbers were recorded and later combined to create geophysical outcrop logs. The resulting line profiles were then used to interpret lithologic, stratigraphic, and facies correlations.

In this study chemical stratigraphy or chemostratigraphy is a technique used to correlate strata through the characterization and correlation of elements.

Chemostratigraphy is particularly useful when attempting correlation in sequences with limited biostratigraphic data and high lateral variability (Ratcliffe et al., 2006). To facilitate chemostratigraphic correlation within the study area, two outcrops were selected (E53 and MC) (Fig 3-3). The selection of the outcrops for chemostratigraphic study was based upon the completeness of the three-meter sampled intervals at the outcrops (accounting for covered sections) and a suitable representation of lithofacies. The selected samples were dissolved using the Na_2O_2 sinter technique as described in Longerich et al., (1990). Whole-rock geochemistry was acquired using inductively coupled plasma-mass spectrometry (ICP-MS) in the Radiogenic Isotope Facility at the University of Alberta. The instrument used to determine the major and trace element compositions by solution mode analysis was a Perkin Elmer Elan 6000 quadrupole ICP-MS (QUAD ICP-MS). The resultant geochemical data included fifty-one element concentrations in parts per million (ppm).

It was determined that the most reliable method of geochemical correlation between the outcrop sections was the comparison of whole rock geochemistry from individual shale and siltstone layers (Bistran, 2009). In sedimentary rocks, absolute concentrations of trace elements are diluted as the concentration of quartz increases with grain size (Spears and Amin, 1981; North et al., 2005). As geochemistry is affected by grain size, the study of coarse-grained sandstone is

not practical in chemostratigraphic analysis (Pearce et al., 1999). Fine grained lithologies are used in this study as error is reduced when using samples of uniform grain size (Ratcliffe et al., 2004). Homogeneous elemental composition and more consistent lateral distribution of shale and siltstone facies are identified to improve the correlation potential (Ratcliffe et al., 2004).

In support of this study, Bistran (2009) at the University of Alberta completed a portion of the chemostratigraphic analysis as an undergraduate thesis. The correlation was completed through the visual interpretation of similarities of the graphical distribution of all elemental concentrations identified. The graphical plots are arranged with elements in increasing atomic number on the X-axis, and elemental concentrations in ppm on the log-scale Y-axis (Appendix D). The resultant data was plotted against outcrop lithologies and gamma-ray logs to observe any similarities and trends (Bistran, 2009).

To supplement the visual correlation analysis described above, additional chemostratigraphic correlations were completed. This methodology involves the normalization of elemental concentrations to Zircon (Zr) to minimize the influence of clastic flux. Whole rock geochemical data normalized to Zr minimizes the influence of subtle variations in content (Pearce et al., 1999). The normalization of the other elements is completed through the division of all elements by the given Zircon concentration for each of the sampled intervals (Appendix C). The resultant normalized elemental concentrations for each element is plotted graphically against the concordant outcrop depth in meters.

The graphical results of each element are placed side by side for comparison and visual interpretation of potential stratal correlations. As outlined in Pearce et al., (1999), immobile elements are less prone to the effects of diagenetic alteration and are also visually compared between the E53 and MC outcrops. Results and interpretations of the chemostratigraphic analysis are presented in chapter 3 of this study.

In addition to chemostratigraphic analyses, biostratigraphic analyses were conducted for this study. Samples for biostratigraphic analyses were collected from carbonate rich intervals suspected to contain high bioclastic content with the intent of eventual conodont analysis. In total 28 one kilogram samples were collected for analysis. Conodont identification and age assignments were completed by M.J. Orchard of the Geological Survey of Canada Pacific. The results of the conodont age analysis were applied to establish biostratigraphic age of the studied outcrop successions and provide enhanced lithologic, stratigraphic, and facies correlation as discussed in chapter 3 of this study.

The data obtained from outcrop descriptions and analyses described above were used to construct facies models that were then grouped into facies associations based upon sedimentological and ichnological criteria. These interpretations provide the basis for the development of depositional models for the facies identified as described in chapter 2 of this study. Stratigraphic correlations were subsequently completed for outcrop sections based upon the facies framework,

along with biostratigraphic, geochemical, lithostratigraphic, and outcrop gamma ray data (chapter 3).

1.5 STRATIGRAPHIC FRAMEWORK

Nomenclature for the correlation of Triassic strata in the WCSB is divided into the front ranges, western foothills, the eastern foothills, and interior plains (Gibson and Barclay, 1989). This study focuses on the Sukunka-Bow River exposures of British Columbia and Alberta of the front ranges and western foothills nomenclature groupings.

In the study area of west-central Alberta, the Spray River Group of the Triassic includes the Sulphur Mountain and Whitehorse formations (Figure 1-1) (Gibson, 1975). The Sulphur Mountain Formation unconformably overlies the Permian Ishbel Group in most of the study area and the Rundle Group in some eastern regions. The Sulphur Mountain Formation is subdivided into four members: the Phroso Siltstone, Vega Siltstone, Whistler, and Llama (Figure 1-1).

The Whitehorse Formation is unconformably overlain by the Jurassic Fernie Formation in the study area as identified by the author and Gibson (1968) (Figure 1-1). The Whitehorse Formation contains three members: the Starlight Evaporite, Brewster, and Winnifred (Gibson, 1975) (Figure 1-1). Due to the prolific abundance of hydrocarbons east of the deformed belt in the Peace River Arch (PRA) area, the majority of subsurface research has focused on the Triassic strata of the eastern foothills and interior plains (Gibson, 1975). For purposes of this

chapter the subdivisions of the Peace River Embayment (PRE) subsurface are applied to the laterally equivalent intervals of the Sukunka-Bow River exposures of British Columbia and Alberta (Figure 1-1). This is done to highlight the generally accepted stratigraphic history of the Triassic in the WCSB (Gibson 1975), (Gibson and Barclay, 1989) (Figure 1-1).

Triassic strata in the PRE subsurface of British Columbia are divided into two groups laterally equivalent to the Spray River Group of the Sukunka-Bow river exposures (Figure 1-1). The two groups are the Diaber Group and the Schooler Creek Group (Figure 1-1). The Diaber Group consists of the Montney Formation and Doig Formation (Figure 1-1). The Schooler Creek Group is made up of the Charlie Lake, Baldonnel, and Pardonet formations (Figure 1-1).

Three major transgressive-regressive cycles are identified in the Triassic of the WCSB (Prdruski et al., 1988; Gibson and Barclay, 1989). The Montney Formation of the first cycle is laterally equivalent to the Vega/Phroso Siltstone Member in the study area (Gibson 1971, 1972, 1975) (Figure 1-1). The Vega/Phroso Siltstone Member is equivalent to the Grayling and lower Toad formations in the Sikanni Chief-Pine River exposures of British Columbia (Gibson 1971, 1972, 1975). The Vega/Phroso Siltstone Member subdivision into the Vega Siltstone Member and Phroso Siltstone Member is not practical due to the lack of a well-defined contact between the two units in the study area (Gibson, 1972, 1975) (Figure 1-1).

Gibson (1975) describes the Vega/Phroso Siltstone Member as a grey to rusty brown, flaggy weathering sequence of dolomitic to calcareous siltstone, finely crystalline to bioclastic limestone, silty shale, and minor very fine sandstone. Recent depositional interpretations identify the sequence and lateral equivalents to be a wave dominated westerly prograding marine shoreline grading into offshore turbidite deposition (Moslow and Davies, 1997; Davies, 1997a).

The second major transgressive-regressive cycle consists of the Whistler, Llama, and Starlight Evaporite members in the study area, laterally equivalent to the Doig, Halfway, and Charlie lake formations (Gibson 1971, 1972, 1975). In the PRE subsurface, the Doig Phosphate Zone overlies the Montney Formation and has been identified as a major marine transgression (Armitage, 1962). The Whistler Member is equivalent to the Doig Phosphate Zone and is equivalent to the Middle Toad Formation in the Sikanni Chief-Pine River exposures.

Gibson (1975) described the Whistler Member to be a dark grey to black weathering siltstone, silty and fossiliferous limestone with minor interbeds of silty shale, dolostone, phosphatic and quartz sandstone, and phosphatic pebble conglomerate. The laterally equivalent Doig Phosphate Zone is recognized as a zone of high total organic carbon (TOC) and phosphate rich siltstone.

Depositional interpretations identify the unit to represent transgressive flooding over the deposits of the Vega/Phroso Siltstone Member. The abrupt contact of the

first and second cycle is interpreted to be a period of non-deposition or submarine erosion of marine transgression (Edwards et al., 1994).

The Llama Member within the second major transgressive-regressive cycle is correlated with the Doig and Halfway formations of the PRE subsurface and the Upper Toad and Liard formations of the Sikanni Chief-Pine River exposures. The Llama Member is described by Gibson (1975) as a resistant succession of thin to thick bedded dolomitic quartz siltstone, silty and bioclastic limestone, and lesser amounts of dolomitic quartz sandstone and dolostone. The contact with the overlying Starlight Evaporite Member (laterally equivalent to the Charlie Lake Formation) is gradational in the Sukunka-Bow River area which includes this study. The contact is placed by Gibson (1975) where the Llama Member grades upward into yellow weathering sandstone, dolostone, and intraformational and/or solution breccia of the Starlight Evaporite Member.

The laterally equivalent Doig Formation is interpreted to be a series of westerly prograding transgressive-regressive sequences of offshore to lower shoreface mudstone, siltstone, and sandstone (Gibson, 1968a, b; Aukes and Webb 1986; Cant, 1986; Gibson and Edwards 1990b). The Doig is identified as gradationally overlain by shoreface sandstones of the Halfway Formation (Gibson, 1968a,b; Gibson, 1975; Aukes and Webb 1986; Cant, 1986; Gibson and Edwards 1990b). The Doig Halfway contact is observed to be sharp in instances where interpreted tidal inlets scour into the Doig Formation (Edwards et al., 1994). However, in the

Sukunka-Bow Rivers region studied by Gibson (1975) the Halfway Formation is not recognizable.

The uppermost formation of the second major transgressive-regressive cycle is the Starlight Evaporite Member of the Whitehorse Formation. This member is laterally equivalent to the Charlie Lake Formation in the PRE subsurface and the Ludington Formation in the Sikanni Chief-Pine River exposures. Gibson (1975) describes the member as a variegated sequence of recessive, yellow brown to grey weathering dolostone, sandstone, siltstone, limestone, and intraformational and/or solution breccia. The contact of the Starlight Evaporite Member with the overlying Brewster Limestone Member is recognized by Gibson (1975) as the point at which where the yellow to grey, calcareous and dolomitic sandstone and siltstone are abruptly overlain by pale to grey weathering, cliff-forming limestone. The Starlight Evaporite Member is interpreted to have been deposited in a back-barrier sabkha and lagoonal, supratidal, or intratidal environment (Gibson, 1975; Aukes and Webb, 1986; Cant 1986; Higgs, 1990; Edwards et al., 1994).

The third and final major transgressive-regressive cycle of the Triassic include the Brewster Limestone Member and the Winnifred Member. According to Gibson (1975), the Brewster Limestone Member is correlative with the Baldonnel Formation north of the Sukunka River and may be correlated with the upper part of the Ludington Formation. Gibson (1975) interpreted the Winnifred Member to be equivalent to the upper most Baldonnel Formation north and east of the Sukunka River and to the upper part of the Ludington Formation and possibly the

lower Pardonet Formation in the Sikanni Chief-Pine River exposures (Gibson, 1975). The Brewster limestone Member is identified to be a distinctive pale grey, resistant, cliff forming sequence of limestone, minor dolostone, and intraformational breccia (Gibson, 1975). The contact of the underlying Starlight Evaporite Member with the Brewster Limestone Member is abrupt and conformable (Gibson, 1975). Identification of the contact is placed at the transition from the yellow to grey calcareous and dolomitic sandstone and siltstone to the cliff forming grey limestone (Gibson, 1975).

The Winnifred Member is described as a recessive, yellow to grey dolostone and limestone, with minor intercalated sandstone beds, siltstone, and intraformational breccia (Gibson, 1975). Gibson (1975) identified the Winnifred Member to be rarely present in the Sukunka-Smokey River area (this study). The Jurassic Fernie Formation unconformably overlies the Winnifred Member in the study area. Gibson and Barclay (1989) and Davies (1997a) describe the depositional environment of the Baldonnel and Pardonet formations as ranging from shallow to deep water marine shelf.

1.6 TECTONIC AND GEOLOGIC SETTING

Triassic strata comprise a range of sedimentary facies representing marine, marginal marine, and sabkha depositional settings (eg. Gibson and Barclay 1989; Gibson, 1993; Arnold, 1994; Zonneveld et al., 1997a, b; Zonneveld et al., 2004; Dixon, 2005; and Zonneveld et al., 2007a). Laterally equivalent units to the Whitehorse Formation and are interpreted to be deposited in an overall progradational sequence of similar mixed siliciclastic and carbonate sediments as

identified by the author and Gibson (1975) (Zonneveld et al., 1997a; Zonneveld et al., 2007a).

The deposition and preservation of the Triassic strata in the WCSB is greatly influenced by a number of structural elements. The structural element interpreted to have the greatest influence on the deposition of sediment during the Triassic is the PRE (Barss et al., 1964; Cant, 1988; Gibson and Barclay, 1989; O'Connell et al., 1990). The PRE is interpreted by some to have developed during the Carboniferous and Permian following the collapse of the PRA (Barss et al., 1964; Cant, 1988; O'Connell et al., 1990). Stratigraphy in the PRA area is largely influenced by Proterozoic and Archean structural features. Cant (1988) describes the formation of the PRA to have resulted from five stages. These stages include: 1) Early Paleozoic uplift, 2) Late Devonian faulting, 3) Mississippian subsidence, 4) Pennsylvanian faulting, and 5) Mesozoic down-warp. The second stage, Late Devonian faulting, is interpreted by Richards (1989) and Henderson (1989) to have resulted in the formation of the PRE.

Other large scale structural elements of the PRA/PRE include the fault sets of the Fort St. John Graben and Dawson Creek Graben Complex (Macauley et al., 1964; Henderson, 1989; Richards, 1989; Barclay et al., 1990). As a result in part of the basement dipping to the west, Triassic strata thicken westward to a maximum of 1200m reached within the collapsed PRA and thin to an erosional edge in the east (Edwards et al., 1994; Ross, 1997). Basinal relief of the PRE lessened through

the Triassic, therefore influencing the overall thickness trends of the Triassic succession (Barss et al., 1964; Cant, 1988; Gibson and Barclay, 1989; O'Connell et al., 1990).

Evidence of tectonic activity during the Triassic in the WCSB has been identified in a number of research papers. Cant (1986) opined that during the deposition of Triassic sediment, tectonic activity reactivated underlying structural elements resulting in small scale gravity faults. Wittenberg (1992, 1993), Qi (1995), and Dixon (2002a) suggest that anomalously thick sand bodies (ATSBs, *sensu* Wittenberg, 1992) identified in Triassic strata of the Doig Formation are the result of structurally created depressions. Wittenberg (1992, 1993) suggests that the accommodation space created for the preservation of the ATSBs is the result of syndepositional growth-fault grabens. Qi (1995) and Berger (2006) identify the influence of basement structures on the preservation of the ATSBs. Evoy and Moslow (1996), Evoy, (1997), and Caplan and Moslow, (1997) additionally identify high-angle normal faulting and synsedimentary tectonism in Triassic successions.

Explanations for the occurrence of tectonic activity in the WCSB include the break up of Pangea, the approach of island arcs in the Panthalassa Ocean and accretion (Monger et al., 1982; Tozer, 1982; Wilson et al., 1991; Davies 1997a; Beranek and Mortensen, 2006, 2007, 2008; Ferri and Zonneveld, 2008). Evidence for the presence of the exotic terranes comes in the form of Triassic and early

Jurassic igneous and carbonate rocks in the western Cordillera of North America (Tozer, 1982; Ferri and Zonneveld, 2008). Researchers interpret these rocks to be accreted island arcs (Monger et al., 1982; Tozer, 1982; and Monger, 1989). Beranek and Mortensen (2006) identify Yukon terranes to accrete during the Triassic. Unfortunately, there is no other evidence identified by the author in current literature that can accurately place the distance of island arcs during the Triassic from the paleocontinental margin of Pangea.

The implications of the proximity of the island arcs to the paleocoast relates to the degree of tectonic activity probable during the Triassic. According to Wilson et al., (1991) the offshore region of Panthalassa was the location of active tectonism including subduction zones, volcanic island arcs, back arc, and intra-arc suboceanic basins, as well as migrating terranes. Gibson and Barclay (1989) assert that the Triassic rocks of the WCSB were deposited before the break-up of Pangea, accretionary events, and identify the western margin as similar to the modern Atlantic passive continental margin. The interpretations of the late Jurassic docking events suggest a more passive and tectonically stable setting persisted during the Triassic (Gibson and Barclay, 1989).

Davies (1997a) contends that tectonism was relatively active on the sedimentary wedge in the Triassic basin. Moderate phases of basin-margin uplift and faulting are interpreted to have resulted in a number of basin-wide eastward-downcutting, erosional unconformities (Davies, 1997a). The study did not reveal any evidence

of major tectonic activity (Davies, 1997a). However, the angular architecture of the Coplin Unconformity suggests a major tectonic event occurred (Hess, 1968). Gibson (1993) interpreted regions of west-central Alberta and northeastern British Columbia to have been a passive margin basin extending from the Late Proterozoic to the Middle Jurassic. In contrast, Davies (1997a) describes sedimentation in the PRA as confined to three tectonically controlled contiguous basins. The three basins include: the Peace River Basin (extensional/transensional type), the Continental Margin Basin (sag type), and the Liard Basin (transensional type) (Davies, 1997a, b).

The lack of exotic sediment observed in Triassic rocks may be explained if the graben systems blocked sediment transport into coastal depositional areas and if uplifted blocks in the western margin source compositionally similar material into the basin to the east (Zonneveld personal communication, 2007). The interpretation that accreting terrains may have been closer to the northwestern margin of North America provides an explanation for active tectonism during the Triassic and is supported by the presence of Carboniferous to Permian Zircon in cratonic Triassic successions (Beranek and Mortensen, 2006, 2007, 2008; Ferri and Zonneveld, 2008). Despite earlier interpretations of a passive tectonic setting during the Triassic, emerging evidence suggests the western North American continental margin may have been more active than previous models indicate (Beranek and Mortensen, 2006, 2007, 2008; Ferri and Zonneveld, 2008).

1.7 PALEOLATITUDE

Paleogeographic reconstructions use in part paleomagnetic data to position the northwestern coast of the Pangaea supercontinent (Golonka et al., 1994). The paleo-coast of west-central Alberta during the Triassic faced westward into the Panthalassa Ocean (Habicht, 1979; Tozer, 1982; Gibson and Barclay, 1989; Edwards et al., 1994) (Figure 1-10). Estimates of paleolatitude position the Proto-Albertan and British Columbian continental margin during the Middle Triassic vary from 25 to 40 degrees north of the paleoequator (Figure 1-11) (Habicht, 1979). The orientation of the Triassic continental margin relative to the present configuration is estimated to be rotated approximately 25 to 30 degrees clockwise (Habicht, 1979; Tozer, 1982; Wilson et al., 1991; Golonka et al., 1994; Smith et al., 1995).

Interpretations of paleolatitude based upon paleomagnetic data are reinforced by lithological and sedimentological data. Carbonate, evaporite, and algal/cyanobacterial mats are commonly formed in latitudes 25 to 40 degrees north and south of the equator in modern depositional environments (Kendall and Skipwith 1969; James and Kendall, 1992). A midlatitudinal interpretation is consistent with the conditions necessary for the formation of lithologies observed in the Triassic strata of this study. Lithologically equivalent units such as the Charlie Lake Formation and platform carbonates of the Baldonnel and Pardonet formations also support this construction (Arnold, 1994, Davies, 1997a, b; Zonneveld and Orchard, 2002; Zonneveld et al., 2004).

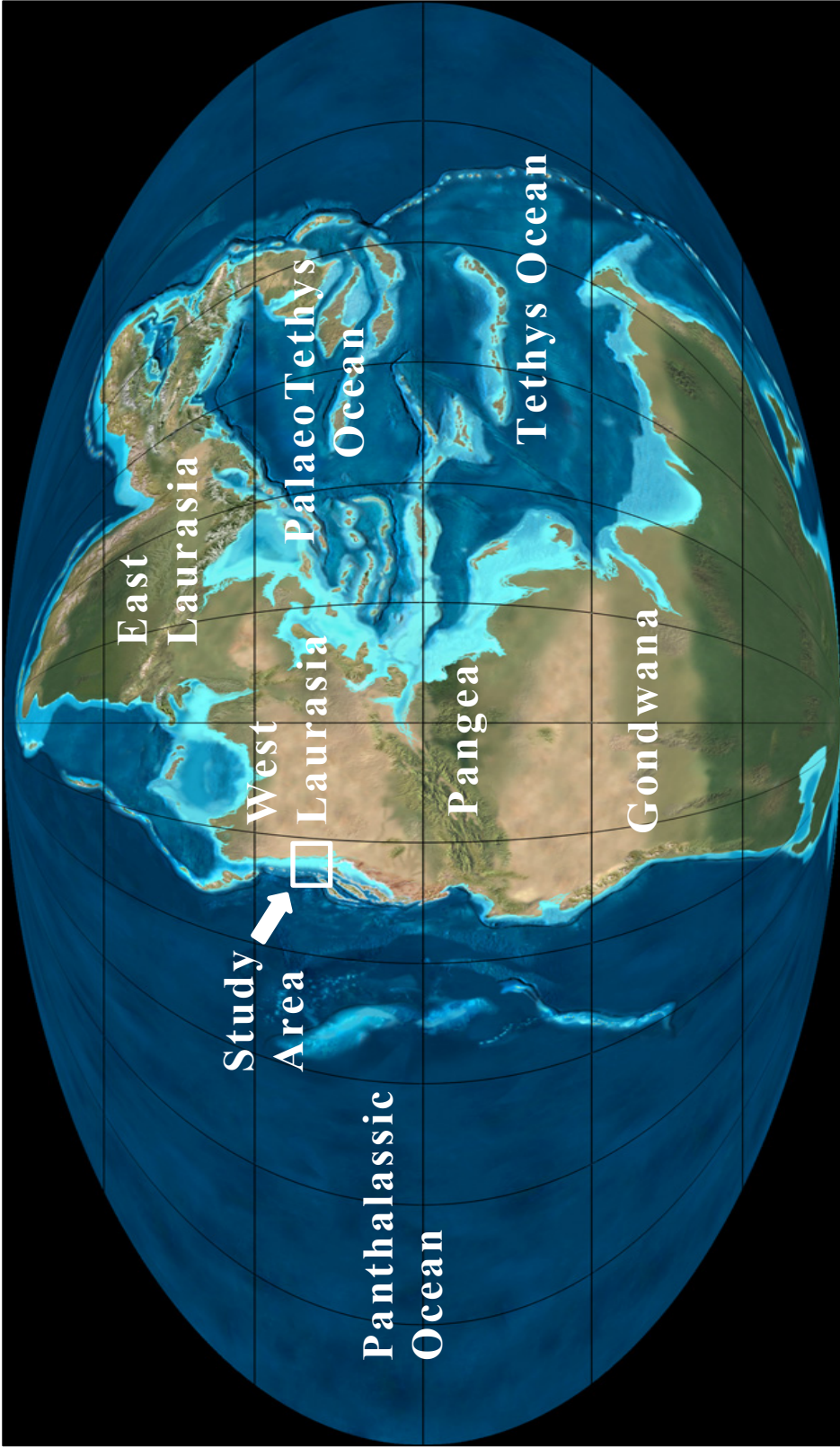


Figure 1-10. Location of west-central Alberta and the study area within the Willmore Wilderness Park in relative position to Pangea during the Early Triassic. After Blakey, R. C., (2011); <http://jan.ucc.nau.edu/~rcb7/index.html>.



Figure 1-11. Paleogeography of the western margin of Pangea during the Middle Triassic and the study area within the Western Canadian Sedimentary Basin (WCSB). After Blakey, R. C., (2011); <http://jan.ucc.nau.edu/~rcb7/index.html>.

1.8 PALEOCLIMATE

Reconstructions of paleoclimate conditions are, in part, based upon modern-day analogs of weather forcing factors including: global oceanographic circulation patterns, thermal gradients, the Coriolis force, and the associated impact of continental distribution upon these factors (Tozer, 1982; Kristan-Tollmann and Tollmann 1982; Golonka et al., 1994). Modern climate conditions of the Saharan, Atacama, and Namibian deserts have been likened to the paleoclimate conditions of the Triassic on the northwestern continental margin of Pangaea (Wittenberg, 1992; Davies, 1997b). The analogs are then compared to paleogeographic models constructed from paleolatitude, paleomagnetic, paleontological, and sedimentological data. Interpretations of paleoclimate conditions during the Triassic deposition of sediment in the WCSB range from temperate and semiarid, to arid (Habicht, 1979; Kristan-Tollmann and Tollmann 1982; Gibson and Barclay, 1989; Gibson and Edwards, 1990a, b; Dickens, 1993; Golonka et al., 1994; Zonneveld et al., 2007a).

Upper Triassic strata in the WCSB contain redbeds, evaporates, and aeolian dune deposits that represent typical deposition in arid to semiarid environments (Barclay and Leckie, 1986; Aukes and Webb, 1986; Gibson and Barclay, 1989; Gibson and Edwards, 1990a, b; Arnold, 1994; Edwards et al., 1994; Davies, 1997a). Evidence of aridity during the Triassic also includes the presence of taeniate bisaccate pollen and polyplicate pollen identified in Lower Montney and Toad successions (Utting et al., 2005; Zonneveld et al., 2007a). Additionally

Davies (1997b) describes coastal arid to semiarid climate conditions interpreted from the presence of desert loess deposits in the Charlie Lake, Baldonnel, and Pardonet formations.

Golonka et al., (1994) suggests that north to northeast trade winds prevailed over much of the present location of the WCSB during the Triassic. These winds are similar to present day trade winds within 35 degrees north of the equator.

Paleocurrent direction measurements of Triassic aeolian sandstone beds observed in northeastern British Columbia were found to support this interpretation (Arnold, 1994). Such arid conditions are ideal for the formation of hypersaline environments resulting in the formation of evaporite minerals and early diagenetic dolomite, as observed in the lithologies of the Whitehorse Formation and laterally equivalent Triassic formations (Davies, 1997a).

Trade winds interpreted to occur during the Triassic are associated with offshore upwelling of cold water (Davies, 1997a). The midlatitudinal position of the continental margin of proto-British Columbia and a paucity of warm water biota (such as megolodons, scleractinians, and sponges) has been interpreted to provide evidence of cool coastal waters (Gibson and Barclay, 1989; Tozer 1992; Davies, 1997a). Zonneveld et al., (2001) cautioned against paleoclimatic interpretations based upon the absence of taxa. The upwelling of colder, nutrient-rich, and possibly anoxic, water is recognized to result in biotic production of phosphatic marine sediment in modern environments (Moslow and Davies, 1992). Examples

of the cold upwelling of ocean currents can be observed in modern environments of similar midlatitudinal settings such as: the coast of southwestern Africa (Namibia), the northern coastal Chile, southern California, and coastal Baja California/Mexico (Davies, 1997a). Phosphate rich intervals are also recognized with this study area.

1.9 PALEO-SEA LEVEL

Previous research has focused on sea level fluctuations during the Triassic which strongly influence sediment distribution (Vail et al., 1977; Haq et al., 1987; Mitchum and Van Wagoner, 1991). Change in relative sea level can be the result of global or local intrabasinal events. Two factors effecting eustatic sea level include glaciation and melting events. Such events may be influence by periods of intense volcanism resulting in greenhouse conditions or extraterrestrial Milankovitch cycles. Changes in sea level may also reflect global or local tectonic events effecting subsidence, loading, extension, and compression.

Gibson and Barclay (1989) identify three major facies assemblages within northeast British Columbia and western Alberta influenced by sea level fluctuation. Within these three major facies assemblages, three major regional transgressive-regressive marine assemblages, several minor cycles have been identified (Wittenberg, 1992; Embry and Gibson, 1995). The three major transgressive-regressive cycles are the Lower Triassic (Induan, Olenekian), Middle Triassic (Anisian, Ladinian), and Upper Triassic (Carnian, Norian).

The Lower Triassic sequence is recognized as beginning with a major marine transgression eastward followed by a regressive sequence consisting of westward deepening distal shelf and shoreline siliciclastics and carbonates (Gibson and Barclay, 1989). This first transgressive-regressive cycle is thought to have resulted in the deposition of the Lower Sulphur Mountain Formation and lateral equivalents (Gibson and Barclay, 1989). The Middle Triassic sequence comprising the second transgressive-regressive assemblage is recognized as a progradational succession composed primarily of shoreline-sabkha siliciclastic, carbonate, and evaporite sediments (Gibson and Barclay, 1989). This cycle is thought to have resulted in the deposition of the Upper Sulphur Mountain Formation sediments (Whistler and Llama Members) (Gibson and Barclay, 1989).

Young (1997) identified Middle Triassic stratigraphy as a westward regression of offlapping parasequences from the Doig Formation to the Halfway and the Lower Charlie Lake formations to the Coplin Unconformity. The third and final major transgressive-regressive sequence resulted in deposition of the Upper Whitehorse Brewster Limestone and Winnifred Members. The Upper Triassic transgressional succession contains smaller progradational parasequence sets (Gibson and Barclay, 1989). The Upper Triassic succession is interpreted to consist of shallow to deep-water shelf and shoreline carbonates (Gibson and Barclay, 1989).

1.10 PALEONTOLOGY AND BIOSTRATIGRAPHY

The Permian mass extinction significantly altered the diversity and distribution of Triassic faunas (Erwin, 1996). The biotic crisis of the Permian resulted in the

extinction of ~ 90% or more of skeletonized marine species (Raup, 1979; Erwin, 1993, 1994). Additionally, this extinction significantly reduced the number of carbonate secreting organisms present in Triassic depositional environments (Zonneveld et al., 2001, 2010a, 2010b). The extinction of many species allowed for the expansion of surviving species into new niches and the evolution of new taxa (Zonneveld et al., 2001, 2010a, 2010b). Paleontological observation in the Willmore Wilderness Park supports but cannot substantiate these results as low diversity of both body and trace fossils were commonly observed. Triassic paleontological assessments in areas to the northeast of the study area do exhibit Triassic successions of more abundant body and trace fossils (Zonneveld et al., 2007b).

In addition to possible residual effects of the impact of the Permian mass extinction on Triassic faunas, the low diversity of both body and trace fossils may reflect the stresses experienced by the marine biota in the depositional environments of the Triassic (Seilacher, 1967; Ekdale, 1988; Frey et al., 1990). Factors such as fluctuating input of siliciclastic sediment, temperature, pressure, salinity, and oxygenation conditions have controlling effects on the distribution and diversity of organisms in a depositional setting (Seilacher, 1967; Ekdale, 1988; Frey et al., 1990). The presence of organisms in a depositional setting is ultimately dependent upon adaptation to a whole range of environmental conditions (Seilacher, 1967; Ekdale, 1988; Frey et al., 1990).

Body fossils identified in this study include: brachiopods, bivalves, gastropods, conodonts, crinoids, and rare blue phosphatic fish bones. Common trace fossils identified during the field study include: *Phycosiphon*, *Thalassinoides*, *Planolites*, *Skolithos*, *Rosselia*, and *Lingulichnus*. Brachiopods are relatively widespread in the study area's Upper Triassic strata, and are well represented in Triassic rocks to the northeast (Zonneveld et al., 2001). Common brachiopods observed in the Triassic include: acrotretids, lingulides, rhynchonellids, spiriferids, and terebratulids (Zonneveld et al., 2007a). However, only lingulids were identified in the study area.

Echinoderms such as crinoids, echinoids, asteroids, and ophiuroids have been identified in the Baldonnel Formation to the northeast and in other Triassic intervals (Zonneveld et al., 2007b). Molluscs including bivalves, gastropods, ammonoids and nautiloids have also been identified as common taxa in Upper Triassic strata (Zonneveld et al., 2001). Zonneveld et al., (2007b) identified the presence of scleractinian coral patch reef deposits in Triassic Carnian deposits in northeastern British Columbia.

Ammonoids and conodonts have been identified in most Triassic stratigraphic sections within western Canada (Orchard and Tozer, 1997). Orchard and Tozer (1997) described the biochronology of conodonts and calibration with the ammonoid standard during the Triassic. The biostratigraphic distribution of conodonts and ammonoids are well documented in the laterally equivalent

Triassic stratigraphy of the Whitehorse Formation. Notably absent in their account is both ammonoid and conodont data for the Whitehorse Formation in the Willmore Wilderness Park (Orchard and Tozer, 1997). Arnold (1994) suggests that difficulties associated with lithostratigraphic correlations of Triassic stratigraphy are a probable result of diachronous units and a lack of stringent biostratigraphic controls. These problems persist, particularly within Upper Triassic rocks of the Whitehorse Formation and will not likely be resolved until further biostratigraphic analyses are completed.

CHAPTER TWO

FACIES DISCRPTIONS, INTERPRETATIONS, AND ASSOCIATIONS

2.1 INTRODUCTION

Fifteen sedimentary facies are distinguished within the Willmore Wilderness Park study area, based upon the analysis of six outcrop sections (Tables 2-1, 2-2, 2-3). The facies are identified on the basis of lithology, primary physical sedimentary structures, biogenic sedimentary structures, bounding surfaces, and fossil composition. Limited diversity, distribution, and abundance of trace fossil assemblages restrict the further subdivision of the lithofacies. Facies data presented confirms many of Arnold's (1994) and Zonneveld's (2004) sedimentological observations of laterally equivalent intervals such as the Doig, Halfway, Charlie Lake, and Baldonnel formations in Northeastern British Columbia. In view of the fact that lithologies under investigation are generally composed of mixed siliciclastic and carbonate sediments, the classification schemes utilized herein for carbonates are those of Dunham (1962), Burchette and Wright (1992), Wright and Burchette (1996; 1998), and for siliciclastics is that of Reading and Collinson (1996).

Subsequent to facies description and interpretation, the fifteen identified facies are grouped into five facies associations. The grouping of facies into facies associations further assists the interpretation of depositional settings. Facies interpreted to be genetically related strata are grouped into the facies associations

Facies Association	Facies	Lithology	Facies Relationships/ Contacts	Lithological Accessories	Physical Sedimentary Structures	Biogenic Sedimentary Structures	Fossils	Interpretation /Depositional Environment
FA1	A	Dolomitic Siltstone	- Lower contact not observed - Gradational upper contact	- Micaceous <5% - Pyrite <3%	- Planar laminae - Undulatory laminae - Low-angle laminae - Cross-laminae - Hummocky cross stratification (HCS) - Dolomitic siltstone bedding 1 to 10 cm - Muddy siltstone bedding 1 to 3 cm	- Very rare <i>Skolithos</i> - Low diversity - Low abundance	- None observed	- Distal offshore transition to offshore transition
FA1	B	Interbedded VF Dolomitic Silty Sandstone and Dolomitic Siltstone	- Gradational lower contact - Sharp upper contact	- Micaceous <3% - Pyrite <3%	- Planar laminae - Undulatory laminae - Low-angle laminae - Cross-laminae - Hummocky cross stratification (HCS) - Symmetric ripples - Siltstone bedding 1-10 cm - Sandstone bedding 5-60cm	- Rare <i>Skolithos</i> - Possible <i>Phycosiphon</i> - Low diversity - Low abundance	- None observed	- Offshore transition to distal lower shoreface
FA2	C	Black Shale	- Sharp lower contact - Gradational upper contact	- High organic content - Phosphate - Pyrite <2%	- Planar laminae - Bedding 0.5-4 cm	- None observed	- Rare phosphatic fish bones (blue)	- Offshore
FA2	D	Muddy Siltstone	- Gradational lower contact - Gradational upper contact	- None observed	- Planar laminae - Bedding 10-15 cm	- Possible <i>Phycosiphon</i> - Cryptic bioturbation - Low diversity - Low abundance	- None observed	- Offshore to distal offshore transition
FA2	E	VF Dolomitic Silty Sandstone	- Gradational lower contact - Sharp upper contact	- Rare phosphate blebs 1-2mm - Rare Vugs	- Undulatory laminae - Low-angle laminae - Hummocky cross stratification (HCS) - Bedding 10-50 cm	- None observed - Possible cryptic bioturbation	- Rare Shell Fragments	- Proximal offshore transition to distal lower shoreface

Table 2-1: Facies descriptions A from sedimentological and ichnological logging of outcrop and core from the Whitehorse Formation.

Facies Association	Facies	Lithology	Facies Relationships /Contacts	Lithological Accessories	Physical Sedimentary Structures	Biogenic Sedimentary Structures	Fossils	Interpretation / Depositional Environment
FA3	K	- VF to F Calcareous Sandstone	- Sharp lower contact - Both sharp and gradational upper contacts	- Rare vugs	- Oscillatory ripples - Low-angle cross-bedding - Low-angle laminae - Siltstone laminae - Bedding 10-35 cm	- <i>Skolithos</i> - Low diversity - Low distribution	- None observed	- Marine/lacustrine
FA4	L	- High-angle Cross-stratified Sandstone	- Sharp lower contact - Sharp upper contact	- None observed	- Planar cross-stratification - Tabular to wedge shaped cross-beds - Bedding 10-100 cm - Horizontal to low-angle planar lamination - Inversely graded laminae	- None observed	- None observed	- Supratidal sabkha (acolian dune)
FA3	M	- Dolomitic Silty Mudstone	- Sharp lower contact - Gradational upper contact	- Vugs 0.3 -5.0 cm - Pressure dissolution features	- VF sand planar laminae (bedding 0.5-3 cm) - Massive dolomitic silty mudstone	- Cryptic bioturbation - <i>Rossetia socialis</i>	- Bivalves - Brachiopods	- Subtidal to intertidal
FA4	N	- Contorted Sandstone	- Gradational lower contact - Sharp upper contact	- None observed	- Planar cross-stratification - Tabular to wedge shaped cross-beds - Bedding 10-100 cm - Horizontal to low-angle planar lamination - Inversely graded laminae - Bedding 10-50 cm	- None observed	- None observed	- Supratidal sabkha (transgressed acolian dune)
FA5	O	- Calcareous Bioclastic Wackestone / Packstone	- Lower contact not observed - Erosionally truncated upper contact	- Wavy aspect to lithology	- Parallel planar laminae - Bedding 1-10 cm	- None observed	- Shell fragments - Bivalves - Gastropods - Brachiopods - Crinoid ossicles	- Offshore

Table 2-2: Facies descriptions B from sedimentological and ichnological logging of outcrop and core from the Whitehorse Formation.

Facies Association	Facies	Lithology	Facies Relationships /Contacts	Lithological Accessories	Physical Sedimentary Structures	Biogenic Sedimentary Structures	Fossils	Interpretation / Depositional Environment
FA2	F	VF Calcareous Sandstone	- Gradational lower contact - Gradational upper contact	- Rare phosphate blebs (1-3 mm)	- Symmetric ripples - Low-angle cross-laminae - Undulatory laminae - Bedding 5-15 cm	- <i>Phycosiphon</i> - <i>Thalassinoides</i> - <i>Skolithos</i> - <i>Planolites</i> - Moderately distributed - Moderate diversity	- Brachiopods (<i>Lingularia selweynti</i>) - Shell fragments - Crinoid ossicles (2-3mm diameter)	- Lower shoreface
FA2	G	Interbedded VF to F Sandstone and Sandy Siltstone	- Erosional lower contact - Upper contact not observed	- Phosphate blebs (2-3mm) - Void vugs and calcite lining (0.3 -0.5 cm) - Rip up clasts (mudstone intraclasts) - Occasionally dolomitic sandstone	- Hummocky cross stratification (HCS) (sandstone) - Undulatory laminae (sandstone) - Symmetric ripples (sandstone) - Parallel and low-angle laminae (sandstone) - Bedding 10-60 cm gradually increasing to 50-75 cm (sandstone) - Low-angle laminae (siltstone) - Cross-laminae (siltstone) - Bedding 1-6 cm (siltstone)	- <i>Skolithos</i> - <i>Planolites</i> - Low diversity - Low abundance	- Shell fragments	- Proximal lower shoreface
FA2	H	- F to C Planar Tabular to Trough Cross-stratified Sandstone and F to M Planar Laminated Sandstone	- Sharp lower contact - Sharp upper contact	- Chert - Phosphate blebs (1-5 mm)	- Planar tabular to trough cross-bedding with bedding 30-50 cm - Planar laminae with bedding 4-10 cm - Asymmetric cross-ripples	- <i>Skolithos</i> - Low diversity - Low distribution	- Fragmented shell debris	- Upper shoreface with amalgamated washover fan or swashzone deposits
FA3	I	- Bindstone Laminate	- Gradational lower contacts - Upper domal convex contacts	- Calcite filled and lined vugs (3-10 mm) - Sulfurous odor - Anhydrite	- Undulatory laminae - Fenestral fabric - Domal stromatolites (possible cyanobacterial) - Bedding 5-10 cm	- None observed	- Rare gastropods - Probable cyanobacterial laminae - Laminar stromatolites	- Supratidal to intertidal flat
FA3	J	- Breccia	- Gradational lower contact - Sharp upper contact	- Calcite filled and void vugs - Sulfurous odor	- Solution collapse of other lithofacies - Angular clasts 0.5-20 cm in length - Chaotically oriented - Primarily matrix supported	- None observed	- None observed	- Solution collapse breccia - Supratidal peritidal (sabkha)

Table 2-3: Facies descriptions C from sedimentological and ichnological logging of outcrop and core from the Whitehorse Formation

as follows. Facies association one consists of facies A and B. This facies association represents the offshore to shoreface transition of the Lower Triassic Vega/Phroso Siltstone Member of the Sulphur Mountain Formation. Facies association two consists of facies C, D, E, F, G, and H. This facies association represents the offshore and shoreface succession of the Whistler, and Llama Members of the Sulphur Mountain Formation. Facies Association three consists of facies I, J, K and M. Facies Association three is interpreted to consist of a subtidal to supratidal sabkha depositional succession within the Starlight Evaporite Member of the Whitehorse Formation. Facies Association four consists of facies L and N. Facies Association four is interpreted to represent aeolian deposition within the Starlight Evaporite Member of the Whitehorse Formation. Facies Association five consists of only Facies O. Facies Association five is interpreted to represent offshore marine carbonate facies of the Brewster Limestone Member of the Whitehorse Formation. Outcrop logs are presented in Appendix A.

2.2 OUTCROP DESCRIPTIONS

Six different outcrop locations were selected for study in the Willmore Wilderness Park from two camp locations. The first campsite, near Eagles Nest Pass, is located at N 53° 27' 46.5" W 118 35' 56.6" with an elevation of 1881 meters. The second campsite near Monaghan Creek and the Sulphur River is located at N 53° 35' 7.4" W 118 55' 16.7" at an elevation of 1575 meters. The three outcrop locations accessed from the Eagles Nest campsite include: A) Poupanee Chute,

B) East 53, and C) Cody Found Horse. From the second campsite an additional three outcrop locations were accessed for study: D) Monaghan Creek, E) Blue Grouse South, and F) Blue Grouse Brewster. Descriptions of the selected outcrops, including location, elevation, GPS accuracy, and the measured section height within the selected outcrop, are displayed in Table 2-4.

2.3 FACIES DESCRIPTIONS AND INTERPRETATIONS

2.3.1 FACIES A: DOLOMITIC SILTSTONE

Description: Lithologically the facies consists of very well sorted slightly dolomitic siltstone interlaminated with muddy siltstone (Figure 2-1). The fissile weathered surfaces of Facies A appear brown, with freshly exposed surfaces appearing dark grey to black (Figure 2-1). The lower contact of the Facies A was not observed due to cover. The upper contact of Facies A with Facies B is gradational. Detrital mica is observed resulting in a weakly speckled appearance to the unit. The bedding consists of alternations of 1-10cm dolomitic siltstone and 1-3 cm beds of muddy siltstone (Figure 2-1). The most predominant sedimentological feature is planar laminae discernible on weathered surfaces (Figure 2-1). The very well sorted nature of the facies makes the discrimination of individual sedimentary features on fresh surfaces difficult, resulting in a largely structureless appearance. Less common undulatory, low-angle, and cross-laminae are observed in the facies increasing in prevalence at the top of the unit. The thinly bedded siltstone facies was measured to be 21 m thick and was only observed in the Poupanee Chute outcrop accessed from camp 1. No body fossils were observed

Outcrop Name	Location Lat./Long. (base of section)	Elevation (base of section)	GPS Accuracy (base of section)	Measured Section Height
Poupanee Chute	N 53° 28' 57.3" W 118° 41' 43.8"	2134 m	10 m	130 m
East 53	N 53° 29' 06.3" W 118° 38' 21.6"	1955 m	3 m	89 m
Cody Found Horse	N 53° 30' 19.8" W 118° 37' 51"	2224 m	3 m	102 m
Monaghan Creek	N 53° 33' 27.4" W 118° 56' 38.5"	1767 m	20 m	261.5 m
Blue Grouse South	N 53° 33' 42.6" W 118° 58' 14.6"	2198 m	5 m	98 m
Blue Grouse Brewster	N 53° 34' 09.5" W 118° 57' 54.9"	2251 m	2 m	63 m

Table 2-4: Outcrop descriptions. Locations referenced to Mount Robson topographic map sheet 1:250 000, 83E NTS selected outcrops including: location, elevation, GPS accuracy and the measured section height within the selected outcrop in displayed in Table 2-4.



Figure 2-1: Facies A, Dolomitic Siltstone. Image A: Planar laminate Siltstone from Vega/Phroso Siltstone Member at the Poupanee Chute outcrop section. Hammer for scale is 25 cm long and the head is pointing up-section. Image B: Symmetrically rippled siltstone from the upper portion of Facies A at the Poupanee chute outcrop section.

in the section. Virtually no trace fossils were observed in Facies A with the exception of rare *Skolithos* burrows towards the top of the unit.

Interpretation: With the exception of rare undulatory, low-angle, and cross-laminae, Facies A is characterized by an absence of higher energy sedimentary structures (Figure 2-1). The finely laminated dolomitic siltstone is likely the result of deposition from suspension. The high degree of sorting observed in Facies A has been interpreted in similar dolomitic siltstone facies of the Montney Formation north of the study area in the Valhalla-La Glace area of west-central Alberta and in north-eastern British Columbia at outcrops along Williston Lake (Davies, 1997a, b; Arnold, 1994; Zonneveld and Moslow, 1997). Suspension fall-out of terrigenous sediment resulting in very well sorted sediment is interpreted in the Valhalla-La Glace area to be the result of aeolian influence on sediment source and transport (Davies, 1997a). Davies (1997a) identified detrital dolomite, mica, and feldspars, possibly from an arid interior, to be consistent with, but not proof of, aeolian sourced sediment in finer grain sizes. Wind blown sediment from aeolian sources has been suggested as an important factor in the distribution of sediment to Triassic deposition centers in the Williston Lake area and recognized in other areas down wind of continental settings (Windom and Chamberlain, 1978; Johnson, 1989; Arnold, 1994). Davies (1997a, b) identified the presence of diagenetic pyrite in the Montney to be a record of the position of a sulfate reduction zone as a result of anoxia (Wignall and Hallam, 1992; Davies, 1997a, b).

The absence of fair-weather influenced sedimentary structures throughout much of Facies A, and the presence of finely laminated siltstone suggest deposition below fair-weather wave base. The undulatory nature of laminae, often with internal erosion surfaces, in the upper section of Facies A is interpreted to be characteristic of hummocky cross stratification (HCS) (Harms et al., 1975; Brenchley, 1985; Leckie and Krystinick, 1989). Discordant laminae and symmetric upper profiles are characteristic of wave produced cross-lamination (Figure 2-1) (De Raaf et al., 1977). The increasing frequency of interpreted HCS towards the top of the unit suggests a shallowing upward succession with an increasing influence of storm related activity (Harms et al., 1975; Brenchley, 1985; Leckie and Krystinick, 1989). The limited occurrence of these structures suggests that only storms of the greatest energy mobilized sediment on the seafloor of Facies A. The increasing abundance of high energy structures towards the top of the unit is interpreted to be evidence of an upwards transition from a depositional environment at or near the mean storm wave base to above storm wave base. The depositional environment interpretation of Facies A is therefore deposition from distal offshore transition to offshore transition. Hamblin and Walker (1979) identify common preservation of HCS in the range from the lower shoreface to proximal offshore transition. The rare observation of HCS in Facies A suggests deposition in the offshore transition zone.

2.3.2 FACIES B: INTERBEDDED VF DOLOMITIC SILTY SANDSTONE AND DOLOMITIC SILTSTONE

Description: The blocky brown weathered surfaces and dark grey fresh surfaces of Facies B appear very similar to (Figure 2-1, 2-2). The lower contact of Facies B is gradational with Facies A. The upper contact of Facies B with Facies C is sharp and disconformable, identified by a prominent lithological change. The distinguishing factor that separates Facies A from Facies B lithologically is the introduction of lower very fine, silty sandstone (Figure 2-2). The silty sandstone is well sorted and variably dolomitic as is the interbedded dolomitic siltstone. The dolomitic concentration is identified to be greater in Facies B than in Facies A. The micaceous component of Facies B is reduced in comparison to Facies A resulting in a less pronounced speckled appearance. The bed thickness of the unit is greater and more variable than in Facies A. Beds of the dolomitic siltstone range from 1-10 cm increasing in thickness towards the top of the unit (Figure 2-2). The bedding of the silty sandstone at the base of the unit averages 5-15 cm increasing in thickness towards the top of the unit to range from 10-60 cm. Upper and lower bedset contacts are observed to occasionally be sharp.

In Facies B, planar laminae, as in Facies A, are the most dominant sedimentological feature (Figure 2-2). In contrast to Facies A, Facies B exhibits more frequent undulatory, low-angle, and cross-laminae (Figure 2-2). Symmetric ripples are commonly identified in Facies B. Decimeter scale structural deformation, present throughout the facies, creates the appearance of wave ripples but is easily distinguished in outcrop. Facies B is measured to be 46.6 m thick



Figure 2-2: Facies B, interbedded VF dolomitic silty sandstone and dolomitic siltstone. Image A: Planar laminate Siltstone from the Vega/Phroso Siltstone Member at the Poupanee Chute outcrop section. Image B: Interbedded VF Dolomitic silty sandstone from the Vega/Phroso Siltstone Member at the Poupanee chute outcrop section.

and is only observed in the Poupanee Chute outcrop accessed from camp 1. No body fossils were observed in the section. The limited diversity and distribution of ichnogenra observed in Facies B is restricted to centimeter sized vertical length *Skolithos* and possible *Phycosiphon*.

Interpretation: The undulatory, low-angle, and cross-laminae present are interpreted to be hummocky cross stratification (HCS) (Harms et al., 1975; Brenchley, 1985; Leckie and Krystinick, 1989). The presence of HCS and symmetric wave ripples leads to an interpretation of deposition in the zone of wave reworking above storm wave base (Brenchley, 1985). Hamblin and Walker (1979) ascertain HCS to be commonly preserved in the lower shoreface to proximal offshore transition. The higher proportion and better developed HCS observed in Facies B in comparison to Facies A suggests deposition in a more proximal shoreface setting. The parallel laminated siltstone is interpreted to be the result of deposition from suspension possibly sourced from an arid continental environment. Storms blowing out of deserts in northern Africa are common and are interpreted to be a potential modern analog for the silty sandstone source in Facies B (Figure 2-3).

The very well sorted nature of the sediment as in facies B makes the identification of internal fabrics very difficult (Davies, 1997a). Gibson (1975) identified similar sandstone lithologies in the Willmore Wilderness Park with flute cast, groove cast, and bouncecast features. Gibson interpreted the features to be associated

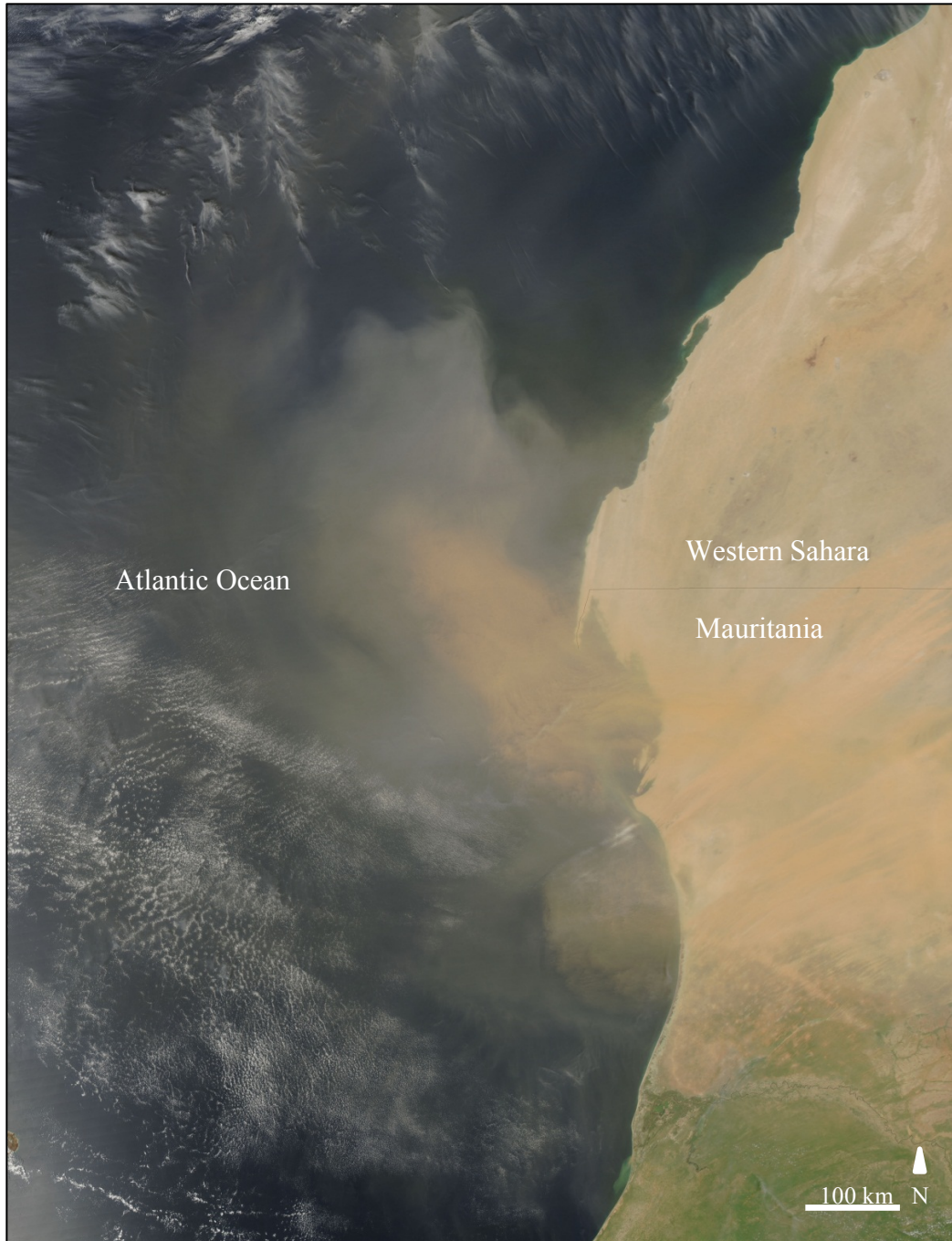


Figure 2-3: Satellite image of dense dust plumes blowing over the Atlantic Ocean, off the coast of western Africa in September 2010. NASA image: Jeff Schmaltz, 2010; MODIS Rapid Response Team at NASA GSFC, <http://earthobservatory.nasa.gov/NaturalHazards/view.php?id=45805>

with shallow water deposition of turbidite facies. Einsele and Seilacher, (1991) identified tempestites to be commonly erosive and incise underlying deposits, potentially resulting in gutter casts, scouring, and sole marks. In the Valhalla-La Glace area and the Williston Lake area similar lithologies have been identified as turbidite deposits (Davies, 1997a, b; Zonneveld et al., 1997). The silty sandstone of Facies B is interpreted to be down-slope gravity driven sediment deposits. The reasons for this description are the inability to identify Bouma subdivisions and the desire to avoid interpretation confusion associated with turbidite and sandy debris flows in the classic deep-water sense (Bouma, 1962; Shanmugam et al., 1995, 1996). Facies B is interpreted to be deposited in the offshore transition to distal lower shoreface with possible emplacement of gravity driven sediment.

2.3.3 FACIES C: BLACK SHALE

Description: The fissile weathered surfaces of Facies C are dark grey to black, with black freshly exposed surfaces. The unit is pervasively planar laminated. The carbonaceous lithology is comprised of weakly dolomitic, silty shale with rare lower very fine sand and silt laminae. The facies is recessive and poorly exposed, as it is commonly partially covered with talus from overlying facies (Figure 2-4). Facies C overlies Facies B separated by a sharp lower contact. Facies C is observed to be gradationally overlain by the muddy siltstone of Facies D. The thickness of Facies C ranges from 1.5-3.5 m, with bedding observed to range from 0.5-4 cm. Covered sections overlying portions of Facies C, precludes the determination of true thickness of the unit. Normally graded planar laminated silt and very fine sand, occur regularly throughout the dolomitic facies and are



Figure 2-4: Facies C, Black Shale. The recessive weathering black planar laminated Siltstone of the Whistler Member, at the Poupanee Chute outcrop. Field assistant for scale, her left hand is indicating up-section. Facies C is poorly exposed and commonly extensively covered by talus from the overlying facies due to the recessive nature of the lithology. Spectral gamma measurements of Facies C are the highest readings observed of all facies studied. This facies is interpreted to be laterally equivalent to the Doig Phosphate Zone.

observed to comprise a very small fraction of the black silty shale (< 5 %). Rare pyrite and blue-black phosphatic fish bones are present in the unit, no other body fossils were observed. No evident biogenic sedimentary structures were observed. Facies C exhibits an exceptionally high gamma-ray signature identified by hand held gamma spectrometer analysis.

Interpretation: Facies C is interpreted to be deposited in the offshore. The black silty shale is interpreted to be the result of a major marine transgression, with the lower contact representing a maximum flooding surface and transgressive surface of erosion. The finely laminated, silty shale, is interpreted to be the result of suspension deposition from the water column below mean storm wave base (Reineck and Singh, 1980; Johnston and Baldwin, 1986). The deposition of rare silt and very fine sand laminae in a quiet marine environment has been interpreted to be the result of input from episodic sediment gravity flows (Reineck and Singh, 1972; Harms et al., 1982; Nelson, 1982; Davis et al., 1989). The rhythmic deposition of planar laminated very fine sand could be the result of episodic deposition following a tempest. A decrease in wave energy following a storm event, would have allowed for sediment to fall-out from suspension after being transported to an offshore environment (Reineck and Singh, 1980; Dott, 1983; Johnston and Baldwin, 1986). The presence of silt and very fine sand has also been interpreted to be the result of aeolian sediment transport during storm events, with later deposition from suspension (Windom and Chamberlain, 1978). Arnold (1994) and Zonneveld et al., (2004) observed the similar presence of silt and sand

laminae in black shale facies at outcrops along Williston Lake in northeastern British Columbia. Both Arnold (1994) and Zonneveld et al., (2004) interpreted the presence of silt and very fine sand laminae to be the result of aeolian sediment transport. The absence shelled organisms, trace fossils, the presence of pyrite, and phosphate in the shale may indicate anoxic conditions during deposition (oxygen levels less than 0.1 ml/L) (Siesser and Rogers 1976; Davies, 1997a; Caplan and Moslow, 1999).

Manko (1960) and Gibson (1975) identified a similar lithology in the Rock Lake area. Manko (1960) describes the Black Siltstone Member, to be a recessive weathering facies that contains prolific *Beyrichites Gymnotoceras* fauna, ammonites, and brachiopods. Gibson (1975) describes the carbonaceous lithology to contain similar fauna including pelecypods. The presence of a phosphatic pebble conglomerate at the base of the section was identified by Gibson (1975). Manko (1960) described nodular limestone beds within this facies that contain nodules of phosphate. Manko (1960) suggests the phosphate marker to afford an excellent correlation marker into the Peace River region. Gibson (1975) assigned the unit to the Whistler Member, conformably overlain by the Llama member. Wittenberg (1992) interpreted the radioactive mudstone beds above the Montney Formation to be a condensed sections, informally referred to as the “Doig Phosphate Zone”. The Doig phosphatic zone has been identified as the source for many oil and natural gas pools in the Triassic (Riediger et al., 1990; Allan and Creaney, 1991).

2.3.4 FACIES D: MUDDY SILTSTONE

Description: Both the weathered and fresh surfaces of Facies D are observed to be dark grey. Lithologically, the muddy siltstone is non-reactive with hydrochloric acid and contains minor amounts of very fine sand (< 5%). Facies D is observed to be interbedded with facies C and E, with gradational upper and lower facies contacts. The thickness of this facies is observed to vary from 3 to 7 meters. The bedding of Facies D is found to be in the range of 10 to 15 centimeters (Figure 2-5). The largely homogeneous facies is dominated by silt sediment. The overall massive appearance of the muddy siltstone occasionally reveals the preservation of planar laminae. No body fossils were observed in Facies D. The exclusive biogenic sedimentary structure described in this facies is the *Phycosiphon* trace.

Interpretation: Lithological, sedimentary, and biogenic characteristics observed in Facies D are indicative of deposition in an environment ranging from the offshore to distal offshore transition. The depositional interpretation of Facies D is additionally derived from the comparison with the more sand prone overlying Facies E, which is comprised of more proximal offshore transition deposits. The occurrence of planar laminae is consistent with deposition below storm wave-base (Boreen and James, 1995). The preservation of finely laminated muddy siltstone suggests deposition from suspension (Reineck and Singh, 1980). The predominantly homogeneous silt sediment is interpreted to contribute to the generally massive appearance of Facies B (Reineck and Singh, 1980).



Figure 2-5: Facies D, Muddy Siltstone: Planar laminate Siltstone, massive in appearance, from the Llama Member at the Monaghan Creek outcrop section. The hammer for scale is 25 cm long and the handle is pointing up-section.

Compaction, dewatering, and pervasive bioturbation may have also contributed to the generation of the overall massive appearance (Forstner et al., 1968; Reineck and Singh, 1980). Bioturbation can result in partial or total lack of preservation of sedimentary structures through the reworking of sediment (Pemberton and Frey, 1985; Pemberton and MacEachern, 1995). The only ichnotaxon identified in facies D is *Phycosiphon*. *Phycosiphon* is identified as a dominant trace in shelf settings (Wetzel and Bromley, 1994; Fu and Werner, 2000).

2.3.5 FACIES E: VF DOLOMITIC SILTY SANDSTONE

Description: Facies E consists of very fine grained dolomitic silty sandstone with very thin (< 1 centimeter) beds of siltstone. Lithological accessories include rare phosphate 1 to 2 millimeter blebs (Figure 2-6). This lithology is characterized by light grey to brown weathered surfaces and a grey coloration of newly exposed surfaces (Figure 2-6). Bedding is observed to be 10 to 30 centimeters. Each bedding unit is massive, with rare undulatory and low-angle laminae observed. The lower contact with Facies D is sharp and abrupt. The upper contact of Facies E is commonly defined by a distinct lithological change. The unit is measured to range in thickness from 3 to 7 meters. No trace fossils or body fossils were observed in this unit.

Interpretation: Facies E is interpreted to have been deposited in the proximal offshore transition to distal lower shoreface. The gradational and coarsening



Figure 2-6: Facies E, VF Dolomitic Silty Sandstone. Image A: Overall massive appearance of Facies E with rarely visible undulatory and low-angle laminae from Llama Member at the Poupanee Chute outcrop section. Hammer for scale is 25 cm long and the head is pointing down-section. Image B: Bedding of Facies E 10-30 cm grading upward into rare 50 cm beds at the Poupanee Chute outcrop section.

upwards nature of Facies D into Facies E is consistent with proximity to the lower shoreface zone. Factors such as deposition by sediment gravity flow, extensive bioturbation, and rapid deposition from suspension can result in the absence of sedimentary structures. In this facies, rare undulatory and low-angle laminae bound some of the sandstones may be interpreted as hummocky cross stratification (HCS) (Benchley, 1985). Benchley (1985), Hamblin and Walker (1979), identify storm dominated shallow marine environments such as the distal lower shoreface to be locations of higher preservation potential for HCS. This suggests that the sandstone of Facies E was deposited during storm events, with silty laminae being deposited by suspension during periods between storm events. The top of Facies E is bound by a sharp contact and the reappearance of Facies C. The deposition of Facies C above Facies E is thought to be representative of a smaller scale transgression event.

2.3.6 FACIES F: VF CALCAREOUS SANDSTONE

Description: Facies F consists of light grey to brown, upper to lower very fine calcareous sandstone, lesser amounts of silt/mud, and abundant bioclastic material (Figure 2-7). Lithological accessories commonly observed in the unit are 1 mm to 3 mm phosphate nodules. The facies is gradational with the underlying Facies D, overlying Facies G, and averages 6 to 9 meters in thickness. The bedding of Facies F ranges from 5 to 15 centimeters, with sharp bases. The sedimentary structures observed include symmetric ripples, undulatory laminae, and low-angle cross-laminae.



Figure 2-7: Facies F, VF Calcareous Sandstone. Image A: VF Calcareous Sandstone displaying a *Lingularia selweyni* brachiopod shell at the Monaghan Creek outcrop section of the Llama Member. The scale bar sections each represent 1 cm. Image B: Brachiopods and unidentified shell fragments of Facies F at the Poupanee Chute outcrop section.

There is a distinct increase in the distribution and diversity of trace fossils in Facies F compared with underlying facies. Trace fossils *Thalassinoides*, *Skolithos*, *Planolites*, and possible *Phycosiphon* are observed in Facies F. The trace fossils are found to increase in abundance within the upper portion of the facies. Body fossils are commonly found within thin beds of the very fine calcareous sandstone (Figure 2-7). These fossils include: brachiopods (*Lingularia selweyni*), unidentified shell fragments, and crinoid ossicles 2-3 mm in diameter (Figure 2-7).

Interpretation: Depositional Environment of Facies F is interpreted to be the lower shoreface. The presence of abundant fragmented and disarticulated bioclastic material suggests that Facies F was influenced by higher energy wave action (Harms et al., 1975; Hunter and Clifton, 1982). The presence of higher energy sedimentary structures, such as symmetric ripples in Facies F, indicates that it was deposited above fair-weather wave base (Harms et al., 1982). The lack of mottled appearance and shallow water fauna (*Lingularia selweyni*) suggests a lower shoreface site of deposition (Zonneveld and Pemberton, 2003). Within the *Cruziana* ichnofacies, vertical, horizontal, and angled burrows are observed (Frey and Pemberton 1985; MacEachern et al., 2007). Vertical *Skolithos* burrows may provide evidence of increased energy, in the coarsening upward facies succession that is interpreted to be progradational in nature. Symmetric ripples and low-angle cross-laminae are common sedimentary structures found within the

Cruziana ichnofacies (Frey and Pemberton, 1985; Pemberton et al., 2001; MacEachern et al., 2007).

2.3.7 FACIES G: INTERBEDDED VF TO F SANDSTONE AND SANDY MUDSTONE

Description: Facies G consists of both weathered and fresh tan to grey surfaces of very fine to medium sandstone, with interbedded sandy mudstone (Figure 2-8). The lower bounding surfaces of Facies G are erosional, with siltstone intraclasts present at the base (Figure 2-8). The upper contact of Facies G was not observed due to cover. Lithological accessories observed within the moderately well sorted sandstone are rare 2 to 3 millimeter phosphate blebs, occasionally dolomitic, void vugs, and vugs filled and lined with calcite 0.3 to 0.5 centimeters in diameter (Figure 2-8). The sandy mudstone displays low-angle laminae and cross-laminae. Bedding of the sandy mudstone ranges from 1 to 6 centimeters gradually decreasing in thickness towards the top of the unit to 1 to 3 centimeters (Figure 2-8). Sedimentary structures within the sandstone include: parallel laminae, undulatory laminae, and symmetric ripples. The bedding of the dolomitic VF to F sandstone is measured to be 10 to 75 centimeters, with sharp lower contacts. The sandstone beds gradually increase in thickness to 50 to 75 centimeters at the top of the unit and decrease in dolomite cement concentration.

The thickness of Facies G is measured to be 22 meters. The moderately bioturbated Facies G displays a low diversity and distribution of biogenic



Figure 2-8: Facies G, Interbedded VF to F Sandstone and Sandy Siltstone. Image A: VF to F sandstone bedding of Facies G of the Llama Member at the Poupanee Chute outcrop section. Hammer for scale is 25 cm long and the head is pointing along-section.

sedimentary structures including: *Skolithos* and *Planolites*. Body fossils consisting of fragmented bioclastic debris are observed within the facies.

Interpretation: The undulatory and low-angle parallel laminated sedimentary structures are interpreted to be HCS (Harms et al., 1975; Hunter and Clifton, 1982; Duke, 1985). The HCS sedimentary structures are indicative of a high-energy storm influenced environment (Duke, 1985; Duke, 1990; Duke et al., 1991). Lower shoreface sand bodies commonly contain HCS with planar lamination or ripple cross-laminae (Leckie and Krystinik, 1989; Duke, 1990; Duke et al., 1991). The coarsening upward grain size and symmetric ripples are common throughout the unit. They are interpreted to indicate a gradually increasing energy regime and deposition above mean fair-weather wave base. The rip-up clasts observed are possibly the result of turbidite sands eroding lower siltstone beds. Sandstone beds typically thicken upwards in the proximal lower shoreface, while shale beds thin and eventually disappear altogether (Walker et al., 1992). Bioturbation is rare in this facies. This is expected in environments where the continual erosive action of storm events removes evidence of bioturbation (Pemberton and Frey, 1984). Storms that destroy fair-weather benthic communities often result in post-storm recovery by opportunistic biogenic structures (Pemberton and Frey, 1984; Pemberton et al., 1992a, b). The biogenic sedimentary features and associated physical sedimentary structures suggest that the depositional environment of Facies G is the proximal lower shoreface.

2.3.8 FACIES H: F TO C PLANAR TABULAR TO TROUGH CROSS-STRATIFIED SANDSTONE AND F TO M PLANAR LAMINATED SANDSTONE

Description: Facies H displays fine to medium planar tabular to trough cross-bedded sandstone and slightly dipping fine to medium planar laminated sandstone (Figure 2-9). The moderately well sorted, fine to coarse grained sandstone, appears very porous with subrounded to subangular quartz grains. The upper and lower bounding surfaces of Facies E are sharp and occasionally erosive. The thickness of Facies H ranges from 3 to 6 meters. The planar tabular to trough cross-bedded sandstone is found to consist of orange to red-brown weathered surfaces and red-brown freshly exposed surfaces. Bed sets are observed to average 30 to 50 centimeters, increasing in bed thickness upward. There is variation in carbonate cementation ranging from basal intervals with no carbonate cement to upper zones rich in calcite cement. The base of individual planar tabular to trough cross-bed sets commonly include: thin abraded lags of chert, shell debris, and phosphatic granules (Figure 2-9). The abundance of fragmented shell debris decreases upward in individual bed sets. A sparse distribution of the *Skolithos* trace fossil is identified in this facies. The slightly dipping, fine to medium grained planar laminated sandstone appears grey on weathered surfaces and tan to grey on fresh surfaces (Figure 2-10). No carbonate cementation was observed in this portion of Facies H. The planar laminae grade uncommonly into asymmetric cross-ripples of 4 to 10 centimeter bed sets with occasional mud draped foresets (Figure 2-10).



Figure 2-9: Facies H, Planar Tabular to Trough Cross-stratified Sandstone and F to M Planar Laminated Sandstone. Image A: Planar Tabular to Trough Cross-stratified Sandstone from Llama Member at the E53 outcrop section. Hammer for scale is 25 cm long and the head is pointing down-section. Image B: Thin abraded lags of chert, shell debris, and phosphatic granules at outcrop section E53.

Interpretation: Several features of Facies H indicate deposition in a high energy environment. The monotypic *Skolithos* assemblage is representative of a high energy setting associated with an actively moving substrate (Howard and Frey, 1984; Frey and Pemberton, 1985; Caplan and Moslow, 1999). Planar tabular cross-stratification observed is interpreted to be the result of high flow velocities produced by migrating sand waves (Howard and Reineck, 1981). The trough cross-bed sets are interpreted to be preserved deposits resulting from bidirectional wave action and possibly longshore currents (Reinson, 1984; Thom et al., 1986). The highly abraded nature of the lag clasts is also indicative of deposition in a high energy setting (Willis and Moslow, 1994). Similar facies characteristics are described in lithologies in the Wembley Field of west central Alberta (Willis and Moslow, 1994). Willis and Moslow (1994) identify planar tabular and trough cross-bedding, separated by erosional surfaces marked by chert grain lags, to be the dominant sedimentary structures of a transgressive barrier island. The occurrence of slightly dipping planar laminae is interpreted to represent washover or swashzone deposition (Figure 2-10). The occurrence of asymmetric ripples is interpreted to be the result of a unidirectional current flow. The presence of mud drapes on the foresets may indicate a more quiescent waning flow or pooling, allowing for finer grained sediment to be deposited (Willis and Moslow, 1994) (Figure 2-10). Willis and Moslow (1994) similarly describe the presence of mud-draped ripple bed forms between washover events on a transgressive barrier island. Zonneveld et al., (1997), describes a similar facies in the Williston Lake area as an amalgamation of shoreface, foreshore and washover fan deposits.



Figure 2-10: Facies H, Planar Tabular to Trough Cross-stratified Sandstone and F to M Planar Laminated Sandstone. Image A: F to M Planar Laminated Sandstone Llama Member at the E53 outcrop section. Image B: The planar laminae grading into asymmetric cross-ripples with mud draped foresets at the E53 outcrop section.

Zonneveld et al., (1997) describes the facies to be strikingly similar to transgressive barrier island deposits described by Willis and Moslow (1994). In addition to this, a similar stratigraphic relationship is identified between the Wembley field and this study. Backbarrier facies in the Wembley Field are overlain by crypt-algal laminated anhydridic dolomite of tidal flat origin (Willis and Moslow, 1994). This is similar to Facies H overlain by the bindstone laminate (facies I) of this study. As the relationship to lateral facies is unknown, this precludes the interpretation of a tidal inlet despite similar facies characteristics as described in Willis and Moslow (1994). Facies H is therefore interpreted to be deposited in the upper shoreface with amalgamated washover or swashzone deposits.

2.3.9 FACIES I: BINDSTONE LAMINITE

Description: Facies I is comprised of a dolomitic siltstone and mudstone with very fine sandstone laminae. Facies I is grey on fresh surfaces and grey to tan on weathered surfaces. The sandstone laminae appear tan on both weathered and fresh surfaces. Bedding occurs in 5 to 10 centimeter beds, with a facies thickness ranging from 0.3 to 0.6 meters. Upper domal contacts are common and gradational lower contacts are present (Figure 2-11). Physical sedimentary structures are regularly spaced wavy to undulatory laminae with 3 to 10 millimeter vugs, fenestral fabric, and possible desiccation cracks. The vugs are commonly found to be arranged in horizontal rows, both filled and lined with calcite (Figure 2-11). Lithological accessories include void vugs, sulfurous odor,

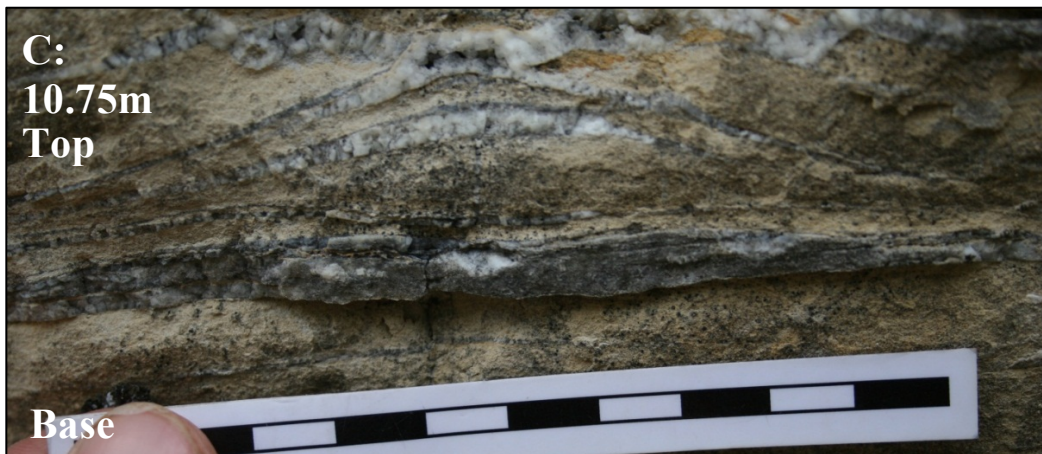
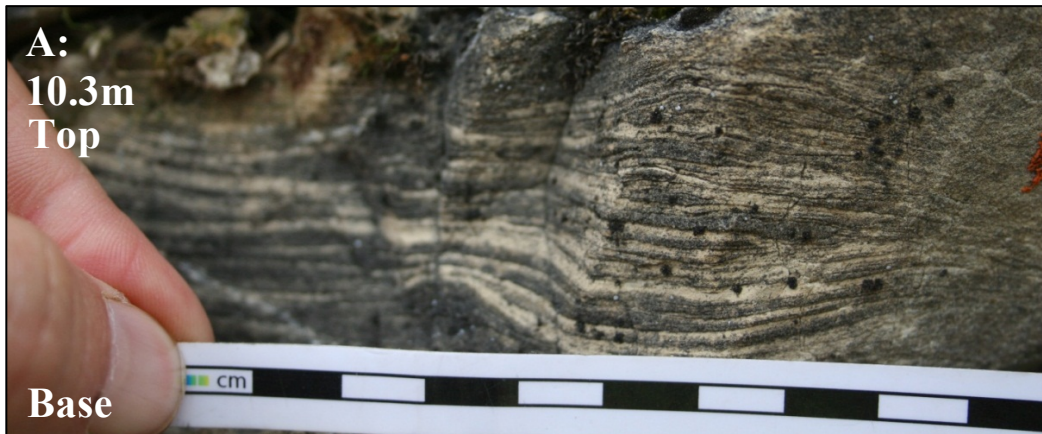


Figure 2-11: Facies I, Bindstone Laminate. Image A: Very fine sandstone laminae of the Bindstone Laminate of Facies I at the E53 outcrop section. Image B: Upper domal contacts of probable cyanobacterial laminae with 1cm scale bar sections. Image C: Vugs arranged in horizontal rows, both filled and lined with calcite at the E53 outcrop section.

and rare anhydrite.

Occasionally minor brecciation is observed within the facies, consisting of dolomitic siltstone clasts. Fossils present include rare gastropods and probable cyanobacterial laminae and laminar stromatolites. No trace fossils are observed in this unit. Facies I is commonly underlain by mudstone (Facies M), overlain by breccia (Facies J), and high-angle cross-stratified sandstone (Facies K).

Interpretation: The depositional environment is interpreted to be an arid supratidal to intertidal flat setting. The mudstone and siltstone is likely deposited during tidal flooding (Warren, 1989). The undulatory laminae, fenestral fabric, and dome structures are typical of cyanobacterial mats interspersed with sediment (Cadée, 1998). As sediment is deposited on cyanobacterial mats by flooding or possibly by wind blown sediment, the cyanobacterial mat establishes new layers on top of the sediment (Shinn, 1983; Hardie and Shinn, 1986). The development of the new layers on top of the sediment is interpreted to result in the vugs observed and overall regular undulatory lamellar appearance. Void vugs and minor brecciation is interpreted to be a result of the post depositional dissolution of evaporite minerals such as anhydrite and gypsum. Lagoons, intertidal, and supratidal settings are best suited for the formation of evaporite minerals and the preservation of such lithological features (Hagan and Logan, 1975). Lagoons are not a likely depositional setting for the facies, as the extent of evaporite mineral deposition is not as extensive as would be expected in such an environment.

Depositional analogs that result in the formation of similar facies are found in modern coastal settings of the Persian Gulf (Butler, 1969; Evans et al., 1969; Kendall and Skipwith, 1969; Purser, 1973; Butler et al., 1982; Warren and Kendall, 1985; Kendall et al., 2002; Alsharhan and Kendall, 2003).

2.3.10: FACIES J BRECCIA

Description: Commonly the matrix of the brecciated Facies J displays a mottled fabric, characterized by tan to grey surfaces (Figure 2-12). The brecciated clasts are usually white to tan in colour on both freshly exposed and weathered surfaces (Figure 2-12). The matrix supported, angular clasts, range in size from 0.5 to 20 centimeters. The thickness of the unit is measured to range between 0.5 to 4 meters. Facies J consists of generally gradational domed lower contacts, often due to the underlying bindstone laminate of Facies I and sharp upper contacts. The predominantly calcareous mud matrix consists of a mix of a dolomitic silty mudstone with both calcite filled and void vugs exhibiting a sulfurous odor. The matrix is less commonly observed to consist of calcareous sandstone. The composition of the brecciated clasts is typically representative of other regularly associated lithofacies. Commonly these clasts consist of dolomitic silty mudstone (Facies M) and sandstone (Facies L)(Figure 2-12). The rare occurrence of clasts composed of the bindstone laminate (Facies I) is also observed. The orientation of the brecciated clasts is random with a slight horizontal bias with respect to bedding. The dolomitic silty mudstone of Facies M and the high-angle cross-stratified sandstone of Facies L commonly overlie Facies J. No body fossils



Figure 2-12: Facies J, Breccia. Image A: Brecciated dolomitic silty mudstone clasts in a sandy mud matrix from the Starlight Evaporite Member at the E53 outcrop section. Image B: Sandstone clasts in a mudstone matrix from Starlight Evaporite Member at the E53 outcrop section.

or trace fossils are observed in this unit.

Interpretation: Facies J is interpreted to be a solution collapse breccia. Solution collapse breccia is formed through post-depositional solution excavation of readily soluble material such as evaporites (Clifton, 1967). The unsupported overlying ceiling rock subsequently collapse into the underlying void space, resulting in the formation of the brecciated clasts (Clifton, 1967). In similar facies, post-depositional solution excavation is interpreted to have occurred in outcrop strata following tectonic uplift, likely through meteoric ground water infiltration (Middleton, 1961; Clifton, 1967; Arnold, 1994).

Evaporite deposits such as gypsum and anhydrite are commonly formed in arid peritidal and supratidal (sabkha) depositional environments (Butler et al., 1982; Hardie and Shinn, 1986; Warren, 1989). The measured thickness of a solution collapse breccia unit is interpreted to be representative of the original thickness of the mineral or lithology subjected to solution excavation. The measured thickness of Facies J (0.5 to 4 meters) would require the dissolution of a similarly thick evaporite. Warren (1989) described the similar formation of thick evaporite deposits in lower supratidal settings. The original emplacement of anhydrite is therefore interpreted to have been in an arid supratidal setting. This is additionally supported by the composition of the brecciated clasts, interpreted to be of peritidal origin and interpreted facies associations. Several studies of the Triassic Whitehorse Formation and the lateral equivalent Charlie Lake Formation

have identified similar solution collapse breccia facies (Manko, 1960; Gibson, 1975; Arnold, 1994; Willis and Moslow, 1994; Young, 1997; Zonneveld et al., 1997; Caplan and Moslow, 1999; Dixon, 2005).

2.3.11 FACIES K: VF TO F CALCAREOUS SANDSTONE

Description: Facies K consist of very fine to fine calcareous sandstone with minor siltstone laminae. The well sorted grey to brown weathered surfaces of Facies K are also grey to brown on freshly uncovered surfaces. Bedding commonly ranges from 10-35 cm in the unit, with an overall measured thickness averaging 3-6m. Facies K is commonly sharply bounded by overlain facies L and M, and gradational underlain with Facies M. Physical sedimentary structures observed in this unit include low angle cross bedding, low angle laminae, and oscillatory ripples (Figure 2-13). The trace fossils observed in Facies K are limited to a monotypic assemblage of *Skolithos*. No body fossils were observed in Facies K.

Interpretation: The depositional setting of Facies K is highly dependent upon the relationship with the overlying and underlying facies. Zonneveld (2008) describes the identification of ephemeral lacustrine and supratidal facies based upon similar stratal relationships. The stratigraphic occurrence and presence of oscillatory ripples suggests deposition is above fair-weather wave base (Harms et al., 1982; Zonneveld, 2008). The deposition of Facies K below the silty mudstone of Facies M indicates deposition in a shoaling zone of a shallow marine

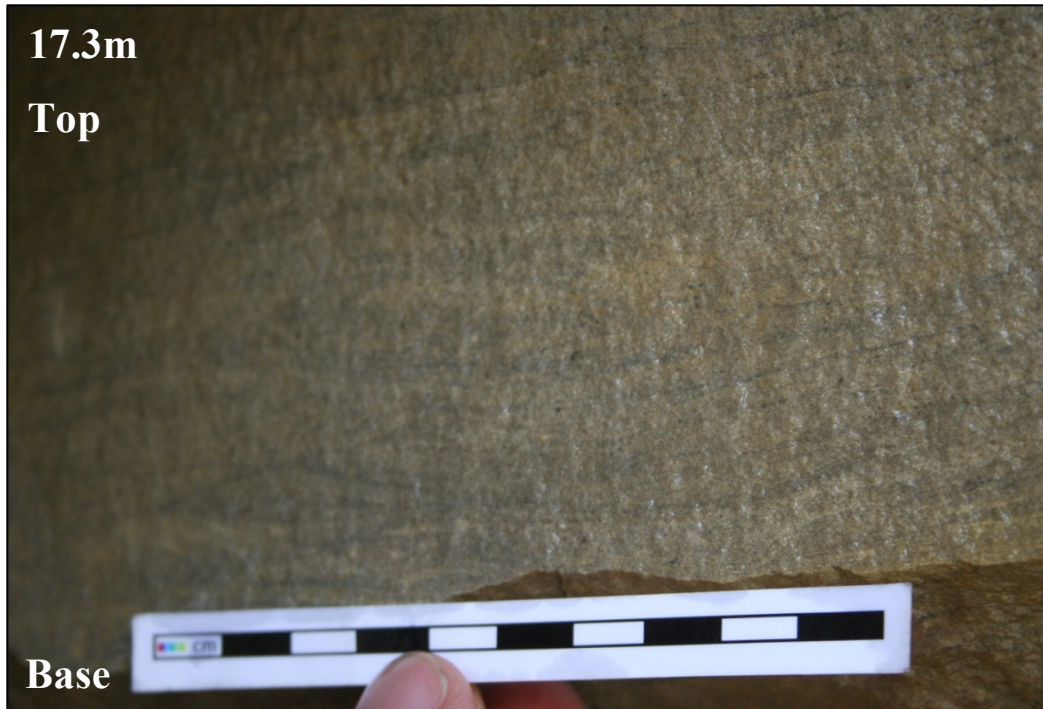


Figure 2-13: Facies K, VF to F Calcareous Sandstone. Image: Oscillatory ripples from the Starlight Evaporite Member at the E53 outcrop section. Scale bar for scale.

environment (Harms et al., 1982; Arnold, 1994). Von der Borch and Lock (1979) describe lacustrine facies that overlie marine and lagoonal carbonate sediments similar to Facies K in the Coorong region in Southern Australia.

The subaqueous occurrence of Facies K interbedded with aeolian Facies L suggests an interdunal ephemeral lacustrine setting (Pye and Tsoar, 1990; Arnold, 1994). Arnold (1994) and Fefchak (2011) identified comparable marine facies in interdunal settings and interpreted the deposition of the facies to be of lacustrine origin. Hummel and Kocurek (1984) described the formation of ephemeral lakes in shallow arid sabkhas following high tide or storm flooding. Aeolian dunes are interpreted to have prograded the interdunal lakes, resulting in the facies sequences observed at outcrops in the Willmore Wilderness Park (Kocurek, 1981; Ruegg, 1983; Hummel and Kocurek, 1984). Ephemeral lakes with similar stratal relationships and sedimentary features have been identified in supratidal settings in the Coorong region of Australia and in upper Triassic successions of the Williston Lake region of north eastern British Columbia (Von der Borch et al., 1975; von der Borch, 1976; von der Borch and Lock 1979; Arnold, 1994; Zonneveld, 2008; Fefchak, 2011). The deposition of Facies K is interpreted to be of shallow marine and lacustrine origin.

2.3.12 FACIES L: HIGH-ANGLE CROSS-STRATIFIED SANDSTONE

Description: Facies L consists of moderately well lithified and well sorted fine to medium grained sandstone, with an overall reddish orange colour. The upper and

lower bounding surfaces are observed to be sharp. The thickness of Facies L is observed to range from 2 to 6 meter. The regularly occurring bed-sets range in size from 10 to 100 centimeters. The primary physical sedimentary structures observed include: planar cross-stratification, tabular to wedge shaped cross-beds, horizontal to low-angle planar lamination, and structureless sand (Figure 2-14). Inversely graded laminae and laminae-sets tapered off up dip. Individual wedge shaped beds and bed-sets are on average dip 20 to 30 degrees. The cross-beds observed, gradually decrease in slope from low-angle to horizontal beds as surfaces are followed laterally (Figure 2-14). Lithological accessories are void vugs ranging from 1 to 3 centimeters. The change in dip occurs over a horizontal distance of 4 to 5 meters on average. No biogenic sedimentary structures or body fossils are observed in Facies L.

Interpretation: The depositional environment of Facies L is interpreted to be in an arid peritidal to supratidal sabkha environment. Several laterally equivalent intervals within the Charlie Lake Formation exhibit aeolian sedimentary characteristics (Higgs, 1990; Arnold, 1994; Zonneveld and Gingras, 2002; Zonneveld et al., 2004; Fefchak, 2011). The high-angle cross-stratified sandstone facies display a lack of marine indicators such as bioturbation and marine body fossils. Biostratigraphic analysis also revealed no conodont samples or other marine indicators such as ichthyoliths. High-angle cross-stratified sandstone is common and distinctive of aeolian facies (Hunter, 1977; Higgs, 1990; Arnold, 1994; Zonneveld and Gingras, 2002; Zonneveld et al., 2004; Fefchak, 2011).



Figure 2-14: Facies L, High-Angle Cross-stratified Sandstone. Image A: High-Angle Cross-stratified Sandstone from the Starlight Evaporite Member at the E53 outcrop section. Hammer for scale is 25 cm long and the head is pointing down-section. Image B: Fine to medium grained sandstone displaying discontinuous laminae that are interpreted to be grainfall strata.

The well sorted fine to medium sized sandstone, displays discontinuous laminae that are interpreted to be grainfall laminae.

Grainfall laminae are produced on the mid-lee slope of dunes where avalanching occurs (Hunter, 1977; 1981; Fryberg and Schenk, 1988; Brookfield, 1992; Pye and Tsor, 1990). When grainfall strata on the lee side of a dune crest exceeds the angle of repose, an erosive sand flow deposit will be created (Pye and Tsor, 1990; Brookfield, 1992). The interpreted sandflow deposit, as observed in this study and others, is interbedded with grainfall sediment (Pye and Tsor, 1990; Brookfield, 1992). The occurrence of inversely graded laminae in Facies J is a strong indicator of aeolian deposition (Hunter 1977; 1981; 1990). Inverse graded planar to low-angle laminae are interpreted to be deposited in an interdunal setting (Fryberger et al., 1979; Hunter, 1990). The preservation space must have been sufficient for the rarely preserved facies to have survived the weathering and erosional processes that commonly destroy such features.

2.3.13 FACIES M: DOLOMITIC SILTY MUDSTONE

Description: The dolomitic silty mudstone of Facies M is weathered grey to tan with grey fresh surfaces. The unit is greatly variable in measured thickness, from 0.5 to 10 meters. Occasionally bedding is observed to be defined by thin sand laminae. The contacts of Facies M are variable dependent upon the facies that bound the unit. The upper contact of Facies M is gradational when associated with the commonly overlying bindstone laminite (facies I). The lower contact of

Facies M is commonly erosional when found to overlie the high-angle cross-stratified sandstone (Facies L). The dolomitic silty mudstone is occasionally sandy when underlain by Facies L. The lower contact with the brecciated Facies J is often difficult to recognize, yet where observed appears sharp. With the exception of rare sand laminae, the dolomitic silty mudstone is massive in appearance and lacks sedimentary structures (Figure 2-15). Lithological accessories include vertical and horizontal fractures with possible pressure dissolution features. Sporadically distributed and moderately common void vugs, ranging in size from 2 mm to 5 cm are observed. Trace fossils observed includes probable cryptic bioturbation and locally abundant *Rosselia socialis*. Bivalve and brachiopod shell material is observed within Facies M, but in low abundance through out the unit.

Interpretation: Facies M is interpreted to have been deposited in a quiescent environment, such as the protected areas of a subtidal lagoon or intertidal setting. The massive appearance of the dolomitic silty mudstone is interpreted to have been the result of extensive bioturbation (Hardie and Shinn, 1986). Stratigraphic positioning and lithological character is primarily used for interpreting the environment of deposition of the unit. Facies M is commonly associated with facies K, I, L, and J. As the dolomitic silty mudstone is commonly gradationally overlain by bindstone laminate, this leads to the interpretation of deposition the in the subtidal to intertidal zone. The presence of bivalve and brachiopod shell



Figure 2-15: Facies M, Dolomitic Silty Mudstone. Image A: The dolomitic silty mudstone is massive in appearance in this photo that displays the vertical and horizontal fractures with possible pressure dissolution features. This sample is from the Starlight Evaporite Member at the E53 outcrop section. Scale bar for scale. Image B: Trace fossil *Rosselia socialis* at the E53 outcrop section

material also indicates marine conditions. Deposition from suspension is consistent with the sedimentary structure and lithology observed in Facies L. In the Coorong region of southern Australia, dolomitic mudstone is recognized to occur in similar peritidal sequences (Von Der Borch et al., 1979, Warren, 1988). Similar sequences have also been identified in coastal environments of Abu Dhabi (Evans et al., 1969). The lack of biogenic sedimentary structures may reflect increased stress in an environment of mixed siliciclastic carbonate deposition and is consistent with other interpreted Triassic subtidal to intertidal settings (Arnold, 1994; Zonneveld et al., 2004). *Rosselia socialis* is the most highly distributed trace observed in this unit (Figure 2-15). *Rosselia socialis* is an indicator of stressed environmental conditions such as areas of fluctuating salinity (Pemberton personal communication, 2008).

2.3.14 FACIES N CONTORTED SANDSTONE

Description: The well sorted fine to medium grained sandstone of Facies N, appears yellow-orange on both weathered and fresh surfaces. Medium grains are occasionally observed to be suspended along parallel laminae in a matrix of well rounded finer grained sand. Distinctive post-depositional folding is observed in Facies N (Figure 2-16). The folding is characterized by units 1.5 to 2.4 meters thick (Figure 2-16). The folding of the sandstone is irregular, slightly overturned in some sections, and completely contorted in others (Figure 2-16). Internal bedding is found to range from 10 to 50 centimeters. The lower most contact is found to be gradational with the high-angle cross-stratified sandstone of Facies L.



Figure 2-16: Facies N, Contorted Sandstone. Image A: The yellow-orange weathered Contorted Sandstone of the Starlight Evaporite Member at the E53 outcrop section. Hammer for scale is 25 cm long and the head is pointing down-section. Image B: Contorted nature of the sandstone of Facies A with gradational lower contact at the E53 outcrop section. Field assistant for scale.

The upper contact is sharp and commonly overlain by the dolomitic silty mudstone of Facies M. Sedimentary structures within the contorted sandstone appear similar to Facies L including: planar cross-stratification, tabular to wedge shaped cross-beds, horizontal to low- angle planar lamination, and inversely graded laminae. The high-angle cross- stratification is observed with laminae sets that pinch out. No trace fossils or body fossils are detected within Facies N.

Interpretation: The distinctive sedimentary features, textures, and facies associations of Facies N reflect characteristics of deposition in an aeolian setting. Aeolian characteristic in other studies and of Facies N include in part: well sorted and well rounded grains, an absence of detrital micas, probable deflation lag of coarser sediment in a finer matrix, and a facies association with arid continental climatic indicators (Arnold, 1994; Davies, 1997b). In addition to this, the high-angle cross-stratification observed is interpreted to be formed as a result of grain deposition on the steep lee side of a sand dune. Such grain fall laminae and sandflow features provide strong evidence of aeolian deposition (Hunter, 1981, Fryberger, 1992). The gradational association of Facies N with the aeolian Facies L suggests the facies are depositionally related. Arnold (1994) interpreted a similar facies association of contorted sandstone and aeolian facies in the Williston Lake region of northeastern British Columbia. The contorted sandstone of the laterally equivalent facies of the Charlie Lake Formation is interpreted to be the result of post-depositional alteration (Arnold, 1994). The alteration is opined to be attributed to the partial preservation and limited reworking of dunes from a

rapid transgression (Glennie and Buller, 1983, Arnold, 1994). However, the presence of fractures suggests that the contorted sandstone is a result of tectonic forces. The common occurrence of the overlying Facies M is consistent with deposition in a transgressive system as discussed in a subsequent section (facies associations).

2.3.15 FACIES O: CALCAREOUS BIOCLASTIC WACKESTONE/PACKSTONE

Description: Facies O consists of a calcareous bioclastic wackestone to packstone. The resistive cliff forming facies is grey on both freshly exposed and weathered surfaces. Upper and lower contacts are not observed in Facies O due to cover and erosional truncation. The thickness of Facies O is measured to be 11.5 meters. Bedding is obscure, but discernable averaging 1 to 10 centimeters with sharp bases and normally graded. Sedimentary structures are largely unobserved with the exception of parallel planar laminae (Figure 2-17). An abundance of body fossils are observed in this unit that include: abraded and fragmented crinoid ossicles, fragmented bivalves and brachiopods, and unidentified shell debris (Figure 2-17). The average diameter of a crinoid ossicle in Facies O is 2.5 millimeters. Biogenic sedimentary are not observed in Facies O. A highly distinctive feature of Facies O is the presence of large chert clasts (Figure 2-17).

Interpretation: Features observed in Facies O such as normal grading, parallel



Figure 2-17: Facies O, Calcareous Bioclastic Wackestone/Packstone. Image A: The yellow-orange weathered Contorted Sandstone of the Brewster Limestone Member at the Blue Grouse Brewster outcrop section. Hammer for scale is 25 cm long and the head is pointing down-section. Image B: Large chert nodule at the Cody Found Horse outcrop section. Image C: Crinoid ossicles and bioclastic material within Facies O at the Blue Grouse Brewster outcrop section.

laminae, and chert is in part suggestive of deposition by turbidity currents.

Calcareous turbidites are typically challenging to identify as internal sedimentary structures are commonly difficult to distinguish (Eberli, 1991a, b). Calcareous turbidites exhibit grading, plane parallel laminae, Bouma type sequences, lateral continuity, unidirectional sole marks, load casting, and chert nodules (Eberli, 1987; Eberli, 1991; Einsele and Seilacher, 1991; Zonneveld, et al., 1997). Gibson (1972) describes the resistive cliff forming bioclastic Brewster Member to contain chert lenses up to 6 inches long. The largest chert clast in this study is measured at 30 cm in length with a 3-4cm variable diameter (Figure 2-17).

Chert nodules observed within Facies O are a microcrystalline or cryptocrystalline sedimentary rock (Malvia and Siever, 1989). Nodular chertification is identified to occur in limestone through the replacement of carbonate material by microcrystalline quartz (Malvia and Siever, 1989; McBride et al., 2006). Silica is precipitated in low (pH) settings with silica concentrations greater than 100 ppm (Blatt, et al., 1980). One potential primary source of silica is from biogenic siliceous spicules, diatoms, and radiolarians. The silica of chert nodules formed in calcareous turbidites has been interpreted to be sourced from the siliceous material transported in the gravity driven sediment from shallow to deep marine settings (Eberli 1991a, b; Haak and Schlager 1989).

Alternatively, aeolian dust-size particles (less than 60 microns) are cited as a potential primary source of SiO₂ (Cecil, 2004). The amorphous silica surface

layer on abraded quartz dust particles is identified to be highly soluble in comparison to structured quartz (Cecil, 2004). The amorphous layer is also interpreted to be volumetrically significant due to the large surface area of the small grains (Cecil, 2004). Malvia and Siever (1989) have determined that heterogeneities in sediment can promote the nucleation of chert nodules. These heterogeneities may be a result of organic matter content, porosity, and biogenic silica concentrations (Malvia and Siever, 1989). The deposition of dust-size particles would require a setting of limited wave reworking such as an offshore setting below mean storm wave base. The calcareous bioclastic Facies O contains many similarities to the Brewster Limestone Member as described by Gibson (1972, 1975). Gibson, (1993), identifies similar lateral equivalent facies in the Ludington and Baldonnel formations to be an amalgamation of fragmented and abraded bivalves, brachiopods, and echinoderms deposited in deep-water distal shelf/upper slope settings. These factors lead to the interpretation that Facies O was deposited in an offshore setting by turbidity currents.

2.4 FACIES ASSOCIATIONS

Triassic strata in the study area are divided into four environmental/depositional subdivisions. These facies associations improve the interpretation of the unique individual facies depositional environments. This is accomplished by the comparison of individual facies within a framework of recurring vertical successions of genetically related facies or facies associations (Gingras et al., 1998). This comparison thereby constrains the probability of facies interpretation

to a more likely depositional setting. According to Gingras et al., (1998) facies associations are useful for characterization of the depositional system, but are not free from perturbations of the facies succession due to local variability and heterogeneities within the depositional environment. Therefore, the application of Wather's Law within a facies association provides a more accurate assessment of depositional environments (Gingras et al., 1998).

2.4.1 FACIES ASSOCIATION 1

Facies Association 1 (FA1) is interpreted to be deposited in an open marine, distal offshore transition to distal lower shoreface setting (*sensu* Burchette and Wright, 1992). FA1 consists of two lithofacies (Facies A and Facies B; Table 2-1).

Facies A is described as being deposited in a distal offshore transition to offshore transition zone. The finely laminated siltstone beds with rare higher energy structures are consistent with deposition above mean storm wave base. Facies A is gradationally overlain by Facies B. Facies B contains deposits closely related to Facies A, representative of deposition in an offshore transition to distal lower shoreface. The planar laminae, coarser nature, and abundance of higher energy structures reflect storm dominated deposition passing into the lower shoreface.

The upper contact of Facies B and FA1 is disconformable and interpreted to be a transgressive surface of erosion resulting from a major flooding event. FA1 is interpreted to be deposited in a prograding distal offshore transition to distal lower depositional system above mean storm wave base to just above mean fair weather

wave base. Gibson and Edwards (1990a) similarly identify laterally equivalent facies of the Grayling, Toad, and Montney formations to be deposited in an open marine distal shelf environment. Edwards (1994), describes the Montney Formation in northeastern British Columbia as deposited on a westward prograding shelf on the paleocontinental margin. This interpretation is consistent with observations of the Vega/Phroso Siltstone Member within FA1.

2.4.2 FACIES ASSOCIATION 2

Facies Association 2 (FA2) consists of facies reflecting deposition in a coarsening upwards, progradational, mixed siliciclastic carbonate, offshore to shoreface succession. FA2 consists of five facies (C, D, E, F, G, and H). Facies C (Black Shale) and Facies D (Muddy Siltstone) are gradational and described as an offshore to shoreface transition zone. It is common for such tranquil depositional environments to display planar laminae deposited from suspension (Boreen and James, 1995). Characteristics of the organic rich Facies C include: planar laminae, very fine sand laminae, unfossiliferous, a lack of observed trace fossils, and a very high gamma signature. The characteristic high organic content and lack of biogenic sedimentary structures in Facies C is consistent with anoxic environments located in proximal to distal offshore environments (Zonneveld et al., 2004). The gamma ray signature of Facies D is decreased with respect to facies C, yet remains relatively high in comparison to all other facies of this study. The bedding of Facies D reveals disrupted planar laminae, interpreted to represent a cryptically bioturbated zone. The cryptically bioturbated appearance of the

finely laminated lithology is consistent with deposition in an open marine sequence (Pemberton and Frey, 1984). Facies D is gradationally overlain by very fine dolomitic silty sandstone of Facies E, very fine calcareous sandstone of facies F, and interbedded very fine to fine sandstone and silty sandstone of Facies G.

Facies E, F, G, and H reflect the deposition of a well sorted, coarsening upward succession, in a proximal offshore transition to lower shoreface setting. Facies E, F, G, and H display higher energy sedimentary structures such as symmetric ripples, trough cross-bedding, and hummocky cross stratification. Hummocky cross stratification is described to be the result of storm combined flows, commonly preserved in the offshore transition and lower shoreface (Hamblin and Walker, 1979; Harms, 1979; Duke, 1985; 1990; Duke et al., 1991). Fossil material is found to be a low diversity assemblage of bivalves, brachiopods, and crinoids. Body fossils observed in this facies association commonly exhibit evidence of abrasion, fragmentation, and are interpreted to be transport to the site of deposition. Sharp-based beds with entrained bioclastic material and mudclasts are interpreted to be tempestites. Such units are often observed in mid-ramp successions (Aigner, 1985; Keller, 1997; Hips, 1998). Trace fossils identified include an assemblage of moderate diversity and distribution including: *Phycosiphon*, *Thalassinoides*, *Skolithos*, *Planolites*, and *Rosselia*. The dwelling and feeding traces commonly occur in the offshore transition to lower shoreface. FA2 is observed overlie FA1 and typically underlies Facies Association 3 (FA3).

A black shale facies (interpreted to be Facies C of this study) is described by Manko (1960), in the Willmore Wilderness Park as being traced laterally northwestward into the Peace River region, particularly into the Peace River subsurface. Gibson (1974) describes a similar phosphate rich Whistler Member to extend southward into the Spray River gorge near Banff. Davies (1997a) identifies the base of the Doig Formation to be marked by phosphatic black shale with a characteristic high gamma-log profile, referred to as the phosphatic zone. The phosphatic zone of the Doig Formation is equivalent to the Whistler Member of the Sulphur Mountain Formation in outcrop (Gibson, 1974, 1975). Ibrahimbas and Riediger (2004) identify the total organic carbon (TOC) values of the phosphatic zone to range from 1.76 wt% to 10.98 wt% with HI values of 189-489 mg HC/g TOC. This indicates an excellent source rock potential (Ibrahimbas and Riediger, 2004).

The remaining facies of the conformable FA2 are interpreted to represent a progradational shoreface sandstone and siltstone succession of the Llama Member of the Sulphur Mountain Formation and laterally equivalent Halfway and Doig formations (Davies, 1997a). The lateral correlation and distinction of Halfway Formation from the Doig Formation is determined to be indistinguishable in FA2. The contact of the Llama Member is placed where the sandstone and siltstone grade upward or is sharply overlain by the yellow weather sandstone, silty dolostone and pelecypod coquinas of the Starlight Evaporite Member of the

Whitehorse Formation (Gibson, 1975). This boundary is recognized at the E53 outcrop where FA3 overlies FA2.

2.4.3 FACIES ASSOCIATION 3

Facies Association 3 (FA3) consists of variable facies deposited in peritidal, ephemeral lacustrine, and supratidal settings. FA3 consists of lithofacies I (bindstone laminate), J (breccia), K (very fine to fine calcareous sandstone), and M (dolomitic silty mudstone). Facies I consists of bindstone laminate (probable cyanobacterial laminate) with a common fenestral fabric, undulatory laminae and rare gastropods. Domal upper contacts are regularly observed when commonly conformably overlain by the breccia of Facies J. Facies I is frequently conformably underlain by the dolomitic silty mudstone Facies M, and occasional very fine to fine calcareous sandstone Facies K. The arid modern day Persian Gulf is thought to provide an analogous depositional setting to the one that formed Facies I. Arid coastlines of the Persian Gulf exhibit cyanobacterial mats on intertidal flats and in supratidal zones (Kendall and Skipwith 1969; James and Kendall, 1992). Body fossils observed in association with the interpreted cyanobacterial laminate are likely grazing gastropods. Rare gastropod body casts have also been recognized in similar bindstone laminate facies in north-eastern British Columbia (Zonneveld et al., 2001).

Facies J consists of matrix supported chaotically brecciated clasts of facies I, M and occasionally aeolian lithologies of Facies Association 4. Facies J is

interpreted to be a solution collapse breccia and not a depositional lithofacies as it is construed to have formed from post-depositional dissolution. Facies J is most commonly observed to be overlying intertidal and subtidal successions, therefore likely to be deposited in a near shore supratidal sabkha setting. Similar solution collapse breccia have been described from the Charlie Lake Formation and interpreted to be deposited in a shore proximal supratidal flat/sabkha succession (Zonneveld, et al., 2004; Fefchak, 2011). Periodic flooding of supratidal environments is interpreted to result in the reoccurring peritidal succession of facies M, I, and J.

Facies K consists of a very fine to fine calcareous sandstone with ripple laminae and a limited monotypic assemblage of rare *Skolithos*. Facies K is observed to be deposited at the boundary where FA3 overlies Facies Association 4 (FA4). Facies K is observed to be commonly deposited below facies M and L bounded by both sharp and gradational contacts. Facies K is interpreted to be deposited in a shallow marine to interdunal ephemeral lake setting.

Facies M consists of dolomitic silty mudstone with common sharp lower contacts and gradational upper contacts. Mud rich sediment is common in intertidal environments as they are largely protected by back barrier islands or reef complexes (James and Kendall, 1992). The lack of burrowing organisms and other diagnostic criteria of Facies M, leads to difficulties in defining the boundaries between intertidal flats and supratidal environments. Therefore

depositional interpretations rely heavily on assessing relationships with adjacent facies and facies associations. Facies M is commonly overlain by the bindstone laminate of Facies I followed by the breccia of Facies J. The dolomitic silty mudstone of Facies M and associated facies are interpreted to occur in arid supratidal settings such as modern setting in the Coorong region of Australia (Von Der Borch et al., 1975). Lake sediments in the Coorong region overlie marine and lagoon sediments (Von Der Borch and Lock, 1979). FA3 is observed to be underlain by FA2 and overlain and underlain by FA4. FA4 regularly appears to conformably overlie FA3. FA4 is occasionally observed to be vertically delayed in some outcrop sections where lithofacies M and K, are seen interbedded with Facies I.

2.4.4 FACIES ASSOCIATION 4

Facies Association 4 (FA4) represents two related facies of aeolian and transgressed aeolian sandstone deposited in a near shoreline supratidal sabkha setting. FA4 consists of high-angle cross-stratified sandstone of lithofacies L and contorted sandstone of lithofacies N. Facies L consists of well sorted fine to medium grained sandstone characterized by high-angle cross-stratification, tabular to wedge shaped cross-beds, and horizontal to low-angle planar lamination. The high-angle cross-stratified sandstone is commonly observed in aeolian settings (Hunter, 1977; 1981; 1990). Ancient examples of the high-angle cross-stratified sandstone exhibit features such as grainfall sediment, high-angle cross-beds, and frosted grains. Pedogenetically altered soil is also a common

feature of arid terrestrial environments. Where observed Facies L is gradational with Facies N and sharply underlain and overlain by FA3. Facies N consists of similar lithological features as in Facies L, with the exception of a distinct contorted appearance. The contorted sandstone of Facies N is likely the result of the expulsion of air during the initial stages of transgression (Glennie and Buller, 1983). As the sand settles, more sediment is overlain, and the air migrates upward creating the contorted appearance (Glennie and Buller, 1983). Facies N is always gradationally underlain by Facies L and is commonly sharply overlain by FA3. Trace fossils and body fossils are not observed in this facies association.

The sequence observed in FA4 is deposited in an arid environment not unlike that of the modern Namibian coastal region of Africa (Krapf, 2003). The Namibian coastline is subject to the influence of an erg desert system in the proximal sabkha. This region is the source of both annual wind sediment transportation and rare events of mass river transport. Both elements are capable of dramatically transferring large quantities of sediment. However, each mechanism of transport does so in alternate temporal scales. Wind transport moves less sediment in a shorter time period but in appreciable abundance over large periods of time. Massive rainfall events are capable of transporting enormous quantities of sediment in a very short period of time (Krapf, 2003). The facies association is significant as it marks the end of the shallowing upward shallow marine succession and the beginning of the terrestrial sequence of the Whitehorse

Formation. The terrestrial sequence FA4 is observed in two of the six outcrops studied and is variable in its occurrence with other facies associations.

2.4.5 FACIES ASSOCIATION 5

Facies Association 5 (FA5) is interpreted to have been deposited in an open marine offshore setting. FA5 consists of a single facies comprised of a calcareous bioclastic wackestone/packstone (Facies O). Facies O is fossiliferous with abundant abraded and fragmented crinoid ossicles, fragmented bivalves and brachiopods, and unidentified shell debris. FA5 is observed to overlie FA4. Despite the observation of FA5 at three outcrop sections, the upper and lower contacts were not observed due to cover and erosional truncation. (Gibson, 1972) designated similar facies to be depositional facies of the Brewster Limestone Member of the Whitehorse Formation. Zonneveld et al., (2004) identified similar facies of the Baldonnel Formation to be deposited in an outer ramp succession deposited below storm wave-base. The characteristic finely laminated beds with discernible scour/erosional surfaces are interpreted to be consistent with storm initiated, bioclastic, turbidite beds (Zonneveld et al., 2004).

2.5 DISCUSSION

The studied Triassic lithologies described within the Willmore Wilderness Park of west-central Alberta comprise five broadly defined facies associations depicted in a schematic representation (Figure 2-18). The facies and facies associations can be related through changes in sediment flux, sea-level change, and preservation or utilization of accommodation space. The volume and rate of sediment flux as

well as the interplay of rate of increase in accommodation space plays a key role in the resultant depositional environment and related facies associations (Van Wagoner et al., 1988). Facies associations and depositional environments in this study are commonly interpreted to transition primarily where these factors result in major alterations in sediment accumulation or bypass.

Factors such as tectonic subsidence and climate change can result in the increase or decrease in sediment flux and accommodation space (Perlmutter and Matthews, 1990). In this study, alterations in such factors are identified to result in depositional environments ranging from offshore deposits (facies association 1), offshore to shoreface (Facies Association 2), ephemeral/lacustrine supratidal (Facies Association 3), aeolian sabkha (Facies Association 4), and offshore turbidite deposits (Facies Association 5).

Schematic Lateral Distribution of Facies

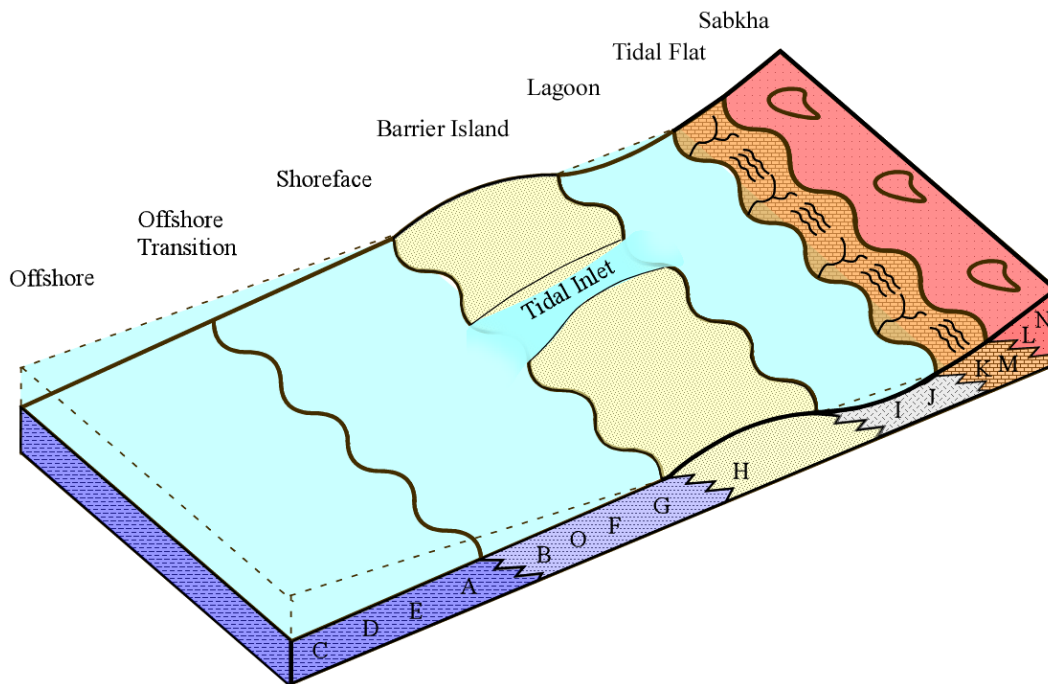


Figure 2-18: Highly schematic three-dimensional depositional model illustrating lateral distribution of facies. Interpreted depositional environments are illustrated and consist of Facies Association 1 offshore deposits (facies A and B), Facies Association 2 offshore to shoreface deposits (facies C, D, E, F, G and H), Facies Association 3 ephemeral/lacustrine supratidal (facies I, J, K, and M), Facies Association 4 aeolian sabkha (facies L and N), and Facies Association 5 offshore turbidite deposits (Facies O). The complete distribution of facies and associated depositional environments are presented in Tables 2-1, 2-2, and 2-3.

The progradation of Facies B over Facies A of Facies Association 1 indicates a gradual rate of increase in the amount of sediment input, relative sea-level fall, or increase in accommodation space. This is identified by the minimal and gradual vertical increase in bed thickness of the facies comprising Facies Association 1. The transition from Facies Association 1 to Facies Association 2 is seemingly abrupt identified by a pronounced lithological change. This is indicative of a potential combination of a rapid increase in sea-level, decrease in localized sedimentation rate and sediment bypass. Facies Association 2 is described as being deposited in offshore to shoreface environments. The development of the overall progradational succession is marked by distinct periods of increased sediment accumulation such as the shoreface facies F, G, and H. Further study is recommend to elucidate the potential of tectonic and climate factors relating to changes in sediment flux and accommodation space.

The transition from Facies Association 2 to Facies Association 3 is progradational in nature and implies a relative increase in sediment accumulation. This is also observed in the transition of Facies Association 3 to Facies Association 4. The progradational succession is recognized by the progressive faces that change systematically up-section. This can relate to an increase in sediment supply or rate and a change in positive accommodation space. Most of the facies contacts are described as gradational and are interpreted to relate to a prolonged period of consistent increase in sediment input, sea level change, and accommodation

space. The differential degree of affect of these factors on sediment accumulation is unknown at this point and recommended for future study.

The unobserved upper and lower contacts of Facies Association 5 and limited occurrence render the determination of the relationship to other facies association speculative. One of the main problems identified in this study is the significance afforded to sharp contacts. The sharp contacts may be sedimentological in nature or a result of changes in depositional environments. The largely coarse resolution of this study did not allowed for detailed description subenvironments therefore the interpretations of sharp contacts are considered tenuous.

CHAPTER THREE

3.1 INTRODUCTION

In this section results and interpretations of biostratigraphy and chemostratigraphy analyses are presented. These interpretations are combined with lithofacies analyses from chapter 2 to create comprehensive log correlations between five outcrop sections in the Willmore Wilderness Park study area. The log correlations are then analyzed to create a stratigraphic framework based upon sequence stratigraphic methodology. The tectonic eustatic implications of the stratigraphic framework are then outlined and discussed.

3.2 BIOSTRATIGRAPHY RESULTS

Thirty three samples were collected from six outcrop sections and submitted by the author for conodont analysis at the Geological Survey of Canada (Pacific). Ten of the samples were found to be barren and twenty three productive samples were identified in the Geological Survey of Canada report No.010-MJO-2009 (Orchard, 2009). Of the twenty three productive samples one was omitted (Curation No.: V-000366) due to possible contamination and three other samples (Curation No: V-000362, V-000363, V-000364) were omitted as the outcrop section was not included for description in this study (outcrop west Blue Grouse). The results of the remaining samples analyzed are identified with respect to age interpretation, associated facies, and identified specimens in Table 3-1 and Table 3-2.

3.3 BIOSTRATIGRAPHY INTERPRETATIONS

GSC Curation No.	Geography Lat/Long NAD83	Interval Above Base of Section (m)	Specimen	Age Interpretation	CAI	Facies
V-000350	53.3317° N 118.5622° W	MC-0	- <i>Neogondolella</i> ex. gr. <i>constricta</i> -Fish ichthyolith -Microgastropod	Middle Triassic	3-4	F
V-000352	53.3317° N 118.5622° W	MC-6.0	- <i>Neogondolella</i> sp. -Fish ichthyolith -Microbivalve -Microgastropod	Phanerozoic	3-4	F
V-000357	53.3317° N 118.5622° W	MC-23.9	-Microgastropod	Phanerozoic	N/A	G
V-000358	53.3317° N 118.5622° W	MC-30.65	-Echinoderm -Microgastropod	Phanerozoic	N/A	G
V-000354	53.3317° N 118.5622° W	MC-104.2	-Fish ichthyolith	Phanerozoic	N/A	M
V-000359	53.3317° N 118.5622° W	MC-259	- <i>Misikella longidentata</i> -Echinoderm -Fish ichthyolith -Microbivalve -Microgastropod	Late Triassic Carnian	2-3	O
V-000365	53.291° N 118.3816° W	E53-0.75	-Fish ichthyolith	Phanerozoic	N/A	G
V-000367	53.291° N 118.3816° W	E53-24.75	-Fish ichthyolith	Phanerozoic	N/A	K
V-000368	53.291° N 118.3816° W	E53-29.0	-Fish ichthyolith	Phanerozoic	N/A	M
V-000370	53.291° N 118.3816° W	E53-39.4	-Foraminiferid -Microgastropod	Phanerozoic	N/A	M
V-000346	53.2837° N 118.4137° W	PC-19.5	- <i>Neogondolella</i> ex. gr. <i>constricta</i> -Fish ichthyolith -Microgastropod	Late Anisian - Early Ladinian	2-3	A

Table 3-1: Biostratigraphy results A. Geological Survey of Canada report results on 23 productive Conodont and microfossil samples submitted for analysis from the Mount Robson map area (83 E/07, /08) British Columbia. Barren and contaminated samples not included in the table; CAI, conodont alteration index; N/A, not applicable; Outcrop original nomenclature AC modified to MC from Report No.010-MJO-2009; Source: Michael Orchard, 2009: Report No.010-MJO-2009.

GSC Curation No.	Geography Lat/Long NAD83	Interval Above Base of Section (m)	Specimen	Age Interpretation	CAI	Facies
V-000342	53.2837° N 118.4137° W	PC-70.5	-? <i>Neogondolella</i> ex. gr. <i>constricta</i> -Fish ichthyolith -Microgastropod	Middle Triassic	3-4	C
V-000344	53.2837° N 118.4137° W	PC-118	- <i>Neogondolella</i> ex. gr. <i>constricta</i> -Echinoderm -Fish ichthyolith - Microgastropod	Late Anisian - Early Ladinian	2-3	F
V-000343	53.2837° N 118.4137° W	PC-124	-? <i>Neogondolella</i> ex. gr. <i>constricta</i> -Fish ichthyolith -Microgastropod	Middle Triassic	3	G
V-000341	53.2837° N 118.4137° W	PC-126.5	- <i>Neogondolella?</i> sp. -Fish ichthyoliths (Specimens appear abraded)	Triassic	3-4	G
V-000345	53.2837° N 118.4137° W	PC-130	-? <i>Neogondolella</i> ex. gr. <i>constricta</i>	Middle Triassic	2.5-3.5	G
V-000371	53.3409° N 118.5754° W	BGB-4.6	-Fish ichthyoliths -Microgastropod	Triassic	3	O
V-000372	53.3409° N 118.5754° W	BGB-11.6	-Fish ichthyoliths -Microgastropod	Triassic	4	O
V-000347	53.3015° N 118.3754° W	CFH-0.5	- <i>Neogondolella</i> ex. gr. <i>Constricta</i> -Fish ichthyoliths -Microgastropod	Ladinian	3-4	F

Table 3-2: Biostratigraphy results B. Geological Survey of Canada report results on 23 productive Conodont and microfossil samples submitted for analysis from the Mount Robson map area (83 E/07, /08) British Columbia. Barren, sections not described, and contaminated samples not included in the table; CAI, conodont alteration index; ND, not described; N/A, not applicable; 1WBG modified to BGB from Report No.010-MJO-2009; Source: Michael Orchard, 2009: Report No.010-MJO-2009.

Biostratigraphic subdivision of the Triassic succession of western Canada has been established by a lineage of Geological Survey of Canada paleontologists starting with F.H. McLearn (1917-1945) and continued by E.T. Tozer (1958-2010) and M.J. Orchard to present. The detailed study of conodonts results in the formation of a temporal framework for stratigraphic study (Tozer, 1967; 1994; Orchard and Tozer, 1997). Ammonoids and conodonts are often intercalibrated with ammonoid zonation as they are often found in similar successions in the fossil record (Mosher, 1973; Tozer, 1984; Orchard, 1983, 1991b; Orchard and Tozer, 1997, Orchard and Zonneveld, 2009). In addition to conodonts, other fossil remains such as fish ichthyoliths, microgastropods, echinoderms, and microbivalves are identified during the analysis of conodont samples that provide further support for depositional and stratigraphic interpretations (Johns et al., 1997).

Six samples collected from different intervals at the Poupanee Chute (PC) outcrop produced identifiable specimens (PC 19.5m, PC 70.5m, PC 118m, PC 124m, PC126.5m, and PC 130). The PC 19.5m sample produced conodont *Neogondolella* ex gr. *constricta*, fish ichthyoliths, and a microgastropods (Mosher and Clark 1965; Orchard, 2009). This sample is the best preserved collection from the PC outcrop (Orchard, 2009). The age range for the sample extracted from Facies A is late Anisian to early Ladinian (Orchard, 2009). The PC 70.5m sample produced conodont *?Neogondolella* ex gr. *constricta*, fish ichthyolith, and microgastropod fossils (Mosher and Clark 1965, Orchard, 2009). The most

detailed age interpretation of the sample removed from Facies C is Middle Triassic, as preservation of the sample is observed to be poor (Orchard, 2009). The PC 118m sample produced conodont *Neogondolella ex gr. constricta*, fish ichthyolith, echinoderm, and microgastropod fossils (Mosher and Clark, 1965; Orchard, 2009). The age interpretation of the sample removed from Facies F is Late Anisian to Early Ladinian, preservation of the fossils is observed to be fair (Orchard, 2009). The remaining samples (PC 124m, PC 126.5m, and PC 130m) of Facies G are interpreted to be Triassic to Middle Triassic determined from similar microfossil samples to PC 19.5m, PC 70.5m, and PC 118m.

The marine microfossil samples obtained from facies A, C, F, and G supports the marine depositional setting interpretations of these facies (Offshore to lower shoreface) (Orchard and Rieber, 1998; Orchard, 2009). The Lower to Middle Triassic stratigraphy is previously identified to range from Lower Griesbachian to Upper Ladinian and Lower Carnian age (Gibson, 1975). The epoch and age interpretation of Middle Triassic, Late Anisian to Early Ladinian of Facies G is consistent with previous age determinations of the Llama Member in the study area (Gibson, 1975). As facies A and G are both interpreted to be of Late Anisian to Early Ladinian age, the application of Steno's law of superposition enables the interpretation of facies B, C, D, E, and F to be of similar Middle Triassic Late Anisian to Early Ladinian age. This interpretation is also supported by the consistent nature of deposition and progression through a shallowing upward succession of these facies. The age determination confirms previous age

interpretations of the Whistler Member (Facies C), and the Llama Member (facies D, E, F, G, and H) (Gibson, 1975). The age interpretation of the Vega/Phroso Siltstone (facies A and B) as Late Anisian to Early Ladinian age is similar to the age of the Upper Vega determined in the Wapiti Lake region north west of the study area (Orchard and Zonneveld, 2009). Orchard and Zonneveld (2009) identify conodonts at the top of the Vega Member to contain *Neogondolella* spp. and possible *Chiosella*, implying an age close to the base of the Anisian.

The CFH 94m sample produced conodont *Neogondolella* ex gr. *constricta*, fish ichthyolith, and microgastropod fossils (Mosher and Clark 1965; Orchard, 2009). This sample is identified to consist of diverse morphology including advanced forms of fair preservation (Orchard, 2009). The sample analyzed from Facies F at the CFH outcrop is interpreted to be Middle Triassic Ladinian age (Orchard, 2009). This is consistent with the age interpretation of Facies F from the PC outcrop of the Llama Member.

The absence of dateable conodont data at the East 53 outcrop is an expected outcome. Many of the facies observed in the East 53 outcrop sequence are interpreted to be deposited in terrestrial depositional environments. Conodonts are deposited in marine settings and the identification of conodonts in non-marine settings is not expected. The samples analyzed produced fish ichthyoliths, foraminiferid, and microgastropod fossils interpreted to be from the Phanerozoic Eon (Orchard, 2009). Fish ichthyolith identified support the marine to lacustrine

Facies K (E53 24.75m) interpretation of the Starlight Evaporite Member of the Whitehorse Formation (Orchard, 2009). Fish ichthyolith, foraminiferid, and microgastropod fossils are also identified and support subaqueous interpretations of the intertidal to subtidal lagoon Facies M (E53 29m, E53 39.4m) of the same member as Facies K (Orchard, 2009).

The interpretation of Triassic lithologies at the Monaghan Creek section is consistent with the age identification of facies observed at the Poupanee chute, Cody Found Horse, and East 53 outcrops. The occurrence of *Neogondolella* ex gr. *constricta*, ichthyolith, and microgastropod fossils at the MC 0m (Facies F) interval and *Neogondolella* sp., fish ichthyolith, microbivalve, microgastropod fossils at MC 6m (Facies F) further confirms the marine and Middle Triassic interpretations of the Llama Member (Mosher and Clark 1965; Orchard, 2009). The marine fossils produced from samples MC 23.9, MC 30.65m, and MC 104.2m further supports the marine interpretations of the Phanerozoic Facies G and Facies M. The MC 259m sample produced *Misikella longidentata*, echinoderm, ichthyolith, microbivalve, and microgastropod fossils from Facies O (Kozur and Mock 1974; Orchard, 2009). The *Misikella longidentata* conodont is interpreted to be possible Carnian age as the preservation was fair (Kozur and Mock 1974; Orchard and Rieber, 1998). The BGB 4.6m sample produced fish ichthyolith and microgastropod fossils from Facies O (Orchard, 2009). Similarly the BGB 11.6m sample also produced ichthyolith and microgastropod fossils from Facies O (Orchard, 2009). The BGB 4.6m and BGB 112.6 samples also

confirm Facies O to be deposited during the Triassic period (Orchard, 2009). The Carnian age of Facies O is consistent with previous age interpretations of the Brewster Limestone Member (Gibson, 1975). This is also consistent with similar Upper Triassic age interpretations of the Baldonnel Formation in northeastern British Columbia (Orchard and Tozer, 1997; Zonneveld, 2004).

3.4 CHEMOSTRATIGRAPHY RESULTS

The results obtained by Bistran (2009), are presented in Appendix D. The elements with the highest concentrations on the order of tens of thousands or hundreds of thousands of ppm were Mg, Al, Si, and Ca. The scatter plots for each element detail the concentration variation (as a normalization ratio) of a particular element in the vertical succession. The data is presented in increasing vertical height in the succession at both the MC and E53 outcrops. Fourteen lithological comparisons between the two outcrops selected were completed, based upon the availability of data. The interpretations for this study focus on further analysis of the Bistran (2009) data and use other graphical methods to attempt a chemostratigraphic correlation between two outcrops in the study area.

The results of geochemical data for normalized to Zr are presented in 8 Figures that show the element to element variation for a given interval at both the E53 and MC outcrops for the 51 elements described (Figure 3-1 to 3-8). A comparison of

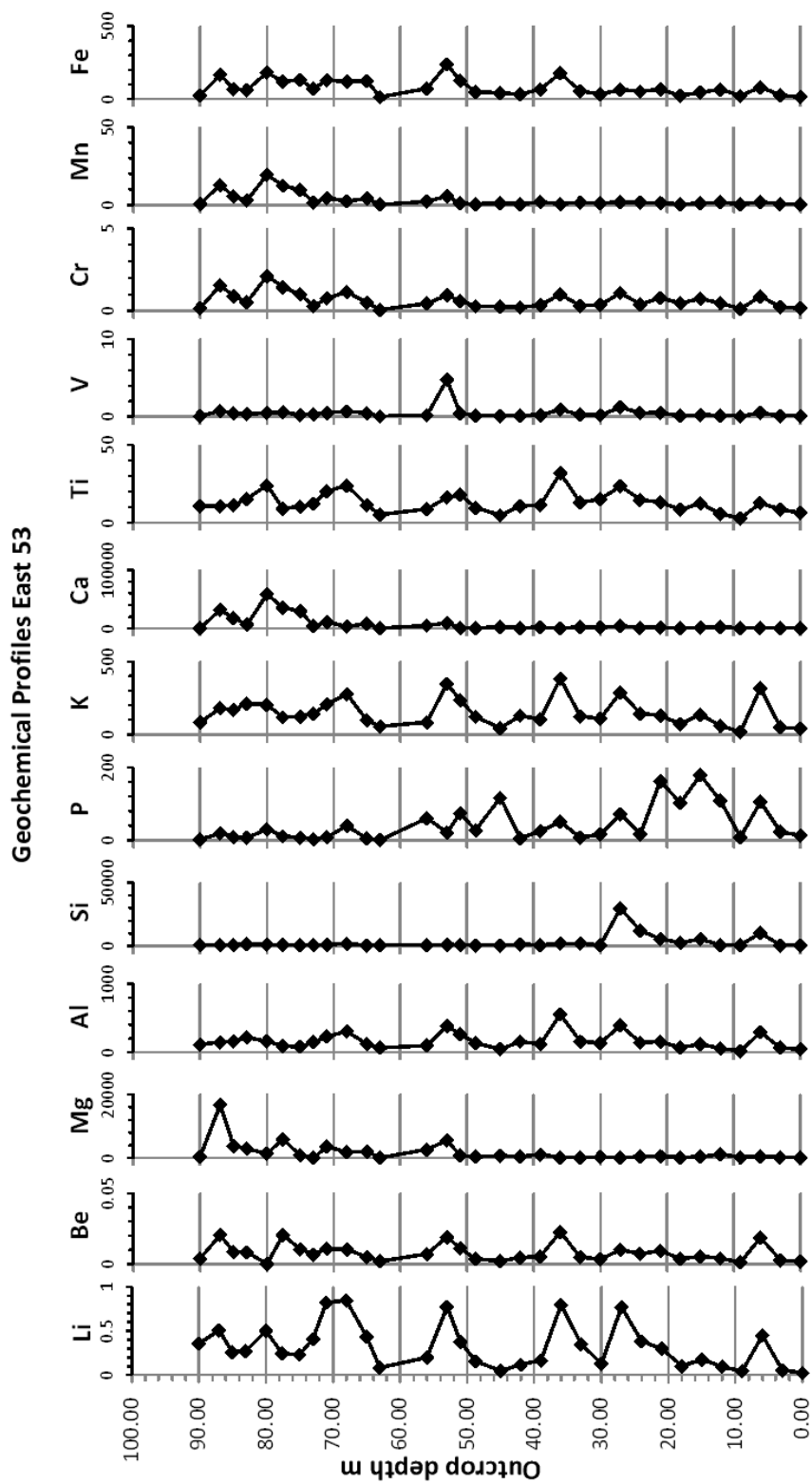


Figure 3-1: Elements Li, Be, Mg, Al, Si, P, K, Ca, Ti, V, Cr, Mn, and Fe geochemical profiles for the study interval from the East 53 outcrop. Data are expressed as parts per million (ppm) normalized to Zr.

Geochemical Profiles East 53

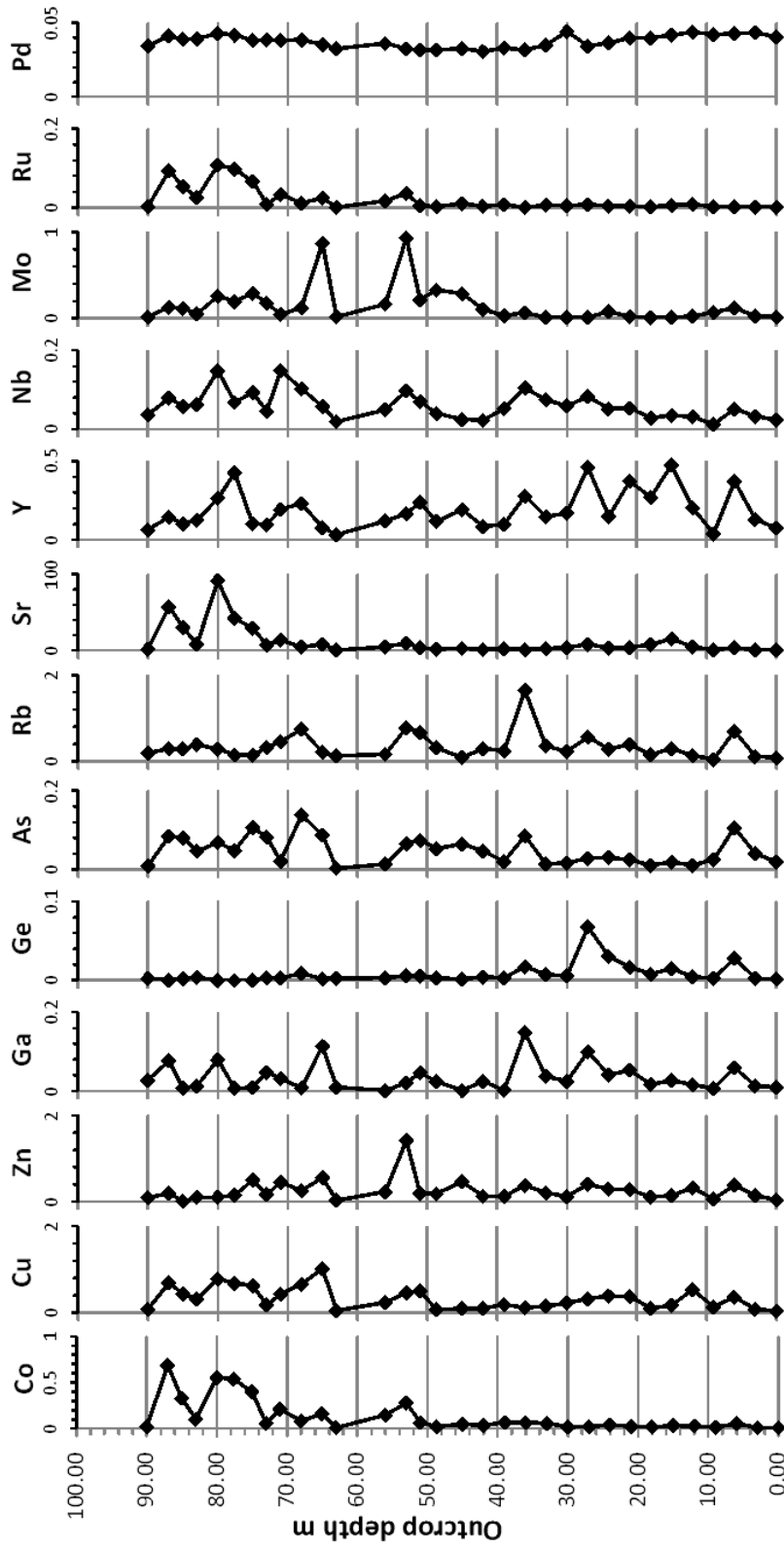


Figure 3-2: Elements Co, Cu, Zn, Ga, Ge, As, Rb, Sr, Y, Nb, Mo, Ru, and Pd geochemical profiles for the study interval from the East 53 outcrop. Data are expressed as parts per million (ppm) normalized to Zr.

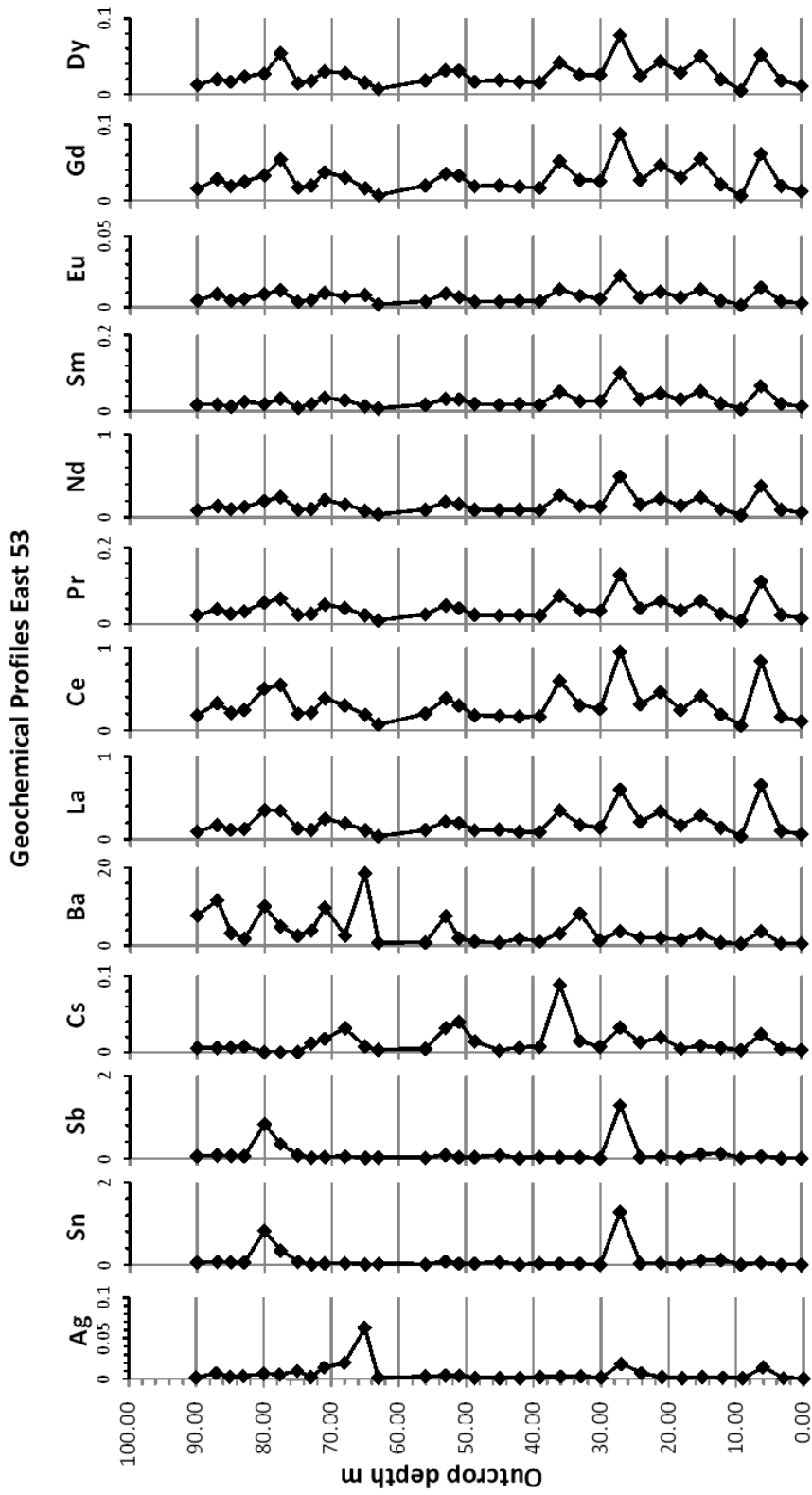


Figure 3-3: Elements Ag, Sn, Sb, Cs, Ba, La, Ce, Pr, Nd, Sm, Eu, Gd, and Dy geochemical profiles for the study interval from the East 53 outcrop. Data are expressed as parts per million (ppm) normalized to Zr.

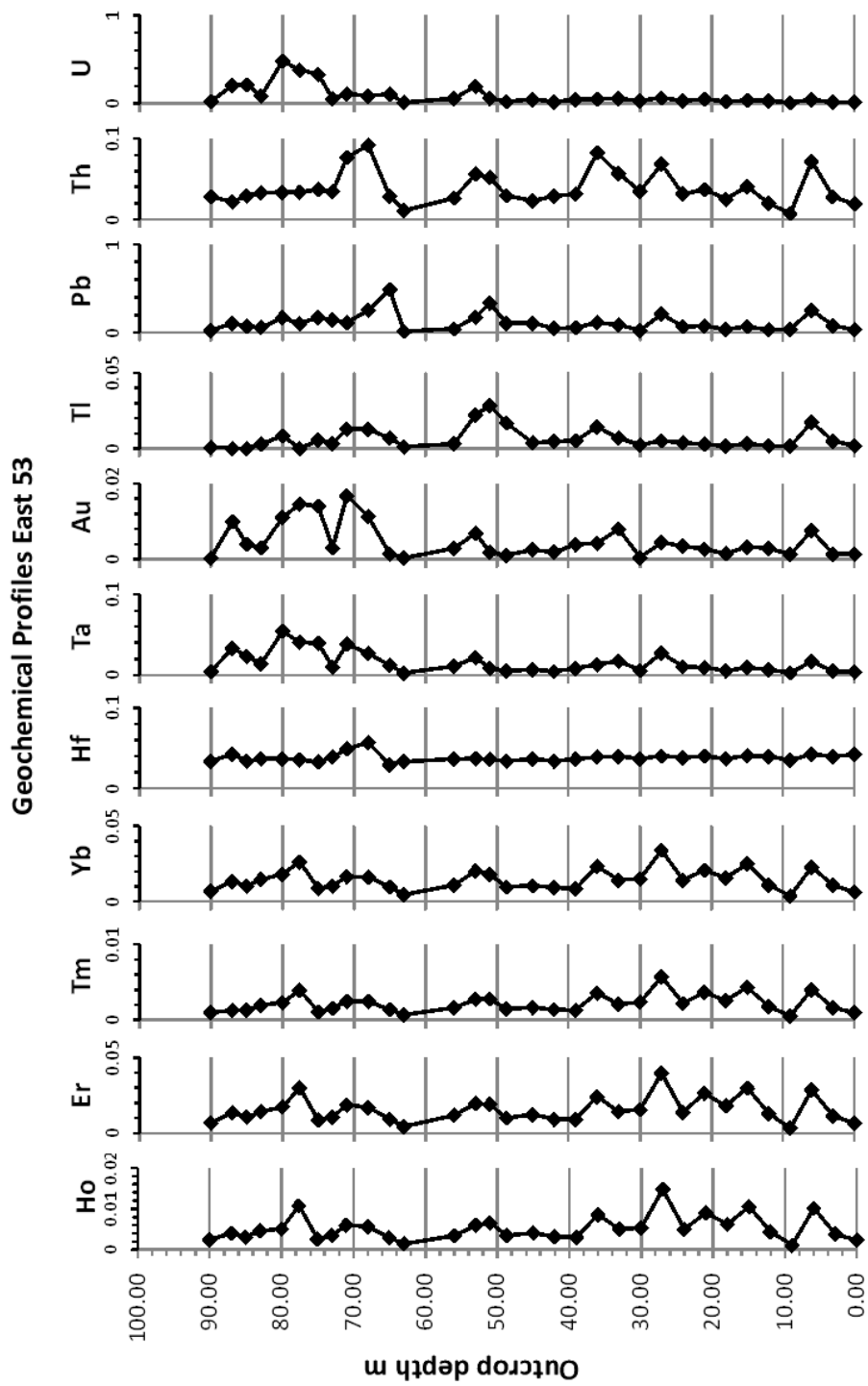


Figure 3-4: Elements Ho, Er, Tm, Yb, Hf, Ta, Au, Tl, Pb, Th, and U geochemical profiles for the study interval from the East 53 outcrop. Data are expressed as parts per million (ppm) normalized to Zr.

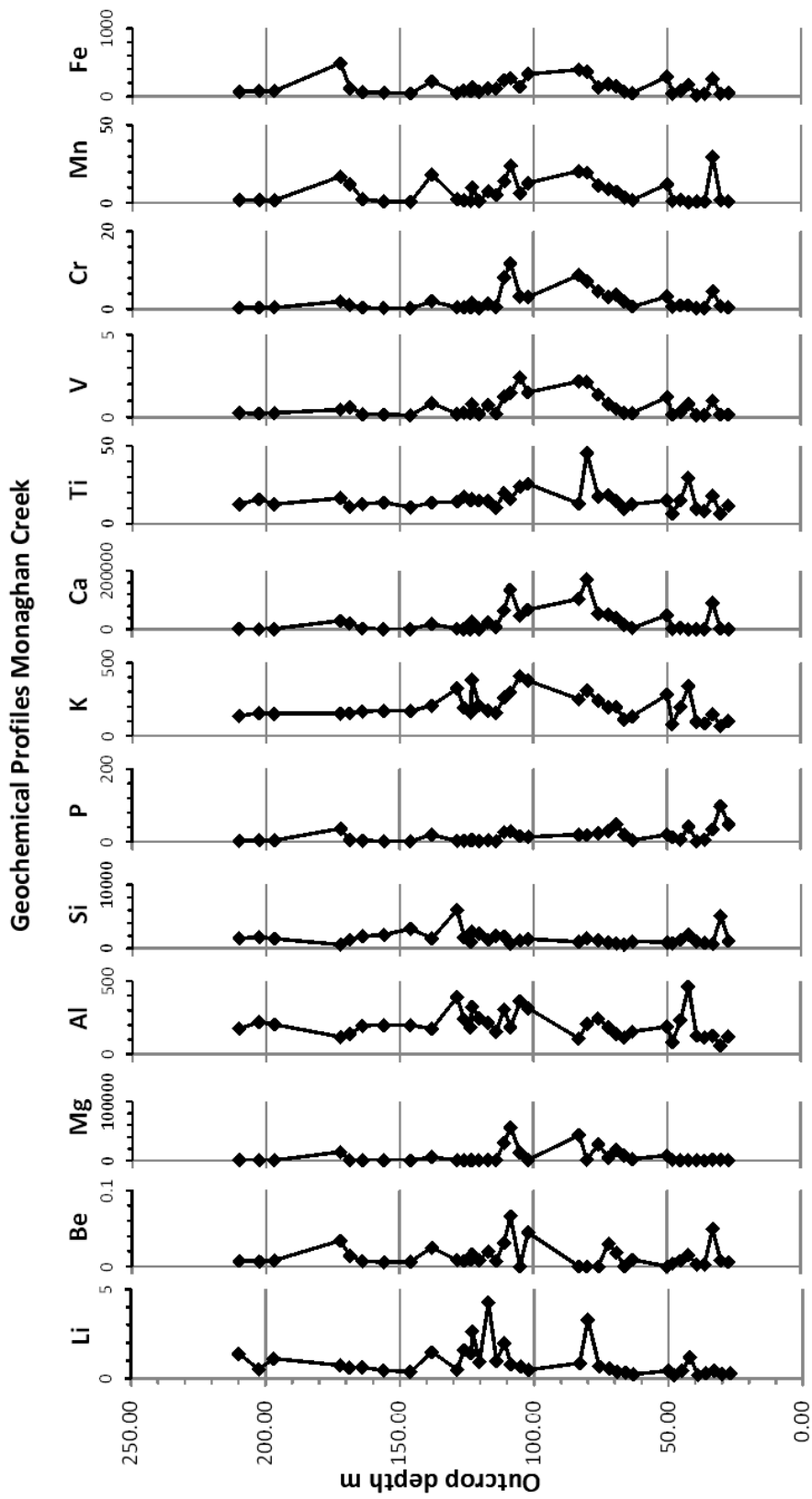


Figure 3-5: Elements Li, Be, Mg, Al, Si, P, K, Ca, Ti, V, Cr, Mn, and Fe geochemical profiles for the study interval from the Monaghan Creek outcrop. Data are expressed as parts per million (ppm) normalized to Zr.

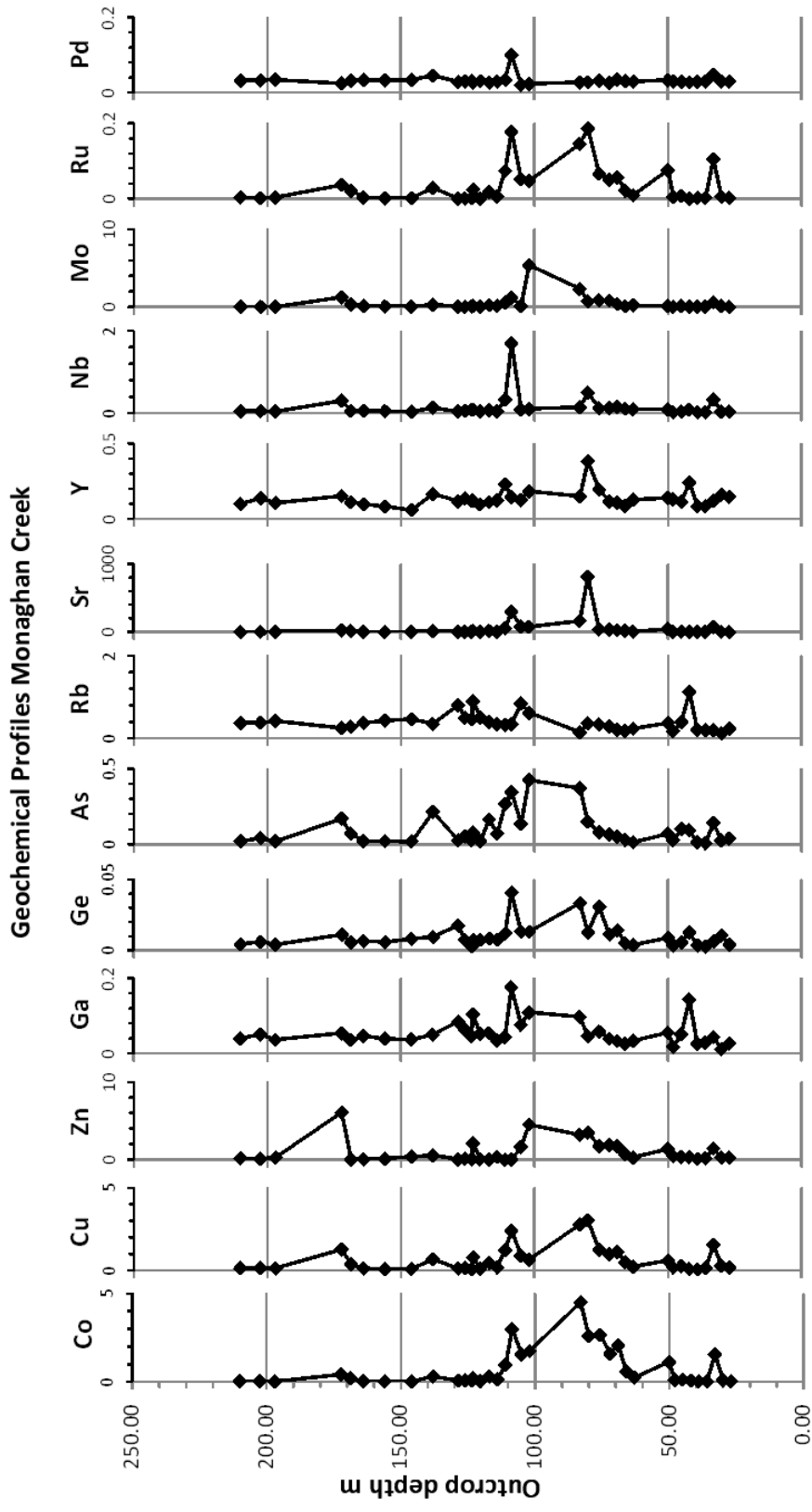


Figure 3-6: Elements Co, Cu, Zn, Ga, Ge, As, Rb, Sr, Y, Nb, Mo, Ru, and Pd geochemical profiles for the study interval from the Monaghan Creek outcrop. Data are expressed as parts per million (ppm) normalized to Zr.

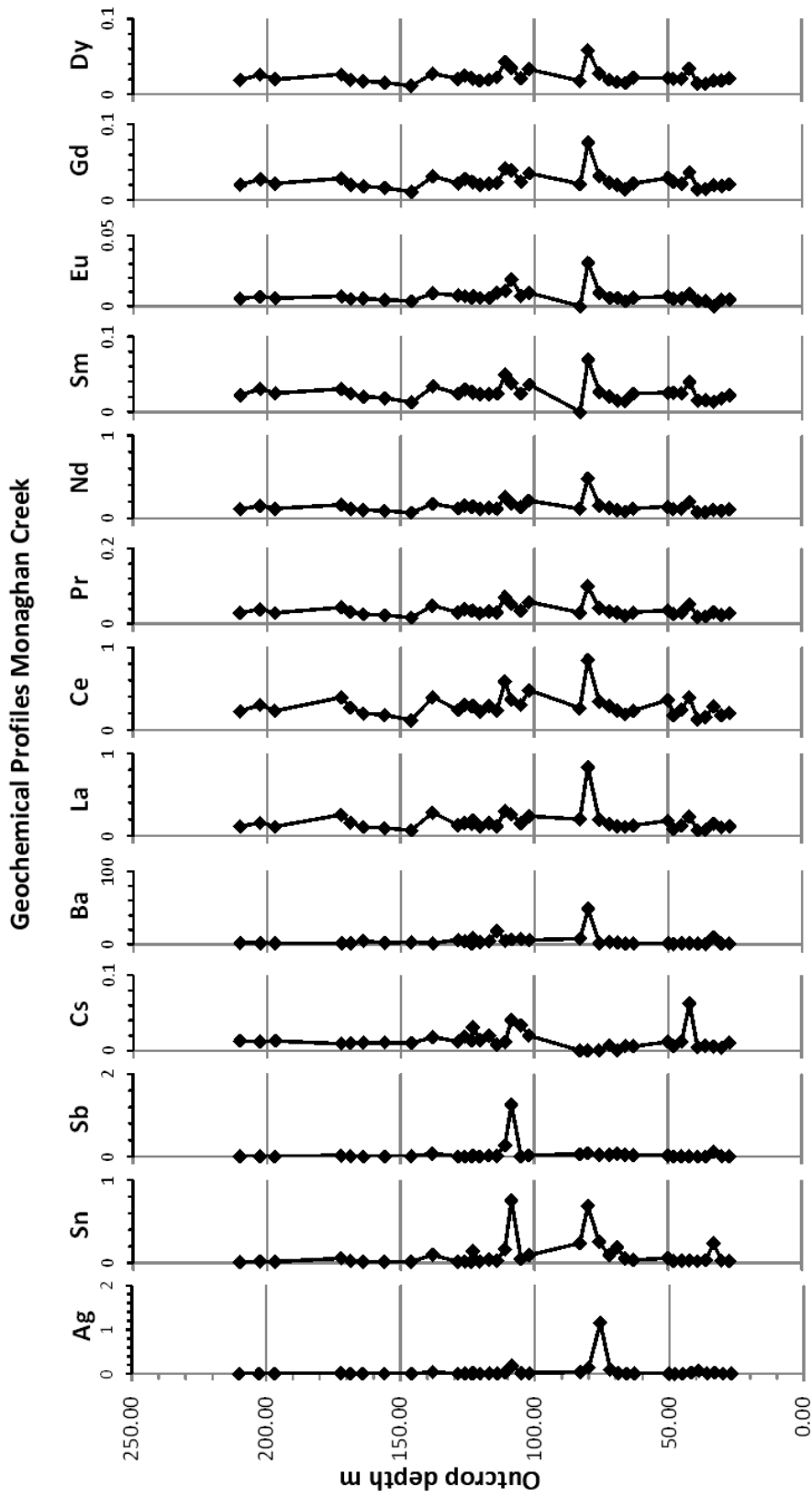


Figure 3-7: Elements Ag, Sn, Sb, Cs, Ba, La, Ce, Pr, Nd, Sm, Eu, Gd, and Dy geochemical profiles for the study interval from the Monaghan Creek outcrop. Data are expressed as parts per million (ppm) normalized to Zr.

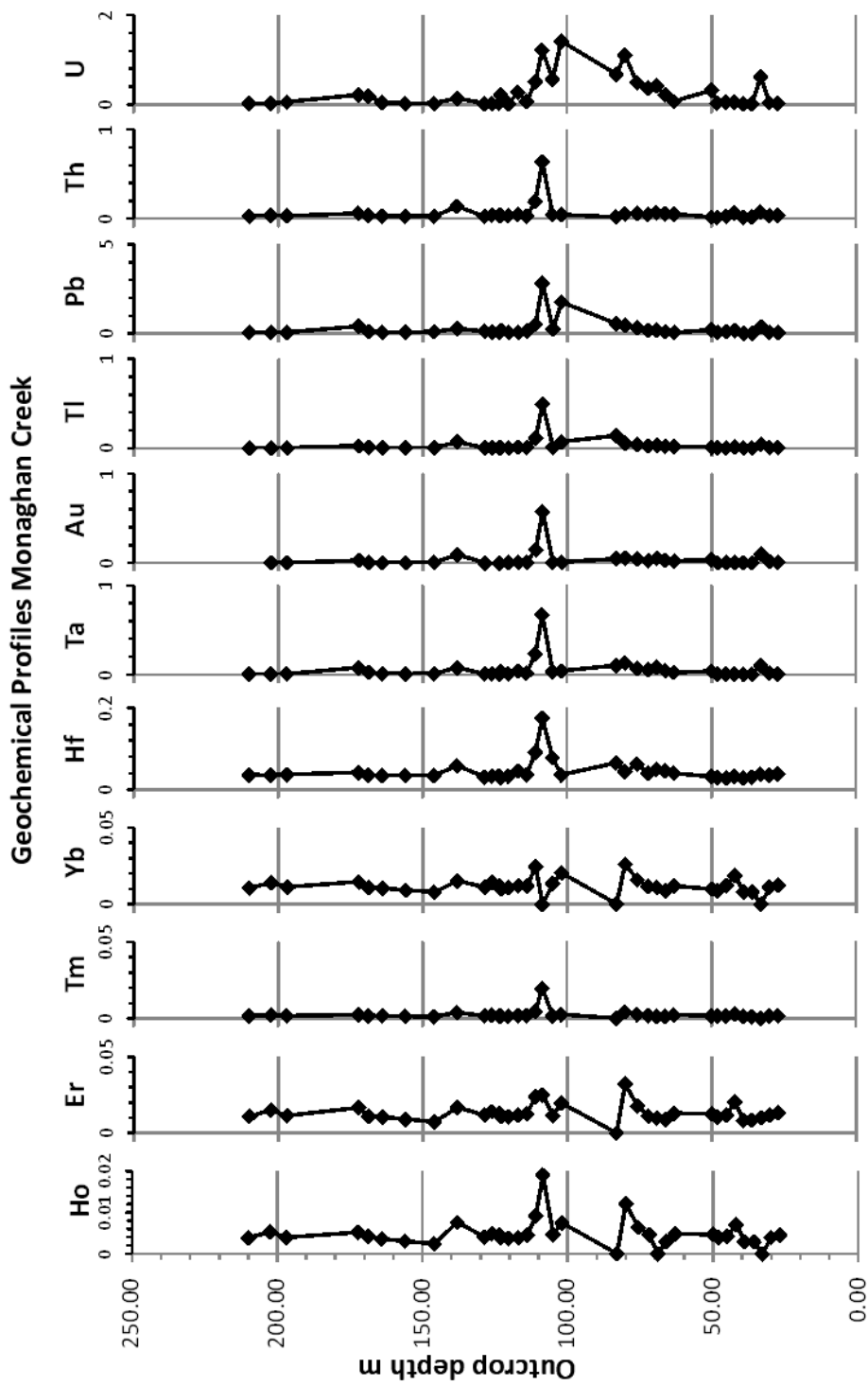


Figure 3-8: Elements Ho, Er, Tm, Yb, Hf, Ta, Au, Tl, Pb, Th, and U geochemical profiles for the study interval from the Monaghan Creek outcrop. Data are expressed as parts per million (ppm) normalized to Zr.

selected immobile elemental data (Nb, Cr, Ti, Al, Hf, and Zr) for each outcrop is presented in Figure 3-9. The resulting geochemical trends are described based upon the distribution of elements laterally, vertically, and at anomalous points in the data. Intervals identified herein are set as average intervals +/- 5m at which specified concentrations are observed to occur. At the E53 outcrop, high elemental values are identified to occur regularly at six separate intervals (Figure 3-1 to 3-8). These intervals include: 6m, 26m, 37m, 53m 70m, and 80m. Low elemental ratios are observed to occur regularly between these intervals with the exception of content between 6m to 37m, where increasing elemental values are noted. In addition, from the 80m interval to the top of the outcrop section overall decreasing elemental ratios are identified there is a decrease in element value marked by periodic variation in moderately high to low content. Anomalous high ratios are occasionally observed at 15m, 45m, and 65m.

At the MC outcrop, high geochemical contents are identified to occur more or less consistently at three intervals (42m, 50m, 77m, 111m, and 175m) (Figure 3-1 to 3-9). From 27m to 42m there is a regular alteration of moderately high and low element value. From 50m to 77m there is a consistent increase in element values to the high content point at 77m. From 77 to 101m no data was available of description. From the high value at 100m to 130m there is a decrease in element ratio marked by periodic fluctuation in moderately high to low content. From 130m to the top of the MC outcrop a gradual switching from high to low ratios is

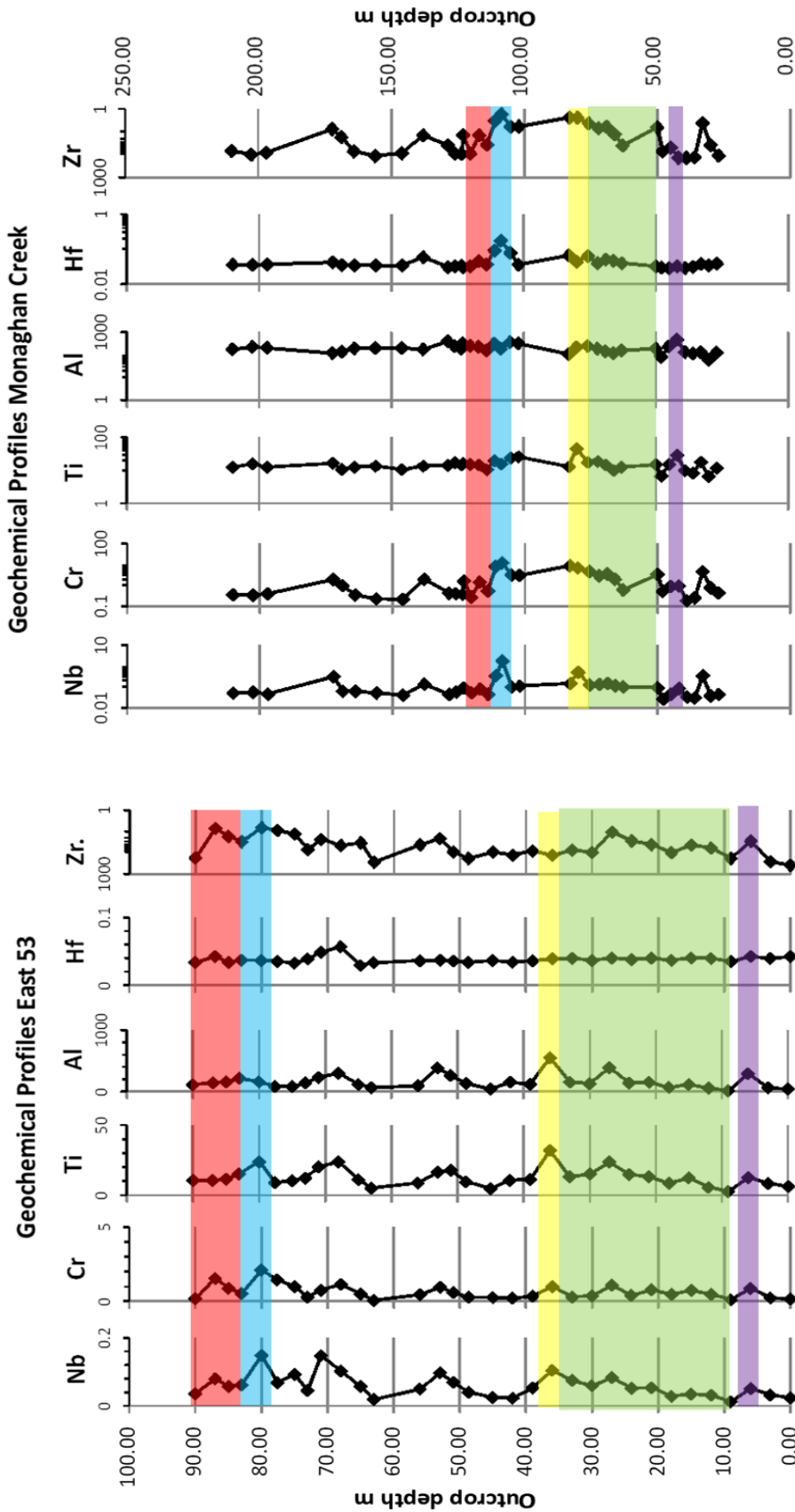


Figure 3-9: Elemental data illustrating correlation of similar ratio values of immobile elements based upon the visual comparison of the study intervals from the East 53 outcrop and Monaghan Creek outcrop. Data are expressed as parts per million (ppm). Like colour bars indicate interpreted chemostratigraphic correlations between the two outcrops.

identified. Anomalous increases are observed to occur irregularly at 145m and 170m.

The distributions of identified immobile elemental values are identified in Figure 3-9. At the E53 outcrop high elemental ratios are identified at 6m, 26m, 37m, 53m, 70m, and 80m. An overall increasing value trend is identified from 6m to the high concentration point at 37m. A consistent fall and rise in content is observed to occur between 37m to 53m. Subsequently another consistent rise and fall in concentration is observed between 53m to 70m. The fall and rise pattern persists from 70m to 80m. From 80m to the top of the outcrop an overall decrease in content is identified. Anomalous values not identified for the immobile elements described.

For the immobile elements at the MC outcrop, high elemental concentrations are identified at 42m, 50m, 77m, 111m, and 175m (Figure 3-9). From 27m to 42m there is a regular variation of moderately high and low element concentrations. From 50m to 77m there is a regular increase to the high content marker at 77m. No data was available of description from 77 to 101m. An oscillation in moderately high to low content culminating in an overall decrease is observed at the 111 to 130m interval. From 130m to the top of the MC outcrop a gradual switching from high to low concentrations are identified. No anomalous increases are observed to occur.

3.5 CHEMOSTRATIGRAPHY INTERPRETATIONS

The visual analysis of results enables the grouping of elemental concentrations at given depths based upon similar concentrations. Of the fourteen graphical plots comparisons by Bistran (2009), nine potential chemostratigraphic correlations were interpreted (Appendix D). The interpreted correlations include: 1) E53 39.0 m and MC 63.0 m, 2) E53 39.0 m and MC 48.0 m, 3) E53 80.0 m and MC 105.0 m, 4) E53 77.6 m and MC 108.6, 111.0 m, 5) E53 83.0 m and MC 108.6, 111.0 m, 6) E53 77.6 m and MC 117.0 m, 7) E53 83.0 m and MC 117.0 m, and 8) E53 85.0 m and MC 117.0 m. These correlations are interpreted to represent the continuous deposition events of equivalent facies. The interpreted chemostratigraphic correlations by Bistran (2009) are supplemented through the additional chemostratigraphic correlation interpretations conducted.

The observed transitions between elemental concentrations of similar depth described in the chemostratigraphy results section are demarked by step changes in concentrations. The comparison of the chemostratigraphic units between the two outcrops then enables the elucidation of correlation potential. The first potential correlation is identified to occur at the E53 6m and MC 42m intervals (Figure 3-1 to 3-9). The E53 interval is preceded by limited data points resulting in the inability to determine the overall character of the chemostratigraphic unit below. The MC 42m interval is preceded by moderately variable values (Figure 3-1 to 3-9). The E53 6m interval is followed vertically by a gradual increase in element ratio and concentrations as is the MC42m interval (Figure 3-1 to 3-9) .

The correlation is strengthened by the similar overlying chemostratigraphic unit and correlation of Facies Association 3 between the two units (E53 6m Facies M and MC 42m Facies K).

The second potential lateral correlation between the two described outcrops is interpreted to occur between the E53 10m to 37m and MC 50m to 72m intervals (Figure 3-1 to 3-9). The E53 and MC intervals both exhibit a gradual increase in elemental values, are preceded by similar high to moderately variable chemostratigraphic units, and are followed upward by a high elemental ratios (Figure 3-1 to 3-9). This interpretation is strengthened by the correlation of Facies Association 3 and Facies Association 4. The third potential lateral correlation is interpreted at the high elemental values at E53 37m and E53 75m (Figure 3-1 to 3-9). The similar nature of the underlying chemostratigraphic units and the interpreted correlation of facies association 4 strengthen the interpretation.

The chemostratigraphic correlation potential between the intervals E53 37m to E53 78m and MC 83 to 102 are unknown due to a lack of data at the MC section (Figure 3-1 to 3-9). The fourth potential chemostratigraphic correlation is interpreted to occur at the E53 80m and MC 111m intervals (Figure 3-1 to 3-9). Both intervals exhibit a high elemental value and concentration and are overlain by an overall decreasing elemental value trend. This interpretation is strengthened by the lateral Facies M correlation of Facies Association 3 between the two outcrops.

The fifth interpreted correlation between the E53 and MC outcrop is at the E53 83m to 90m interval and MC 117m to 123m intervals (Figure 3-1 to 3-9). The similar underlying geochemical signatures and similar overall decreasing elemental value supports the interpretation. The interpretation is strengthened by the lateral correlation of Facies Association 3. Based upon the analysis of integrated chemostratigraphic, biostratigraphy, lithofacies, and gamma-ray data the most probable correlations are determined to be: 1) E53 37 m to MC 63 m and 2) E53 80 m to MC 111 m. both correlations correspond to Facies Association 3.

The graphical display of elemental values plotted to depth allows for the visual differentiation of units and enable correlation of the similarities seen in the profiles (Figure 3-1 to 3-9). As sediment is transported to sites of deposition they are subject to forces that may result in the alteration of chemical composition. An example of minerals that are prone to dissolution and diagenetic alteration include feldspar and clay (Pearce et al., 1999). As dissolution occurs the feldspar chemical concentrations of Ca, Na, K, Pb, Rb, Sr and certain rare earth elements can change considerably (Pearce et al., 1999). As outlined in Pearce et al., 1999 immobile elements (Al, Ti, Nb, Cr, Zr) are less prone to the effect of diagenetic alteration and therefore used for the correlation between the E53 and MC outcrops (Figure 3-9). Immobile elements in this study are not identified to contain anomalously high or low values. This supports the interpretation that anomalous values observed are a possible result of diagenetic effect on mobile element concentrations.

Element profiles for each of the immobile elements studied are strikingly consistent for both outcrops and illustrate the strength of chemostratigraphic correlation in laterally variable depositional settings when supported by facies correlation. To further improve the correlation potential Pearce et al., (1999) suggests the use of a discriminant function analysis for a more accurate assessment of the chemostratigraphic correlation.

3.6 LOG CORRELATION

Outcrop correlations are completed on the basis of chemostratigraphic, biostratigraphic, lithological, and gamma-ray data. As identified in this study and by Gibson (1968a), the correlation of lateral facies is uncertain as there is a high degree of lithological variability between outcrops. In addition to this, the chemostratigraphic and biostratigraphic data is less than desirable between outcrops, as only two outcrops were chemostratigraphically analyzed and many of the biostratigraphy samples were either barren or contained no high-resolution conodont samples (Bistran, 2009; Orchard, 2009). Of the outcrops logged, three of the six outcrops are more confidently correlated (PC, E53, and MC). This is a result of the vertical distribution of facies, chemostratigraphic correlation, and relatively abundant biostratigraphic data at these outcrops. The BGB outcrop is less confidently correlated as the outcrop was of limited thickness, contacts were not observed, and the outcrops consisted of only one facies (Facies O) and single facies association (FA5). The CFH outcrop is thought to be weakly correlated resulting from extensive cover and a high degree of structural shortening. The

BGS outcrop did not receive correlation to the other outcrops as facies identification was beyond the scope of work for this study. Log correlations are presented in Figure 3-10.

Correlation based upon biostratigraphic results of conodont data suggests a high likelihood of correlation potential between analyzed outcrops within the study area. This is supported by the similar ages observed across the outcrops analyzed. The resolution of the biostratigraphic data is insufficient for individual bed correlations based solely on conodont data. However, when the data is combined with chemostratigraphic, gamma-ray, and lithofacies the data supports coarser scale outcrop correlations. Chemostratigraphic interpretations provide a high-resolution constraint for correlations between outcrops E53 and MC. The comparison of chemostratigraphic data with facies, biostratigraphic, and gamma-ray data greatly improves the confidence of correlations between the two outcrops. Gamma-ray data additionally supplements the correlation of chemostratigraphic data between the two outcrops and the other outcrops lacking chemostratigraphic interpretations. The correlation of similar lithofacies between outcrops has proven to be difficult due to the high lateral variability, but is nonetheless a vital correlation tool in this study.

3.7 STRATIGRAPHIC FRAMEWORK

Outcrop Log Correlation of Lithofacies, Chemostratigraphic, Biostratigraphic, and Gamma-ray Data

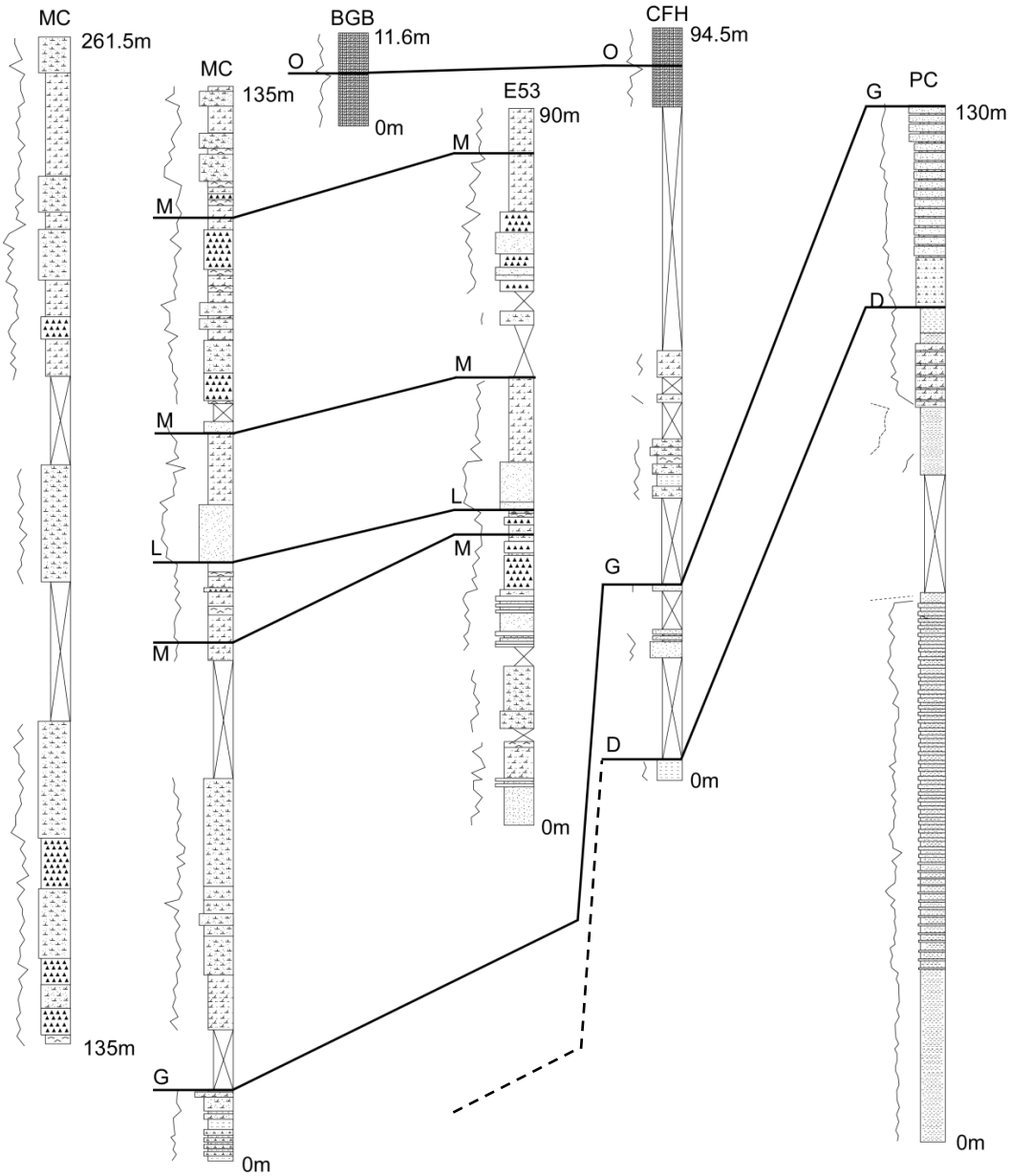


Figure 3-10: The log correlations of outcrops within the study area are presented from west to east. Gamma ray data, chemostratigraphic, biostratigraphic, and lithofacies data are combined to create the correlations in this figure. The correlated facies (O, M, L, G, and D) are identified in this correlation. Notably the high degree of lateral facies variability greatly limits correlations of the studied outcrops (MC, Monaghan Creek; BGB, Blue Grouse Brewster; E53, East 53; CFH, Cody Found Horse; PC, Poupanee Chute). Gamma-ray data is presented to the left of the outcrop logs in counts per second (0-200) and is available in detail in appendix A.

Sequence stratigraphic analysis is completed based upon the integration of multiple data sets. The use of several data sets increases the probability of accurate identification of significant surfaces formed by sedimentary processes (Catuneanu et al., 2008). The stratal architecture of the described facies, associated bounding surfaces, and interpreted depositional system provides the basis for the determination of the sequence stratigraphic framework in the study area. The selected scale of observation for this analysis is a coarse resolution interpretation of two outcrops (PC and E53) with reference to surrounding outcrops. The PC and E53 outcrops are selected as they provide the most complete representation of interpreted facies. The interpreted stratigraphic facies relationship model for the depositional sequence of this study is presented in Table 3-3 and Table 3-4.

From the base of the PC outcrop to the 67.5 m interval, a single regressive succession interpreted to consist of the Vega/Phroso Member is identified. The first regressive succession is overlain by an interpreted maximum flooding surface and transgressive surface of erosion. This surface is interpreted to mark the top of the Vega/Phroso Member and the base of the Whistler Member. This point also marks the beginning of the second coarse scale regressive succession identified at the PC outcrop. This coarsening upward succession is interpreted to consist of The Whistler Member and the Llama Member. A small scale transgressive regressive succession is observed within this package, identified by the reappearance of facies C and D of the Whistler Member initiated at 100.5m

Lithology	Depositional Environment	Facies	Inferred Sea Level Curve and Stratigraphic Facies Relationships	Stratigraphic Surfaces
Dolomitic Silty Mudstone	Subtidal	M		Regression? FS
Solution Collapse Breccia	Supratidal peritidal (sabkha)	J		Regression FS (small scale)
High-angle Cross-stratified Sandstone	Supratidal sabkha	L		4 th major Regression
Solution Collapse Breccia	Supratidal peritidal (sabkha)	J		
Contorted Sandstone	Supratidal sabkha	N		
High-angle Cross-stratified Sandstone	Supratidal sabkha	L		
Solution Collapse Breccia	Supratidal peritidal (sabkha)	J		FS
VF to F Calcareous Sandstone	Marine/ lacustrine	K		
Dolomitic Silty Mudstone	Subtidal	M		3 rd major Regression
Contorted Sandstone	Supratidal sabkha	N		
High-angle Cross-stratified Sandstone	Supratidal sabkha	L		
VF to F Calcareous Sandstone	Marine/ lacustrine	K		
Bindstone Laminate	Supratidal to intertidal flat	I		
Solution Collapse Breccia	Supratidal peritidal (sabkha)	J		
Dolomitic Silty Mudstone	Subtidal	M		
Solution Collapse Breccia	Supratidal peritidal (sabkha)	J		
Dolomitic Silty Mudstone	Subtidal	M		
Solution Collapse Breccia	Supratidal peritidal (sabkha)	J		
VF to F Calcareous Sandstone	Marine/ lacustrine	K		FS
High-angle Cross-stratified Sandstone	Supratidal sabkha	L		

Table 3-3. Stratigraphic profile B. Relative position of facies (coarsening left) and stratigraphic surfaces observed in the Willmore Wilderness Park. Described data obtained at outcrops PC (facies A to G) and E53 (facies H to N); SB, sequence boundary; TSE, transgressive surface of erosion; MFS, maximum flooding surface; FS, flooding surface.

Lithology	Depositional Environment	Facies	Inferred Sea Level Curve and Stratigraphic Facies Relationships	Stratigraphic Surfaces
VF to F Calcareous Sandstone	Marine/ lacustrine	K		2 nd major Regression LST?
High-angle Cross-stratified Sandstone	Supratidal sabkha	L		
VF to F Calcareous Sandstone	Marine/ lacustrine	K		
Bindstone Laminate	Supratidal to intertidal flat	I		
Dolomitic Silty Mudstone	Subtidal	M		SB
F to C Planar Tabular to Trough Cross-stratified Sandstone and F to M Planar Laminated Sandstone	Upper shoreface with amalgamated washover fan or swashzone deposits	H		Regression ~0m E53 ~130m PC LST?
Interbedded VF to F Sandstone and Sandy Siltstone	Proximal lower shoreface	G		Regression
VF Calcareous Sandstone	Lower shoreface	F		FS (small scale)
Muddy Siltstone	Offshore to distal offshore transition	D		Regression
Black Shale	Offshore	C		TSE/MFS
VF Dolomitic Silty Sandstone	Proximal offshore transition to distal lower shoreface	E		1 st major Regression
Muddy Siltstone	Offshore to distal offshore transition	D		
Black Shale	Offshore	C		
Interbedded VF Dolomitic Silty Sandstone and Dolomitic Siltstone	Offshore transition to distal lower shoreface	B		
Dolomitic Siltstone	Distal offshore transition to offshore transition	A	0m PC	

Table 3-4. Stratigraphic profile B. Relative position of facies (coarsening left) and stratigraphic surfaces observed in the Willmore Wilderness Park. Described data obtained at outcrops PC (facies A to G) and E53 (facies H to N); SB, sequence boundary; TSE, transgressive surface of erosion; MFS, maximum flooding surface; FS, flooding surface; LST, lowstand systems tract.

(Table 3-4; Appendix A).

Facies at the PC outcrop are correlated to the base of the MC outcrop and the poorly exposed CFH outcrop (Figure 3-10). The lack of observed contacts between Facies G and Facies H proves to be problematic, as no determination of continued progradation between the two facies can be explicitly proven. However, the transition of depositional interpretations from the proximal lower shoreface (Facies G) to upper shoreface (Facies H) suggests continued progradation. The lack of identified upper bounding surfaces and restricted lateral correlation, results in the inability to confirm a depositional sequence tract within the PC outcrop. It is postulated that the progradational sequence represents a potential lowstand systems tract, as the succession is underlain by a sequence boundary and is likely overlain by a transgressive surface (E53 29m). Dixon (2002a) indicates that an unconformity likely separates the base of the Charlie Lake Formation from Halfway and Doig strata. This study suggests a continued progradational succession of facies from the Llama Member into the Starlight Evaporite Member. However, the author is suspicious of sandstone beds at the top of Facies H at the E53 outcrop that may represent a subaerial unconformity. The lack of supporting data for this interpretation is regrettable and is recommended for future work.

The E53 29m and E53 45m intervals mark the initiation of the third and fourth coarse scale regressive successions. The successions are often punctuated by

smaller scale regression and transgression events. The transition of these events is primarily interpreted to be representative of regular peritidal sequences (Facies M, Facies I, and Facies J) often capped by terrestrial facies (facies L and N). Arnold (1994) identified a similar cyclicity of subtidal, intertidal, supratidal, and sabkha facies repeated within the Charlie lake Formation of the Williston Lake area.

The E53 and MC outcrops are not interpreted to represent the entire sequence of the Starlight Evaporite Member, as the uppermost contacts are not observed. In addition to this, the fact that observed facies are not easily correlated due to lateral facies variability restricts the interpretation of systems tracts. The peritidal successions observed at the E53 outcrop are also observed in the MC outcrop. The primary difference is that only one aeolian sabkha facies is interpreted to cap peritidal successions in the MC outcrop. The result is a large number of minor subtidal, intertidal, and supratidal peritidal sequences, consisting of facies M, I, and J. This precludes the interpretation of the coarser scale regressional or transgression nature of the Starlight Evaporite Member.

As the lower contact of the Brewster limestone Member (FA5) is not observed, systems tract analysis is restricted. However, the occurrence of the offshore Brewster Limestone Member above the often terrestrial Starlight Evaporite Member implies a significant transgression event occurred between the two

members. The coarse scale transgressional flooding surfaces described are identified on the strip log provided in appendix A.

3.8 TECTONIC AND EUSTATIC IMPLICATIONS

The regressive events representing sea level fall may have been the result of a number of factors. The flexural fore-bulge created by the weight of approaching accreting terranes is one possible mechanism for local sea-level rise (DeCelles and Giles, 1996). The instances of rising sea level observed may indicate regional tectonic subsidence (Collier, et al., 1990). Long-term eustasy variation caused by sea-floor spreading during the initiation of super-continental breakup of Pangea may have also had a large role (Heller, et al., 1996). The alteration in global cooling and warming trends attributed to alteration in albedo effect as result of the continental breakup may have also played a role. These factors in combination with global cooling and warming trends attributed to orbital forcing is also a widely recognized mechanism for sea level variation (Varadi, et al., 2003).

CHAPTER FOUR

4.1.0 Conclusion and Summary

This study describes geological characteristics of the Spray River Group in the Willmore Wilderness Park of west-central Alberta. In total six outcrops are examined, with five of the outcrop analyzed in detail. Of the outcrops studied, multiple data sets are described and interpreted to better understand the depositional history of the Spray River Group. In this study fifteen lithofacies are described and interpreted. The lithofacies are placed into five facies associations based upon sedimentological and depositional characteristics. Biochronological data set analyses is conducted to better constrain outcrop correlations and establish age relationships of the studied lithologies. Additionally, chemostratigraphic data set analyses completed enables high-resolution correlation between the outcrops. Results and interpretations established in this study identify the need for further analysis in the study area.

Facies descriptions from the study area were created using sedimentological and ichnological logging of outcrops. Lithologies of the facies are primarily composed of mixed siliciclastic-carbonate sediment. Of the lithologies, fifteen facies are described in the study area representing depositional environments that range from offshore marine to supratidal sabkha environments. Facies described in this study are similar to facies descriptions and environmental interpretations of equivalent Montney, Doig, and Charlie lake formation stratigraphy to the northeast (Arnold, 1994; Zonneveld, et al., 2004).

Facies Association 1 (FA1) is interpreted to be deposited in the offshore transition to lower shoreface. FA1 is interpreted to be the Vega/Phroso Siltstone Member laterally equivalent of the upper Montney Formation. The lower most portion of FA1 is interpreted to be deposited offshore to lower shoreface transition. Facies C and D are interpreted to comprise the Whistler Member, laterally equivalent to the Doig phosphate zone. The remaining facies of FA2 are interpreted to consist of the Llama Member, laterally equivalent to the Doig Formation. Facies Association 3 (FA3) is interpreted to have been deposited in environments ranging from subtidal to ephemeral lacustrine settings. FA3 is interpreted to be a component of the Starlight Evaporite Member, laterally equivalent to the Charlie Lake Formation. Facies Association 4 (FA4) is interpreted to represent deposition by aeolian dunes in a supratidal sabkha depositional setting. FA4 is also a component of the Starlight Evaporite Member, laterally equivalent to the Charlie Lake Formation. Facies Association 5 (FA5) consists of a single facies consisting of calcareous bioclastic wackestone/packstone, deposited in an offshore setting. FA5 is interpreted to be the Brewster Limestone Member, potentially laterally equivalent to the Baldonnel Formation. Many differences exist between the Brewster Limestone Member and the Baldonnel Formation and the correlation cannot be confirmed or denied in this study.

To facilitate outcrop correlation and establish lithological age relationships within the study area biochronological dating of conodont material was completed.

Several analyzed samples failed to provide high-resolution data and further biostratigraphic analysis is recommended. Chemostratigraphic analysis of homogenous fine-grained lithologies was also completed between two outcrops (East 53 and Monaghan Creek). Results of the analysis identify strong correlation potential between two lithological intervals. In order to complete the correlation between all of the outcrops other further chemostratigraphic analyses is suggested.

Of the five outcrops three are confidently correlated: Poupanee, East 53, and Monaghan Creek. Two of the five outcrops are less confidently correlated: Cody Found Horse and Blue Grouse Brewster. The inability to confidently correlate the Cody Found Horse outcrop is primarily the result of the extensive cover and structural shortening. The second outcrop that could not be confidently correlated is the Blue Grouse Brewster outcrop. This outcrop was not easily correlated for two primary reasons. Firstly, the Blue Grouse Brewster outcrop displays a single relatively unique facies (Facies O). This facies is only observed at one other outcrop section. Unfortunately the other occurrence of Facies O is at the Cody Found Horse outcrop. Biostratigraphic constrains and facies association models however, enable low-resolution correlation between these outcrops. Following outcrop correlations, sequence stratigraphic analysis was completed.

Stratigraphic analysis was completed through the use of multiple data sets described in chapter 3. The analysis reveals four coarse scale regressive and

transgressive sequences. The regressive successions observed are represented by the East 53 and Poupanee Chute outcrops. Further sequence stratigraphic study is needed to describe the transgressive and regressive cycles present as the high degree of lateral variability and limited outcrop sections decreased the ability to identify system tracts.

In addition to sequence stratigraphic analysis, further work is needed for a complete characterization of the Spray River Group in the Willmore Wilderness Park. To improve correlations between outcrops in this study, it is recommended that chemostratigraphic analysis be completed for the remaining outcrops and extended to available core. In addition to more extensive biostratigraphic analysis between outcrops, core study should also be completed. With this data, large-scale correlation between outcrops of this study and subsurface core sections identified to the east would improve regional understanding of lateral relationships. The correlation and comparison of Triassic lithologies in west central Alberta northeastern British Columbia with those of this study would also improve understanding. Such an analysis would provide key insights into the depositional history of the Spray River Group and subsurface.

REFERENCES

- Aigner, T., 1985. Storm depositional systems: dynamic stratigraphy in modern and ancient shallow-marine sequences. *Lecture Notes in Earth Sciences*, v. 3, Berlin, New York, p. 174.
- Armitage, J. H., 1962. Triassic oil and gas occurrences in northeastern British Columbia, Canada; *J. Alberta Society of Petroleum Geology*, v. 10, no. 2 p. 35-56.
- Arnold, K.J. 1994. Origin and distribution of aeolian sandstones in the Triassic Charlie Lake Formation, northeastern British Columbia. M.Sc. thesis, University of Alberta, Edmonton, Alberta, 320p.
- Aukes, P.G. and Webb, T.K. 1986. Triassic Spirit River Pool, northwestern Alberta. In: *Canadian Society of Petroleum Geologists, 1986 Core Conference*, Calgary, Alberta, Canada. N.C. Meijer Drees (ed.). p. 3.1-3.34.
- Barclay, J.E. and Leckie, D.A. 1986. Tidal inlet reservoirs of the Triassic Halfway Formation, Wembley Region, Alberta. In: *1986 Core Conference*. N.C. Meijer Drees (ed.). *Canadian Society of Petroleum Geologists*, Calgary, Alberta, p. 4.1-4.6.
- Barclay, J.E., Krause, F.F., Campbell, R.I. and Utting, J. 1990. Dynamic casting and growth faulting of the Dawson Creek Graben Complex: Carboniferous-Permian Peace River Embayment, Western Canada. In: *Geology of the Peace River Arch*. S.C. O'Connell and J.S. Bell (eds.). *Bulletin of Canadian Petroleum Geology*, v. 38A, p. 115-145.
- Barss, D.L., Best, E.W., Meyers, N., 1964. Geologic history of Western Canada. In: *McCrossan, G., Glasster, P.O (Eds.). Alberta Society of Petroleum Geologists*, pp. 113-137 (chap. 9).
- Berger, Z. 2006 (Abstract). Detection and analysis of basement structures and their influence on hydrocarbon plays in northeast British Columbia. *Canadian Society of Petroleum Geologists, Reservoir*, v.33, Issue 2, p15.
- Best, E.W., 1958. The Triassic of the North Saskatchewan-Athabasca Rivers area; *Alberta Soc. Petrol. Geol., Guidebook; Eight Ann. Field Conf.*, p. 39-49.
- Blakey, R. C., 2011. <http://jan.ucc.nau.edu/~rcb7/index.html>. NAU Geology Web Page. Northern Arizona University, Flagstaff, AZ. Department of Geology.

- Blatt, H., Middleton, G., and Murray, R., 1980. *Origin of Sedimentary Rocks*. 2nd ed., Printice-Hall Inc., New Jersey, Engle Wood Cliffs.
- Boreen, T.D., and James, N.P., 1995. Stratigraphic sedimentology of Tertiary cool water limestones, SE Australia. *Journal of Sedimentary Research*, v. B65, p. 142-159.
- Brenchley, P.J. 1985. Storm Influenced Sandstone Beds. *Modern Geology*, v. 9, p. 369-396
- Brookfield, M.E. 1992. *Eolian systems; in Facies Models: Response to Sea Level Change*, Walker, R.G. and James, N.P., Geological Association of Canada. *Geotext 1*: pages 143–156.
- Buatois, L.M., Mangano, G., Gingras, M.K., MacEachern, J.A., Martin, A., Netto, R., Pemberton, S.G. and Zonneveld, J-P. 2004. Colonization of brackish-water systems through time: evidence from the trace fossil record. *Palaios*, v. 20, No. 4, p. 321-347.
- Burchette, T.P. and Wright, V.P. 1992. Carbonate ramp depositional systems. *Sedimentary Geology*, v. 79, p. 3-57.
- Butler, G.P, Harris, P.M. and Kendall, C.G.St.C. 1982. Recent evaporites from the Abu Dhabi coastal flats. *In: Depositional and Diagenetic Spectra of Evaporites - a Core Workshop*. C.R. Handford, R.G. Loucks and C.R. Davies (eds.). Society of Economic Paleontologists and Mineralogists, Core Workshop No. 3, p. 33-64.
- Cadée, G.C., 1998. Intertidal fauna and vegetation. In Eisma, D. (Ed.). *Intertidal deposits: river mouths, tidal flats and coastal lagoons*. Marine Science Series. CRC Press, Boca Raton, FL p. 383-438.
- Callaway, J.M. and Brinkman, D.B. 1989. Ichthyosaurs (Reptilia, *Ichthyosauria*) from the Lower and Middle Triassic Sulphur Mountain Formation Wapiti lake area, British Columbia, Canada. *Canadian Journal of Earth Sciences*, v. 26, p. 1491-1500.
- Campbell, C.V., Dixon, R.J. and Forbes, D.M. 1989. Updip erosional truncation of Halfway and Doig shoreline sequences: a new model for exploration in west central Alberta (Abstract). In: *Exploration Update 1989 – Integration of Technologies, Program and Abstracts*. Canadian Society of Petroleum Geologists Convention, Calgary, Alberta, p. 138.
- Campbell, C.V. and Hassler, G. 1989. Stratigraphy and facies of the Triassic Halfway and Doig Formations in west-central Alberta. *C.S.P.G. Reservoir, Abstract*, v.16, p. 2.

- Cant, D.J. 1986. Hydrocarbon trapping in the Halfway Formation (Triassic), Wembley Field, Alberta. *Bulletin of Canadian Petroleum Geology*, v. 34, p. 329-338.
- Cant, D.J., 1988. Regional structure and development of the Peace River Arch, Alberta: A Paleozoic failed-rift system? *Bulletin of Canadian Petroleum Geology* 36, 284-295.
- Cant, D. J., 2004. Subsurface facies analysis: Facies models response to sea level change. Edited by Walker R. and James N, p.27-46.
- Caplan, M.L., and Moslow T.F., 1997. Tectonic controls on preservation of Middle Triassic Halfway reservoir facies, Peejay Field, Northeastern British Columbia: a new hydrocarbon exploration model, *in* Moslow, T.F., and Wittenberg, J., eds., *Triassic of the Western Canada Sedimentary Basin*: *Bulletin of Canadian Petroleum Geology*, v. 45, p. 434-460.
- Caplan, M.L. and Moslow, T.F.1999. Depositional origin and facies variability of a Middle Triassic barrier island complex, Peejay Field, northeastern British Columbia. *American Association of Petroleum Geologists Bulletin*, v. 83, p. 128-154.
- Carlson, S.J., 1991. A phylogenetic perspective on articulate brachiopod diversity and the Permo-Triassic extinction. In: E. Dudley, Editor, *The Unity of Evolutionary Biology*, Proceedings of the 4th International Congress of Systematic and Evolutionary Biology, Dioscorides Press, Potland (1991), pp. 119-142.
- Catuneanu O., Abreu V., Bhattacharya J.P., Blum M.D., Dalrymple R.W., Eriksson P.G., Fielding C.R., Fisher W.L., Galloway W.E., Gibling M.R., Giles K.A., Holbrook J.M., Jordan R., Kendall C.G.St.C., Macurda B., Martinsen O.J., Miall A.D., Neal J.E., Nummedal D., Pomar L., Posamentier H.W., Pratt B.R., Sarg J.F., Shanley K.W., Steel R.J., Strasser A., Tucker M.E., and Winker C., 2008. Towards the standardization of sequence stratigraphy. In: *Earth-Science Reviews* 92 (2009) p. 1-33.
- Cecil, C.B., 2004. Eolian dust and the origin of sedimentary chert. Open-File Report, No.1089, USA Geological survey p. 11.
- Clark, D. R., 1961. Primary Structures of the Halfway sand in the Milligan Creek oil Fields, British Columbia; *J. Alberta Society of Petroleum Geology*, v. 9, no. 4 p. 109. Cockford, M. B. B., 1949. Geology of the Ribbon Creek area, Alberta, Res. Council Alberta, Rept. 42.

- Clifton, E. 1967. Solution-collapse and cavity filling in the Windsor Group, Nova Scotia, Canada. *Geological Society of America Bulletin*, v. 78, p. 819-832.
- Collier, R. E. L., Leeder, M. R., and Maynard, J. R., 1990. Transgressions and regressions; a model for the influence of tectonic subsidence, deposition and eustasy, with application to Quaternary and Carboniferous examples. *Geological Magazine*; v. 127; no. 2; p. 117-128.
- Creaney S. and Allan J. 1990. Hydrocarbon generation and migration in the Western Canadian Sedimentary Basin. In *Classical Petroleum Provinces* (ed. J. Brooks); Geological Society Special Publication. 50,189-202.
- Davies, G.R., 1997a. The Triassic of the Western Canada Sedimentary Basin: tectonic and stratigraphic framework, paleogeography, paleoclimate and biota, *in* Moslow, T.F., and Wittenberg, J., eds., *Triassic of the Western Canada Sedimentary Basin: Bulletin of Canadian Petroleum Geology*, v. 45, p. 434-460.
- Davies, G.R., 1997b. Aeolian sedimentation and bypass, Triassic of Western Canada, *in* Moslow, T.F., and Wittenberg, J., eds., *Triassic of the Western Canada Sedimentary Basin: Bulletin of Canadian Petroleum Geology*, v. 45, p. 624-642.
- Davis, H.R. and Byers, C.W., 1989. Shelf sandstones in the Mowry shale: evidence for deposition during Cretaceous sea level falls: *Journal of Sedimentary Petrology*, v59, p. 548-560.
- Dawson, G.M., 1881. Report on the exploration from Port Simpson on the Pacific Coast to Edmonton on the Saskatchewan, embracing a portion of the Northern part of British Columbia and the Peace River country. *Geol. Nat. Hist. Surv., Canada, Report of Progress 1879-80, part B*, p. 1-177.
- DeCelles, P.G., and Giles, K.A., 1996. Foreland Basin System. *Basin Res.* 8, p. 105-125. p. 432-453.
- Dixon, J. 1999. Isopach maps of Triassic units in the Trutch (94-G) map area (Central Forelands Natmap). Geological Survey of Canada Open File 3765.
- Dixon, J., 2002a. A modification of Wittenberg's model for the deposition of thick sandstone bodies in the Triassic Doig Formation, Wembley area, west-central Alberta: *Bulletin of Canadian Petroleum Geology*, v. 50, p. 393-406.

- Dixon, J., 2002b (Abstract). A regional unconformity associated with the Middle Triassic Halfway Formation, Western Canada Sedimentary Basin. Canadian Society of Petroleum Geologists, Annual Convention 2002, Program and Abstracts, p.111.
- Dixon, J. 2002c. Triassic stratigraphy in the subsurface of the Trutch (94-G) map-sheet, northeast British Columbia, Central Foreland Natmap Project. Geological Survey of Canada Open File 3465.
- Dixon, J. 2002d. Regional correlations within the Triassic Doig, Halfway and lower Charlie Lake formations, Western Canada Sedimentary Basin. Geological Survey of Canada, Open File 3908 (CD).
- Dixon, J. 2004. Evidence for a major unconformity in Middle Triassic strata (Doig, Halfway and lowermost Charlie Lake formations) of the Grande Prairie area (map-sheet 84M: Townships 70 to 80, Ranges 1W6 to 13W6) west-central Alberta. Geological Survey of Canada, Open File 1580 (CD).
- Dixon, J., 2005. A major unconformity at the of the Upper Triassic Charlie Lake Formation in the Western Canada Sedimentary Basin:area, Bulletin of Canadian Petroleum Geology, v. 53, p. 432-453.
- Dixon, J. 2007. Regional facies trends in the lowermost beds of the Upper Triassic Charlie Lake Formation, in the subsurface of western Canada. Bulletin of Canadian Petroleum Geology, v. 55, p. 1–20.
- Dixon, J. 2008. Triassic stratigraphy in the subsurface of the plains area of Dawson Creek (93P) and Charlie Lake (94A) map-sheets, northeast British Columbia
- Dott, H.R. 1983. 1982 SEPM Presidential Adress: Episodic Sedimentation – How Normal is Average? How Rare is Rare? Does it Matter? Journal of Sedimentary Petrology 53, p. 5-23.
- Dowling, D.B., 1907. Report on the Cascade Coal Basin, Alberta; Geol. Surv. Can., Publ. 949, p. 37.
- Duke, W.L., 1985. Hummocky cross stratification, tropical Hurricanes, and intense winter storms: Sedimentology, v. 32, p. 167-194.
- Duke, W.L., 1990. Geostrophic circulation or shallow marine turbidity currents? The dilemma of paleoflow patterns in storm-influenced prograding shoreline systems: Journal of Sedimentary Petrology v. 60, p. 870-883.

- Duke, W.L., Arnott, R.W., and Cheel, R.J., 1991. Shelf sandstones and hummocky cross stratification; new insights on a stormy debate: *Geology*, v. 19, p. 625-628.
- Dunham, R.J. 1962. Classification of carbonate rocks according to depositional textures. In: *Classification of carbonate rocks*. W.E. Ham (ed.). American Association of Petroleum Geologists, Memoir 1, p. 108-121.
- Eberli, G. P., 1991a. Carbonate turbidite sequences deposited in rift-basins of the Jurassic Tethys Ocean (eastern Alps, Switzerland). *Sedimentology*, 34:363-388.
- Eberli, G.P., 1991b. Calcareous turbidites and their relationship to sea-level fluctuations and tectonism. In: Einsele, G., Ricken, W. A. and Seilacher, A., *Cycles and events in Stratigraphy*, 320-359. Dortmund: Springer-Verlag.
- Edwards, D.E., Barclay, J.E., Gibson, D.W., Kvill, G.E., and Halton, E., 1994. Triassic strata of the Western Canada Sedimentary Basin. In: *Geological Atlas of the Western Canada Sedimentary Basin*. G.D. Mossop and I. Shetsen (comps). Canadian Society of Petroleum Geologists and Alberta Research Council, p. 257–275.
- Einsele, G and Seilacher, A. 1991. Distinction of tempestites and turbidites. *In: Cycles and Events in Stratigraphy*. G. Einsele, W. Ricken and A. Seilacher (eds). Springer-Verlag, p. 377-382.
- Ekdale, A.A., 1988. Pitfalls of paleobathymetric interpretations based on trace fossil assemblages. *Palaios*, 3, p. 464-472.
- Embry, A.F., and Gibson, D.W., 1995. T-R sequences analysis of the Triassic succession of Western Canada Sedimentary Basin. In: *Proceedings of the Oil and Gas Forum '95 – Energy from Sediments*. J. S. Bell, T.D. Bird, T.L. Hiller and P.L. Greener (eds). Geological Survey of Canada, Open file 3058, p. 25–28.
- Erwin, D.H., 1993. *The Great Paleozoic Crisis*, Columbia University Press, New York (1993).
- Erwin, D.H., 1994. The Permo-Triassic extinction, *Nature* 367 (1994), pp. 231–236.
- Erwin, D.H., and Hua-Zhang, P., 1996. Recoveries and radiations: gastropods after the Permo-Triassic mass extinction, *in* Hart, M.B. ed., *Biotic recovery from mass extinction events: Geological Society Special Publication*, v. 102, p. 223–229.

- Evans, G., Schmidt, V., Bush, P. and Nelson, H. 1969. Stratigraphy and geologic history of the Sabkha, Abu Dhabi, Persian Gulf, *Sedimentology*, 12, 145-159.
- Evoy, R.W., 1997. Lowstand shorefaces in the Middle Triassic Doig Formation: Implications for hydrocarbon exploration in the Fort St. John area, northeastern British Columbia. In: Moslow, T.F., Wittenberg, J. (Eds.). *Triassic of the Western Canada Sedimentary Basin*, *Bulletin of Canadian Petroleum Geology*, 45, p. 525-537.
- Evoy, R.W. 1995. *The Role of Sediment Bypassing In Siliclastic Facies Variability on the Continental Shelf: Examples from the Fraser River delta foreslope and the Middle Triassic Doig Formation*. Ph.D thesis, University of Alberta, Edmonton, Alberta, 452 p.
- Evoy, R.W. and Moslow, T.F. 1995. Lithofacies associations and depositional environments in the Middle Triassic Doig Formation, Buick Creek Field, northeastern British Columbia. *Bulletin of Canadian Petroleum Geology*, v. 43, p.461-475.
- Evoy, R.W., Moslow, T.F., 1996. Lithofacies associations and depositional environments in the Middle Triassic Doig Formation, Buick Creek field, northeastern British Columbia. *Bulletin of Canadian Petroleum Geology* 43, p. 461-475.
- Fedorov, Yu.N., Ivanov, K.S., Erokhin, Yu. V., and Ronkin Yu. L., 2007. Inorganic Geochemistry of the Oil of West Siberia: First ICP-MS Data. *Doklady Earth Sciences*, v.414, p. 634-637.
- Fefchak, C. 2011. *Sedimentology of the Charlie Lake Formation*. MSc thesis University of Alberta, Edmonton, p. 1-128.
- Ferri , F., and Zonneveld, J-P., 2008. Were Triassic rocks of the Western Canada Sedimentary Basin deposited in a foreland? *Source: Reservoir* [1484-2238] yr: 2008 vol:35 iss:10 p.12-14.
- Forstner, U. and Muller, G., Reineck, H. E. 1968. Sedimente und Sedimentgefuge des Rheindeltas im Bodensee. *Neues Jahrb. Mineral, Abhandl*, v. 109, p.33-62.
- Frey, R.W. and Pemberton, S.G. 1985. Biogenic structures in outcrops and cores I— approaches to ichnology: *Bulletin of Canadian Petroleum Geology*, v. 33, p. 72–115.
- Frey, R.W., Pemberton, G.S., Saunders, T.D., 1990. Ichnofacies and bathymetry: a passive relationship. *Journal of Paleontology*, 64, 1, p. 155-158.

- Fryberger, S.G, Ahlbrandt, T.S., and S. Andrews, 1979. Origin, sedimentary features, and significance of low-angle eolian "sand sheet" deposits, Great Sand Dunes National Monument and vicinity, Colorado. *Journal of Sedimentary Petrology*, v.49, p. 733-746.
- Fu, S. and Werner, F. 2000. Distribution, ecology and taphonomy of the organism trace, *Scolicia*, in northeast Atlantic deep-sea sediments: *Paleogeography, Paleoclimatology, Paleoecology*, v. 156, p. 289-300.
- Gibson, D.W., 1965. Triassic Stratigraphy near the Northern Boundary of Jasper National Park, Alberta; Geological Survey of Canada, Paper, p. 64-9.
- Gibson, D.W., 1968a. Triassic Stratigraphy between the Athabasca and Smoky Rivers of Alberta; Geological Survey of Canada, Paper, p. 67-65.
- Gibson, D.W., 1968b. Triassic Stratigraphy between the Athabasca and Brazeau Rivers of Alberta; Geological Survey of Canada, Paper, p. 68-11.
- Gibson, D.W., 1969. Triassic Stratigraphy of the Bow River-Crowsnest Pass Region, Rocky Mountains of Alberta and British Columbia; Geological Survey of Canada, Paper, p. 68-29.
- Gibson, D.W., 1970. Triassic Stratigraphy, Pine Pass Area, Northeastern British Columbia; Edmonton Geological Society, Field Conference Guidebook, p. 23-28.
- Gibson, D.W., 1971. Triassic Stratigraphy of the Sikanni Chief River-Pine Pass Region, Rocky Mountain Foothills, Northeastern British Columbia; Geological Survey of Canada, Paper, p. 70-31.
- Gibson, D.W., 1972. Triassic stratigraphy of the Pine Pass–Smoky River area, Rocky Mountain Foothills and Front Ranges of British Columbia and Alberta: Geological Survey of Canada, Paper, p. 71–30.
- Gibson, D.W., 1974. Triassic Rocks of the Southern Canadian Rocky Mountains: Geological Survey of Canada, Paper, p. 71–30.
- Gibson, D.W., 1975. Triassic rocks of Rocky Mountain Foothills and Front Ranges of northeastern British Columbia and west-central Alberta: Geological Survey of Canada, Bulletin no. 247, p. 1–61.
- Gibson, D.W., and Barclay, J.E., 1989. Middle Absaroka Sequence, The Triassic stable craton, *in* Ricketts, B.E., ed., *Western Canada Sedimentary Basin: Canadian Society of Petroleum Geologists, Special Publication 30*, p. 219-232.

- Gibson, D. W., and Edwards, D. E., 1990a. Triassic stratigraphy of the Williston Lake area, northeastern British Columbia. Field Trip Guide, Basin Perspectives, 1990. Canadian Society of Petroleum Geologists Convention, Calgary, p. 75.
- Gibson, D. W., and Edwards, D. E., 1990b. An overview of Triassic stratigraphy and depositional environments in the Rocky Mountain Foothills and Western Interior Plains, Peace River Arch area, northeastern British Columbia. Bulletin of Canadian Petroleum Geology, v.38A, p. 146-158.
- Gibson, D.W., 1993. Upper Triassic Coquina Channel Complexes, Rocky Mountain Foothills, Northeastern British Columbia: Bulletin of Canadian Petroleum Geology, v. 41, no.1, p. 59.
- Gingras, M.K., Mac Eachern, J.A., and Pemberton, S.G., 1998. A comparative analysis of the Ichnology of wave- and river-dominated allomembers of the Upper Cretaceous Dunvegan Formation: Bulletin of Canadian Petroleum Geology, vol.46, No 1 (March, 1998), p. 51-73.
- Glennie, K.W., and A.T. Buller, 1983. The Permian Weisslied of NW Europe: the partial deformation of aeolian dune sands caused by the Zechstein Transgression. Sedimentary Geology, v. 35, p. 43-81.
- Golonka, J., Ross, M.I. and Scotese, C.R., 1994. Phanerozoic and paleogeographic and paleoclimate modeling maps. In: Pangea: Global Environments and Resources. A.F. Embry, B. Beauchamp and D. Glass (eds.). Canadian society of Petroleum Geologists, Memoir 17, p. 1-47.
- Habicht, J.K.A., 1979. Paleoclimate, paleomagnetism, and continental drift. A.A.P.G. Studies in Geology 9, 1-29.
- Hamblin, A.P. and Walker, R.G. 1979. Storm dominated shallow marine deposits: the Fernie-Kootenay (Jurassic) transition, southern Rocky Mountains. Canadian Journal of Earth Sciences, v. 16, p. 1673-1690.
- Hagan, G.M., Logan, B.W., 1975. Recent tidal deposits, Abu Dhabi, U.A.E Arabian Gulf. In: Ginsberg, R.N. (Ed.). Tidal Deposits: a Casebook of Recent Examples and Fossil Counterparts. Springer, Berlin, p. 209-214.
- Haq, B.V., Hardenbol, J., Vail, P.R., Colin, J.P., Ioannides, N., Stonver, L.E., Jan DuChene, R., Wright, R.C., Sarq, J.F., and Morgan, B.E., 1987. Mesozoic-Cenozoic Cycle Chart, Version 3.1B, American Association Petroleum Geologists.
- Hardie, L.A., and Shinn, 1986. Carbonate depositional environments, modern and ancient. Part 3: tidal flats: Colorado School of Mines, Quarterly, v. 81, p. 74.

- Harms, J.C., Southard, J.B., Spearing, D.R., and Walker, R.G., 1975. Depositional environments as interpreted from primary sedimentary structures and stratification sequences: Society of Economic Paleontologists and Mineralogists, Short Course 2, p. 161.
- Harms, J.C. 1979. Primary sedimentary structures. *Annual Review of Earth and Planetary Science*, v. 7, p. 227-248.p. 579-595.
- Harms, J.C., Southard, J.B., and Walker, R.G, 1982. Structures and sequences in clastic rocks. S.E.P.M. Short Course No. 9.
- Harris, R.G. and Bustin, M.R. 2000. Diagenesis, reservoir quality, and production trends of the Doig Formation sand bodies in the Peace River area of Western Canada. *Bulletin of Canadian Petroleum Geology*, v. 48, p. 339-359.
- Heller, P.L., Anderson, D.L., and Angevine, C.L. 1996. Is the Middle Cretaceous pulse of rapid sea-floor spreading real or necessary? *Geology*; v. 24; no. 6; p. 491-494.
- Henderson, C.M. 1989. Absaroka Sequence - The Lower Absaroka Sequence: Upper Carboniferous and Permian. In: *Western Canada Sedimentary Basin - A Case History*. B.D. Ricketts (ed.). Canadian Society of Petroleum Geologists, Special Publication No. 30, Calgary, Alberta, p. 203-217.
- Hess, E.B. 1968. Charlie Lake study - correlation and nomenclature. British Columbia Ministry of Energy, Mines and Petroleum Resources, Petroleum Resources Branch, Assessment Report 1970 (7 cross sections), 31p.
- Higgs, R., 1990. Sedimentology and petroleum geology of the Artex Member (Charlie Lake Formation), northeastern British Columbia. Abstracts, Canadian Society of Petroleum Geologists Convention, Calgary, Alberta, May 27-30, 1990, *Bulletin of Canadian Petroleum Geology*, v. 38, p. 166.
- Hips, K. 1998. Lower Triassic storm-dominated ramp sequence in northern Hungary: an example of evolution from homoclinal through distally steepened ramp to Middle Triassic flat-topped platform. In: *Carbonate Ramps*. V.P. Wright and T.P. Burchette (eds.). Geological Society, London, Special Publication 149, p. 315-338.
- Howard, J.D., and Frey, R.W., 1984. Characteristic trace fossils in nearshore to offshore sequences, Upper cretaceous of east and central Utah: *Canadian Journal of Earth Sciences*, 21: p. 200-219.

- Hunt, A.D., and RATCLIFFE, J.D., 1959. Triassic Stratigraphy, Peace River area, Alberta and British Columbia, Canada; *Bulletin of American Association of Petroleum Geology*, v.43, p. 563-589
- Hunter, R.E. 1977. Basic types of stratification in small eolian dunes. *Sedimentology*, v.24, p. 361-387.
- Hunter, R.E. 1981. Stratification styles in eolian sandstones: some Pennsylvanian to Jurassic examples from the western interior U.S.A. In: *Recent and ancient nonmarine depositional environments*. F. Ethridge and R.M. Flores (eds.). Society of Economic Paleontologists and Mineralogists Special Publication 31, p. 315-330.
- Hunter, R.E., 1990. A primer on eolian fine structures. In: *Ancient eolian and erg-migration deposits*, 1990 SEPM Field Guidebook, Chan, M.A., Loope, D.B., and R. Hunter (Eds.) p. 4-12.
- Irish, E.J.W., 1951. Pierre Greys Lakes Map-Area, Alberta; Geological Survey of Canada, Mem. 258.
- Irish, E.J.W., 1954. Kvass Flats, Alberta; Geological Survey of Canada, Mem. 334.
- Irish, E.J.W., 1965. Geology of the Rocky Mountain Foothills, Alberta. Geological Survey of Canada, Paper 69-11, p. 154.
- Irish, E.J.W., 1970. Halfway River Map area, British Columbia. Geological Survey of Canada, Paper 69-11, p. 154.
- James, N. P., and Kendall A. C., 1992. Introduction to carbonate and evaporate facies models: Facies models response to sea level change. Edited by Walker R. and James N., p.265-276.
- Johnstone, H.D., and Baldwin, C.T., 1986. Shallow siliciclastic seas. In H.G. Reading (Ed.), *Sedimentary Facies and Environments* (Second edition), p. 229-282.
- Johns, M.J., Barnes, C.R., and Orchard, M.J., 1997. Taxonomy and biostratigraphy of Middle and Upper Triassic elasmobranch ichthyoliths from northeastern British Columbia. Geological Survey of Canada Bulletin, 502, 235 pp.
- Keller, M. 1997. Evolution and sequence stratigraphy of an Early Devonian carbonate ramp, Cantabrian Mountains, Northern Spain. *Journal of Sedimentary Research*, v. 67, p. 638-652.
- Kendall, C.G., and Skipwith, P.A., 1969. Geomorphology of a recent shallow-water carbonate province: Khor Al Bazam, Trucial Coast, southwest Persian Gulf: *Geological Society of America Bulletin*, v.80, p. 865-892.

- Kindle, E. D., 1924. Standard Paleozoic section of the Rocky Mountains near Banff, Alberta; *Pan-American Geol.*, v 42.
- Kirstan-Tollmann, V.E., and Tollmann, A., 1982. Die Entwicklung der Tethystrias und Herkunft ihrer Fauna. The development of the Triassic within the Tethys realm and the origin of its faunas. *Geol. Rundschau*, v 71, no. 3, p. 987-1019.
- Kocurek, G., 1981, Significance of interdune deposits and bounding surfaces in aeolian dune sands. *Sedimentology*, v.28, p. 753-780
- Krapf, C., 2003. Ephemeral river systems at the Skeleton Coast, NW-Namibia: Dissertation zur Erlangung des naturwissenschaftlichen Doktorgrades der Bayerischen Julius-Maximilians-Universität Würzburg.
- Lambe, L. M., 1916. Ganoid fishes from near Banff, Alberta; *Trans. Roy. Soc. Can.*, Ser. 3, sec. 4, v. 10, p. 37-38.
- Laudon, L.R., Deidrick, E., Hamilton, W.B., Lewis, P.J., McBee, W., Spreng, A.C., and Stoneburner, R., 1949. Devonian and Mississippian Stratigraphy, Wapiti Lake Area, British Columbia; *Edmonton Geological Society, Field Conference Guidebook*, p. 1-14.
- Longerich, H.P., Jenneer, G. A., Fryer, B. J., and Jackson, S. E., 1990. Inductively coupled plasma-mass spectrometric analysis of geological samples: a critical evaluation based on case studies: *Chemical Geology*, v. 83, p.105-118.
- Macauley, G., Procter, R.M. and Tisdall, W.H. 1964. Carboniferous In: *Geological History of Western Canada*, R.G. McCrossan and R.P. Glaister (eds.). Alberta Society of Petroleum Geologists, Calgary, Alberta, p. 89-102.
- MacEachern, J.A., Pemberton, G. S., Gingras, M.K. and Bann, K.L. 2007. The Ichnofacies Paradigm: Fifty-Year Retrospective. In Miller, W. III (ed), *Trace Fossils: Concepts, Problems, Prospects*, p. 52-77.
- Maliva, R., and Siever, R., 1989. Nodular Chert Formation in Carbonate Rocks. *The Journal of Geology*, Vol. 97, No. 4 (Jul., 1989), pp. 421-433.
- Manspeizer W., 1994. The breakup of Pangea and its impact on climate: consequences of Variscan–Alleghanide orogenic collapse. In: G.D. Klein, Editor, *Pangea: Paleoclimate, Tectonics, and Sedimentation During Accretion, Zenith, and Breakup of a Supercontinent*, Boulder, Geological Society of America Special Paper vol. 288 (1994), pp. 169–185.

- Manko, E. M., 1960. The Triassic of the Rock Lake Area. In: Rock Lake, Second Annual Field Trip Guide Book, Edmonton Geological Society, p. 25.
- McBride, AntarAbdel-Wahab and Ahmed Reda M. El-Younsy, 1999. Origin spheroidal chert nodules, Drunka Formation (Lower Eocene), Egypt. *Journal of Sedimentology* Vol46, Issue 4PP733
- McConnell R.G., 1887. Report on the geological structure of the Rocky Mountains; *Geol. Nat. Hist. Surv. Canada, Ann. Rept. 1886, Pt D.*
- McConnell R.G., 1891. Report on a portion of the District of Athabasca comprising the country between Peace River and the Athabasca River north of Lesser Slave Lake; *Geological Survey of Canada, Ann. Rept. v. V, part I, part D.*
- McLearn, F.H., 1930. A preliminary study of the faunas of the Upper Triassic Schooler Creek Formation, western Peace River, B.C. *Transactions of the Royal Society of Canada, series 3, section 4, v. 24, p. 13–19.*
- McLearn, F.H., 1937. Contributions to the Triassic of Peace River: *Canadian Field Naturalist, v. 51, p. 127–131.*
- McLearn, F.H., 1940a. Triassic of Beattie Hill, Peace River Foothills. B.C.: *The Canadian Field Naturalist, v. 54, p. 79–82.*
- McLearn, F.H., 1940b. Preliminary study of Triassic pelecypods and ammonoids from the Peace River Foothills. B.C.: *The Canadian Field Naturalist, v. 54, p. 111–116.*
- McLearn, F.H., 1941a. Triassic stratigraphy of Brown Hill, Peace River Foothills, B.C.: *Transactions of the Royal Society of Canada, v. 55, p. 93–104.*
- McLearn, F.H., 1941b. Triassic stratigraphy, Mahaffy Cliffs to Red Rock Spur, Peace River Foothills, B.C.: *Canadian Field Naturalist, v. 55, p. 95–100.*
- McLearn, F.H., and Kindle, E.D., 1950. *Geology of northeastern British Columbia Geological Survey of Canada, Memoir, 259.*
- McLearn, F. H., 1953. Correlations of the Triassic formations of Canada. *Bulletin of the Geological Society of America, v. 64, p. 1205-1228.*
- Middleton, G., 1961. Evaporite solution breccias from the Mississippian of southwest Montana. *Journal of Sedimentary Petrology, v. 31, p. 189-195.*
- Mitchum, R.M., and Van Wagoner, J.C., 1991. High frequency sequences and their stacking patterns: sequence-stratigraphic evidence of high-frequency eustatic cycles. *Sedimentary Geology, v. 70, p. 131-160.*
- Mosher, L.C. 1973. Triassic conodonts from British Columbia and the northern Arctic Islands. *Geological Survey of Canada. Bulletin 222, p. 141-193.*

- Moslow, T.F., and Davies, G.R., 1992. Triassic reservoir facies and exploration trends: Western Canada Sedimentary Basin: Short course guide, Environments of Exploration 1992, Canadian Society of Petroleum Geology Convention, Calgary, p. 166.
- Moslow and Davies 1997. The Upper Triassic Baldonnel and Pardonet formations, Western Canada Sedimentary Basin. In: Triassic of the Western Canada Sedimentary Basin. T.F. Moslow and J. Wittenberg (eds.). Bulletin of Canadian Petroleum Geology, v. 45, p. 643-674.
- Mountjoy, E. W., 1960. Structure and stratigraphy of the Miette and adjacent areas, eastern Jasper National Park, Alberta; Univ. of Toronto, Ph. D, thesis.
- Nelson, C.H., 1982. Modern shallow-water graded sand layers from storm surges, Bering Shelf: a mimic of Boma sequences and turbidite systems. Journal of Sedimentary Petrology, v. 52 p. 537-545. Nio, S.D. and Yang, C. 1991. Diagnostic attributes of clastic tidal deposits. In. Clastic tidal sediments (Smith, D.G., Reinson, G.E. Zaitlin, B.A. and Rahmani, R.A. eds) Canadian Society of Petroleum Geologists Memoir 16, p. 3-28.
- North, C.P., Hole, M.J., Jones, D.G., 2005. Geochemical correlation in deltaic successions: A reality check. Geological Society of America Bulletin, v. 117, p. 620-632.
- O'Connell, S.C., Dix, G.R., and Barclay, J.E. 1990. The origin, history, and regional structural development of the Peace River Arch, Western Canada. Bulletin of Canadian Petroleum Geology, v. 38A, p. 4-24.
- Orchard, M.J. 1983. Epigondolella populations and their phylogeny and zonation in the Norian (Upper Triassic). Fossils and Strata, no. 15, p. 177-192.
- Orchard, M.J. 1991. Upper Triassic conodont biochronology and new index species from the Canadian cordillera. In: Ordovician to Triassic Conodont Paleontology of the Canadian Cordillera. M.J. Orchard and A.D. McCracken (eds.). Geological Survey of Canada Bulletin 417, p. 299-335.
- Orchard, M.J. and Tozer, E.T., 1997. Triassic conodont biochronology, its calibration with the ammonoid standard, and biostratigraphic summary for the Western Canada Sedimentary Basin. Bulletin of Canadian Petroleum Geology, v. 45, p. 675-692.
- Orchard, M.J. and Rieber, H., 1998. Multielement *Neogondolella* (Conodonta, Upper Permian-Middle Triassic). Proceedings of ECOS7, Bologna-

Modena, Italy, June 1998. Bollettino della Societa Palaeontologica Italiana, v. 37, no.2-3: p. 475-488.

Orchard, M.J., 2009. Report on 33 (23 productive) microfossil samples submitted for analysis by D. Nordheimer (2008) Mount Robson map area (83 E/07/08), British Columbia. Geological Survey of Canada, Paleontological Report Number 10-MJO-2009, 18 pp.

Pearce, T.J. et al. 1999. Chemostratigraphy: a method to improve interwell correlation in barren sequences — a case study using onshore Duckmantian/Stephanian sequences West Midlands, U.K.). Journal of Sedimentary Geology. 124, 197-220.

Pelletier, B.R. 1960. Triassic stratigraphy, Rocky Mountain Foothills, northeastern British Columbia 94J and I. Geological Survey of Canada, Paper 60-2.

Pelletier, B.R. 1961. Triassic stratigraphy of the Rocky Mountains and Foothills, northeastern British Columbia. Geological Survey of Canada, Paper 61-8.

Pelletier, B. R., 1963. Triassic stratigraphy of the Rocky Mountains and Foothills, Peace River district, British Columbia. Geological Survey of Canada Paper 62-26.

Pelletier, B.R. 1964. Triassic stratigraphy of the Rocky Mountain Foothills between Peace and Muskwa rivers, northeastern British Columbia, Geological Survey of Canada, Paper 63-33.

Pelletier, B. R., 1965. Paleocurrents in the Triassic northeastern British Columbia. In Middleton, G.V. (Ed.), Primary sedimentary structures and their hydrodynamic interpretation. Society of Economic Palaeontologists and Mineralogists Special Publication No. 35 Tulsa, p. 237 -259 Geological Survey of Canada Paper 62-26.

Pemberton, S.G., and Frey, R.W., 1984. Ichnology of storm-influenced shallow marine sequence; Cardium Formation (Upper Cretaceous) at Seebe, Alberta. In D.F. Stott and D.L. Glass (Eds.), the Mesozoic of middle North America. CSPG Memoir 9, p. 281-304.

Pemberton, S.G. and Frey, R. W. 1985. The *Glossifungites* ichnofacies: modern examples from the Georgia coast, USA In: Curran, H.A. (ed.) *Biogenic Structures: Their Use in Interpreting Depositional Environments*. Society of Economic Paleontologists and Mineralogists, Special Publications, Tulsa, Oklahoma, 35, p. 237-259.

Pemberton, S.G., Ranger, M.J., and MacEachern, J.A., 1992a. The conceptual framework of ichnology: In S.G Pemberton ed., Application of Ichnology

Petroleum Exploration, A Core Workshop. Society of Economic Paleontologists and Mineralogists, Core Workshop Notes 17: 1-32.

- Pemberton, S.G., MacEachern, J.A., and Ranger, M.J., 1992b. Ichnology and event stratigraphy: The use of trace fossils in recognizing tempestites: In S.G Pemberton ed., Application of Ichnology to Petroleum Exploration, A Core Workshop. Society of Economic Paleontologists and Mineralogists, Core Workshop Notes 17: 85-117.
- Pemberton, S.G., Spila, M., Pulham, A., Saunders, T., MacEachern, J., Robbins, D. and Sinclair, I. 2001. *Ichnology and Sedimentology of Shallow and Marginal Marine Systems: Ben Nevis and Avalon Reservoirs, Jean D' Arc Basin*. Geological Association of Canada, St John's, Newfoundland, Short Course Notes, 15.
- Perlmutter, M.A. and Matthews, M.D., 1990. Global cyclostratigraphy - a model. In Cross, T.A. (Ed.) *Quantitative Dynamic Stratigraphy*. Prentice Hall, 233-260
- Price, R. A. and Ollerenshaw, N. C., 1971. Geology, Scalp Creek (East and West), Alberta, Geol. Surv. Can., Maps 1275A, 1276A.
- Pye, K. and Tsoar, H. 1990. Aeolian Sand and Sand Dunes; London, *Unwin Hyman Ltd.*, 396 pages.
- Qi, Fazheng, 1995. Seismic stratigraphy and sedimentary facies of the Middle Triassic strata, Western Canada Sedimentary Basin, northeastern British Columbia. Unpublished PhD thesis, University of Alberta, Edmonton, 219p.
- Rahman, B. and Henderson, M. 2005. The Nature and Significance of Erosional Surfaces in the Middle Triassic Doig and Halfway Formations, WCSB. CSPG Core Conference, Core Papers and Abstracts, June 23-24, 2005, Calgary, Alberta, p. 298.
- Raup, D.M., 1979. Size of the Permo-Triassic bottleneck and its evolutionary implications. *Science*, v. 206, p. 217-218
- Ratcliffe, K. T., Wright, A. M., Hallsworth, C., Morton, A., Zaitlin, B.A., Potocki, D., and Wray, D.S., 2004. An example of alternative correlation techniques in a low-accommodation setting, nonmarine hydrocarbon system: The (Lower Cretaceous) Mannville Basal Quartz succession of southern Alberta. *AAPG Bulletin*, v. 88, p. 1419-1432.
- Ratcliffe, K. T., Martin, J., Pearce, T.J., Hughes, A.D., Lawton, D.E., Wray D.S., and Bessa, F., 2006. A regional chemostratigraphically-defined correlation framework for the late Triassic TAG-I Formation in Blocks 402 and 405a, Algeria. *Petroleum Geoscience*, v. 12, p. 3-12.

- Reading, H.G. and Collinson, J.D. 1996. Clastic Coasts. In: Sedimentary environments: Processes, facies and stratigraphy. H.G. Reading (ed.). 3rd edition. Blackwell Science, Oxford, p. 154-231.
- Reineck, H.E. and Singh, I.B. 1972. Genesis of laminated sand and graded rhythmites in storm-sand layers of shelf mud. *Sedimentology*, v. 18, p. 123-128.
- Reinson, G.E., 1984. Barrier-island and associated strand-plain systems: In: R.G. Walker ed., *Facies Models* second edition. Geoscience Canada, ReprintSeries 1, Geological Association of Canada, p. 119-140.
- Richards, B.C. 1989. Upper Kaskaskia Sequence: uppermost Devonian and Lower Carboniferous. In: *Western Canada Sedimentary Basin - A Case History*. B.D. Ricketts (ed.). Canadian Society of Petroleum Geologists, Special Publication no. 30, Calgary, Alberta, p. 164-201.
- Riediger, C.L., Fowler, M.G., Brooks, P.W. and Snowdon, L.R. 1990a. Lower and Middle Triassic source rocks, thermal maturation, and oil-source rock correlations in the Peace River Embayment area, Alberta and British Columbia. *Bulletin of Canadian Petroleum Geology*, v. 38A, p.218-235.
- Riediger, C., Carrelli, G. G. and Zonneveld, J-P., 2004. Hydrocarbon source rock characterization and thermal maturity of the Upper Triassic Baldonnel and Pardonet formations, northeastern British Columbia, Canada. *Bulletin of Canadian Petroleum Geology*, 52: 277-301.
- Ross, G.M., Gehrels, G.E., and Patchett, P.J., 1997. Provenance of Triassic strata in the miogeocline, western Canada, in Moslow, T.F., and Wittenberg, J., eds., *Triassic of the Western Canada Sedimentary Basin*: *Bulletin of Canadian Petroleum Geology*, v. 45, p. 461-473.
- Ruegg, D.M., and R.E. Hunter, 1985. Periglacial eolian evenly laminated sandy deposits in the Late Pleistocene of NW Europe, a facies unrecorded in modern sedimentological handbooks. In: Brookfield, M.E. and T.S. Ahlbrandt (Eds.), *Eolian Sediments and Processes*, p. 455-482.
- Schaeffer, B. and Mangus, M. 1976. An Early Triassic Fish Assemblage from British Columbia. *Bulletin of the American Museum of Natural History*, 156, p. 515-564.
- Schmaltz, J., 2010. NASA Earth Observatory; MODIS Rapid Response Team NASA GSFC. <http://earthobservatory.nasa.gov/NaturalHazards/view.php?id=45805>.
- Seilacher, A., 1967. Bathymetry of Trace Fossils. *Marine Geology*, 5, p. 413- 428

- Selwyn, A.R.C., 1877. Report on exploration in British Columbia 1875. Geological Survey of Canada; Report of Progress 1875-1876, p. 97.
- Shinn, 1983. Tidal flat. In: Scholle, P.A., Bebout, D.G., Moore, C.H. (Eds.) Carbonate Depositional Environments, 33. American Association of Petroleum Geologists, Memoir p. 171-210.
- Siberling, N. J. and Tozer, E. T., 1968. Biostratigraphic classification of the marine Triassic in North America. Geological Society of America Special Paper 110.
- Soreghan, M.J., and Soreghan, G.S. (Lynn), 2007. Whole-rock geochemistry of Upper Paleozoic loessite, western Pangaea: Implications for paleo - atmospheric circulation. Earth and Planetary Science Letters, v. 255, p. 117-132.
- Spears, D.A., Amin, M.A., 1981. A mineralogical and geochemical study of turbidite sandstones and interbedded shales, Mam Tor, Derbyshire, UK. Clay Minerals, v. 16, p. 333-345.
- Thom, B.G., Roy P.S., Short, A.D., Hudson, J., and Davis Jr. R.A., 1986. Modern coastal and estuarine environments of deposition in southeastern Australia: Guide for Excursion 4A, 12th International Sedimentological Congress, Canberra, p. 279.
- Tozer, E.T., 1961. The sequence of marine Triassic faunas in western Canada. Geological Survey of Canada Paper 61-69.
- Tozer, E.T. 1962. Illustrations of Canadian Fossils, Triassic of Western and Arctic Canada. Geological Survey of Canada, Paper 62-19, p. 1-5.
- Tozer, E.T. 1963. *Liquidates* and *Maclearnoceras*, new Triassic ammonoids from the 141 *Nathorstites* Zone of northeastern British Columbia. Geological Survey of Canada, Bulletin 96, part 2, p. 31-38.
- Tozer, E.T. 1965. Lower Triassic Stages and Ammonoid Zones of Arctic Canada. Geological Survey of Canada, Paper 65-12, p. 1-14.
- Tozer, E.T., 1967. A standard for Triassic time. Geological Survey of Canada Bulletin 156.
- Tozer, E.T., 1982. Marine Triassic faunas of North America, their significance for assessing plate and terrane movements: Geologische Rundschau v. 71, p. 1077-1104.

- Tozer, E.T., 1984. The Triassic and its ammonoids: The evolution of a time scale. Geological Survey of Canada Miscellaneous Report 35, 171p.
- Tozer, E.T., 1994. Canadian Triassic ammonoid faunas. Geological Survey of Canada, Bulletin 467, p. 663
- Utting, J., Zonneveld, J. P., MacNaughton, R. B., and Fallas K. M., 2005. Palynostratigraphy, lithostratigraphy and thermal maturity of the Lower Triassic Toad and Grayling, and Montney Formations of Western Canada, and comparisons with coeval rocks of the Sverdrup Basin, Nunavut (in Central Foreland NATMAP Project; stratigraphic and structural evolution of the Cordilleran foreland; Part 2, Lane,) Bulletin of Canadian Petroleum Geology (March 2005), 53(1): p. 5-24.
- Vail, P.R., Mitchum, R.M, Todd, R.G., Widmer, J.M., Thompson, J.M., Sangree, J.B., Bubb, J.M., and Hatlelid, W.G., 1977. Seismic stratigraphy and global changes in sealevel. In: C.W. Payton, edit., Seismic Stratigraphy-Applications to hydrocarbon exploration. American Association Petroleum Geologists, Memoir 26, p. 49-212.
- Varadi, F., Runnegar, B., and Ghil M. 2003. Successiv Refinements in Long – Term Integrations of Planetary Orbits. The Astrophysical Journal 592: 620–630.
- Veevers, J.J., 1994. Pangea: evolution of a supercontinent and its consequences for Earth's paleoclimate and sedimentary environments. In: G.D. Klein, Editor, Pangea: Paleoclimate, Tectonics, and Sedimentation During Accretion, Zenith, and Breakup of a Supercontinent, Boulder, Geological Society of America Special Paper vol. 288 (1994), pp. 13–23.
- Von Der Borch, C.C. and Lock, D., 1979. Geological significance of Coorong dolomites. Sedimentology v. 26, Issue 6, p. 813-824.
- Van Wagoner, J.C., Posamentier, H.W., Mitchum, R.M., Vail, P.R., Sarg, J.F., Loutit, T.S., Hardenbol, J., 1988, An overview of sequence stratigraphy and key definitions. In: Wilgus, C.K., Hastings, B.S., Kendall, C.G.St.C., Posamentier, H.W., Ross, C.A., Van Wagoner, J.C. (Eds.), Sea Level Changes—An Integrated Approach, vol. 42. SEPM Special Publication, pp. 39–45.
- Walker, R.G., 1984. Shelf and shallow marine sands, In: R.G. Walker (Ed.), Facies Models (2nd edition), Geoscience Canada, Reprint Series 1, p .141-170.

- Walker, R. G., and Plint A. G., 1992. Wave- and Storm-Dominated Shallow Marine Systems: Facies models response to sea level change. Edited by Walker R. and James N.P., p.219-238.
- Warren, P. S., 1927. Banff area, Alberta; Geological Survey of Canada. Mem. 153.
- Warren, P. S., 1945. Triassic faunas in the Canadian Rockies; Amer J. Sci., v. 71, p. 145-152.
- Warren, J.K. 1989. Evaporite Sedimentology. Prentice Hall Advanced Reference Series, p. 1-285.
- Wetzel, A. and Bromley, R. 1994. *Phycosiphon Incertum* Revisited: *Anconichnus Horizontalis* Is Its Junior Subjective Synonym. Journal of Paleontology, v. 68(6), p.1396-1402.
- Wignall, P.B., and Hallam, A., 1992. Anoxia as a cause of the Permian/Triassic mass extinction: Facies evidence from northern Italy and the western United States: Palaeogeography, Palaeoclimatology, Palaeoecology, v. 93, p. 21–46.
- Willis, A.J. and Moslow, T.F. 1994. Stratigraphic setting of transgressive barrier island reservoirs with an example from the Triassic Halfway Formation, Wembley Field, Alberta, Canada. American Association of Petroleum Geologists, Bulletin, v. 78, p. 775-791.
- Wilson, K.M., Hay, W.W., and Wold, C.N., 1991, Mesozoic evolution of exotic terranes and marginal seas, Western North America: Marine Geology, v. 102, p.311–361.
- Windom, H.L. and Chamberlain, C.F. 1978. Dust-storm transport of sediments to the north Atlantic Ocean. Journal of Sedimentary Petrology v. 48, p. 385-388.
- Wittenberg, J. and Moslow, T.F. 1991. Origin and variability of overthickened sandstones in the Doig Formation, west-central Alberta (Abstract). In: Opportunities for the Nineties, Program and Abstracts, 1991 Canadian Society of Petroleum Geologists Convention, Calgary, p. 146.
- Wittenberg, J. 1992. Origin and stratigraphic significance of anomalously thick sandstone trends in the Middle Triassic Doig Formation of west-central Alberta. MSc thesis University of Alberta, Edmonton, pp. 1-600.
- Wittenberg, J. 1993. The significance and recognition of mass wasting events in cored sequences, impact on the genesis of several anomalously thick sandstone bodies in the Middle Triassic Doig Formation of west-central Alberta. In: Karvonen, R., den Haan, J., Jang, K., Robinson, D., Smith,

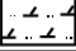

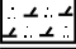
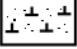
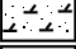
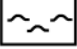

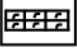

- G., Webb, T., Wittenberg, J., (Eds.). Carboniferous to Jurassic Pangea Core Workshop. Pp. 131-161.
- Wright, V.P. and Burchette, T.P. 1996. Shallow-water carbonate environments. In: Sedimentary environments: Processes, facies and stratigraphy. Reading, H.G. (ed.). 3rd edition. Blackwell Science, Oxford, p. 325-394.
- Wright, V.P. and Burchette, T.P. 1998. Carbonate ramps: an introduction. In: Carbonate Ramps. V.P. Wright and T.P. Burchette (eds.). Geological Society of London, Special Publication 149, p. 1-5.
- Young, G.R., 1997. Iconoclastic view of mid-Triassic stratigraphy, Umbach Wargen area, British Columbia, *in* Moslow, T.F., and Wittenberg, J., eds., Triassic of the Western Canada Sedimentary Basin: Bulletin of Canadian Petroleum Geology, v. 45, p. 577-594.
- Zonneveld, J-P, Moslow, T.F. and Gingras, M.K., 1997a. Sequence Stratigraphy and Sedimentary Facies of the Lower and Middle Triassic of Northeastern British Columbia: Progradational shoreface associations in a mixed carbonate siliciclastic system. Field trip guide, Sedimentary Events-Hydrocarbon Systems. 1997. Canadian Society of Petroleum Geologists - Society for Sedimentary Geology (SEPM) joint convention, Calgary, Alberta. 118p.
- Zonneveld, J-P., Moslow, T.F., and Henderson, C.M., 1997b. Lithofacies associations and depositional environments in a mixed siliciclastic-carbonate depositional system, Upper Liard Formation, Triassic, northeastern British Columbia: Bulletin of Canadian Petroleum Geology, v. 45, p. 553-575.
- Zonneveld, J.-P., 1999. Sedimentology and sequence biostratigraphic framework of a mixed siliciclastic-carbonate depositional system, Middle Triassic, northeastern British Columbia. Unpublished PhD Dissertation, University of Alberta, Edmonton, 287 pp
- Zonneveld, J-P. 2001, Middle Triassic biostromes from the Liard Formation, British Columbia, Canada: oldest examples from the Mesozoic of NM Pangea: Sedimentary Geology, v. 145, p. 317-341.
- Zonneveld, J-P, Gingras, M.K., and Pemberton, S.G., 2001. Trace fossil assemblages in a Middle Triassic mixed siliciclastic-carbonate marginal marine depositional system, British Columbia. : Palaios, Palaeogeography, Palaeoclimatology, Palaeoecology, 166, (2001) p. 249-276.

- Zonneveld, J-P., and Orchard, M.J. 2002. Stratal relationships of the Baldonnel Formation (Upper Triassic), Williston Lake, northeastern British Columbia. Geological Survey of Canada Current Research 2002-A8: 15p.
- Zonneveld, J-P., and Pemberton, S.G., 2003. Ichnotaxonomy and Behavioral Implications of Lingulide-Derived Trace Fossils from the lower and Middle Triassic of Western Canada. *Ichnos*, 10: p. 25-39.
- Zonneveld, J-P, Carrelli, G.G., and Riediger, C., 2004. Sedimentology of the Upper Triassic Charlie Lake, Baldonnel and Pardonet formations from outcrop exposures in the southern Trutch region, northeastern British Columbia. *Bulletin of Canadian Petroleum Geology*, v.52, no.4 (December, 2004), p.343-375.
- Zonneveld, J-P, Beatty, T.W., and Pemberton, S.G., 2007a. Lingulide Brachiopods and the Trace Fossil *Lingulichnus* from the Triassic of the western Canada: Implications for Faunal Recovery after the end-Permian Mass Extinction: *Palaios*, Research Report, v. 22, p. 74–97.
- Zonneveld, J-P, Henderson, C.M., Stanley Jr., G.D., Orchard, M.J., and Gingras, M.K., 2007b. Oldest scleractinian coral reefs on the North American craton; Upper Triassic (Carnian), northeastern British Columbia, Canada. *Palaeogeography, palaeoclimatology, palaeoecology* [0031-0182] vol:243 iss:3-4 p.421-450
- Zonneveld, J-P, 2008. Triassic sedimentary framework and sequence stratigraphy, Williston Lake, British Columbia. Calgary: Canadian Society of Petroleum Geologists. Field Trip Guidebook,201p.

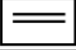
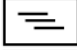

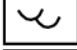



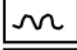


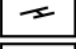
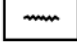
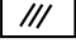
APENDIX A: OUTCROP LOGS

Legend

Lithology

	Dolomitic Siltstone		Siltstone
	Dolomitic Silty Sandstone		Calcareous Sandstone
	Dolomitic Sandstone		Bindstone Laminate
	Sandstone		Bioclastic Wackestone/Packstone
	Breccia		

Physical Structures

	Planar Laminae		Planar Tabular Bedding
	Undulatory laminae		Trough Cross Bedding
	Low-angle laminae		Hummocky Cross Stratification
	Current Ripples		Convolute Bedding
	Symmetric Ripples		Stylolites
	Low-Angle Cross-laminae		Scour
	High-Angle Cross-stratification		



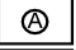
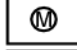

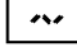
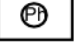
Ichnofossils

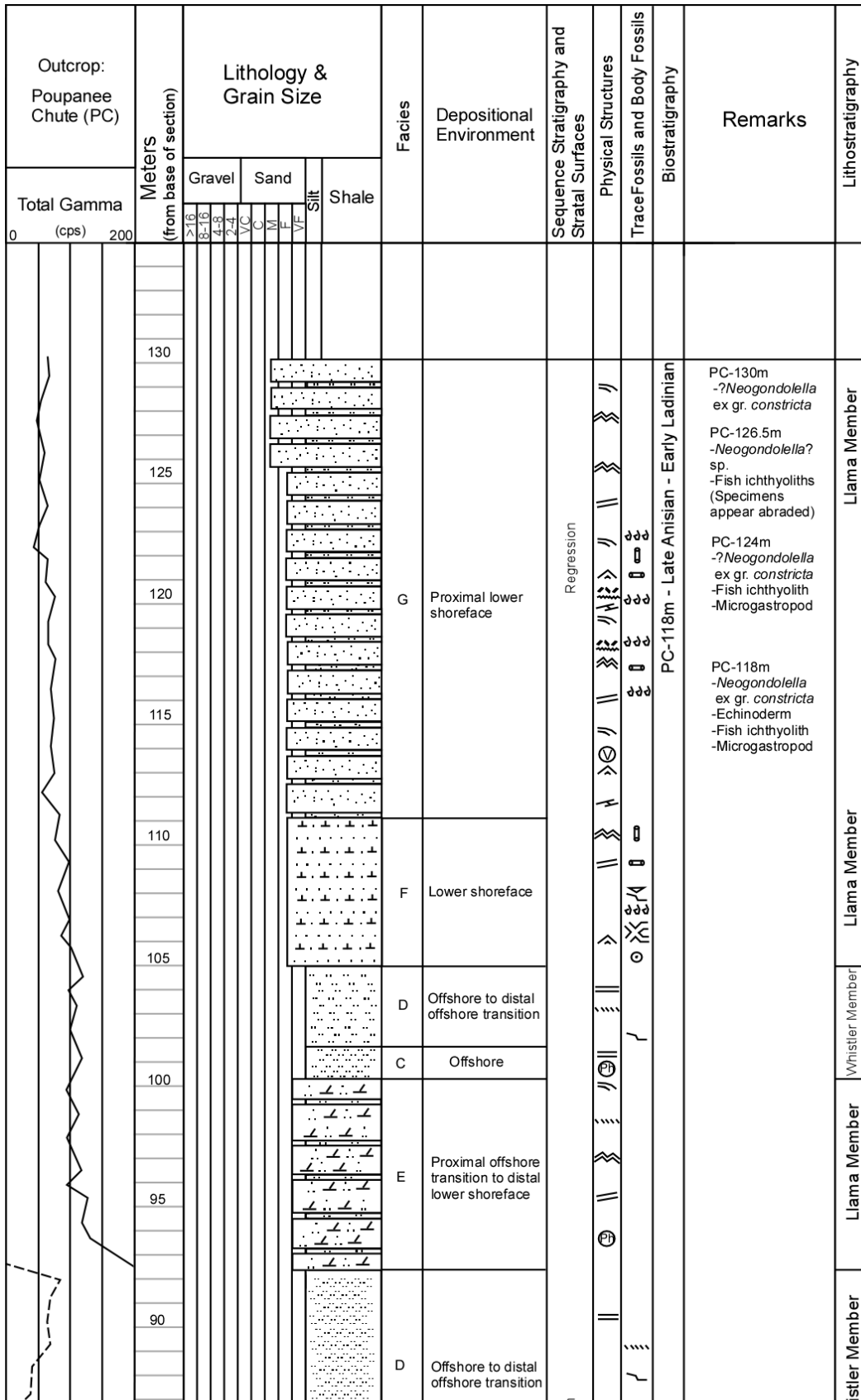
	Rosselia		Cryptic Bioturbation
	Skolithos		Thalassinoides
	Planolites		
	Phycosiphon		

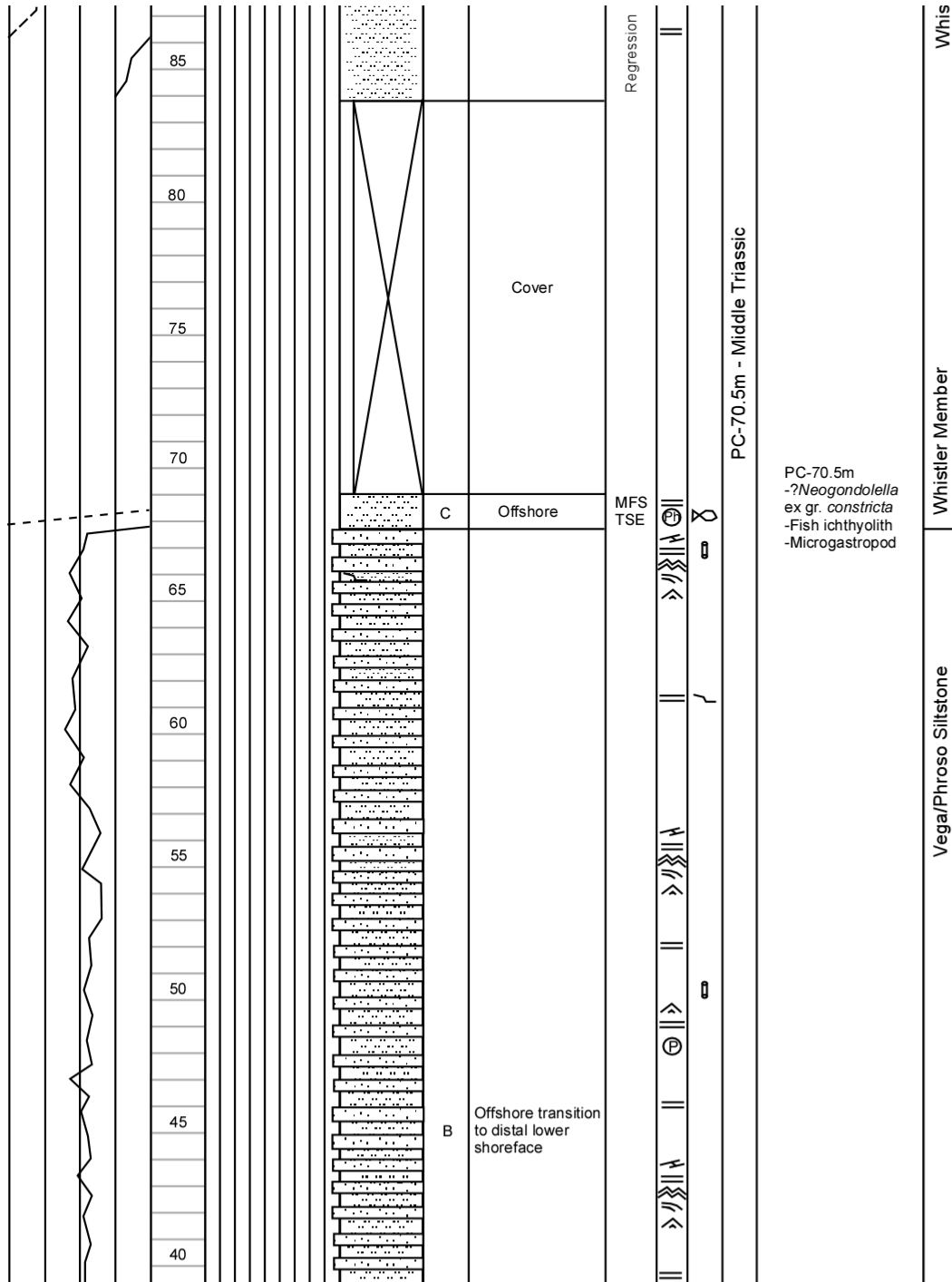
Fossils

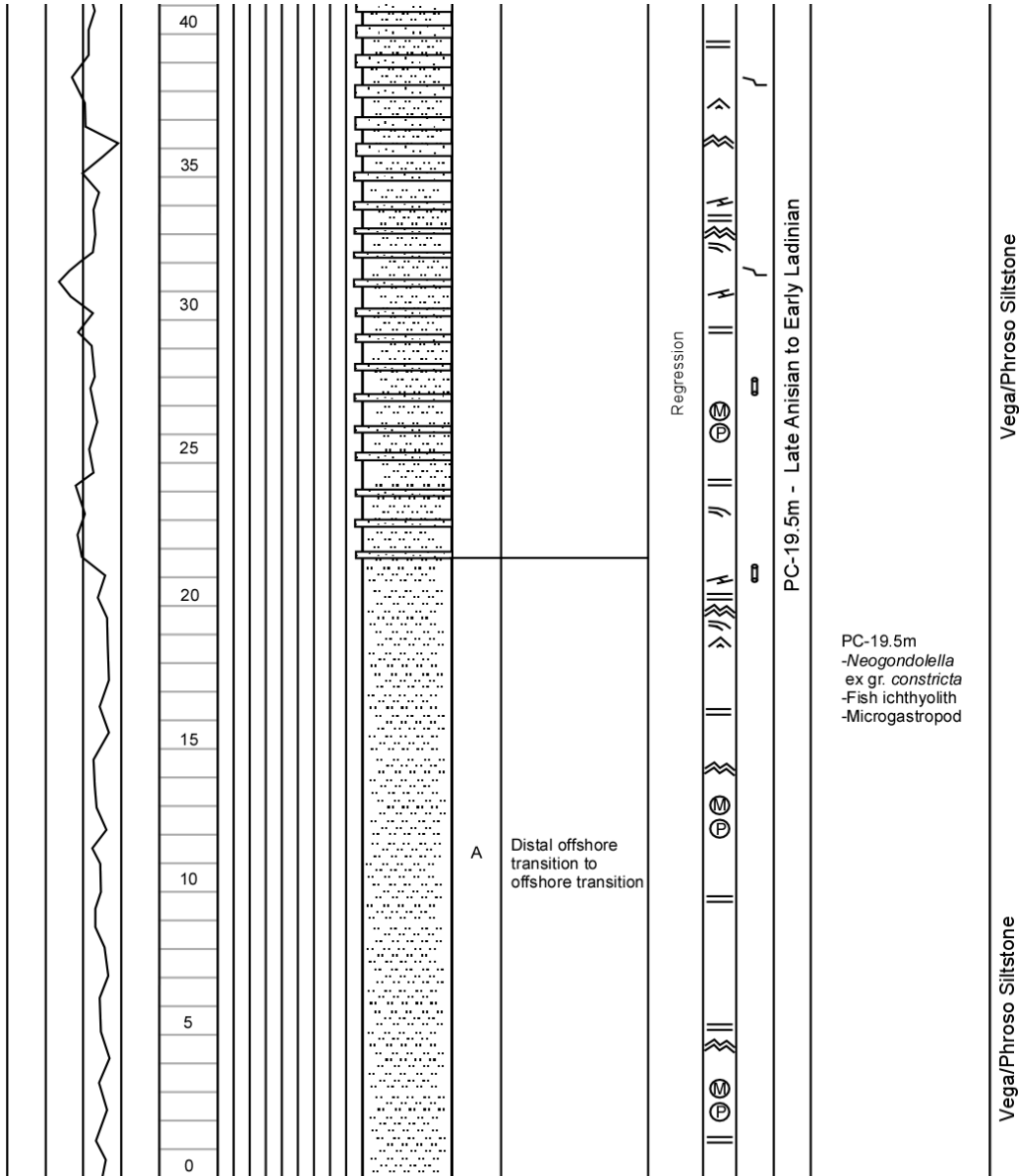
	Brachiopods		Cyanobacteria/Stromatolite
	Bivalve		Crinoids
	Gastropods		Shell Fragments
	Fish Remains		

Lithological Accessories

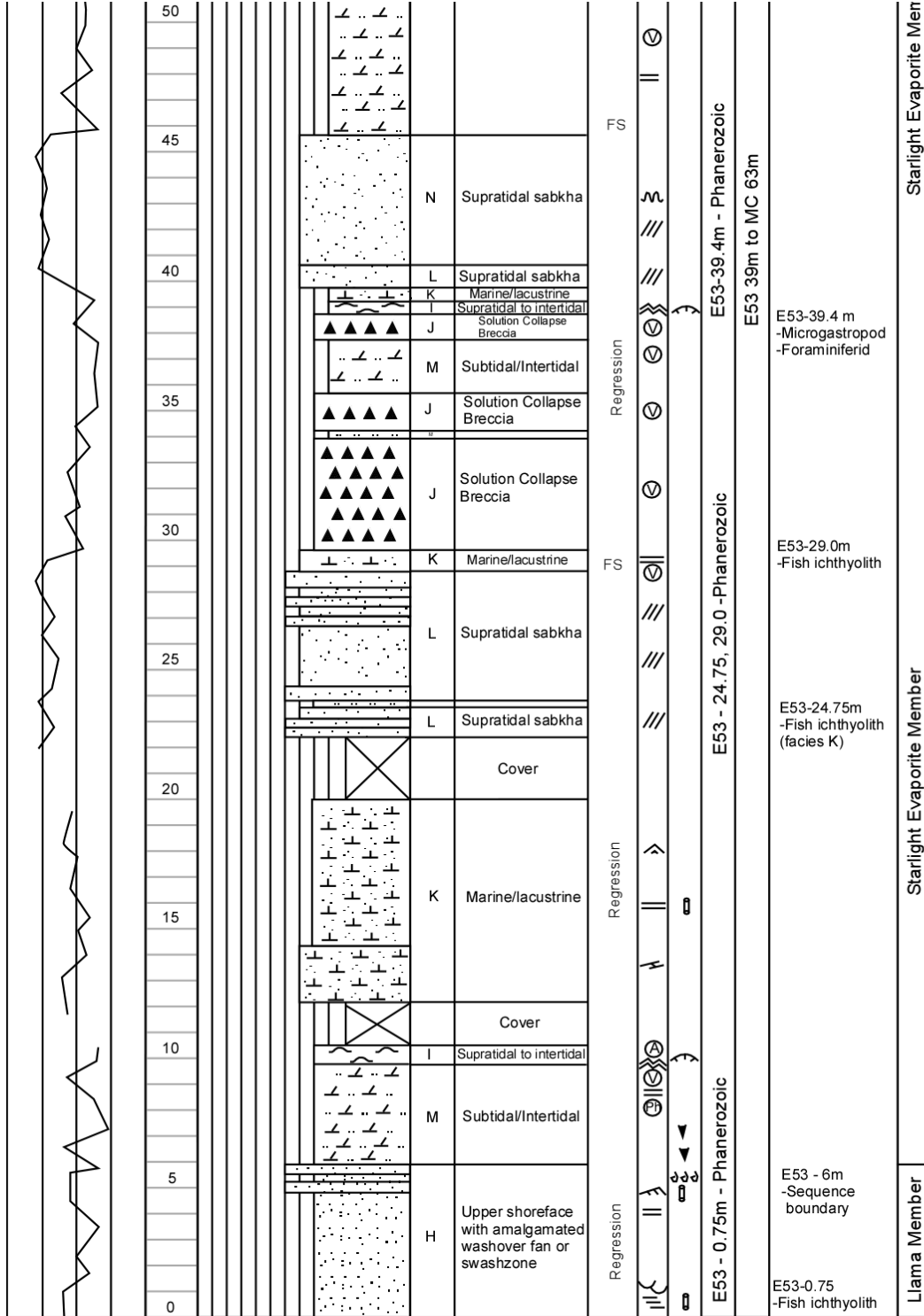
	Pyrite		Vugs
	Anhydritic		Micaceous
	Chert		Rip Up Clasts
	Phosphate		

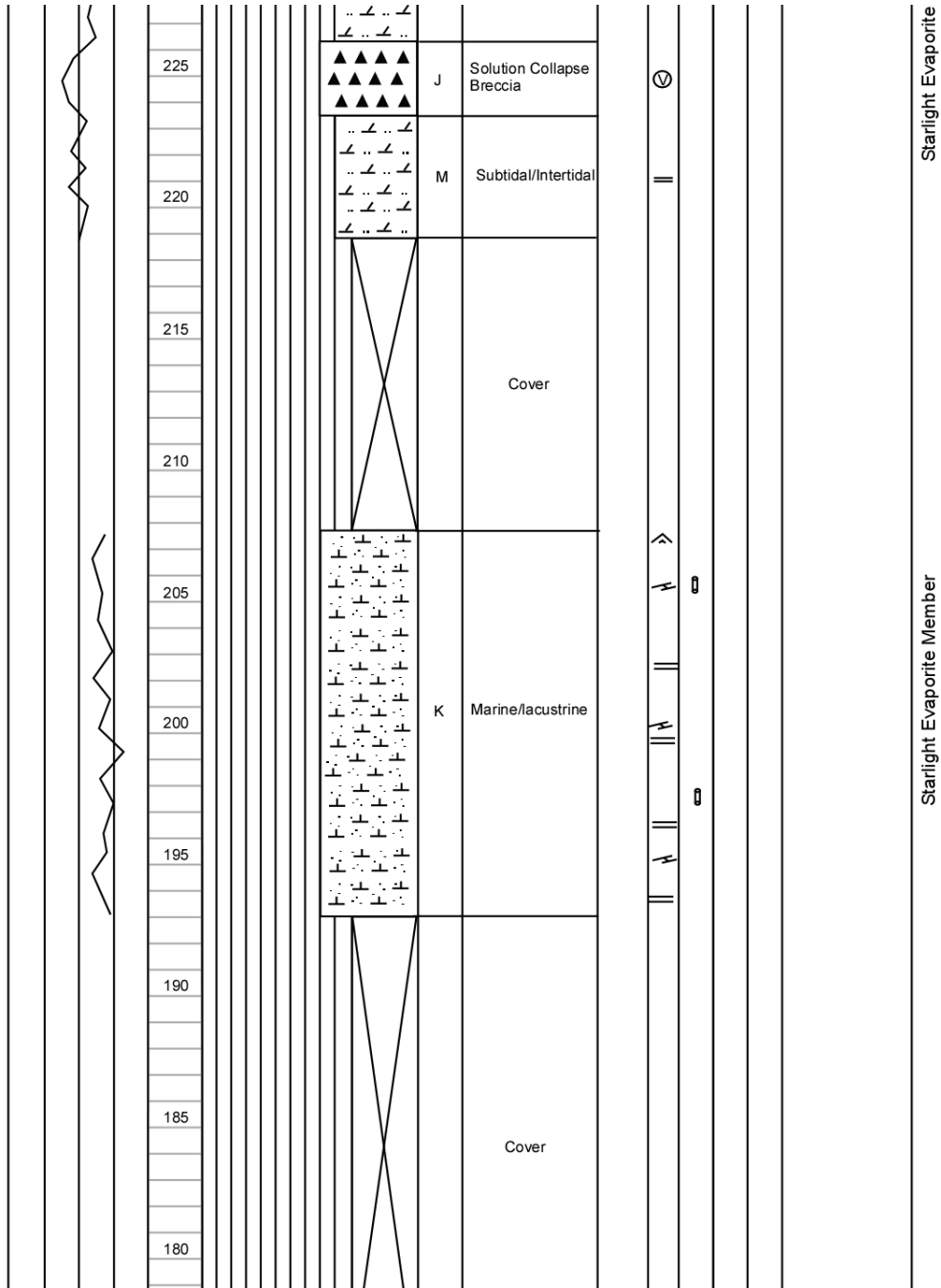






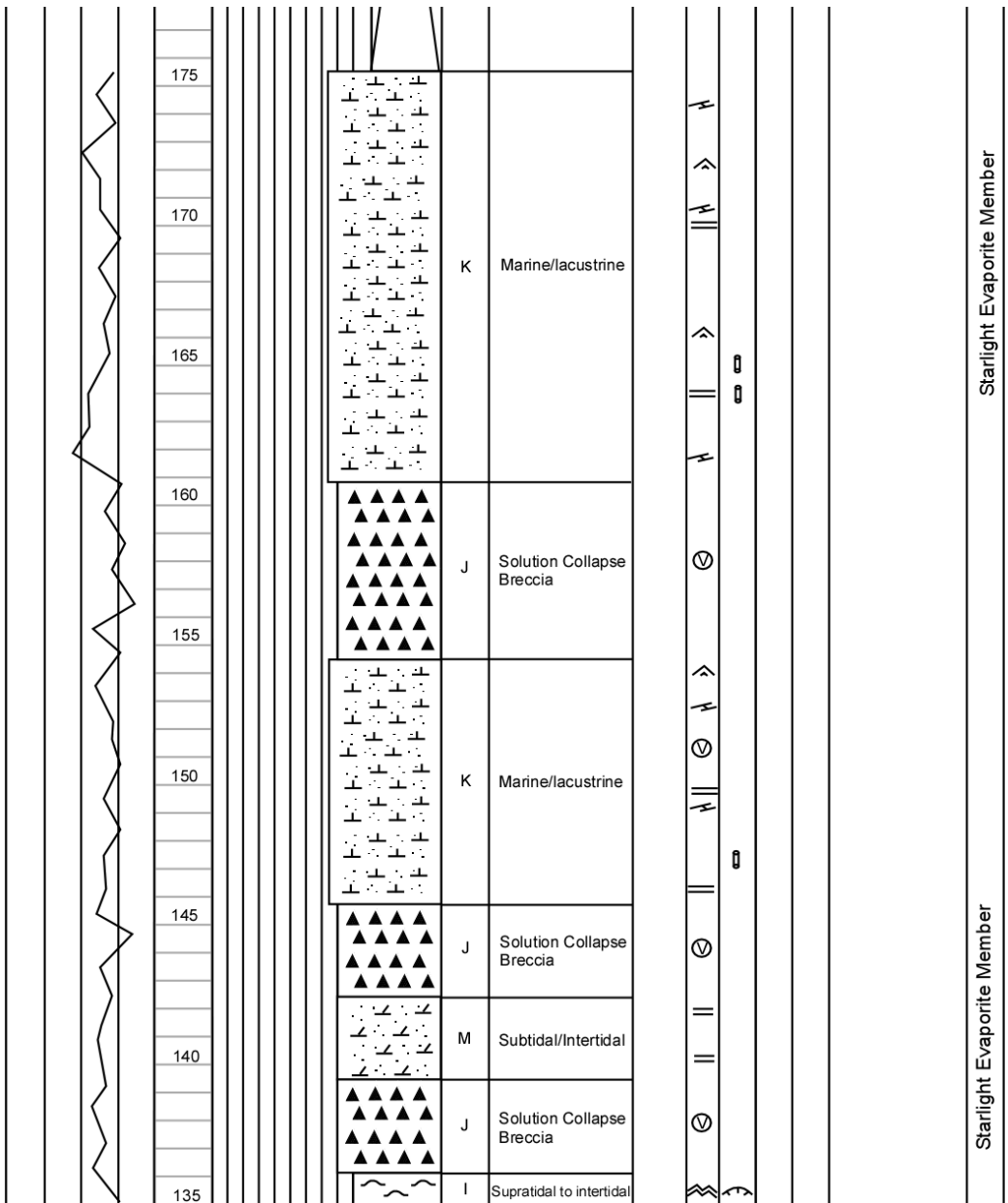
Outcrop: East 53 (E53)		Lithology & Grain Size						Facies	Depositional Environment	Sequence Stratigraphy and Stratal Surfaces	Physical Structures	Trace Fossils and Body Fossils	Biostratigraphy	Chemostratigraphy	Remarks	Lithostratigraphy
Total Gamma (cps)	Meters (from base of section)	Gravel	Sand	Silt	Shale											
0	200	>16	8-16	4-8	2-4	VC	C	M	F	VF						
	90															
	85							M	Subtidal/Intertidal	Regression?	⊙	⊙	⊙			
	80										⊙	⊙	⊙			
	75							J	Solution Collapse Breccia	Regression	⊙	⊙	⊙			
	70							L	Supratidal sabkha	Regression	⊙	⊙	⊙			
								J	Solution Collapse Breccia	Regression	⊙	⊙	⊙			
								N	Supratidal sabkha	Regression	⊙	⊙	⊙			
								L	Supratidal sabkha	Regression	⊙	⊙	⊙			
								J	Solution Collapse	Regression	⊙	⊙	⊙			
	65								Cover							
								K	Marine/lacustrine	Regression	⊙	⊙	⊙			
	60								Cover							
	55															
	50							M	Subtidal/Intertidal		⊙	⊙	⊙			
E53 85 m to MC 117 m																
Starlight Evaporite Member																
Member																





Starlight Evaporite

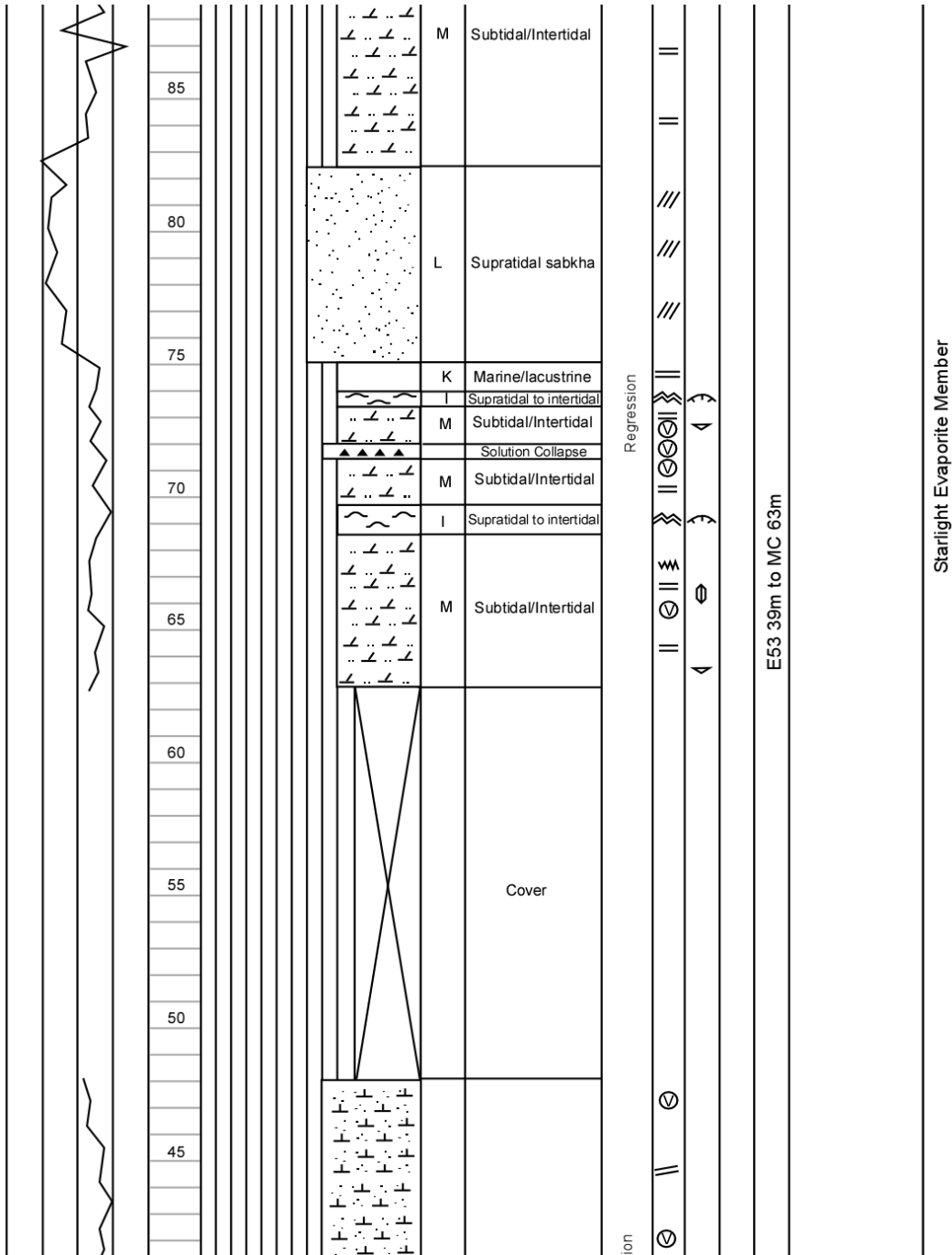
Starlight Evaporite Member

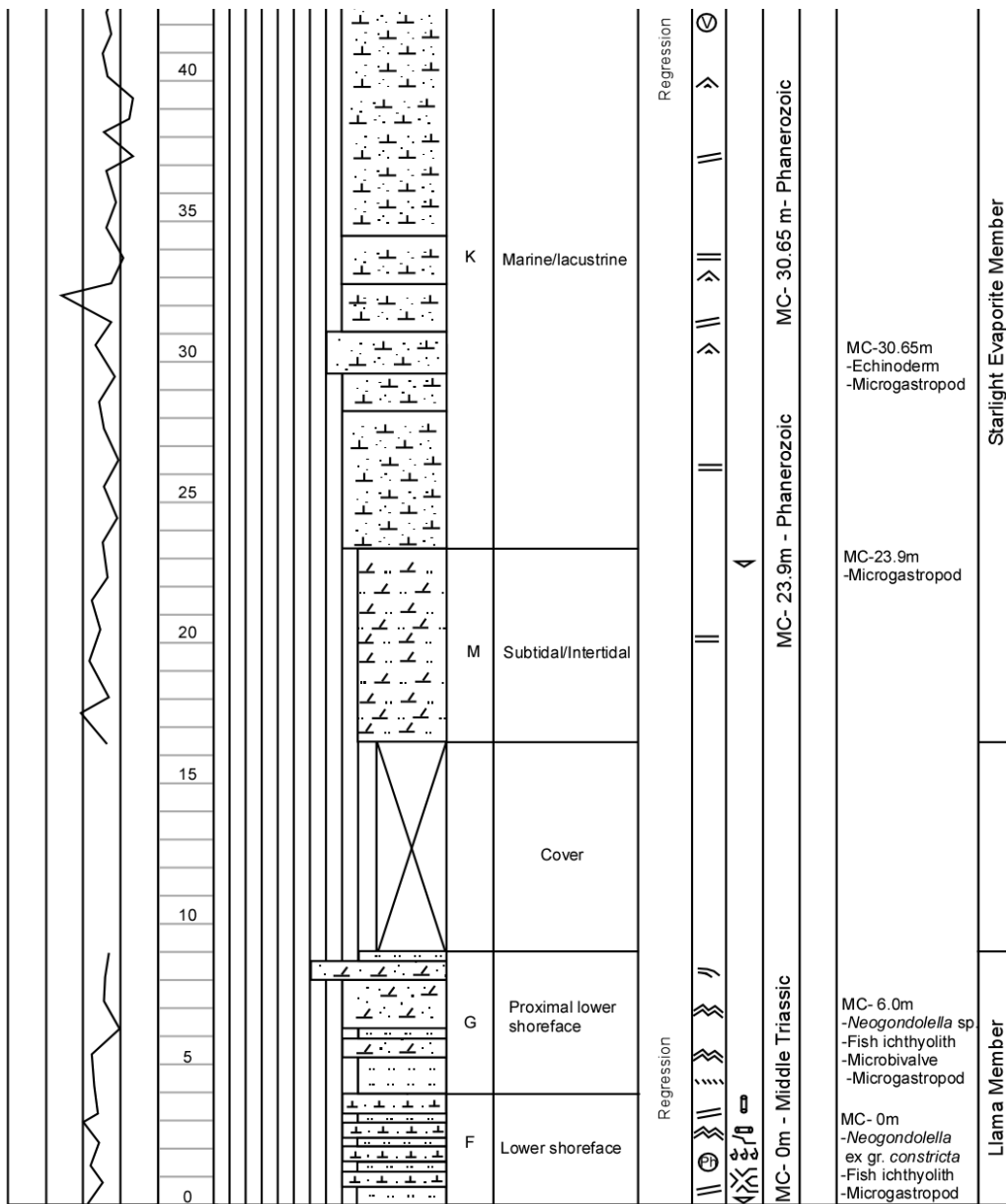


Starlight Evaporite Member

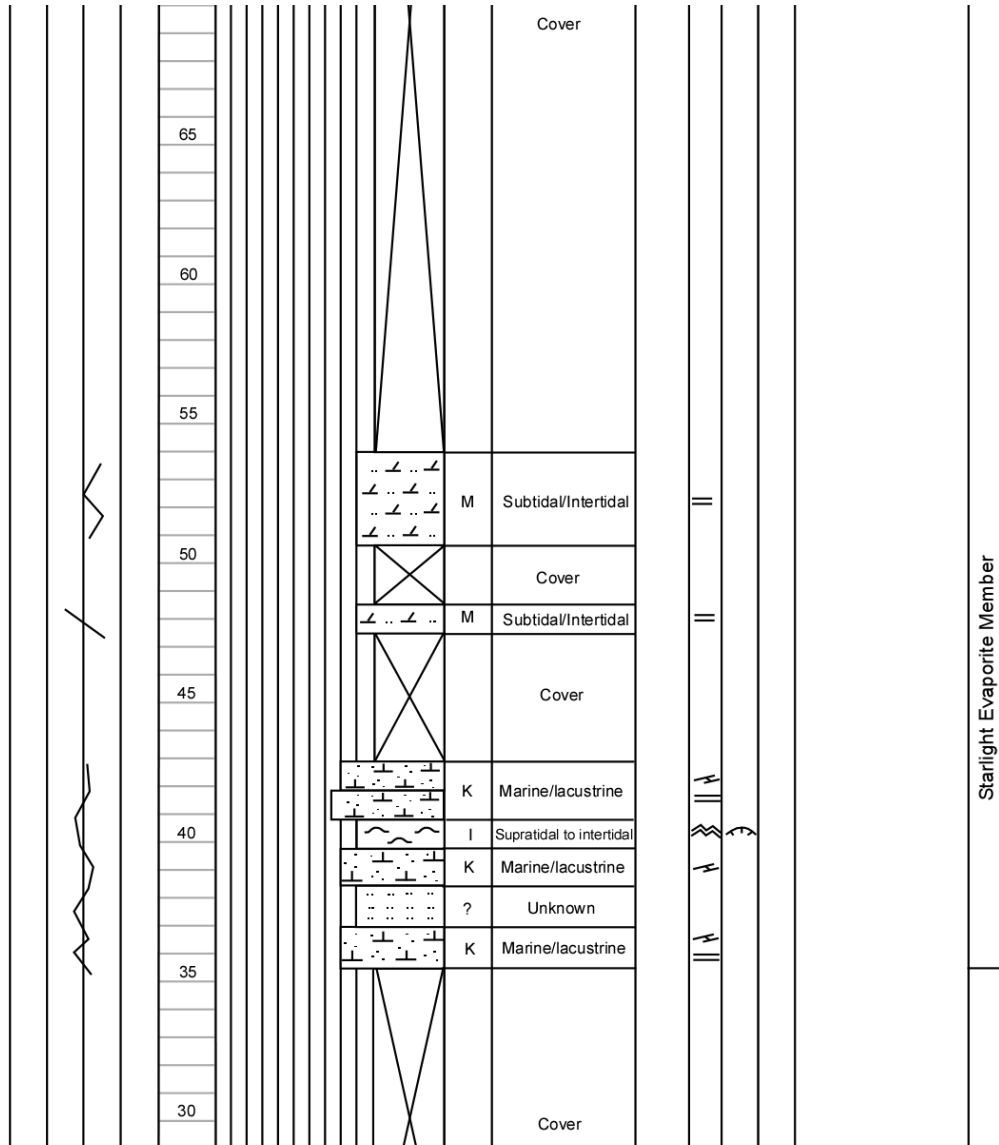
Starlight Evaporite Member

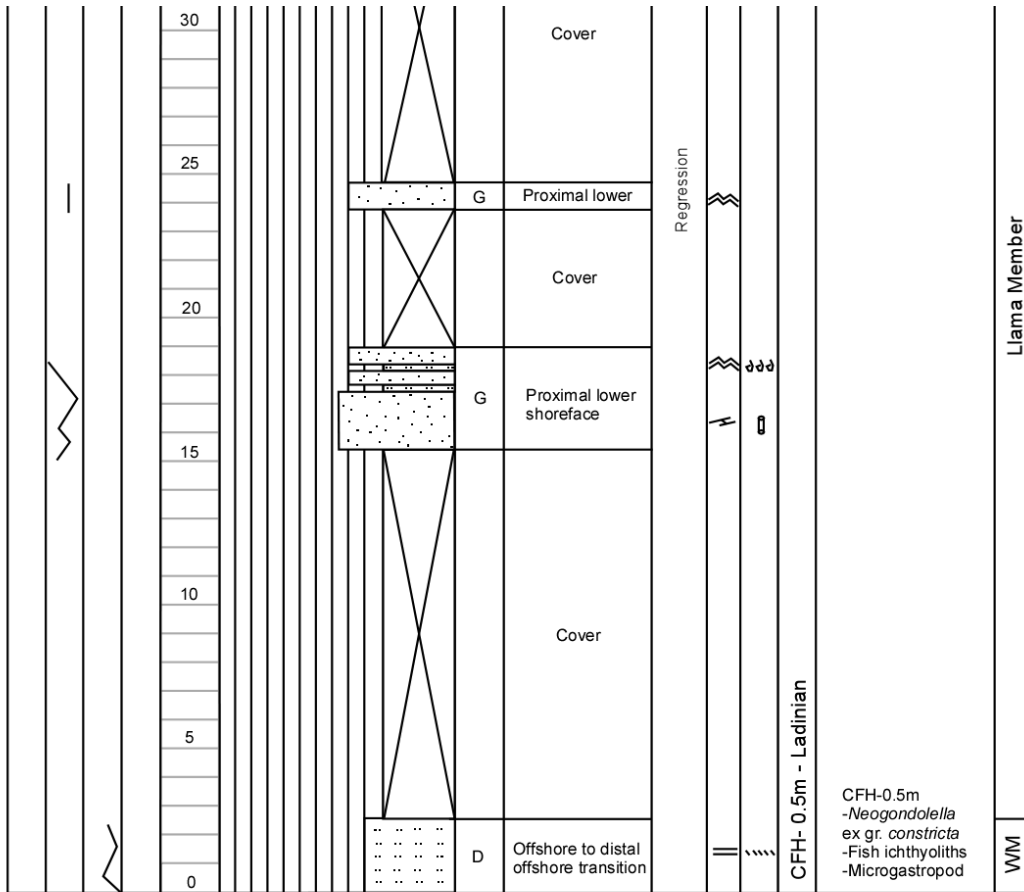
Outcrop: Monaghan Creek (MC)	Total Gamma 0 (cps) 200	Meters (from base of section)	Lithology & Grain Size					Facies	Depositional Environment	Sequence Stratigraphy and Stratal Surfaces	Physical Structures	Trace Fossils and Body Fossils	Biostratigraphy	Chemostratigraphy	Remarks	Lithostratigraphy
			Gravel	Sand	Silt	Shale										
			>1/16 8-1/16 4-8 2-4 1/4 C M F VF													
		130					M	Subtidal/Intertidal								
							K	Marine/lacustrine								
							M	Subtidal/Intertidal								
							K	Marine/lacustrine								
		125					I	Supratidal to intertidal								
							K	Marine/lacustrine								
							I	Supratidal to intertidal								
							M	Marine/lacustrine								
		120					J	Solution Collapse								
							I	Supratidal to intertidal								
							M	Subtidal/Intertidal								
		115					J	Solution Collapse Breccia								
							I	Supratidal to intertidal								
		110					M	Subtidal/Intertidal								
							I	Supratidal to intertidal								
							M	Subtidal/Intertidal								
		105					K	Marine/lacustrine								
							M	Subtidal/Intertidal								
							K	Marine/lacustrine								
		100					M	Subtidal/Intertidal								
							J	Solution Collapse Breccia								
		95					I	Supratidal to intertidal								
								Cover								
		90					?									
							M	Subtidal/Intertidal								
MC-104.2m - Phanerozoic												E53 85 m to MC 117 m				
MC-104.2m - Fish ichthyolith																
Starlight Evaporite Member																





Outcrop: Cody Found Horse (CFH)		Meters (from base of section)	Lithology & Grain Size						Facies	Depositional Environment	Sequence Stratigraphy and Stratal Surfaces	Physical Structures	Trace Fossils and Body Fossils	Biostratigraphy	Remarks	Lithostratigraphy
Total Gamma 0 (cps) 200	Gravel		Sand		Silt	Shale										
	>16	8-16	4-8	2-4	VC	C	M	LF								
		100														
		95														
		90							O	Offshore	FS?	☉ ☉	◊ ◊ ◊	◊ ◊ ◊		
		85											◊ ◊ ◊	◊ ◊ ◊		
		80											◊ ◊ ◊	◊ ◊ ◊		
		75											◊ ◊ ◊	◊ ◊ ◊		
		70								Cover						
															Brewster Limestone Member	





APENDIX B: RAW GEOCHEMISTRY DATA

Outcrop: Monaghan Creek		Original Data (values in ppm)			
Height in vertical section (meters)	1	2	3	4	5
	Li	Be	Mg	Al	Si
27.00	29.7	0.6	65215		129262
30.00	8.4	0.3	38655	2257	190284
33.00	1.8	0.2	5109	515	3093
36.00	38.5	0.3	3756	14445	114325
39.00	24.5	0.3	20928	17050	143770
42.00	158	2.0	12403	62092	286205
45.00	20.6	0.4	2773	11420	66742
48.00	13.2	0.3	81694	5801	58171
50.00	2.7	No data	52821	1180	6176
63.00	8.9	0.4	90656	6146	43786
66.00	4.3	No data	107528	1483	8145
69.00	2.3	0.1	108832	831	4915
72.00	3.9	0.2	35532	1310	6581
75.75	2.9	No data	117379	1042	5192
80.00	7.8	No data	2642	499	3818
83.00	2.0	No data	102026	254	2435
102.00	2.8	0.3	3864	1859	8550
105.00	3.9	No data	79362	2173	7305
108.60	1.4	0.1	96441	314	1353
111.00	6.7	0.1	100713	1037	6295
114.00	34.4	0.3	12911	5560	70644
117.00	60.9	0.3	6638	3113	19358
120.30	84.0	0.7	7100	22231	205568
123.00	36.3	0.2	8197	4453	36423
123.50	129	0.8	46272	16872	96763
126.00	145	0.7	10950	21664	155450
128.60	19.5	0.3	2472	15485	238660
138.00	20.9	0.4	77401	2458	22180
146.00	31.8	0.5	2419	16823	261033
156.00	50.9	0.6	5408	22606	243523
164.00	45.1	0.5	4538	14017	138078
168.70	10.6	0.3	5014	2418	23818
172.20	5.5	0.3	107625	886	4407
197.00	89.4	0.6	6304	16480	124626
202.50	50.4	0.6	32011	21454	173142
210.00	93.8	0.5	63927	11840	106110

Outcrop: Monaghan Creek		Original Data (values in ppm)			
Height in vertical section (meters)	6	7	8	9	10
	P	K	Ca	Ti	V
27.00	5266	10657	125000	1260	18.5
30.00	3688	2520	126657	246	5.88
33.00	143	612	375665	73.2	4.17
36.00	798	10922	227908	1065	19.1
39.00	297	13115	180371	1307	16.6
42.00	5770	45554	16905	3969	110
45.00	322	9595	295083	737	16.4
48.00	890	5581	185594	470	11.2
50.00	124	1763	308473	93.6	7.68
63.00	196	5296	212519	499	10.0
66.00	259	1429	239164	129	3.62
69.00	295	1179	241584	87.0	3.01
72.00	212	1365	353846	131	5.60
75.75	106	1038	233582	75.7	5.93
80.00	45	737	411232	109	5.12
83.00	48	590	247450	30.7	5.16
102.00	79	2218	397966	151	8.87
105.00	95	2455	281950	143	14.6
108.60	50	511	234102	26.9	2.54
111.00	90	876	220312	66.5	4.25
114.00	83	5603	289517	371	8.35
117.00	61	2436	368394	208	10.4
120.30	209	18742	113228	1354	20.0
123.00	76	5239	373027	220	11.0
123.50	451	14706	171660	1374	24.0
126.00	311	17269	183189	1577	26.2
128.60	109	12792	122979	563	7.88
138.00	280	2900	267302	192	12.2
146.00	139	14369	134951	894	9.57
156.00	266	19569	148961	1549	19.4
164.00	239	11973	237726	911	13.5
168.70	100	2684	380025	187	10.9
172.20	273	1142	224551	124	3.52
197.00	348	12210	238343	1023	20.8
202.50	413	15107	128251	1545	22.5
210.00	266	9189	152724	844	17.8

Outcrop: Monaghan Creek		Original Data (values in ppm)			
Height in vertical section (meters)	11	12	13	14	15
	Cr	Mn	Fe	Co	Cu
27.00	47.5	101	6044	4.60	18.8
30.00	29.4	63.5	1610	4.38	10.7
33.00	18.7	122	1064	6.38	6.3
36.00	33.2	130	5071	5.51	18.4
39.00	24.9	139	2783	6.26	11.2
42.00	127.6	72.5	23432	10.6	12.6
45.00	43.9	111	4239	7.01	12.7
48.00	37.1	97.3	2936	7.21	12.9
50.00	20.7	76.5	1837	7.11	3.75
63.00	24.1	73.2	1936	9.66	9.28
66.00	25.8	49.7	940	7.67	6.49
69.00	21.3	44.2	906	12.4	6.59
72.00	20.9	62.9	1330	11.1	6.75
75.75	19.9	49.7	603	11.4	5.34
80.00	16.9	46.5	862	6.22	7.24
83.00	20.6	48.4	936	10.7	6.60
102.00	17.8	75.6	1927	10.3	3.87
105.00	19.0	37.6	862	9.37	5.31
108.60	20.1	41.1	467	5.12	4.16
111.00	27.3	47.3	805	3.25	4.15
114.00	19.9	183	4098	5.27	7.33
117.00	20.7	107	1694	4.45	6.63
120.30	24.9	112	6409	5.64	11.5
123.00	22.6	138	1887	3.03	10.9
123.50	35.4	127	6950	7.43	9.56
126.00	36.9	164	8205	7.02	12.6
128.60	17.1	99.6	2113	2.69	4.82
138.00	28.0	258	3152	4.39	9.51
146.00	18.6	70.4	3769	2.22	8.46
156.00	26.1	109	6246	2.62	8.73
164.00	25.2	171	4568	3.04	9.38
168.70	17.1	215	2133	3.77	6.31
172.20	14.7	129	3680	3.19	9.57
197.00	32.3	138	6473	2.14	10.9
202.50	33.3	181	7876	4.46	14.0
210.00	24.3	134	4646	2.88	10.4

Outcrop: Monaghan Creek		Original Data (values in ppm)			
Height in vertical section (meters)	16	17	18	19	20
	Zn	Ga	Ge	As	Rb
27.00	29.0	2.87	0.41	3.96	25.6
30.00	10.2	0.44	0.39	0.98	4.74
33.00	5.88	0.18	0.03	0.57	0.84
36.00	24.5	3.78	0.36	0.87	24.9
39.00	11.3	3.53	0.48	1.34	27.1
42.00	45.1	19.2	1.68	12.2	151
45.00	17.3	2.53	0.28	4.91	19.2
48.00	32.8	1.24	0.24	1.81	12.0
50.00	8.55	0.35	0.06	0.44	2.33
63.00	11.4	1.33	0.15	0.52	9.32
66.00	9.79	0.33	0.07	0.37	2.43
69.00	10.2	0.20	0.08	0.28	1.27
72.00	13.1	0.28	0.08	0.44	2.09
75.75	7.32	0.25	0.13	0.34	1.44
80.00	8.31	0.11	0.03	0.35	0.86
83.00	7.49	0.23	0.08	0.88	0.34
102.00	26.6	0.64	0.08	2.50	3.66
105.00	9.63	0.46	0.08	0.82	5.06
108.60	No data	0.30	0.07	0.59	0.60
111.00	No data	0.15	0.04	0.89	1.09
114.00	12.6	1.27	0.27	2.48	12.2
117.00	0.11	0.78	0.12	2.32	5.71
120.30	5.78	4.68	0.67	1.84	46.0
123.00	28.6	1.43	0.10	1.04	12.4
123.50	4.26	4.29	0.29	2.41	42.2
126.00	10.4	5.90	0.67	4.70	45.1
128.60	0.90	3.35	0.69	1.04	31.8
138.00	7.62	0.71	0.14	3.03	4.94
146.00	32.4	3.12	0.68	1.50	39.4
156.00	15.4	4.45	0.66	2.26	48.6
164.00	4.55	3.33	0.47	1.43	26.6
168.70	<DL	0.63	0.10	1.19	4.80
172.20	45.7	0.40	0.08	1.28	1.88
197.00	19.8	2.97	0.32	1.58	34.1
202.50	10.3	4.94	0.58	3.93	37.2
210.00	13.1	2.73	0.29	1.37	24.8

Outcrop: Monaghan Creek		Original Data (values in ppm)			
Height in vertical section (meters)	21	22	23	24	25
	Sr	Y	Zr	Nb	Mo
27.00	173	15.9	107	4.67	3.10
30.00	134	6.00	37.2	1.40	4.97
33.00	292	0.49	4.10	1.39	2.51
36.00	216	10.7	128	3.73	2.33
39.00	192	11.0	134	4.23	0.90
42.00	149	32.4	134	11.2	3.75
45.00	327	5.58	49.0	2.20	6.00
48.00	172	9.10	70.0	1.77	1.24
50.00	275	0.87	6.28	0.58	0.74
63.00	193	5.09	39.7	3.98	7.83
66.00	172	1.15	13.1	1.52	1.14
69.00	160	0.65	5.95	0.88	2.23
72.00	223	0.81	6.98	0.90	5.75
75.75	168	0.84	4.30	0.53	3.67
80.00	1935	0.92	2.39	1.18	1.69
83.00	386	0.35	2.37	0.34	5.50
102.00	441	1.08	5.88	0.64	31.7
105.00	475	0.74	6.00	0.58	0.62
108.60	505	0.25	1.71	2.91	1.94
111.00	186	0.77	3.37	1.12	1.83
114.00	236	4.49	35.8	1.56	4.37
117.00	230	1.60	14.2	1.10	3.23
120.30	156	8.70	89.8	4.67	2.39
123.00	279	1.63	13.7	1.17	1.67
123.50	195	11.1	91.5	7.78	5.74
126.00	208	12.2	90.5	5.13	3.14
128.60	145	4.58	39.5	1.70	1.63
138.00	207	2.36	14.2	1.87	4.17
146.00	213	4.97	84.7	3.39	4.03
156.00	172	9.34	114	5.63	6.76
164.00	218	7.01	71.9	4.31	8.29
168.70	235	1.94	17.5	1.07	6.14
172.20	174	1.15	7.54	2.30	9.23
197.00	224	8.55	81.0	3.64	0.76
202.50	148	13.6	97.9	5.34	0.98
210.00	170	6.65	67.4	3.39	0.55

Outcrop: Monaghan Creek		Original Data (values in ppm)			
Height in vertical section (meters)	26	27	28	29	30
	Ru	Pd	Ag	Sn	Sb
27.00	0.20	3.21	0.32	1.73	1.54
30.00	0.20	1.12	0.14	0.90	0.77
33.00	0.43	0.19	0.13	0.95	0.46
36.00	0.24	3.79	2.56	3.57	0.41
39.00	0.24	3.83	9.58	2.08	0.47
42.00	No data	3.66	4.28	3.34	1.04
45.00	0.34	1.43	0.26	1.05	0.29
48.00	0.35	2.10	0.09	1.07	0.27
50.00	0.47	0.21	0.08	0.34	0.15
63.00	0.36	1.16	0.23	1.25	1.64
66.00	0.28	0.40	0.10	0.71	0.71
69.00	0.33	0.21	0.09	1.07	0.46
72.00	0.36	0.18	0.69	0.61	0.34
75.75	0.28	0.13	4.98	1.08	0.21
80.00	0.44	0.07	0.35	1.63	0.20
83.00	0.34	0.06	0.10	0.56	0.14
102.00	0.28	0.14	0.12	0.53	0.20
105.00	0.31	0.13	0.07	0.26	0.08
108.60	0.30	0.17	0.31	1.29	2.16
111.00	0.25	0.12	0.11	0.54	0.94
114.00	0.24	1.07	0.13	0.77	0.69
117.00	0.25	0.38	0.17	0.58	0.46
120.30	No data	2.72	0.57	1.02	0.43
123.00	0.32	0.37	0.23	1.90	0.31
123.50	0.15	2.78	0.19	0.71	0.37
126.00	0.04	2.66	0.23	1.11	0.45
128.60	No data	1.12	0.06	0.37	0.28
138.00	0.40	0.64	0.59	1.32	1.07
146.00	0.12	2.85	0.21	1.13	0.67
156.00	0.08	3.71	0.24	0.88	0.50
164.00	0.20	2.39	0.18	0.85	0.36
168.70	0.37	0.56	0.05	0.31	0.23
172.20	0.27	0.18	0.08	0.38	0.21
197.00	0.23	2.76	0.16	0.82	0.38
202.50	0.12	3.21	0.16	1.35	0.42
210.00	0.23	2.17	0.11	0.37	0.30

Outcrop: Monaghan Creek		Original Data (values in ppm)			
Height in vertical section (meters)	31	32	33	34	35
	Cs	Ba	La	Ce	Pr
27.00	1.12	102	12.7	22.4	2.99
30.00	0.13	32.5	3.94	6.60	0.877
33.00	0.02	41.4	0.62	1.16	0.127
36.00	0.81	95.2	9.65	19.9	2.52
39.00	0.57	147	9.29	17.8	2.38
42.00	8.39	290	31.4	52.9	6.96
45.00	0.58	74.9	6.07	12.0	1.50
48.00	0.40	43.7	5.86	12.5	1.89
50.00	0.07	10.6	1.16	2.28	0.227
63.00	0.23	54.1	5.07	9.20	1.22
66.00	0.08	14.1	1.48	2.50	0.289
69.00	No data	15.4	0.73	1.43	0.175
72.00	0.05	25.8	1.02	2.02	0.230
75.75	No data	8.53	0.86	1.48	0.182
80.00	No data	116	1.99	2.02	0.238
83.00	No data	18.6	0.48	0.62	0.070
102.00	0.12	34.1	1.40	2.83	0.344
105.00	0.20	46.4	0.93	1.83	0.210
108.60	0.07	11.9	0.45	0.62	0.091
111.00	0.04	16.6	1.03	1.98	0.240
114.00	0.28	657	4.38	8.44	1.07
117.00	0.27	60.9	2.26	4.11	0.488
120.30	1.25	254	10.4	20.0	2.56
123.00	0.43	119	2.61	4.04	0.505
123.50	1.18	116	13.5	26.1	3.20
126.00	1.67	412	14.2	27.6	3.54
128.60	0.47	240	5.20	9.52	1.20
138.00	0.26	21.7	4.03	5.62	0.688
146.00	0.84	259	5.94	10.1	1.42
156.00	1.22	236	10.8	20.4	2.63
164.00	0.75	340	7.91	14.4	1.86
168.70	0.17	25.9	2.84	4.67	0.555
172.20	0.07	12.3	1.94	2.98	0.329
197.00	1.05	131	9.17	18.7	2.36
202.50	1.14	177	15.6	29.7	3.80
210.00	0.88	155	7.96	15.2	1.95

Outcrop: Monaghan Creek		Original Data (values in ppm)			
Height in vertical section (meters)	36	37	38	39	40
	Nd	Sm	Eu	Gd	Dy
27.00	11.5	2.34	0.53	2.23	2.24
30.00	3.36	0.68	0.17	0.69	0.68
33.00	0.41	0.06	No data	0.08	0.07
36.00	9.64	1.98	0.44	1.87	1.78
39.00	9.45	2.02	0.49	1.89	1.89
42.00	26.3	5.30	1.15	4.95	4.57
45.00	5.69	1.21	0.27	1.03	1.01
48.00	7.92	1.78	0.36	1.65	1.44
50.00	0.87	0.16	0.04	0.18	0.13
63.00	4.63	0.97	0.23	0.87	0.87
66.00	1.08	0.19	0.05	0.19	0.19
69.00	0.61	0.09	0.04	0.12	0.10
72.00	0.87	0.14	0.04	0.16	0.13
75.75	0.68	0.11	0.04	0.14	0.12
80.00	1.15	0.17	0.07	0.18	0.14
83.00	0.27	No data	No data	0.05	0.04
102.00	1.25	0.21	0.06	0.21	0.19
105.00	0.81	0.14	0.04	0.15	0.13
108.60	0.31	0.07	0.03	0.07	0.06
111.00	0.86	0.17	0.04	0.14	0.14
114.00	4.21	0.87	0.35	0.81	0.80
117.00	1.81	0.34	0.09	0.30	0.27
120.30	9.92	2.09	0.53	1.76	1.60
123.00	1.97	0.35	0.10	0.32	0.28
123.50	12.2	2.47	0.56	2.25	2.02
126.00	13.7	2.70	0.65	2.52	2.25
128.60	4.74	0.95	0.30	0.87	0.80
138.00	2.46	0.48	0.13	0.44	0.39
146.00	5.57	1.07	0.31	0.91	0.93
156.00	10.1	2.07	0.51	1.80	1.74
164.00	7.13	1.45	0.39	1.29	1.23
168.70	2.01	0.42	0.09	0.36	0.33
172.20	1.23	0.23	0.05	0.21	0.20
197.00	9.36	2.00	0.46	1.76	1.59
202.50	14.6	2.98	0.66	2.67	2.55
210.00	7.46	1.51	0.36	1.38	1.27

Outcrop: Monaghan Creek		Original Data (values in ppm)			
Height in vertical section (meters)	41	42	43	44	45
	Ho	Er	Tm	Yb	Hf
27.00	0.49	1.42	0.212	1.35	4.08
30.00	0.15	0.43	0.060	0.41	1.29
33.00	No data	0.04	No data	No data	0.15
36.00	0.38	1.08	0.155	1.05	3.92
39.00	0.39	1.12	0.165	1.10	3.88
42.00	0.94	2.73	0.394	2.53	4.24
45.00	0.21	0.58	0.085	0.59	1.37
48.00	0.28	0.76	0.101	0.62	2.06
50.00	0.03	0.08	0.012	0.06	0.20
63.00	0.19	0.51	0.085	0.47	1.58
66.00	0.04	0.12	0.020	0.11	0.61
69.00	No data	0.06	0.009	0.06	0.30
72.00	0.03	0.08	0.013	0.08	0.28
75.75	0.03	0.08	0.011	0.07	0.27
80.00	0.03	0.08	0.010	0.06	0.10
83.00	No data	No data	No data	No data	0.16
102.00	0.04	0.11	0.015	0.12	0.21
105.00	0.03	0.07	0.011	0.08	0.47
108.60	0.03	0.04	0.034	No data	0.30
111.00	0.03	0.08	0.015	0.08	0.31
114.00	0.16	0.45	0.069	0.43	1.30
117.00	0.06	0.17	0.026	0.17	0.65
120.30	0.33	0.96	0.143	0.98	2.92
123.00	0.05	0.15	0.023	0.14	0.42
123.50	0.41	1.19	0.165	1.11	3.08
126.00	0.45	1.29	0.190	1.27	2.95
128.60	0.16	0.46	0.066	0.44	1.22
138.00	0.11	0.24	0.054	0.22	0.83
146.00	0.20	0.62	0.100	0.66	2.89
156.00	0.35	1.05	0.155	1.04	3.89
164.00	0.26	0.75	0.117	0.75	2.47
168.70	0.07	0.19	0.031	0.19	0.61
172.20	0.04	0.13	0.018	0.11	0.31
197.00	0.32	0.93	0.137	0.91	2.98
202.50	0.51	1.48	0.212	1.36	3.47
210.00	0.26	0.74	0.107	0.71	2.41

Outcrop: Monaghan Creek		Original Data (values in ppm)			
Height in vertical section (meters)	46	47	48	49	50
	Ta	Au	Tl	Pb	Th
27.00	1.01	0.93	0.79	6.21	4.23
30.00	0.55	0.61	0.33	2.71	1.24
33.00	0.43	0.41	0.17	1.62	0.30
36.00	0.60	0.41	0.21	3.18	2.36
39.00	0.58	0.33	0.24	3.63	2.28
42.00	1.05	0.33	1.52	22.9	8.97
45.00	0.47	0.27	0.30	5.61	1.52
48.00	0.37	0.26	0.18	4.72	1.05
50.00	0.24	0.22	0.05	1.32	0.11
63.00	0.97	0.77	0.71	2.43	2.05
66.00	0.60	0.40	0.31	1.50	0.74
69.00	0.48	0.32	0.20	1.20	0.41
72.00	0.40	0.19	0.19	1.30	0.35
75.75	0.30	0.19	0.17	1.43	0.25
80.00	0.32	0.13	0.13	1.12	0.14
83.00	0.24	0.11	0.34	1.31	0.04
102.00	0.24	0.06	0.42	10.4	0.26
105.00	0.21	0.02	0.06	1.46	0.29
108.60	1.15	0.98	0.85	4.82	1.09
111.00	0.78	0.50	0.38	1.79	0.66
114.00	0.66	0.23	0.26	5.10	1.07
117.00	0.55	0.12	0.17	1.18	0.69
120.30	0.72	0.07	0.38	6.99	3.26
123.00	0.41	0.03	0.10	2.39	0.48
123.50	0.68	No data	0.34	6.08	3.53
126.00	0.66	0.03	0.45	8.42	3.72
128.60	0.35	No data	0.18	5.11	0.98
138.00	1.11	1.31	0.98	3.92	1.96
146.00	0.89	0.57	0.71	9.50	2.21
156.00	0.93	0.36	0.51	8.48	3.48
164.00	0.68	0.23	0.32	4.55	2.06
168.70	0.44	0.11	0.14	1.98	0.63
172.20	0.59	0.21	0.21	3.14	0.44
197.00	0.59	0.14	0.29	5.20	2.65
202.50	0.74	0.05	0.34	8.54	3.82
210.00	0.49	-0.03	0.24	5.58	2.09

Outcrop: Monaghan Creek		Original Data (values in ppm)			
Height in vertical section (meters)	51				
	U				
27.00	2.13				
30.00	1.33				
33.00	2.56				
36.00	2.19				
39.00	2.83				
42.00	6.61				
45.00	2.18				
48.00	2.02				
50.00	1.98				
63.00	2.70				
66.00	2.83				
69.00	2.45				
72.00	2.50				
75.75	2.10				
80.00	2.64				
83.00	1.60				
102.00	8.33				
105.00	3.34				
108.60	2.08				
111.00	1.69				
114.00	2.28				
117.00	3.82				
120.30	1.20				
123.00	3.06				
123.50	2.83				
126.00	1.63				
128.60	0.80				
138.00	1.95				
146.00	2.18				
156.00	2.17				
164.00	3.21				
168.70	3.24				
172.20	1.62				
197.00	4.37				
202.50	2.36				
210.00	2.04				

Outcrop: East 53			Original Data (values in ppm)		
Height in vertical section (meters)	1	2	3	4	5
	Li	Be	Mg	Al	Si
0.00	10.0	0.7	42155	16955	212294
3.00	14.2	0.7	49453	16465	170655
6.00	12.9	0.5	14549	8368	304521
9.00	8.4	0.2	44197	2846	157780
12.00	5.7	0.2	66176	3283	60824
15.00	7.6	0.2	15810	5054	240239
18.00	9.9	0.4	15647	6620	274038
21.00	12.3	0.4	23172	6288	235320
24.00	10.6	0.2	11510	3898	339048
27.00	8.2	0.1	473	4170	317874
30.00	12.2	0.3	28962	12808	90968
33.00	26.0	0.4	4198	11770	156623
36.00	105	3.0	23296	72982	278099
39.00	13.5	0.4	86915	9528	71317
42.00	14.9	0.6	62084	19470	189051
45.00	4.4	0.2	65214	4038	49327
48.70	28.7	0.7	71631	24403	115666
51.00	35.1	1.0	73006	24467	101854
53.00	16.4	0.4	118203	8191	28438
56.00	8.5	0.3	112624	4101	33657
63.00	23.0	0.5	37109	17788	266745
65.00	14.9	0.2	68149	4110	21814
68.00	38.2	0.5	84118	13725	88583
71.00	18.9	0.2	83000	5276	29648
73.00	28.5	0.5	4429	10215	69897
75.00	3.0	0.1	10481	1027	9174
77.60	2.2	0.2	54501	794	8907
80.00	3.3	No data	8922	1041	8350
83.00	8.2	0.2	90199	6555	49552
85.00	4.4	0.1	63347	2703	18541
87.00	3.7	0.1	121797	1047	6737
90.00	61.8	0.7	65223	19214	179836

Outcrop: East 53			Original Data (values in ppm)		
Height in vertical section (meters)	6	7	8	9	10
	P	K	Ca	Ti	V
0.00	5165	15307	86595	2464	26.1
3.00	6203	12855	101423	2225	22.1
6.00	3048	9181	34954	364	15.2
9.00	1621	3116	102617	498	10.3
12.00	6520	3509	164238	337	11.1
15.00	7650	5770	72302	531	9.40
18.00	10062	6903	63409	825	11.1
21.00	6695	5314	73428	542	20.4
24.00	465	3961	35694	408	13.3
27.00	767	3065	46509	250	12.8
30.00	1608	10404	161444	1458	18.2
33.00	557	9255	208494	971	20.0
36.00	6672	50642	32769	4210	122
39.00	2064	8408	180076	913	16.7
42.00	734	16176	108697	1348	21.2
45.00	10938	3941	254898	437	7.66
48.70	5193	22390	130899	1782	32.3
51.00	6895	22022	135732	1666	39.0
53.00	458	7349	200820	344	101
56.00	2559	3500	207971	371	8.13
63.00	340	14751	83694	1420	14.6
65.00	167	3350	279353	385	15.8
68.00	1810	12553	158479	1079	30.9
71.00	203	4731	247909	463	11.7
73.00	239	9980	298735	848	21.9
75.00	100	1564	380938	133	3.23
77.60	106	1064	327509	83.2	5.14
80.00	198	1324	381490	157	3.14
83.00	214	6341	211231	461	10.9
85.00	152	2851	296216	190	7.28
87.00	139	1310	230814	76.4	5.39
90.00	388	14340	112620	1864	17.8

Outcrop: East 53			Original Data (values in ppm)		
Height in vertical section (meters)	11	12	13	14	15
	Cr	Mn	Fe	Co	Cu
0.00	61.5	160	5419	4.62	13.1
3.00	61.4	176	6617	2.96	20.2
6.00	25.0	55.1	2325	1.59	10.2
9.00	22.0	97.3	3784	2.65	23.1
12.00	28.1	99.9	3907	1.78	31.6
15.00	31.9	48.3	1916	1.41	7.20
18.00	46.3	45.7	2231	1.70	9.18
21.00	31.9	59.1	2745	1.07	15.5
24.00	11.1	41.6	1446	1.08	10.5
27.00	11.5	21.0	679	0.24	3.41
30.00	34.8	92.5	3255	1.72	21.3
33.00	22.8	123	4052	4.54	11.0
36.00	133	98.0	23402	8.70	14.9
39.00	28.6	152	5354	5.52	15.1
42.00	26.9	68.6	4246	4.38	11.5
45.00	25.6	119	3836	4.45	8.62
48.70	51.6	98.4	9297	4.20	12.9
51.00	55.8	86.5	11818	6.02	46.3
53.00	20.1	122	5034	5.93	9.72
56.00	19.3	94.3	3068	6.22	9.82
63.00	19.2	79.7	3715	3.03	12.0
65.00	17.1	146	4209	5.51	34.7
68.00	51.8	111	5425	3.79	29.7
71.00	17.5	105	2953	4.84	9.71
73.00	20.3	107	5017	4.00	12.1
75.00	12.8	125	1677	5.12	8.02
77.60	13.2	113	1088	4.90	6.19
80.00	13.8	127	1181	3.63	5.10
83.00	16.0	88.4	1872	3.06	9.40
85.00	14.9	94.6	1158	5.56	7.32
87.00	11.2	92.6	1211	4.97	4.98
90.00	27.4	121	4194	3.57	12.7

Outcrop: East 53			Original Data (values in ppm)		
Height in vertical section (meters)	16	17	18	19	20
	Zn	Ga	Ge	As	Rb
0.00	16.8	3.81	0.65	7.55	32.2
3.00	36.8	3.40	0.62	10.5	28.5
6.00	11.2	1.71	0.81	3.07	20.1
9.00	11.5	1.10	0.43	4.62	7.45
12.00	19.1	0.97	0.27	0.63	7.86
15.00	6.13	1.16	0.62	0.79	12.5
18.00	10.4	1.64	0.76	1.02	15.1
21.00	11.8	2.18	0.68	1.03	16.0
24.00	8.04	1.13	0.84	0.83	7.77
27.00	4.30	1.06	0.72	0.30	6.01
30.00	11.9	2.38	0.55	1.59	21.8
33.00	15.3	2.77	0.54	1.05	26.2
36.00	49.6	19.7	2.27	11.3	218
39.00	10.2	0.15	0.24	1.65	19.5
42.00	16.2	3.09	0.50	5.91	36.9
45.00	43.1	0.14	0.13	6.02	7.99
48.70	34.3	4.42	0.51	9.85	57.5
51.00	17.6	4.29	0.51	6.90	61.9
53.00	30.2	0.45	0.12	1.40	16.4
56.00	9.88	0.05	0.13	0.58	6.79
63.00	8.20	2.68	0.69	0.93	33.7
65.00	19.1	3.90	0.06	3.00	7.10
68.00	11.6	0.36	0.39	6.26	33.7
71.00	10.4	0.73	0.06	0.49	10.4
73.00	11.7	3.31	0.23	5.78	22.3
75.00	6.46	0.11	No data	1.38	1.81
77.60	1.32	0.06	No data	0.44	1.38
80.00	0.69	0.52	No data	0.45	1.81
83.00	3.19	0.38	0.10	1.41	11.7
85.00	0.16	0.12	0.04	1.35	4.79
87.00	1.44	0.56	No data	0.61	2.10
90.00	15.9	4.69	0.43	1.62	32.9

Outcrop: East 53			Original Data (values in ppm)		
Height in vertical section (meters)	21	22	23	24	25
	Sr	Y	Zr	Nb	Mo
0.00	217	29.1	392	9.02	6.21
3.00	173	34.1	263	8.46	6.95
6.00	103	10.7	28.8	1.47	3.50
9.00	128	6.73	182	2.14	12.8
12.00	288	12.2	60.0	1.85	1.48
15.00	649	20.2	42.7	1.46	0.49
18.00	765	26.4	98.1	2.80	0.84
21.00	157	15.3	41.2	2.19	0.80
24.00	91.4	4.10	27.7	1.43	2.12
27.00	86.2	4.91	10.7	0.88	0.16
30.00	370	16.3	96.4	5.67	1.29
33.00	177	10.9	74.7	5.55	0.90
36.00	152	36.6	132	13.8	8.47
39.00	175	8.02	81.7	4.24	2.46
42.00	169	10.5	126	2.81	12.8
45.00	271	17.9	93.7	2.31	26.9
48.70	362	21.7	186	7.34	61.0
51.00	332	22.1	93.3	6.49	20.1
53.00	205	3.54	21.3	2.06	19.8
56.00	200	5.05	42.5	2.07	7.01
63.00	166	8.95	275	5.27	5.23
65.00	269	2.62	34.3	1.97	29.8
68.00	215	10.4	45.3	4.65	5.58
71.00	314	4.43	23.0	3.40	1.04
73.00	515	6.66	70.0	3.16	12.4
75.00	376	1.32	12.9	1.19	3.72
77.60	387	3.87	9.13	0.62	1.81
80.00	598	1.72	6.53	0.97	1.68
83.00	252	3.75	30.2	1.87	1.58
85.00	511	1.70	16.8	0.97	1.92
87.00	415	1.04	7.24	0.57	0.93
90.00	319	11.1	174	6.32	2.88

Outcrop: East 53			Original Data (values in ppm)		
Height in vertical section (meters)	26	27	28	29	30
	Ru	Pd	Ag	Sn	Sb
0.00	0.19	15.9	0.41	2.38	0.92
3.00	0.25	11.4	0.34	1.09	0.59
6.00	0.06	1.24	0.42	1.56	0.34
9.00	0.35	7.66	0.23	2.89	0.58
12.00	0.52	2.63	0.11	7.03	0.29
15.00	0.25	1.79	0.10	4.60	0.30
18.00	0.16	3.90	0.14	2.15	0.32
21.00	0.15	1.65	0.09	1.96	0.28
24.00	0.10	1.01	0.20	1.04	0.33
27.00	0.08	0.37	0.20	13.7	0.28
30.00	0.44	4.25	0.19	0.82	0.29
33.00	0.47	2.62	0.26	2.30	1.25
36.00	0.01	4.21	0.43	3.78	1.54
39.00	0.61	2.70	0.21	2.87	0.46
42.00	0.40	3.87	0.18	1.54	0.52
45.00	0.92	3.06	0.13	6.84	0.38
48.70	0.47	5.91	0.28	6.41	0.38
51.00	0.43	2.96	0.42	2.84	0.38
53.00	0.77	0.69	0.10	1.82	0.20
56.00	0.71	1.53	0.14	0.85	0.19
63.00	0.21	8.97	0.41	7.31	0.36
65.00	0.83	1.21	2.16	0.51	0.40
68.00	0.50	1.75	0.91	2.07	0.73
71.00	0.76	0.88	0.33	0.91	0.42
73.00	0.61	2.70	0.20	1.38	0.50
75.00	0.86	0.49	0.13	1.06	0.27
77.60	0.89	0.38	0.05	3.19	0.15
80.00	0.70	0.28	0.04	5.38	0.18
83.00	0.77	1.19	0.11	1.79	0.17
85.00	0.90	0.66	0.05	1.05	0.15
87.00	0.68	0.30	0.05	0.55	0.11
90.00	0.41	6.02	0.32	10.0	0.36

Outcrop: East 53			Original Data (values in ppm)		
Height in vertical section (meters)	31	32	33	34	35
	Cs	Ba	La	Ce	Pr
0.00	0.99	239	24.7	41.9	5.86
3.00	1.22	157	25.4	43.7	6.21
6.00	0.68	108	18.8	24.1	3.21
9.00	0.42	89.0	6.67	11.0	1.40
12.00	0.32	47.6	8.37	11.3	1.54
15.00	0.36	130	12.4	17.8	2.62
18.00	0.47	146	16.5	24.2	3.50
21.00	0.81	82.6	13.8	19.0	2.51
24.00	0.36	57.3	5.90	8.77	1.14
27.00	0.35	39.7	6.36	10.1	1.39
30.00	0.66	132	13.4	25.2	3.30
33.00	1.07	610	13.1	22.7	2.73
36.00	11.8	420	45.8	79.2	9.80
39.00	0.58	84.5	7.27	13.9	1.83
42.00	0.80	229	10.9	20.9	2.87
45.00	0.21	70.1	11.0	16.3	2.09
48.70	2.60	201	20.2	33.7	4.47
51.00	3.72	175	18.2	28.1	3.84
53.00	0.68	161	4.57	8.26	1.03
56.00	0.20	36.9	4.70	8.55	1.08
63.00	0.84	193	9.77	19.0	2.56
65.00	0.25	638	3.72	6.41	0.776
68.00	1.43	117	8.57	13.6	1.88
71.00	0.40	224	5.68	8.87	1.16
73.00	0.80	267	7.74	15.0	1.85
75.00	No data	32.5	1.67	2.57	0.311
77.60	No data	44.4	3.16	5.00	0.608
80.00	No data	65.7	2.29	3.29	0.366
83.00	0.23	53.0	3.81	7.47	0.998
85.00	0.11	54.9	1.95	3.58	0.448
87.00	0.04	83.8	1.22	2.38	0.283
90.00	0.94	1354	15.9	32.1	3.96

Outcrop: East 53			Original Data (values in ppm)		
Height in vertical section (meters)	36	37	38	39	40
	Nd	Sm	Eu	Gd	Dy
0.00	23.4	4.82	1.02	4.74	4.32
3.00	24.3	4.99	1.06	5.07	4.69
6.00	11.0	1.88	0.40	1.77	1.51
9.00	5.42	1.08	0.24	1.05	0.94
12.00	5.91	1.19	0.28	1.28	1.18
15.00	10.5	2.24	0.53	2.34	2.13
18.00	14.0	2.96	0.67	3.02	2.78
21.00	9.39	1.90	0.44	1.92	1.78
24.00	4.31	0.85	0.19	0.75	0.67
27.00	5.27	1.07	0.24	0.94	0.83
30.00	12.4	2.55	0.54	2.48	2.40
33.00	10.3	2.00	0.60	2.04	1.88
36.00	36.1	6.84	1.62	6.88	5.54
39.00	7.05	1.32	0.34	1.36	1.25
42.00	11.3	2.29	0.54	2.28	2.01
45.00	8.19	1.54	0.37	1.85	1.73
48.70	17.6	3.45	0.72	3.50	3.05
51.00	15.0	2.86	0.67	3.05	2.89
53.00	4.00	0.67	0.21	0.76	0.67
56.00	4.02	0.72	0.17	0.84	0.77
63.00	10.1	2.03	0.49	1.93	1.87
65.00	2.82	0.46	0.29	0.56	0.52
68.00	7.09	1.28	0.33	1.39	1.26
71.00	4.83	0.80	0.23	0.86	0.69
73.00	6.98	1.30	0.35	1.38	1.23
75.00	1.21	0.11	0.05	0.22	0.19
77.60	2.27	0.30	0.11	0.50	0.49
80.00	1.28	0.12	0.06	0.22	0.18
83.00	3.88	0.74	0.17	0.75	0.70
85.00	1.69	0.20	0.08	0.32	0.27
87.00	1.00	0.13	0.07	0.21	0.14
90.00	15.2	3.01	0.81	2.70	2.18

Outcrop: East 53			Original Data (values in ppm)		
Height in vertical section (meters)	41	42	43	44	45
	Ho	Er	Tm	Yb	Hf
0.00	0.91	2.59	0.381	2.54	16.5
3.00	0.99	2.99	0.425	2.79	10.4
6.00	0.29	0.83	0.116	0.66	1.22
9.00	0.20	0.60	0.096	0.64	6.34
12.00	0.26	0.78	0.106	0.66	2.38
15.00	0.45	1.28	0.186	1.07	1.72
18.00	0.61	1.78	0.251	1.53	3.62
21.00	0.37	1.09	0.151	0.86	1.64
24.00	0.14	0.39	0.061	0.40	1.06
27.00	0.16	0.42	0.061	0.36	0.43
30.00	0.52	1.51	0.225	1.46	3.53
33.00	0.37	1.07	0.156	1.06	2.96
36.00	1.13	3.20	0.470	3.10	5.13
39.00	0.25	0.75	0.104	0.70	2.97
42.00	0.40	1.18	0.173	1.16	4.25
45.00	0.38	1.16	0.156	0.99	3.42
48.70	0.65	1.88	0.266	1.82	6.31
51.00	0.61	1.78	0.258	1.68	3.35
53.00	0.13	0.42	0.058	0.43	0.78
56.00	0.14	0.50	0.067	0.46	1.54
63.00	0.40	1.20	0.188	1.30	9.12
65.00	0.10	0.32	0.047	0.34	1.00
68.00	0.25	0.77	0.111	0.73	2.57
71.00	0.14	0.43	0.057	0.38	1.12
73.00	0.24	0.74	0.107	0.72	2.71
75.00	0.03	0.11	0.014	0.11	0.42
77.60	0.10	0.27	0.036	0.24	0.32
80.00	0.03	0.11	0.015	0.12	0.24
83.00	0.14	0.43	0.059	0.44	1.12
85.00	0.05	0.18	0.022	0.17	0.56
87.00	0.03	0.10	0.009	0.10	0.31
90.00	0.42	1.22	0.171	1.20	5.84

Outcrop: East 53			Original Data (values in ppm)		
Height in vertical section (meters)	46	47	48	49	50
	Ta	Au	Tl	Pb	Th
0.00	1.62	0.55	0.72	12.8	7.58
3.00	1.20	0.36	1.28	20.8	7.30
6.00	0.48	0.22	0.50	7.31	2.08
9.00	0.52	0.23	0.26	7.34	1.30
12.00	0.40	0.17	0.11	1.95	1.18
15.00	0.39	0.14	0.13	2.99	1.74
18.00	0.53	0.14	0.16	3.59	2.46
21.00	0.39	0.11	0.12	3.05	1.53
24.00	0.29	0.09	0.10	1.95	0.87
27.00	0.29	0.05	0.05	2.24	0.73
30.00	0.58	0.04	0.21	2.56	3.35
33.00	1.30	0.60	0.52	6.64	4.24
36.00	1.73	0.55	1.89	15.1	10.9
39.00	0.67	0.32	0.43	4.75	2.56
42.00	0.55	0.23	0.59	5.66	3.63
45.00	0.62	0.23	0.35	10.2	2.14
48.70	0.92	0.19	3.13	19.7	5.47
51.00	0.80	0.17	2.66	31.3	4.86
53.00	0.46	0.15	0.47	3.72	1.20
56.00	0.46	0.12	0.13	1.86	1.12
63.00	0.73	0.09	0.34	3.99	2.98
65.00	0.42	0.05	0.24	16.7	0.97
68.00	1.21	0.51	0.58	11.5	4.17
71.00	0.88	0.39	0.30	2.61	1.76
73.00	0.70	0.21	0.23	10.1	2.39
75.00	0.51	0.18	0.07	2.22	0.47
77.60	0.37	0.13	No data	0.95	0.31
80.00	0.36	0.07	0.05	1.10	0.22
83.00	0.43	0.09	0.09	1.80	0.98
85.00	0.39	0.07	No data	1.25	0.49
87.00	0.24	0.07	No data	0.76	0.16
90.00	0.76	0.05	0.14	4.60	4.85

Outcrop: East 53		Original Data (values in ppm)			
Height in vertical section (meters)	51				
	U				
0.00	5.51				
3.00	2.92				
6.00	1.32				
9.00	1.63				
12.00	1.84				
15.00	1.55				
18.00	2.29				
21.00	2.03				
24.00	0.83				
27.00	0.68				
30.00	3.14				
33.00	4.14				
36.00	6.81				
39.00	3.54				
42.00	2.54				
45.00	4.44				
48.70	4.00				
51.00	5.70				
53.00	4.13				
56.00	2.51				
63.00	3.09				
65.00	3.64				
68.00	3.85				
71.00	2.51				
73.00	3.69				
75.00	4.28				
77.60	3.46				
80.00	3.14				
83.00	2.63				
85.00	3.55				
87.00	1.48				
90.00	4.01				

APENDIX C: GEOCHEMISTRY DATA NORMALIZED TO ZIRCON

Outcrop: Monaghan Creek		Data Normalized to Zr in ppm				
Height in vertical section (meters)	1	2	3	4	5	
	Li	Be	Mg	Al	Si	
27.00	0.277047	0.005909	607.3441	121.3356	1203.802	
30.00	0.225494	0.007666	1038.532	60.63059	5112.352	
33.00	0.433399	0.049538	1244.877	125.555	753.7856	
36.00	0.300045	0.00252	29.30614	112.713	892.0733	
39.00	0.18345	0.00256	156.7187	127.6805	1076.615	
42.00	1.17646	0.014936	92.49023	463.0366	2134.302	
45.00	0.419888	0.007777	56.64065	233.2955	1363.421	
48.00	0.188047	0.004077	1167.27	82.88587	831.1599	
50.00	0.432134	No data	8413.787	187.9042	983.8009	
63.00	0.225292	0.008849	2284.932	154.9097	1103.593	
66.00	0.326792	No data	8191.913	112.9684	620.4806	
69.00	0.39067	0.017868	18283.81	139.5556	825.6727	
72.00	0.564322	0.029646	5087.747	187.631	942.2764	
75.75	0.681353	No data	27315.28	242.5259	1208.307	
80.00	3.285198	No data	1106.798	208.9089	1599.746	
83.00	0.850849	No data	43105.93	107.42	1028.742	
102.00	0.476701	0.044551	657.0918	316.0762	1454.065	
105.00	0.652751	No data	13225.21	362.0484	1217.411	
108.60	0.809675	0.066231	56347.69	183.454	790.573	
111.00	1.977886	0.03126	29884.01	307.7956	1867.917	
114.00	0.961182	0.007065	360.2731	155.1405	1971.232	
117.00	4.2734	0.0196	466.0062	218.5648	1358.951	
120.30	0.936048	0.008124	79.0988	247.6794	2290.317	
123.00	2.646801	0.016152	597.1753	324.3769	2653.483	
123.50	1.412424	0.008776	505.6809	184.3845	1057.476	
126.00	1.597163	0.007357	120.9982	239.3816	1717.692	
128.60	0.49368	0.008282	62.5413	391.7929	6038.253	
138.00	1.470739	0.024719	5457.91	173.343	1564.005	
146.00	0.37512	0.00621	28.57309	198.7249	3083.501	
156.00	0.447683	0.0055	47.60346	198.995	2143.674	
164.00	0.627944	0.006965	63.1254	194.9621	1920.524	
168.70	0.607098	0.014406	287.1359	138.4777	1364.08	
172.20	0.727205	0.033846	14268.87	117.5231	584.3306	
197.00	1.102913	0.007818	77.80578	203.3909	1538.062	
202.50	0.514538	0.006596	326.859	219.0604	1767.923	
210.00	1.390612	0.007372	948.1543	175.6027	1573.79	

Outcrop: Monaghan Creek		Data Normalized to Zr in ppm				
Height in vertical section (meters)	6	7	8	9	10	
	P	K	Ca	Ti	V	
27.00	49.04583	99.25025	1164.119	11.73328	0.172461	
30.00	99.07706	67.6979	3402.879	6.604538	0.158101	
33.00	34.83019	149.1136	91538.9	17.82841	1.017222	
36.00	6.226117	85.22737	1778.357	8.310547	0.148757	
39.00	2.223359	98.20788	1350.705	9.788886	0.124035	
42.00	43.02652	339.7063	126.0643	29.59999	0.819793	
45.00	6.586824	196.0144	6027.994	15.0538	0.33409	
48.00	12.72219	79.74786	2651.826	6.713436	0.160511	
50.00	19.70012	280.8849	49136.73	14.91496	1.223799	
63.00	4.929088	133.4718	5356.419	12.58427	0.252683	
66.00	19.71442	108.882	18220.39	9.792285	0.275941	
69.00	49.58924	198.1427	40585.95	14.61362	0.50634	
72.00	30.37717	195.4943	50665.71	18.7013	0.801298	
75.75	24.61242	241.5197	54356.7	17.61592	1.379333	
80.00	18.93187	308.6072	172299.9	45.58563	2.143671	
83.00	20.14357	249.0756	104547.3	12.95142	2.180005	
102.00	13.50354	377.1631	67681.87	25.65468	1.508692	
105.00	15.88307	409.1655	46985.18	23.90921	2.427739	
108.60	29.29415	298.4983	136779	15.73743	1.482132	
111.00	26.7244	260.0201	65371.89	19.73123	1.25998	
114.00	2.315462	156.3463	8078.586	10.36325	0.232948	
117.00	4.260887	171.0349	25861.84	14.59451	0.729916	
120.30	2.332397	208.8113	1261.515	15.08631	0.223265	
123.00	5.548863	381.6832	27175.35	16.05175	0.798647	
123.50	4.925965	160.7109	1875.991	15.0187	0.262057	
126.00	3.436131	190.8243	2024.209	17.42189	0.289562	
128.60	2.769287	323.6496	3111.448	14.24267	0.19941	
138.00	19.72842	204.4675	18848.82	13.57322	0.861722	
146.00	1.636842	169.7397	1594.14	10.5577	0.113066	
156.00	2.340089	172.2606	1311.268	13.63762	0.170508	
164.00	3.329586	166.5365	3306.539	12.66682	0.187228	
168.70	5.725422	153.7256	21764.35	10.73627	0.62358	
172.20	36.2455	151.3541	29770.79	16.45449	0.466646	
197.00	4.29651	150.6933	2941.503	12.62487	0.256985	
202.50	4.219325	154.2504	1309.547	15.77366	0.229691	
210.00	3.948506	136.2942	2265.166	12.52338	0.263286	

Outcrop: Monaghan Creek		Data Normalized to Zr in ppm				
Height in vertical section (meters)	11	12	13	14	15	
	Cr	Mn	Fe	Co	Cu	
27.00	0.442434	0.939414	56.2894	0.042837	0.175427	
30.00	0.789619	1.707011	43.24657	0.117663	0.286945	
33.00	4.561734	29.74951	259.2718	1.553668	1.54699	
36.00	0.258947	1.014054	39.5689	0.04303	0.143959	
39.00	0.18654	1.042645	20.84346	0.046877	0.083643	
42.00	0.95188	0.540343	174.7368	0.078831	0.094302	
45.00	0.897206	2.267957	86.59767	0.143133	0.259893	
48.00	0.529661	1.390204	41.95024	0.102957	0.18421	
50.00	3.293777	12.18091	292.56	1.131998	0.597024	
63.00	0.607409	1.845663	48.80381	0.243396	0.233921	
66.00	1.962532	3.789955	71.60344	0.584355	0.494505	
69.00	3.58493	7.429629	152.1892	2.078134	1.107931	
72.00	2.988206	9.000316	190.417	1.590285	0.965902	
75.75	4.63687	11.5583	140.3706	2.657661	1.242643	
80.00	7.074687	19.49768	361.2268	2.606215	3.033845	
83.00	8.700013	20.45438	395.3589	4.505988	2.787146	
102.00	3.026397	12.84934	327.6793	1.75479	0.658912	
105.00	3.168242	6.270204	143.6056	1.561919	0.885269	
108.60	11.75113	23.98608	272.7873	2.988923	2.430931	
111.00	8.0861	14.04687	238.9805	0.964607	1.231603	
114.00	0.554217	5.105434	114.3354	0.147025	0.20456	
117.00	1.451267	7.518357	118.9434	0.312063	0.465181	
120.30	0.277124	1.248617	71.40137	0.062808	0.128343	
123.00	1.645619	10.08974	137.4389	0.220748	0.793743	
123.50	0.386608	1.388999	75.94903	0.081217	0.104424	
126.00	0.407546	1.816807	90.66738	0.077571	0.138831	
128.60	0.432	2.52015	53.45863	0.068174	0.12204	
138.00	1.972269	18.18628	222.2495	0.309316	0.670398	
146.00	0.21973	0.831903	44.52269	0.026242	0.099985	
156.00	0.230044	0.955176	54.98552	0.023088	0.076836	
164.00	0.35008	2.379997	63.53993	0.042227	0.130489	
168.70	0.980568	12.30646	122.1853	0.215854	0.361137	
172.20	1.951981	17.07885	487.8388	0.42339	1.26927	
197.00	0.398201	1.703414	79.88421	0.026377	0.135102	
202.50	0.340311	1.851723	80.41917	0.045529	0.143172	
210.00	0.360808	1.982762	68.91208	0.042747	0.153704	

Outcrop: Monaghan Creek		Data Normalized to Zr in ppm				
Height in vertical section (meters)	16	17	18	19	20	
	Zn	Ga	Ge	As	Rb	
27.00	0.270539	0.026757	0.003852	0.036841	0.238154	
30.00	0.274104	0.011861	0.010464	0.026252	0.127446	
33.00	1.433918	0.044205	0.00634	0.139171	0.204979	
36.00	0.19149	0.029527	0.002771	0.006793	0.194214	
39.00	0.084664	0.026449	0.003561	0.010019	0.20328	
42.00	0.336103	0.143537	0.012519	0.091156	1.126132	
45.00	0.352705	0.051684	0.005688	0.100253	0.391508	
48.00	0.467956	0.01766	0.003438	0.02585	0.172077	
50.00	1.361327	0.055707	0.008803	0.070097	0.371553	
63.00	0.288195	0.033571	0.003727	0.013144	0.234891	
66.00	0.745934	0.025195	0.004973	0.028297	0.185428	
69.00	1.710828	0.03337	0.014047	0.047323	0.213214	
72.00	1.876745	0.039617	0.011392	0.062656	0.298953	
75.75	1.703378	0.058055	0.030887	0.078348	0.334095	
80.00	3.482977	0.046377	0.012562	0.148711	0.35918	
83.00	3.163877	0.097545	0.033359	0.371166	0.142876	
102.00	4.51937	0.109285	0.01312	0.425215	0.622123	
105.00	1.604592	0.076422	0.013311	0.136112	0.842686	
108.60	No data	0.175476	0.04068	0.345343	0.348272	
111.00	No data	0.044212	0.011948	0.26504	0.324341	
114.00	0.352168	0.035491	0.007609	0.069193	0.341733	
117.00	0.00761	0.054688	0.008255	0.163183	0.400543	
120.30	0.06436	0.052125	0.007446	0.02052	0.512548	
123.00	2.083079	0.103861	0.007373	0.075421	0.902688	
123.50	0.046514	0.046926	0.003217	0.026288	0.461355	
126.00	0.114818	0.065221	0.007393	0.051884	0.498837	
128.60	0.022845	0.084643	0.01745	0.026298	0.803788	
138.00	0.53742	0.050233	0.009562	0.213634	0.348594	
146.00	0.383102	0.036835	0.008065	0.017702	0.46533	
156.00	0.136001	0.039208	0.005802	0.019928	0.428226	
164.00	0.063257	0.046348	0.006523	0.019878	0.370477	
168.70	No data	0.036102	0.00582	0.068129	0.274765	
172.20	6.065271	0.053669	0.01112	0.169656	0.249472	
197.00	0.244081	0.03667	0.00397	0.019475	0.420384	
202.50	0.105396	0.050426	0.005954	0.040111	0.38031	
210.00	0.194023	0.040479	0.004371	0.020268	0.36755	

Outcrop: Monaghan Creek		Data Normalized to Zr in ppm			
Height in vertical section (meters)	21	22	23	24	25
	Sr	Y	Zr	Nb	Mo
27.00	1.614573	0.147948	1	0.043517	0.028867
30.00	3.597944	0.161236	1	0.037525	0.133577
33.00	71.14182	0.118336	1	0.337733	0.610614
36.00	1.684948	0.083325	1	0.029138	0.018217
39.00	1.43722	0.082636	1	0.031713	0.006719
42.00	1.112453	0.241584	1	0.083839	0.027985
45.00	6.680171	0.114018	1	0.044912	0.122527
48.00	2.452035	0.130046	1	0.025307	0.017764
50.00	43.73031	0.13897	1	0.091726	0.118123
63.00	4.872116	0.12838	1	0.100233	0.197371
66.00	13.1078	0.087727	1	0.11558	0.086625
69.00	26.85104	0.108467	1	0.147675	0.375068
72.00	31.89908	0.116319	1	0.128747	0.823553
75.75	38.98775	0.194326	1	0.122688	0.853757
80.00	810.5261	0.383661	1	0.49615	0.707434
83.00	163.0633	0.149747	1	0.143346	2.32297
102.00	75.02738	0.182864	1	0.109107	5.390993
105.00	79.23544	0.123854	1	0.09645	0.103516
108.60	294.8972	0.146246	1	1.701313	1.133615
111.00	55.1469	0.229262	1	0.331834	0.541643
114.00	6.582067	0.125339	1	0.043665	0.121935
117.00	16.13135	0.112535	1	0.077343	0.22686
120.30	1.734516	0.096983	1	0.051988	0.026573
123.00	20.36078	0.119047	1	0.08497	0.121769
123.50	2.127842	0.12171	1	0.084969	0.062783
126.00	2.301055	0.135321	1	0.0567	0.034646
128.60	3.666288	0.115834	1	0.04291	0.041213
138.00	14.57904	0.166724	1	0.132119	0.294083
146.00	2.511281	0.058745	1	0.040038	0.047565
156.00	1.515813	0.082258	1	0.049563	0.059515
164.00	3.037189	0.097508	1	0.059882	0.115375
168.70	13.47773	0.11106	1	0.061365	0.351739
172.20	23.05754	0.152039	1	0.304296	1.223868
197.00	2.768956	0.105565	1	0.044915	0.009409
202.50	1.512009	0.138369	1	0.054543	0.010018
210.00	2.518107	0.098684	1	0.050296	0.008183

Outcrop: Monaghan Creek		Data Normalized to Zr in ppm				
Height in vertical section (meters)	26	27	28	29	30	
	Ru	Pd	Ag	Sn	Sb	
27.00	0.001885	0.029906	0.002987	0.016156	0.014368	
30.00	0.005482	0.030024	0.003642	0.024263	0.020763	
33.00	0.104569	0.047417	0.031061	0.230394	0.111332	
36.00	0.001879	0.029555	0.019943	0.027866	0.003226	
39.00	0.001776	0.028686	0.071711	0.015607	0.003542	
42.00	No data	0.02731	0.031952	0.024899	0.007778	
45.00	0.006941	0.029167	0.005255	0.021532	0.005964	
48.00	0.004993	0.030031	0.001291	0.0153	0.00387	
50.00	0.075549	0.033028	0.013134	0.054549	0.023547	
63.00	0.00902	0.029248	0.00576	0.031459	0.041322	
66.00	0.021655	0.030391	0.007589	0.053821	0.053883	
69.00	0.055953	0.035273	0.015806	0.179122	0.077281	
72.00	0.050905	0.025565	0.098558	0.087147	0.047975	
75.75	0.066158	0.030947	1.158247	0.251759	0.048308	
80.00	0.186439	0.027543	0.146296	0.684896	0.084111	
83.00	0.145125	0.02677	0.040945	0.234963	0.061071	
102.00	0.046777	0.023106	0.019804	0.090277	0.034767	
105.00	0.052434	0.020998	0.012495	0.04375	0.014077	
108.60	0.176881	0.100444	0.183851	0.752034	1.259368	
111.00	0.074164	0.034306	0.033248	0.16011	0.280234	
114.00	0.006721	0.029794	0.003549	0.021357	0.019357	
117.00	0.017699	0.027027	0.011742	0.040911	0.032541	
120.30	No data	0.030335	0.006388	0.01132	0.004807	
123.00	0.023605	0.026784	0.016636	0.138315	0.022294	
123.50	0.00169	0.030352	0.002107	0.007719	0.004087	
126.00	0.000482	0.029445	0.002585	0.012238	0.004959	
128.60	No data	0.028394	0.001554	0.009414	0.007034	
138.00	0.028422	0.044957	0.041444	0.093315	0.075253	
146.00	0.001384	0.03366	0.002444	0.013358	0.007931	
156.00	0.000747	0.032672	0.002073	0.007725	0.004438	
164.00	0.0028	0.033265	0.002519	0.011886	0.00497	
168.70	0.021458	0.032337	0.002871	0.017648	0.013278	
172.20	0.036073	0.024265	0.010278	0.050743	0.027494	
197.00	0.002856	0.034083	0.00202	0.010157	0.00475	
202.50	0.001195	0.032777	0.001609	0.013817	0.004316	
210.00	0.003394	0.032161	0.001648	0.005505	0.004498	

Outcrop: Monaghan Creek		Data Normalized to Zr in ppm				
Height in vertical section (meters)	31	32	33	34	35	
	Cs	Ba	La	Ce	Pr	
27.00	0.010415	0.947376	0.118246	0.208679	0.02789	
30.00	0.00359	0.873863	0.10595	0.177362	0.023549	
33.00	0.005078	10.08787	0.150025	0.282746	0.030843	
36.00	0.00634	0.743169	0.075265	0.155511	0.019655	
39.00	0.004286	1.100598	0.069559	0.133191	0.01782	
42.00	0.062554	2.160103	0.234353	0.394229	0.051901	
45.00	0.011766	1.529285	0.124016	0.245364	0.030586	
48.00	0.005739	0.623924	0.083716	0.178216	0.02703	
50.00	0.011761	1.687148	0.185508	0.362515	0.036202	
63.00	0.005798	1.363399	0.127832	0.231916	0.0308	
66.00	0.005828	1.072535	0.112493	0.190082	0.02198	
69.00	No data	2.591422	0.123018	0.239805	0.029323	
72.00	0.007113	3.696684	0.146453	0.28892	0.032916	
75.75	No data	1.984256	0.199237	0.34508	0.042357	
80.00	No data	48.6842	0.835306	0.845647	0.099874	
83.00	No data	7.876586	0.203185	0.263255	0.029744	
102.00	0.019929	5.800461	0.238578	0.481584	0.058435	
105.00	0.033217	7.7347	0.154875	0.304667	0.034967	
108.60	0.040579	6.95059	0.260709	0.364903	0.053261	
111.00	0.011251	4.93675	0.304761	0.586429	0.071304	
114.00	0.0077	18.33978	0.12218	0.235637	0.029769	
117.00	0.019292	4.274045	0.158975	0.288661	0.034281	
120.30	0.013876	2.832515	0.115648	0.222313	0.028492	
123.00	0.031037	8.642969	0.190139	0.294031	0.036793	
123.50	0.012878	1.269546	0.147859	0.28478	0.034944	
126.00	0.018472	4.55426	0.157358	0.305314	0.039121	
128.60	0.011869	6.074615	0.131626	0.240945	0.030331	
138.00	0.018019	1.52998	0.284155	0.396069	0.048518	
146.00	0.009936	3.062039	0.070112	0.119149	0.016787	
156.00	0.010706	2.075948	0.094906	0.17916	0.023126	
164.00	0.010388	4.725295	0.110086	0.200925	0.025864	
168.70	0.009882	1.485826	0.162718	0.267397	0.031761	
172.20	0.009114	1.631722	0.256545	0.395581	0.04361	
197.00	0.012928	1.613298	0.113128	0.230731	0.029072	
202.50	0.011595	1.807154	0.159521	0.303749	0.038851	
210.00	0.013082	2.293166	0.118076	0.225792	0.02897	

Outcrop: Monaghan Creek		Data Normalized to Zr in ppm				
Height in vertical section (meters)	36	37	38	39	40	
	Nd	Sm	Eu	Gd	Dy	
27.00	0.107314	0.021787	0.004922	0.020753	0.020822	
30.00	0.090143	0.018145	0.00444	0.01847	0.018303	
33.00	0.099883	0.013536	No data	0.019653	0.018238	
36.00	0.075255	0.015426	0.003422	0.014565	0.013853	
39.00	0.070773	0.015132	0.003701	0.01418	0.014119	
42.00	0.195876	0.039516	0.008573	0.036893	0.034092	
45.00	0.116232	0.024728	0.005445	0.0211	0.020553	
48.00	0.113227	0.02541	0.005195	0.023644	0.02059	
50.00	0.139082	0.02543	0.006864	0.029318	0.021453	
63.00	0.116706	0.024326	0.005877	0.021914	0.021932	
66.00	0.082009	0.01456	0.003528	0.01419	0.014733	
69.00	0.101676	0.015204	0.00591	0.020132	0.016455	
72.00	0.124615	0.020647	0.006	0.023013	0.019206	
75.75	0.157123	0.026706	0.009616	0.031615	0.027522	
80.00	0.481384	0.069232	0.030546	0.075819	0.058348	
83.00	0.11428	No data	No data	0.02086	0.017525	
102.00	0.212614	0.036201	0.009375	0.035299	0.033153	
105.00	0.135121	0.02409	0.007372	0.02429	0.021186	
108.60	0.180342	0.038082	0.019025	0.039129	0.034649	
111.00	0.253792	0.049571	0.010913	0.041609	0.04287	
114.00	0.117425	0.024171	0.009701	0.022634	0.022196	
117.00	0.127344	0.023803	0.006003	0.021126	0.019252	
120.30	0.110525	0.023273	0.00588	0.019561	0.017858	
123.00	0.143344	0.02542	0.007157	0.023588	0.020173	
123.50	0.132948	0.026985	0.006112	0.024555	0.022119	
126.00	0.15123	0.029809	0.007157	0.02783	0.024889	
128.60	0.119884	0.02402	0.007657	0.022079	0.020216	
138.00	0.173483	0.03392	0.009079	0.031305	0.027342	
146.00	0.065795	0.01259	0.003618	0.010799	0.011005	
156.00	0.089102	0.018252	0.004469	0.015833	0.015304	
164.00	0.099115	0.020115	0.005455	0.017924	0.017094	
168.70	0.115117	0.024046	0.005219	0.020463	0.018805	
172.20	0.162617	0.030362	0.00699	0.028495	0.026159	
197.00	0.115553	0.024704	0.005667	0.0217	0.019648	
202.50	0.148717	0.030438	0.006785	0.027287	0.026053	
210.00	0.110632	0.022377	0.005405	0.020398	0.018793	

Outcrop: Monaghan Creek		Data Normalized to Zr in ppm				
Height in vertical section (meters)	41	42	43	44	45	
	Ho	Er	Tm	Yb	Hf	
27.00	0.004578	0.013256	0.001972	0.01259	0.037975	
30.00	0.003994	0.011622	0.00161	0.011086	0.034674	
33.00	No data	0.010021	No data	No data	0.037293	
36.00	0.002961	0.008447	0.001208	0.008169	0.030578	
39.00	0.002899	0.008414	0.001232	0.008205	0.029052	
42.00	0.007026	0.020327	0.00294	0.018866	0.031643	
45.00	0.004264	0.011868	0.001732	0.012045	0.027885	
48.00	0.00393	0.010812	0.00144	0.008892	0.029424	
50.00	0.004671	0.012664	0.001959	0.009911	0.031904	
63.00	0.004839	0.012965	0.002137	0.011875	0.039931	
66.00	0.002961	0.008968	0.001561	0.008669	0.046406	
69.00	No data	0.00995	0.001584	0.010902	0.049787	
72.00	0.004603	0.011075	0.001889	0.011573	0.039798	
75.75	0.006385	0.017812	0.00249	0.015913	0.062465	
80.00	0.01213	0.032243	0.004319	0.026194	0.043766	
83.00	No data	No data	No data	No data	0.065508	
102.00	0.007466	0.019521	0.002588	0.020511	0.035865	
105.00	0.004624	0.011445	0.001846	0.013535	0.078358	
108.60	0.018953	0.024849	0.019728	No data	0.17499	
111.00	0.009215	0.024097	0.004449	0.024486	0.091638	
114.00	0.004531	0.012643	0.001918	0.011888	0.036324	
117.00	0.003882	0.011663	0.001854	0.012087	0.045362	
120.30	0.003709	0.010742	0.001593	0.010941	0.032561	
123.00	0.003961	0.010839	0.001668	0.009859	0.03074	
123.50	0.00453	0.013056	0.001804	0.012134	0.03364	
126.00	0.00495	0.01422	0.002101	0.01404	0.032595	
128.60	0.004009	0.011637	0.001665	0.011108	0.030781	
138.00	0.007599	0.016749	0.003795	0.015313	0.05835	
146.00	0.002384	0.007313	0.00118	0.007791	0.034188	
156.00	0.00307	0.009204	0.001361	0.009165	0.034219	
164.00	0.003566	0.010432	0.001625	0.010417	0.034292	
168.70	0.004169	0.0109	0.001765	0.010994	0.034784	
172.20	0.005203	0.016648	0.00235	0.014596	0.041758	
197.00	0.003944	0.011494	0.001692	0.011202	0.036768	
202.50	0.005258	0.015109	0.002162	0.013935	0.035399	
210.00	0.003836	0.011034	0.001586	0.010586	0.035785	

Outcrop: Monaghan Creek		Data Normalized to Zr in ppm				
Height in vertical section (meters)	46	47	48	49	50	
	Ta	Au	Tl	Pb	Th	
27.00	0.009406	0.00869	0.007356	0.057863	0.039386	
30.00	0.014902	0.016371	0.00895	0.07275	0.033298	
33.00	0.105628	0.100433	0.041529	0.393894	0.07228	
36.00	0.004706	0.003237	0.001664	0.024824	0.018385	
39.00	0.004336	0.002435	0.001761	0.027171	0.017078	
42.00	0.007818	0.002441	0.011333	0.17055	0.06691	
45.00	0.009581	0.005433	0.00603	0.114585	0.03108	
48.00	0.005268	0.003657	0.002597	0.06751	0.015042	
50.00	0.038538	0.035271	0.007826	0.210531	0.017573	
63.00	0.024403	0.019527	0.017961	0.061246	0.051693	
66.00	0.045395	0.030099	0.023577	0.114196	0.056054	
69.00	0.080355	0.05387	0.033361	0.202242	0.068775	
72.00	0.057177	0.027609	0.02677	0.186536	0.049645	
75.75	0.069465	0.04505	0.040336	0.333315	0.059312	
80.00	0.132636	0.053168	0.052646	0.469716	0.057464	
83.00	0.101607	0.046209	0.141593	0.553919	0.018762	
102.00	0.041386	0.010617	0.071045	1.771757	0.044967	
105.00	0.035739	0.004099	0.00968	0.243632	0.048021	
108.60	0.670954	0.573454	0.496306	2.816473	0.634851	
111.00	0.231025	0.148497	0.11295	0.532185	0.195299	
114.00	0.01838	0.006318	0.007374	0.14238	0.029921	
117.00	0.038603	0.008566	0.012229	0.082977	0.048669	
120.30	0.008056	0.000751	0.004238	0.077892	0.036361	
123.00	0.029733	-0.00211	0.00731	0.174051	0.035054	
123.50	0.007417	No data	0.003676	0.066439	0.038561	
126.00	0.007307	-0.00032	0.005008	0.093002	0.04108	
128.60	0.008759	No data	0.004591	0.129181	0.024785	
138.00	0.077993	0.092223	0.069332	0.276606	0.13814	
146.00	0.010478	0.006791	0.008406	0.112276	0.026137	
156.00	0.008198	0.003165	0.004524	0.074682	0.030601	
164.00	0.009509	0.00326	0.004445	0.063355	0.02862	
168.70	0.025132	0.006322	0.007919	0.113472	0.036262	
172.20	0.07761	0.027853	0.027671	0.416906	0.058772	
197.00	0.00724	0.001776	0.003519	0.064178	0.032699	
202.50	0.007525	0.00055	0.003465	0.087152	0.03897	
210.00	0.007283	0.000429	0.003528	0.08281	0.030993	

Outcrop: Monaghan Creek		Data Normalized to Zr in ppm			
Height in vertical section (meters)	51				
	U				
27.00	0.019859				
30.00	0.035785				
33.00	0.624396				
36.00	0.017127				
39.00	0.021183				
42.00	0.04929				
45.00	0.044622				
48.00	0.028807				
50.00	0.315978				
63.00	0.068111				
66.00	0.21542				
69.00	0.41187				
72.00	0.358455				
75.75	0.489642				
80.00	1.104857				
83.00	0.678041				
102.00	1.41662				
105.00	0.55649				
108.60	1.217036				
111.00	0.501853				
114.00	0.063495				
117.00	0.268253				
120.30	0.013352				
123.00	0.223126				
123.50	0.030897				
126.00	0.018028				
128.60	0.020351				
138.00	0.137313				
146.00	0.025807				
156.00	0.019101				
164.00	0.044717				
168.70	0.185808				
172.20	0.214908				
197.00	0.053984				
202.50	0.024136				
210.00	0.030235				

Outcrop: East 53		Data Normalized to Zr in ppm				
Height in vertical section (meters)	1	2	3	4	5	
	Li	Be	Mg	Al	Si	
0.00	0.025408	0.001768	107.4627	43.22279	541.1873	
3.00	0.054133	0.002581	188.3086	62.69647	649.8277	
6.00	0.447269	0.018576	504.6764	290.2857	10563.42	
9.00	0.046436	0.001066	243.4923	15.67763	869.2421	
12.00	0.0946	0.003937	1102.194	54.67459	1013.066	
15.00	0.176839	0.005163	369.9478	118.2669	5621.427	
18.00	0.101317	0.003575	159.4787	67.47018	2793.06	
21.00	0.297879	0.009267	562.6726	152.6808	5714.241	
24.00	0.382222	0.007021	415.1514	140.5855	12229.1	
27.00	0.768007	0.010091	44.38257	391.4834	29842.16	
30.00	0.127042	0.003282	300.5385	132.9116	943.9747	
33.00	0.348438	0.004796	56.18982	157.5466	2096.493	
36.00	0.796373	0.022551	176.0994	551.6861	2102.194	
39.00	0.165685	0.005165	1063.252	116.5544	872.4364	
42.00	0.118096	0.004439	493.2847	154.6989	1502.089	
45.00	0.047213	0.002006	696.025	43.09928	526.4585	
48.70	0.154212	0.003702	385.4475	131.3132	622.4004	
51.00	0.37601	0.011034	782.5709	262.2712	1091.797	
53.00	0.771544	0.019006	5560.15	385.2908	1337.709	
56.00	0.199343	0.007006	2653.093	96.61894	792.8716	
63.00	0.083661	0.001831	134.7021	64.56954	968.2496	
65.00	0.432969	0.004784	1986.284	119.7823	635.8113	
68.00	0.843167	0.01015	1855.16	302.6884	1953.635	
71.00	0.822066	0.010723	3608.475	229.3884	1288.974	
73.00	0.407405	0.006575	63.3165	146.026	999.1828	
75.00	0.23227	0.010401	813.5241	79.72724	712.0153	
77.60	0.243781	0.020392	5971.197	86.9466	975.8356	
80.00	0.501923	No data	1365.503	159.362	1277.968	
83.00	0.271644	0.008126	2989.385	217.2634	1642.258	
85.00	0.258799	0.008408	3764.997	160.6627	1102.003	
87.00	0.507028	0.020489	16819.6	144.5622	930.3434	
90.00	0.355191	0.003812	374.6749	110.3767	1033.078	

Outcrop: East 53		Data Normalized to Zr in ppm				
Height in vertical section (meters)	6	7	8	9	10	
	P	K	Ca	Ti	V	
0.00	13.16776	39.02134	220.7509	6.280645	0.06649	
3.00	23.62134	48.95139	386.2015	8.471996	0.084277	
6.00	105.7237	318.4664	1212.511	12.62579	0.527425	
9.00	8.92849	17.16709	565.3382	2.741348	0.056686	
12.00	108.6008	58.44917	2735.474	5.619686	0.184956	
15.00	179.0111	135.0062	1691.812	12.41469	0.219921	
18.00	102.5495	70.3571	646.2815	8.407956	0.113134	
21.00	162.563	129.0486	1783.031	13.16177	0.495101	
24.00	16.76021	142.8781	1287.441	14.70799	0.48075	
27.00	71.99613	287.7076	4366.323	23.46481	1.20586	
30.00	16.68544	107.958	1675.298	15.12735	0.188872	
33.00	7.452111	123.8806	2790.814	12.99702	0.268346	
36.00	50.43245	382.8128	247.7086	31.82532	0.923995	
39.00	25.24607	102.858	2202.91	11.16327	0.204903	
42.00	5.835377	128.528	863.6416	10.70693	0.168138	
45.00	116.7414	42.06395	2720.493	4.663216	0.081754	
48.70	27.9424	120.4807	704.3671	9.589489	0.174013	
51.00	73.91342	236.0641	1454.945	17.85352	0.417991	
53.00	21.55957	345.6942	9446.417	16.1916	4.765534	
56.00	60.27635	82.45465	4899.206	8.751376	0.19143	
63.00	1.23373	53.54325	303.7976	5.153883	0.05286	
65.00	4.87443	97.64512	8142.136	11.23081	0.460898	
68.00	39.91849	276.8437	3495.132	23.80226	0.682269	
71.00	8.81709	205.6843	10777.93	20.12616	0.508803	
73.00	3.422732	142.6679	4270.434	12.11792	0.313545	
75.00	7.774588	121.41	29566.94	10.31178	0.250576	
77.60	11.65668	116.6082	35882.21	9.118536	0.563603	
80.00	30.33728	202.6437	58386.45	23.96954	0.480366	
83.00	7.098344	210.1611	7000.671	15.26249	0.360311	
85.00	9.014946	169.4537	17605.52	11.29056	0.432601	
87.00	19.20752	180.8392	31874.4	10.54927	0.744051	
90.00	2.228581	82.37434	646.9535	10.70706	0.102478	

Outcrop: East 53		Data Normalized to Zr in ppm				
Height in vertical section (meters)	11	12	13	14	15	
	Cr	Mn	Fe	Co	Cu	
0.00	0.156845	0.408659	13.8139	0.011766	0.033487	
3.00	0.23393	0.669249	25.19544	0.011268	0.077034	
6.00	0.867855	1.912874	80.63401	0.055048	0.353285	
9.00	0.121267	0.535952	20.84772	0.014614	0.127418	
12.00	0.467324	1.664155	65.07855	0.029619	0.527049	
15.00	0.745717	1.131027	44.83035	0.032942	0.168376	
18.00	0.471437	0.465449	22.74138	0.017283	0.093522	
21.00	0.774342	1.436039	66.65143	0.025918	0.375766	
24.00	0.401957	1.499668	52.16045	0.039052	0.378407	
27.00	1.080911	1.967552	63.74504	0.022896	0.320121	
30.00	0.361543	0.960193	33.77602	0.017831	0.220792	
33.00	0.305296	1.648865	54.24429	0.060825	0.147855	
36.00	1.002076	0.740755	176.9015	0.065794	0.11245	
39.00	0.35033	1.856244	65.49904	0.067534	0.184971	
42.00	0.213567	0.545145	33.73974	0.034799	0.091728	
45.00	0.272838	1.268619	40.93901	0.047507	0.091989	
48.70	0.277521	0.529577	50.02587	0.022627	0.069499	
51.00	0.597743	0.927616	126.6827	0.06456	0.496169	
53.00	0.945801	5.733547	236.7937	0.278723	0.457014	
56.00	0.453683	2.220297	72.27201	0.146642	0.231349	
63.00	0.069853	0.289423	13.48379	0.010998	0.043524	
65.00	0.497066	4.242579	122.6845	0.160547	1.01212	
68.00	1.142397	2.439325	119.6467	0.083682	0.654681	
71.00	0.760998	4.549859	128.3674	0.210272	0.421971	
73.00	0.290356	1.529635	71.72204	0.057118	0.172544	
75.00	0.997074	9.729459	130.1382	0.397634	0.622266	
77.60	1.441842	12.40868	119.2359	0.536516	0.677768	
80.00	2.10443	19.41753	180.7422	0.555309	0.780963	
83.00	0.531351	2.930642	62.02863	0.101339	0.311445	
85.00	0.884047	5.624593	68.79602	0.330211	0.434791	
87.00	1.553065	12.79294	167.2849	0.686996	0.688365	
90.00	0.157568	0.694895	24.09423	0.020494	0.072814	

Outcrop: East 53		Data Normalized to Zr in ppm				
Height in vertical section (meters)	16	17	18	19	20	
	Zn	Ga	Ge	As	Rb	
0.00	0.042793	0.009705	0.001657	0.019236	0.082119	
3.00	0.140034	0.012956	0.00236	0.040138	0.108626	
6.00	0.387399	0.059265	0.027949	0.106339	0.696718	
9.00	0.063514	0.006077	0.002363	0.025456	0.041063	
12.00	0.317521	0.016158	0.004443	0.010484	0.130945	
15.00	0.143322	0.027189	0.014589	0.018528	0.292819	
18.00	0.106441	0.016733	0.00775	0.010408	0.154253	
21.00	0.287486	0.052906	0.016475	0.02506	0.389029	
24.00	0.290157	0.040729	0.030272	0.030065	0.280278	
27.00	0.404028	0.099423	0.06751	0.028447	0.564407	
30.00	0.122968	0.024709	0.005719	0.016448	0.225761	
33.00	0.204703	0.037036	0.007183	0.014107	0.350874	
36.00	0.375058	0.148709	0.017189	0.085717	1.646751	
39.00	0.125078	0.001861	0.002991	0.020231	0.2387	
42.00	0.12901	0.02457	0.003988	0.046951	0.292837	
45.00	0.45987	0.001541	0.001377	0.064219	0.085241	
48.70	0.184358	0.023807	0.002769	0.053009	0.309564	
51.00	0.188691	0.045968	0.005462	0.073925	0.663789	
53.00	1.41959	0.020993	0.005718	0.065648	0.772141	
56.00	0.232692	0.001147	0.00295	0.013624	0.159877	
63.00	0.029781	0.009712	0.002503	0.003393	0.122228	
65.00	0.556402	0.113717	0.001836	0.087456	0.207032	
68.00	0.256682	0.007831	0.00869	0.138137	0.742137	
71.00	0.451	0.031809	0.002741	0.021087	0.453225	
73.00	0.167433	0.047248	0.003353	0.08265	0.318708	
75.00	0.501445	0.008908	No data	0.106739	0.140261	
77.60	0.144509	0.00618	No data	0.047951	0.150659	
80.00	0.104858	0.079354	No data	0.068507	0.277732	
83.00	0.105764	0.012463	0.003426	0.046641	0.387201	
85.00	0.009693	0.007082	0.002168	0.080023	0.284423	
87.00	0.199142	0.0771	No data	0.084717	0.289327	
90.00	0.091239	0.026941	0.002491	0.00928	0.18899	

Outcrop: East 53		Data Normalized to Zr in ppm			
Height in vertical section (meters)	21	22	23	24	25
	Sr	Y	Zr	Nb	Mo
0.00	0.552904	0.074081	1	0.022998	0.01583
3.00	0.658341	0.129767	1	0.032224	0.02648
6.00	3.583435	0.370894	1	0.050827	0.121346
9.00	0.705485	0.03705	1	0.011805	0.070256
12.00	4.804536	0.203001	1	0.030827	0.024726
15.00	15.19203	0.472311	1	0.034185	0.011356
18.00	7.797335	0.269581	1	0.0285	0.008597
21.00	3.821388	0.371679	1	0.053074	0.019499
24.00	3.298258	0.147965	1	0.051609	0.07632
27.00	8.09202	0.461332	1	0.082696	0.014782
30.00	3.838689	0.169445	1	0.058862	0.013376
33.00	2.36559	0.146298	1	0.07428	0.012031
36.00	1.150292	0.276694	1	0.10437	0.063995
39.00	2.140604	0.098112	1	0.051864	0.03007
42.00	1.343346	0.083706	1	0.022294	0.10152
45.00	2.891906	0.190554	1	0.024636	0.287517
48.70	1.950346	0.116668	1	0.039516	0.328175
51.00	3.561299	0.236489	1	0.069518	0.215428
53.00	9.651957	0.16656	1	0.096999	0.930151
56.00	4.700749	0.118995	1	0.048838	0.165055
63.00	0.603972	0.032485	1	0.019122	0.018985
65.00	7.851474	0.076288	1	0.057353	0.868813
68.00	4.744893	0.230341	1	0.102559	0.123151
71.00	13.66793	0.192717	1	0.14788	0.045155
73.00	7.357969	0.095244	1	0.045165	0.177947
75.00	29.20228	0.102237	1	0.092252	0.289065
77.60	42.41191	0.424196	1	0.068047	0.19832
80.00	91.51849	0.263313	1	0.14822	0.257712
83.00	8.342853	0.124399	1	0.062086	0.052486
85.00	30.36869	0.101148	1	0.057431	0.11397
87.00	57.2729	0.143933	1	0.078856	0.128754
90.00	1.83095	0.063872	1	0.036299	0.016523

Outcrop: East 53		Data Normalized to Zr in ppm				
Height in vertical section (meters)	26	27	28	29	30	
	Ru	Pd	Ag	Sn	Sb	
0.00	0.000475	0.040576	0.001049	0.006067	0.002343	
3.00	0.00096	0.043444	0.001309	0.004161	0.002237	
6.00	0.002252	0.042863	0.014401	0.054041	0.011692	
9.00	0.001942	0.042183	0.00126	0.015914	0.003177	
12.00	0.008647	0.043837	0.001884	0.117144	0.004837	
15.00	0.005889	0.041884	0.002452	0.107545	0.006996	
18.00	0.001653	0.039769	0.001376	0.021914	0.003267	
21.00	0.003646	0.039983	0.00229	0.047513	0.006766	
24.00	0.003616	0.036435	0.00723	0.037678	0.012013	
27.00	0.007448	0.034412	0.018759	1.285134	0.026399	
30.00	0.004609	0.044134	0.001975	0.008479	0.002989	
33.00	0.006266	0.035058	0.00345	0.030825	0.016728	
36.00	0.000112	0.031854	0.003281	0.028602	0.011623	
39.00	0.00742	0.033053	0.002531	0.03505	0.005673	
42.00	0.003186	0.030765	0.00141	0.012199	0.004141	
45.00	0.009791	0.032631	0.001356	0.07304	0.004023	
48.70	0.002522	0.031804	0.001485	0.034479	0.002031	
51.00	0.004595	0.031733	0.004551	0.030448	0.004059	
53.00	0.0361	0.032587	0.004587	0.08571	0.00923	
56.00	0.01666	0.036126	0.003324	0.019954	0.004423	
63.00	0.000761	0.032561	0.001501	0.026535	0.001312	
65.00	0.024153	0.035406	0.062967	0.014914	0.011712	
68.00	0.01097	0.03858	0.019963	0.045646	0.016083	
71.00	0.033214	0.038329	0.014431	0.039489	0.018422	
73.00	0.008688	0.038592	0.002807	0.019721	0.007209	
75.00	0.066515	0.038309	0.010153	0.081934	0.020771	
77.60	0.097612	0.042006	0.005559	0.349985	0.016341	
80.00	0.107834	0.043003	0.00681	0.824002	0.027262	
83.00	0.025493	0.039319	0.003697	0.059181	0.005517	
85.00	0.053466	0.039039	0.003158	0.062623	0.00894	
87.00	0.093478	0.041261	0.007206	0.076127	0.014844	
90.00	0.002359	0.034607	0.001865	0.057664	0.002065	

Outcrop: East 53		Data Normalized to Zr in ppm				
Height in vertical section (meters)	31	32	33	34	35	
	Cs	Ba	La	Ce	Pr	
0.00	0.002517	0.609091	0.062927	0.106733	0.01495	
3.00	0.004654	0.598308	0.096679	0.166392	0.023665	
6.00	0.023699	3.748466	0.652012	0.834952	0.111494	
9.00	0.002321	0.490183	0.036755	0.060398	0.007738	
12.00	0.005343	0.792997	0.139325	0.188725	0.025573	
15.00	0.00841	3.048515	0.289321	0.416792	0.061335	
18.00	0.00483	1.491946	0.167892	0.246168	0.03566	
21.00	0.019593	2.006012	0.334432	0.460738	0.060859	
24.00	0.012841	2.067242	0.212742	0.316442	0.041204	
27.00	0.032819	3.72858	0.596787	0.95017	0.130738	
30.00	0.00681	1.369774	0.138611	0.261929	0.034239	
33.00	0.014373	8.161902	0.174783	0.303958	0.036518	
36.00	0.089122	3.175117	0.346065	0.598856	0.07405	
39.00	0.007066	1.033185	0.088962	0.169631	0.02241	
42.00	0.006366	1.821343	0.086538	0.165798	0.022784	
45.00	0.002276	0.747859	0.117204	0.173541	0.022259	
48.70	0.014003	1.081848	0.108727	0.181388	0.02403	
51.00	0.039855	1.878061	0.194644	0.301123	0.041145	
53.00	0.031978	7.578939	0.215192	0.388697	0.048498	
56.00	0.004629	0.869745	0.110682	0.201442	0.025523	
63.00	0.003055	0.702073	0.035459	0.069122	0.009291	
65.00	0.007325	18.59494	0.108421	0.186786	0.022603	
68.00	0.031518	2.586775	0.189039	0.299902	0.041397	
71.00	0.017351	9.732088	0.246733	0.385778	0.050564	
73.00	0.011503	3.823297	0.110628	0.214738	0.026444	
75.00	No data	2.523945	0.129639	0.199665	0.024128	
77.60	No data	4.869976	0.345963	0.547851	0.066576	
80.00	No data	10.053	0.349742	0.503445	0.055994	
83.00	0.007463	1.758109	0.126214	0.247548	0.033085	
85.00	0.006319	3.261657	0.116176	0.212535	0.026603	
87.00	0.005297	11.57811	0.169145	0.32823	0.039022	
90.00	0.005399	7.779887	0.091607	0.184453	0.022728	

Outcrop: East 53		Data Normalized to Zr in ppm				
Height in vertical section (meters)	36	37	38	39	40	
	Nd	Sm	Eu	Gd	Dy	
0.00	0.059528	0.012287	0.002604	0.012088	0.011025	
3.00	0.092659	0.018983	0.004044	0.019296	0.017858	
6.00	0.381889	0.065334	0.013803	0.061538	0.052366	
9.00	0.02985	0.005969	0.001349	0.005763	0.005157	
12.00	0.098411	0.019843	0.004581	0.021327	0.019651	
15.00	0.245645	0.052348	0.012378	0.054755	0.049944	
18.00	0.142481	0.030197	0.006788	0.030745	0.02838	
21.00	0.227974	0.046035	0.010709	0.046647	0.043222	
24.00	0.155321	0.030542	0.006739	0.02719	0.024201	
27.00	0.494964	0.100858	0.022081	0.087785	0.077785	
30.00	0.128332	0.026433	0.005654	0.02572	0.024952	
33.00	0.137712	0.026834	0.008	0.02726	0.025162	
36.00	0.272555	0.051681	0.012222	0.052003	0.041905	
39.00	0.086285	0.016193	0.004197	0.016604	0.015272	
42.00	0.089713	0.018225	0.004278	0.018094	0.015973	
45.00	0.087389	0.016457	0.003963	0.019795	0.018425	
48.70	0.094554	0.018565	0.003858	0.018827	0.016401	
51.00	0.160494	0.030653	0.007219	0.032744	0.030933	
53.00	0.188285	0.031665	0.009647	0.035592	0.031427	
56.00	0.094689	0.017041	0.00399	0.019882	0.018195	
63.00	0.036523	0.007379	0.001784	0.007	0.006791	
65.00	0.082243	0.013532	0.00847	0.01629	0.015283	
68.00	0.15631	0.028149	0.007323	0.030667	0.027715	
71.00	0.210201	0.03486	0.009852	0.03748	0.030005	
73.00	0.099841	0.018527	0.004932	0.019682	0.017626	
75.00	0.093585	0.008864	0.003807	0.016961	0.014471	
77.60	0.248856	0.033331	0.011639	0.054241	0.053795	
80.00	0.195517	0.018086	0.00914	0.033432	0.026854	
83.00	0.12854	0.02444	0.005676	0.024793	0.023197	
85.00	0.100505	0.011933	0.004563	0.019178	0.016226	
87.00	0.137882	0.017653	0.009063	0.028402	0.019608	
90.00	0.087321	0.017304	0.004681	0.015533	0.012544	

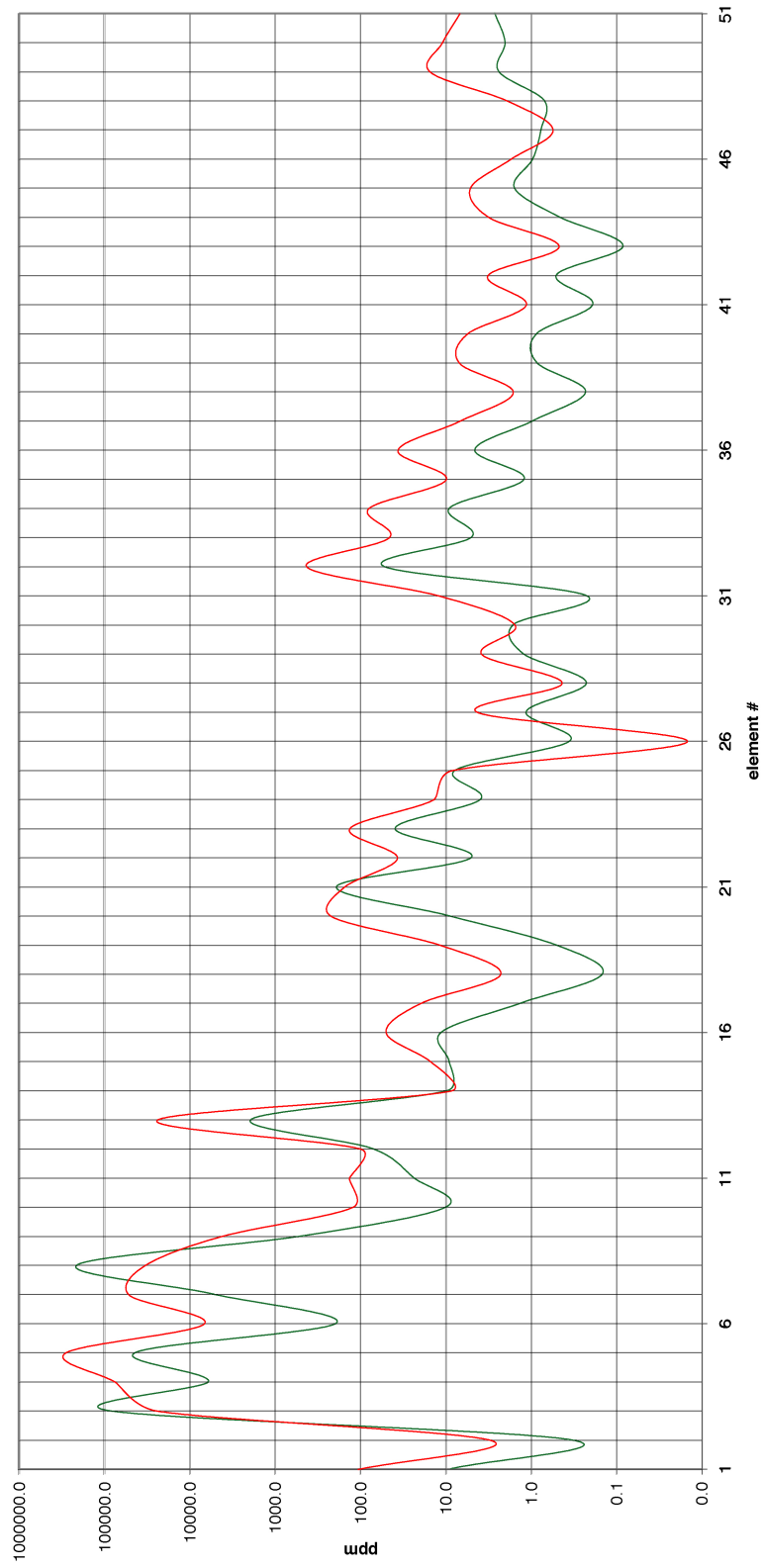
Outcrop: East 53		Data Normalized to Zr in ppm				
Height in vertical section (meters)	41	42	43	44	45	
	Ho	Er	Tm	Yb	Hf	
0.00	0.002328	0.006591	0.000972	0.006487	0.04201	
3.00	0.003784	0.011372	0.001617	0.01063	0.039456	
6.00	0.010151	0.028648	0.004031	0.023013	0.042416	
9.00	0.001092	0.003291	0.000531	0.003528	0.03494	
12.00	0.004352	0.013045	0.001773	0.010937	0.039652	
15.00	0.010535	0.029987	0.004342	0.025038	0.040359	
18.00	0.006227	0.018104	0.002555	0.015563	0.036879	
21.00	0.009028	0.026446	0.00366	0.020762	0.039755	
24.00	0.005002	0.01397	0.002203	0.01432	0.038094	
27.00	0.014773	0.039669	0.005706	0.034038	0.040043	
30.00	0.005433	0.015665	0.002338	0.015122	0.036638	
33.00	0.004986	0.01434	0.002093	0.014165	0.039576	
36.00	0.008566	0.024153	0.003549	0.023418	0.038809	
39.00	0.003055	0.009137	0.001275	0.008594	0.036312	
42.00	0.0032	0.009367	0.001378	0.009196	0.033802	
45.00	0.004101	0.012344	0.001662	0.010578	0.03651	
48.70	0.003516	0.010102	0.00143	0.009811	0.033933	
51.00	0.006557	0.019094	0.002765	0.018055	0.035888	
53.00	0.006019	0.019624	0.002736	0.020223	0.036911	
56.00	0.003411	0.011856	0.00159	0.010733	0.036304	
63.00	0.001444	0.004357	0.000683	0.004706	0.033107	
65.00	0.002923	0.009374	0.001381	0.009767	0.029214	
68.00	0.005616	0.016937	0.002448	0.016198	0.056786	
71.00	0.006054	0.018745	0.002467	0.016521	0.048781	
73.00	0.003499	0.010571	0.001532	0.010241	0.038799	
75.00	0.002609	0.008632	0.001077	0.008772	0.03268	
77.60	0.010744	0.03004	0.003942	0.026172	0.03542	
80.00	0.005071	0.017453	0.002298	0.018182	0.036636	
83.00	0.004614	0.014269	0.001953	0.014671	0.037054	
85.00	0.003097	0.010688	0.001289	0.010278	0.033518	
87.00	0.004027	0.01348	0.001272	0.013412	0.04234	
90.00	0.002413	0.006997	0.000981	0.006911	0.033524	

Outcrop: East 53		Data Normalized to Zr in ppm				
Height in vertical section (meters)	46	47	48	49	50	
	Ta	Au	Tl	Pb	Th	
0.00	0.004129	0.001404	0.001831	0.032751	0.019314	
3.00	0.004554	0.001379	0.004865	0.079088	0.027797	
6.00	0.016796	0.007596	0.017327	0.253586	0.072123	
9.00	0.002845	0.001244	0.001435	0.040444	0.007176	
12.00	0.006692	0.002901	0.001837	0.032509	0.019612	
15.00	0.009037	0.003253	0.003116	0.069913	0.040663	
18.00	0.005415	0.001449	0.001615	0.036555	0.025024	
21.00	0.009375	0.002712	0.002851	0.073956	0.037125	
24.00	0.010303	0.003423	0.003651	0.070171	0.031273	
27.00	0.027442	0.00444	0.005151	0.210251	0.06831	
30.00	0.006005	0.000458	0.002146	0.026604	0.034808	
33.00	0.017375	0.008019	0.006986	0.088886	0.056812	
36.00	0.013048	0.004185	0.014294	0.11426	0.082548	
39.00	0.00823	0.003911	0.005208	0.0581	0.031309	
42.00	0.004391	0.001861	0.004713	0.044935	0.028864	
45.00	0.006624	0.002503	0.003716	0.109255	0.022892	
48.70	0.004958	0.001023	0.01686	0.105907	0.029412	
51.00	0.008577	0.001828	0.028485	0.335939	0.052107	
53.00	0.021734	0.006878	0.022199	0.175082	0.056427	
56.00	0.010853	0.002894	0.003053	0.043779	0.026434	
63.00	0.002636	0.000333	0.001217	0.014485	0.010812	
65.00	0.01217	0.001417	0.006904	0.486813	0.028349	
68.00	0.026686	0.011289	0.012779	0.253902	0.091982	
71.00	0.038314	0.01677	0.012977	0.113283	0.076664	
73.00	0.009954	0.00303	0.003234	0.143767	0.034186	
75.00	0.03939	0.014023	0.005435	0.172308	0.036766	
77.60	0.04069	0.014619	No data	0.104492	0.033669	
80.00	0.054471	0.011059	0.008398	0.168304	0.033681	
83.00	0.014254	0.002976	0.002917	0.059696	0.032643	
85.00	0.023089	0.003974	No data	0.07416	0.029162	
87.00	0.033205	0.009968	No data	0.105558	0.021793	
90.00	0.004349	0.000308	0.000818	0.026437	0.027881	

Outcrop: East 53		Data Normalized to Zr in ppm			
Height in vertical section (meters)	51				
	U				
0.00	0.014054				
3.00	0.011105				
6.00	0.045908				
9.00	0.008964				
12.00	0.030614				
15.00	0.036239				
18.00	0.023364				
21.00	0.049317				
24.00	0.029771				
27.00	0.063927				
30.00	0.032601				
33.00	0.055454				
36.00	0.051487				
39.00	0.043354				
42.00	0.020182				
45.00	0.047349				
48.70	0.021521				
51.00	0.0611				
53.00	0.19424				
56.00	0.059064				
63.00	0.01121				
65.00	0.106228				
68.00	0.084801				
71.00	0.109143				
73.00	0.052716				
75.00	0.332096				
77.60	0.378663				
80.00	0.480869				
83.00	0.087082				
85.00	0.211117				
87.00	0.204261				
90.00	0.023014				

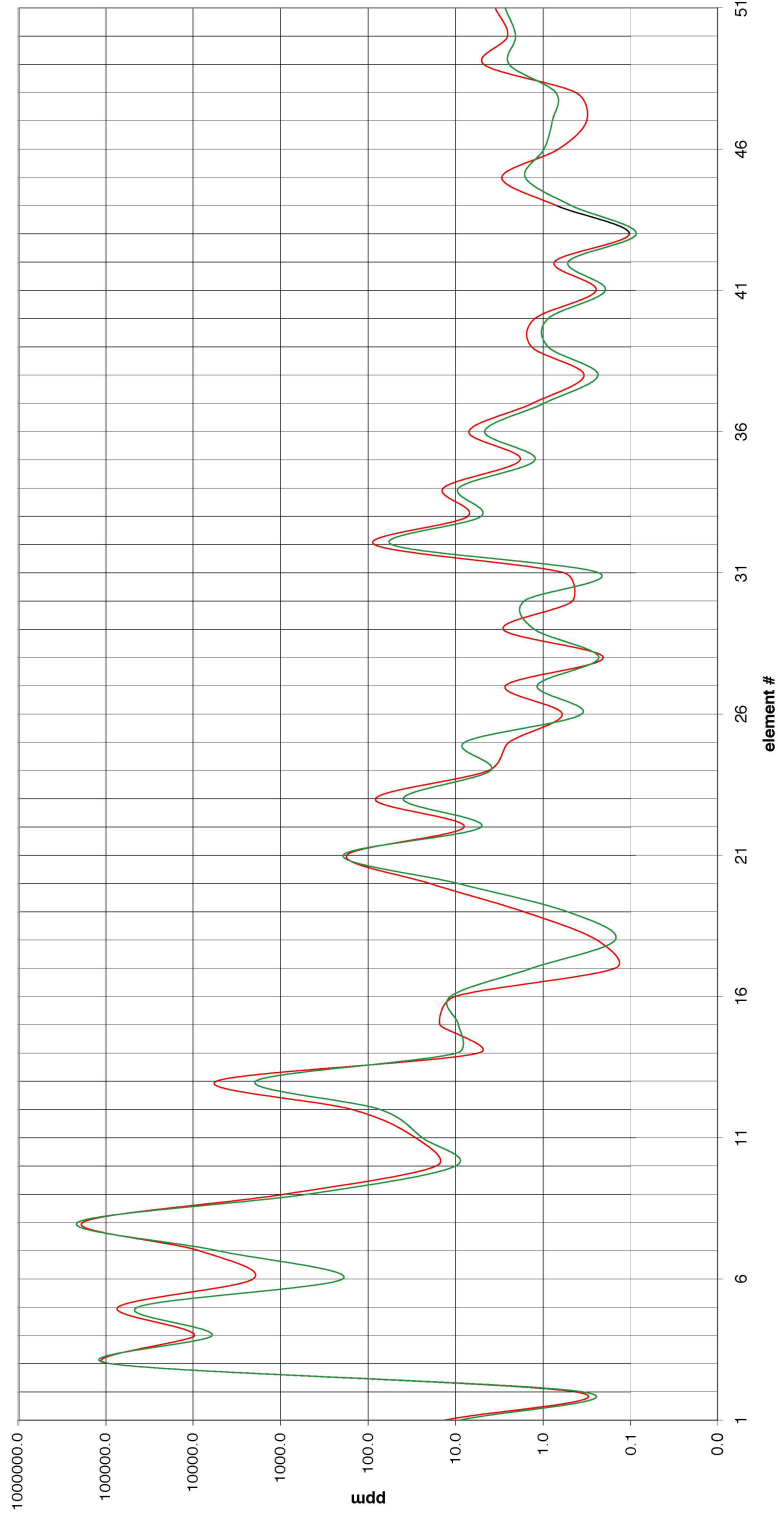
APENDIX D: GEOCHEMISTRY GRAPHS, BISTRAN 2009

Overlay Geochemical Plots of E53 36 m and MC 63 m



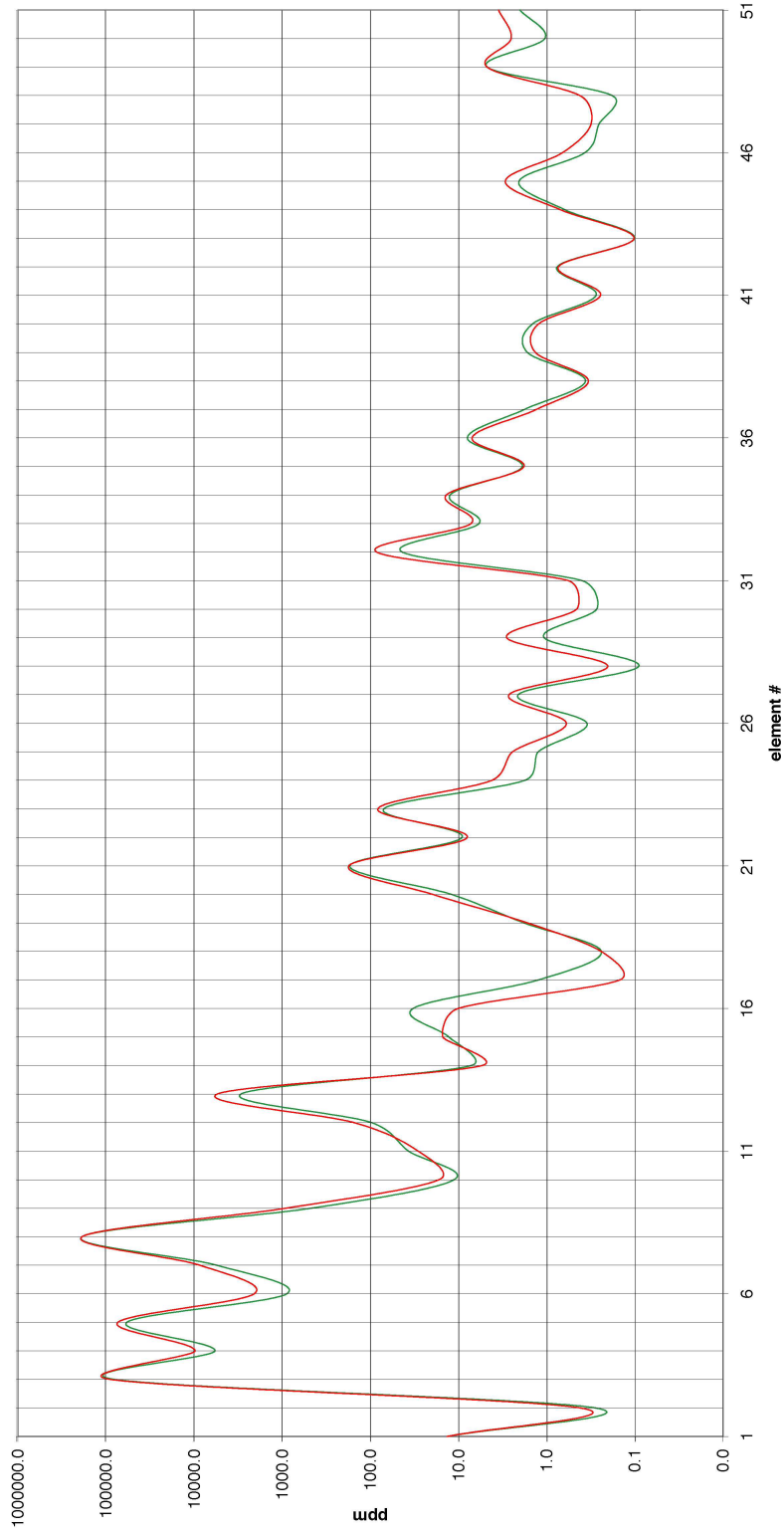
In this graph selected intervals, represented by individual lines, are overlain to illustrate the differences and similarities between the concentration in parts per million (ppm) and element number (#). The comparison of the lithology at 36 m in E53 with the lithology at 63 m in MC is shown in this graph (Bistran, 2009). For a detailed summary of the elements identified and specific concentrations please refer to Bistran (2009).

Overlay Geochemical Plots of E53 39 m and MC 63 m



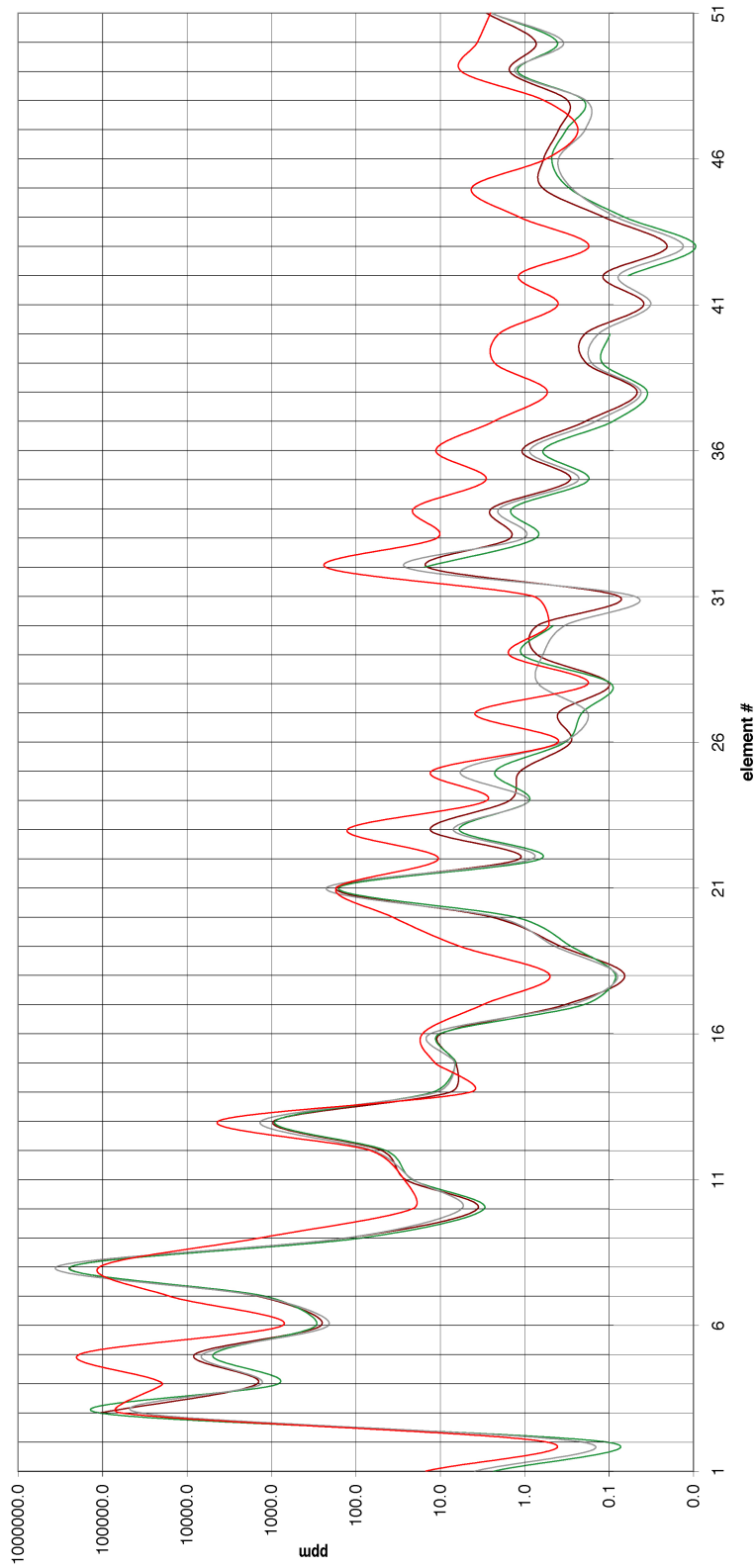
In this graph selected intervals, represented by individual lines, are overlain to illustrate the differences and similarities between the concentration in parts per million (ppm) and element number (#). The comparison of the lithology at 39 m in E53 with lithology at 63 m in MC is shown in this graph (Bistran, 2009). For a detailed summary of the elements identified and specific concentrations please refer to Bistran (2009).

Overlay Geochemical Plots of E53 39 m and MC 48 m



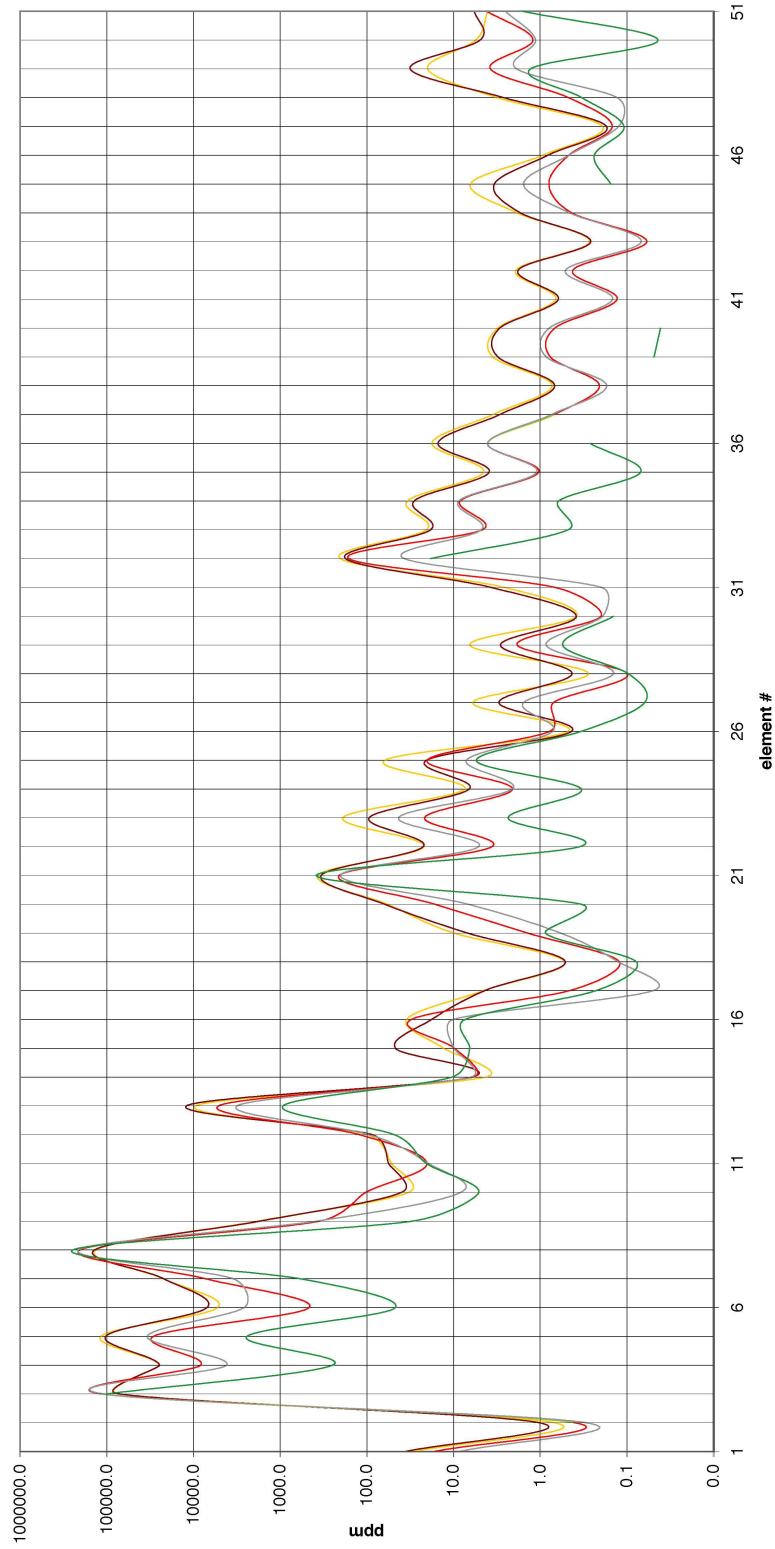
In this graph selected intervals, represented by individual lines, are overlain to illustrate the differences and similarities between the concentration in parts per million (ppm) and element number (#). The comparison of the lithology at 39 m in E53 with the lithology at 48 m in MC is shown in this graph (Bistran, 2009). For a detailed summary of the elements identified and specific concentrations please refer to Bistran (2009).

Overlain Geochemical Plots of E53 42 m and MC 66 m, 72 m



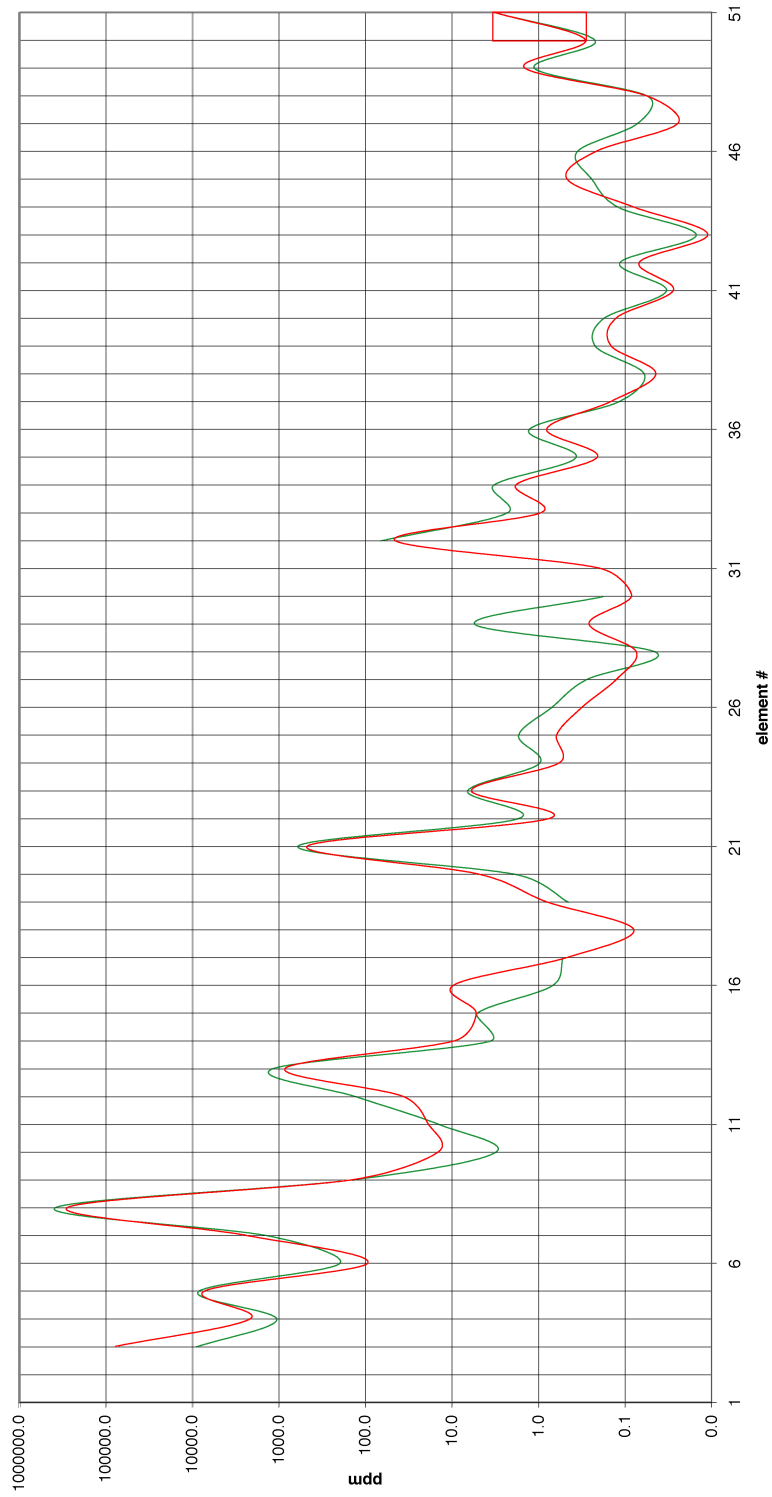
In this graph selected intervals, represented by individual lines, are overlain to illustrate the differences and similarities between the concentration in parts per million (ppm) and element number (#). The comparison of the lithology at 42 m in E53 with the lithology at 66 and 72 m in MC is shown in this graph (Bistran, 2009). For a detailed summary of the elements identified and specific concentrations please refer to Bistran (2009).

Overlay Geochemical Plots of E53 48.7 m, 56 m and MC 83 m



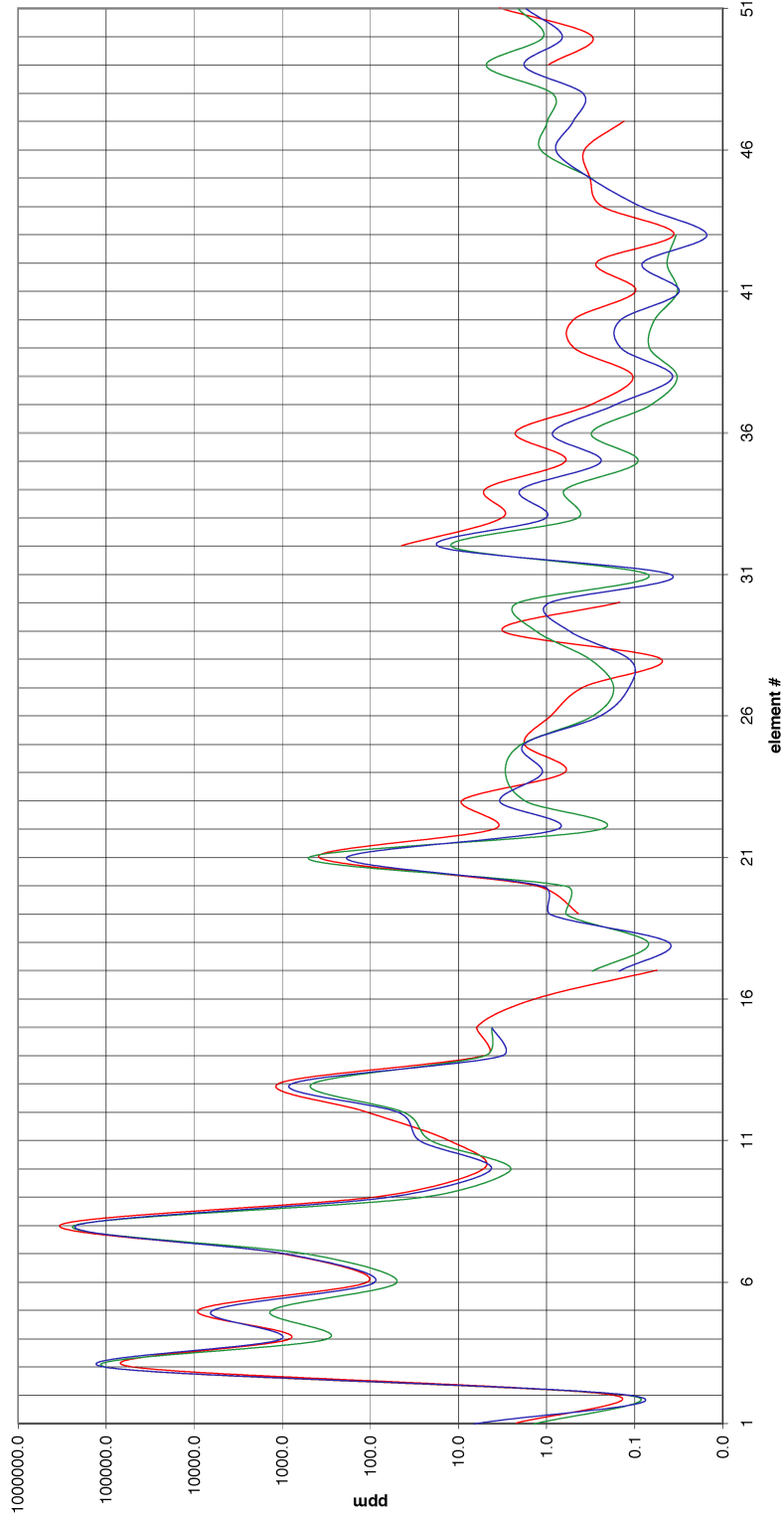
In this graph selected intervals, represented by individual lines, are overlain to illustrate the differences and similarities between the concentration in parts per million (ppm) and element number (#). The comparison of the lithology at 48.7 and 56 m in E53 with the lithology at 83 m in MC is shown in this graph (Bistran, 2009). For a detailed summary of the elements identified and specific concentrations please refer to Bistran (2009).

Overlay Geochemical Plots of E53 80 m and MC 105 m



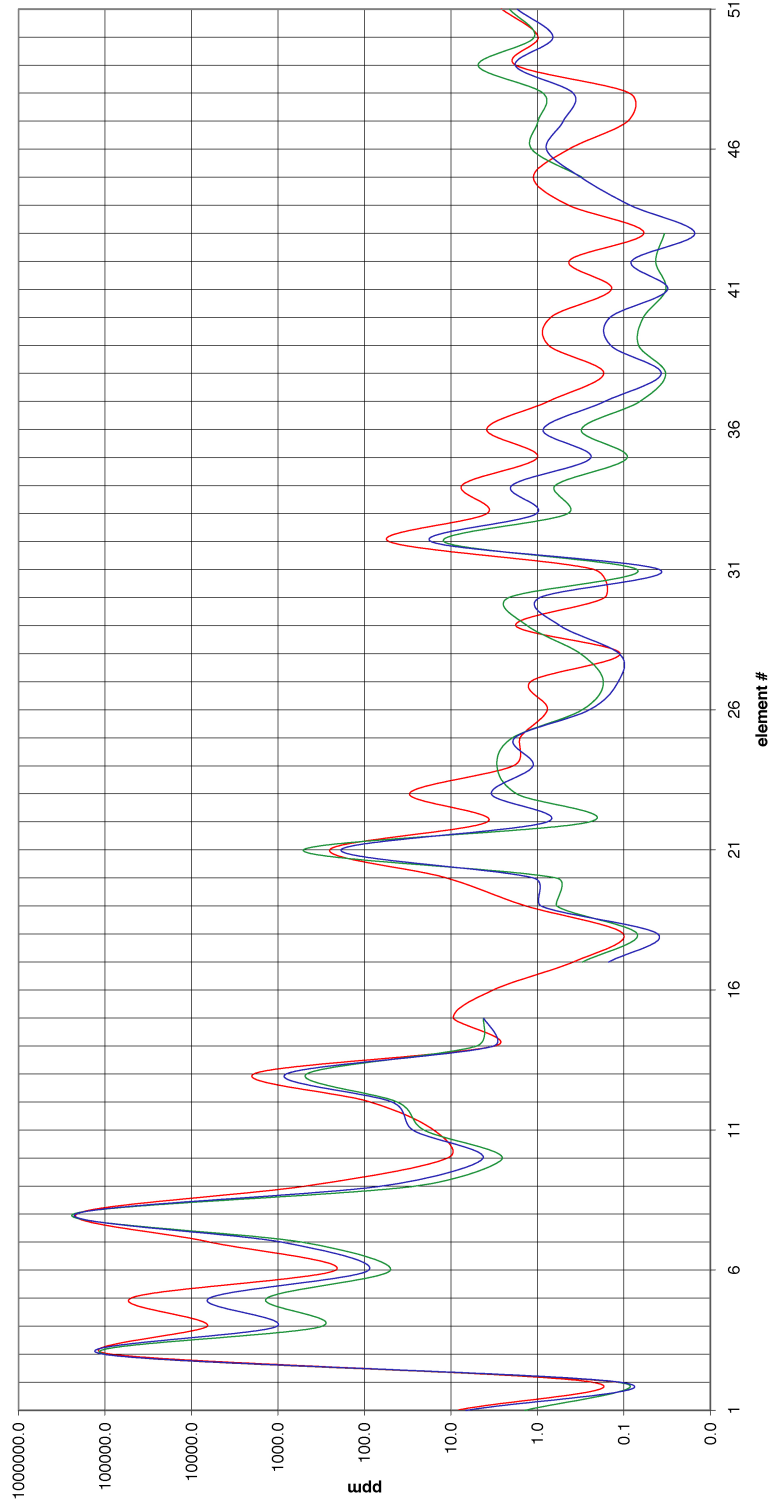
In this graph selected intervals, represented by individual lines, are overlain to illustrate the differences and similarities between the concentration in parts per million (ppm) and element number (#). The comparison of the lithology at 80 m in E53 with the lithology at 105 m in MC is shown in this graph (Bistran, 2009). For a detailed summary of the elements identified and specific concentrations please refer to Bistran (2009).

Overlap Geochemical Plots of E53 77.6 m and MC 108.6 m, 111 m



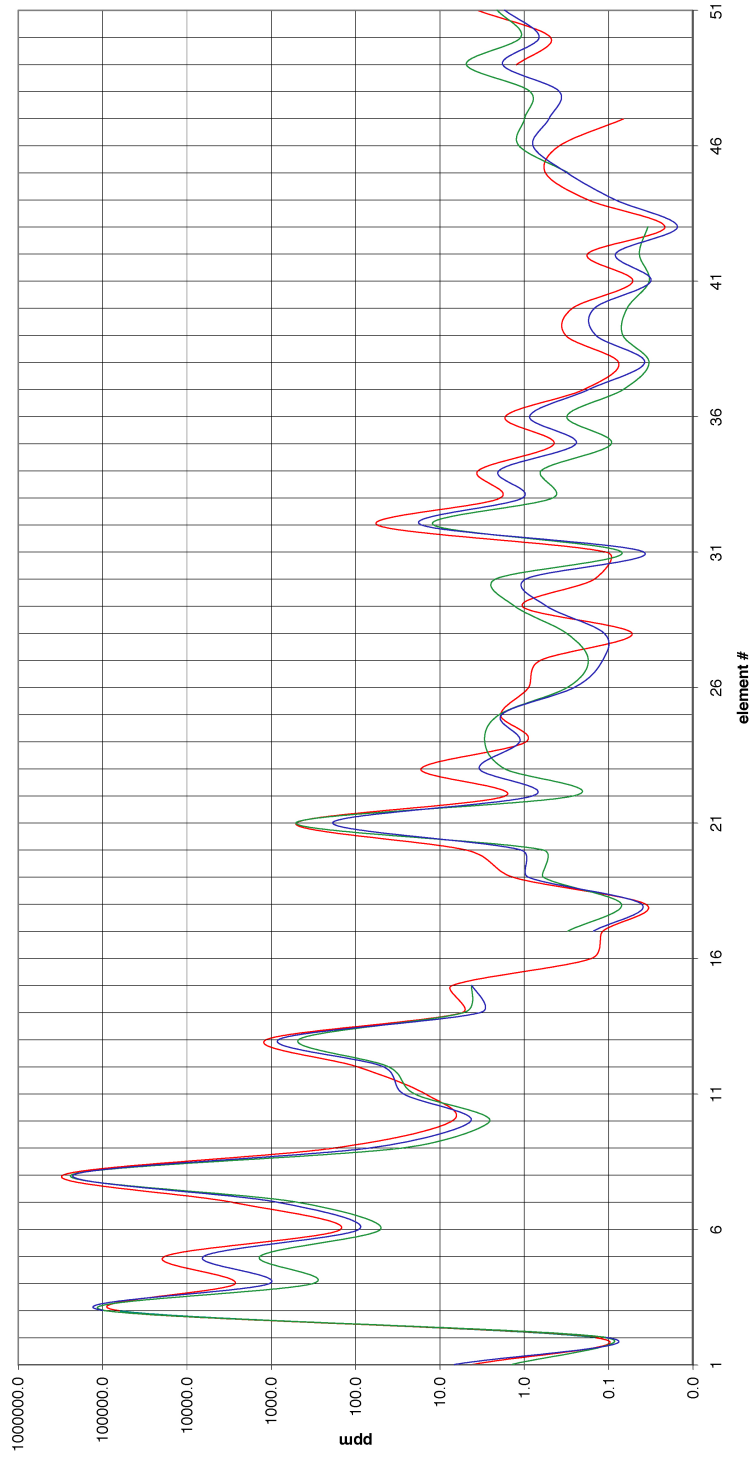
In this graph selected intervals, represented by individual lines, are overlain to illustrate the differences and similarities between the concentration in parts per million (ppm) and element number (#). The comparison of the lithology at 77.6 m in E53 with the lithology at 108.6 and 111 m in MC is shown in this graph (Bistran, 2009). For a detailed summary of the elements identified and specific concentrations please refer to Bistran (2009).

Overlay Geochemical Plots of E53 83 m and MC 108.6 m, 111 m



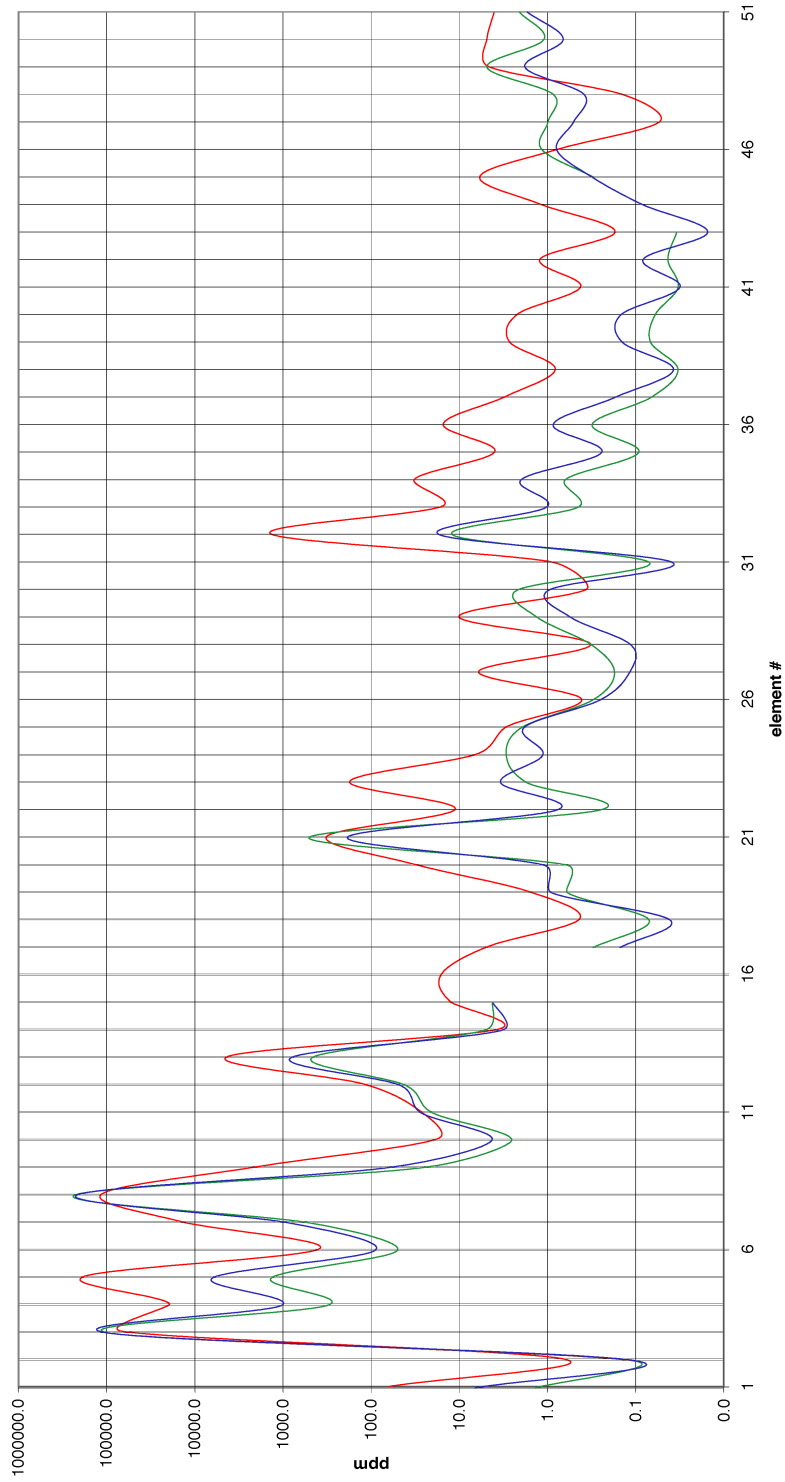
In this graph selected intervals, represented by individual lines, are overlain to illustrate the differences and similarities between the concentration in parts per million (ppm) and element number (#). The comparison of the lithology at 83 m in E53 with the lithology at 108.6 and 111 m in MC is shown in this graph (Bistran, 2009). For a detailed summary of the elements identified and specific concentrations please refer to Bistran (2009).

Overlay Geochemical Plots of E53 85 m and MC 108.6 m, 111 m



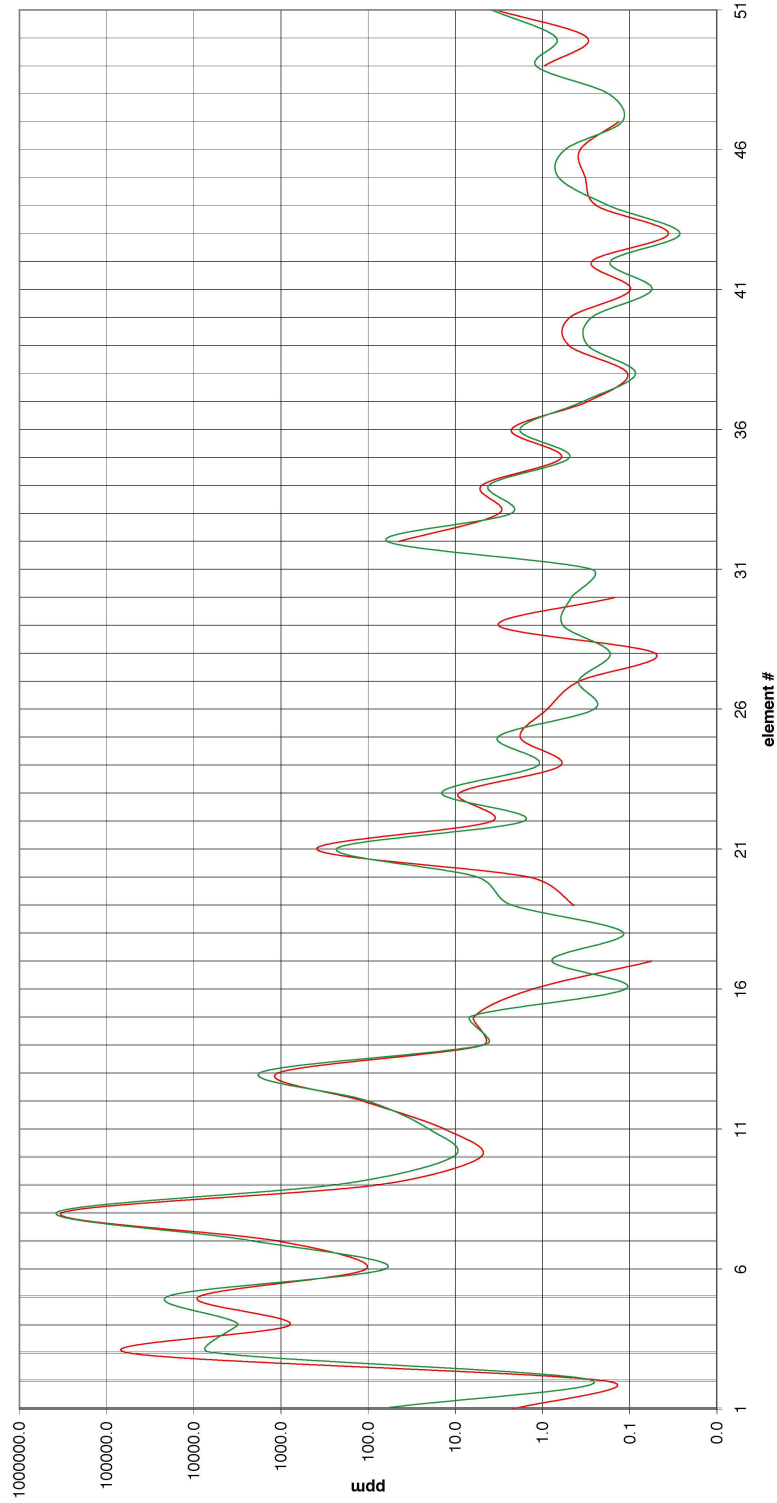
In this graph selected intervals, represented by individual lines, are overlain to illustrate the differences and similarities between the concentration in parts per million (ppm) and element number (#). The comparison of the lithology at 85 m in E53 with the lithology at 108.6 and 111 m in MC is shown in this graph (Bistran, 2009). For a detailed summary of the elements identified and specific concentrations please refer to Bistran (2009).

Overlay Geochemical Plots of E53 90 m and MC 108.6 m, 111



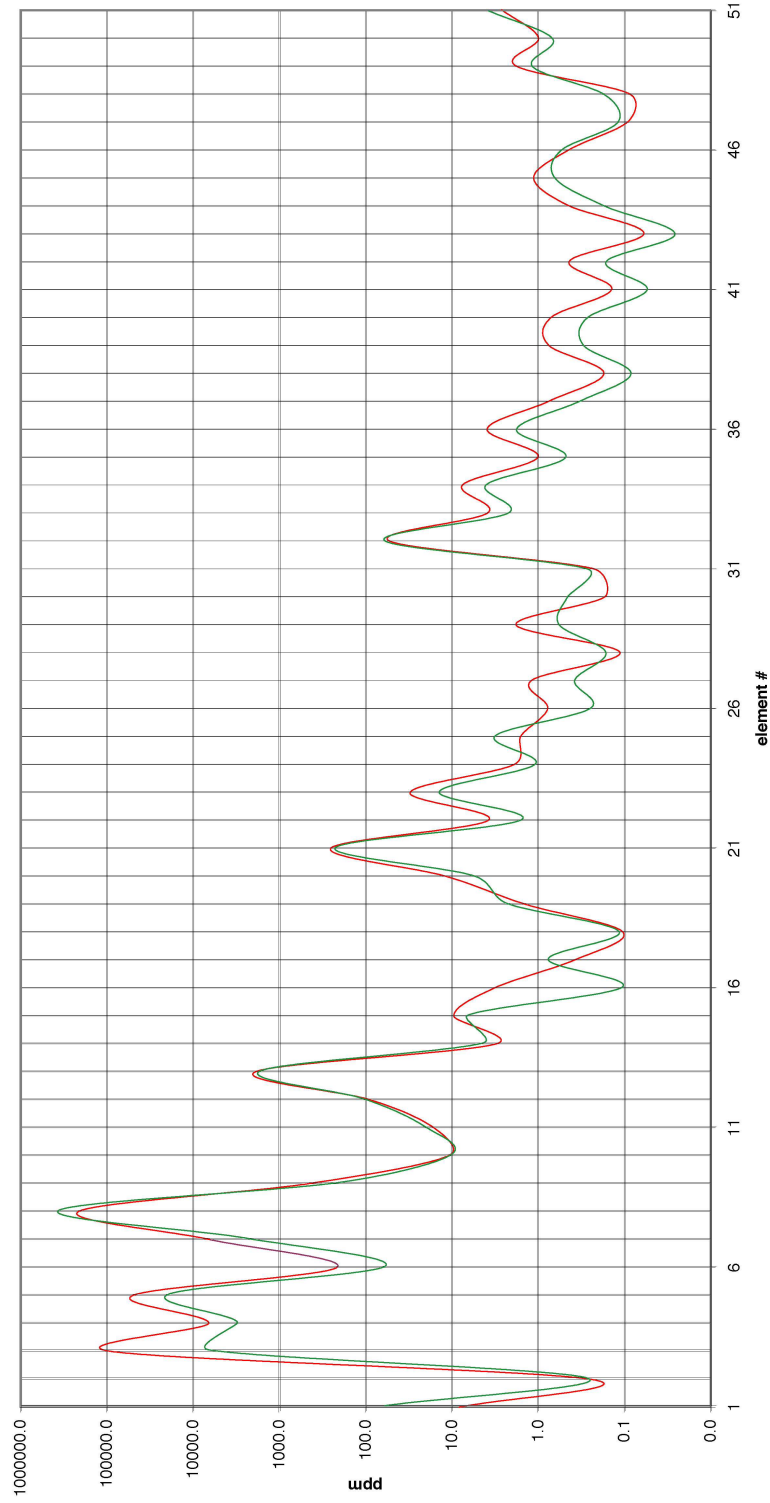
In this graph selected intervals, represented by individual lines, are overlain to illustrate the differences and similarities between the concentration in parts per million (ppm) and element number (#). The comparison of the lithology at 90 m in E53 with the lithology at 108.6 and 111 m in MC is shown in this graph (Bistran, 2009). For a detailed summary of the elements identified and specific concentrations please refer to Bistran (2009).

Overlay Geochemical Plots of E53 77.6 m and MC 117 m



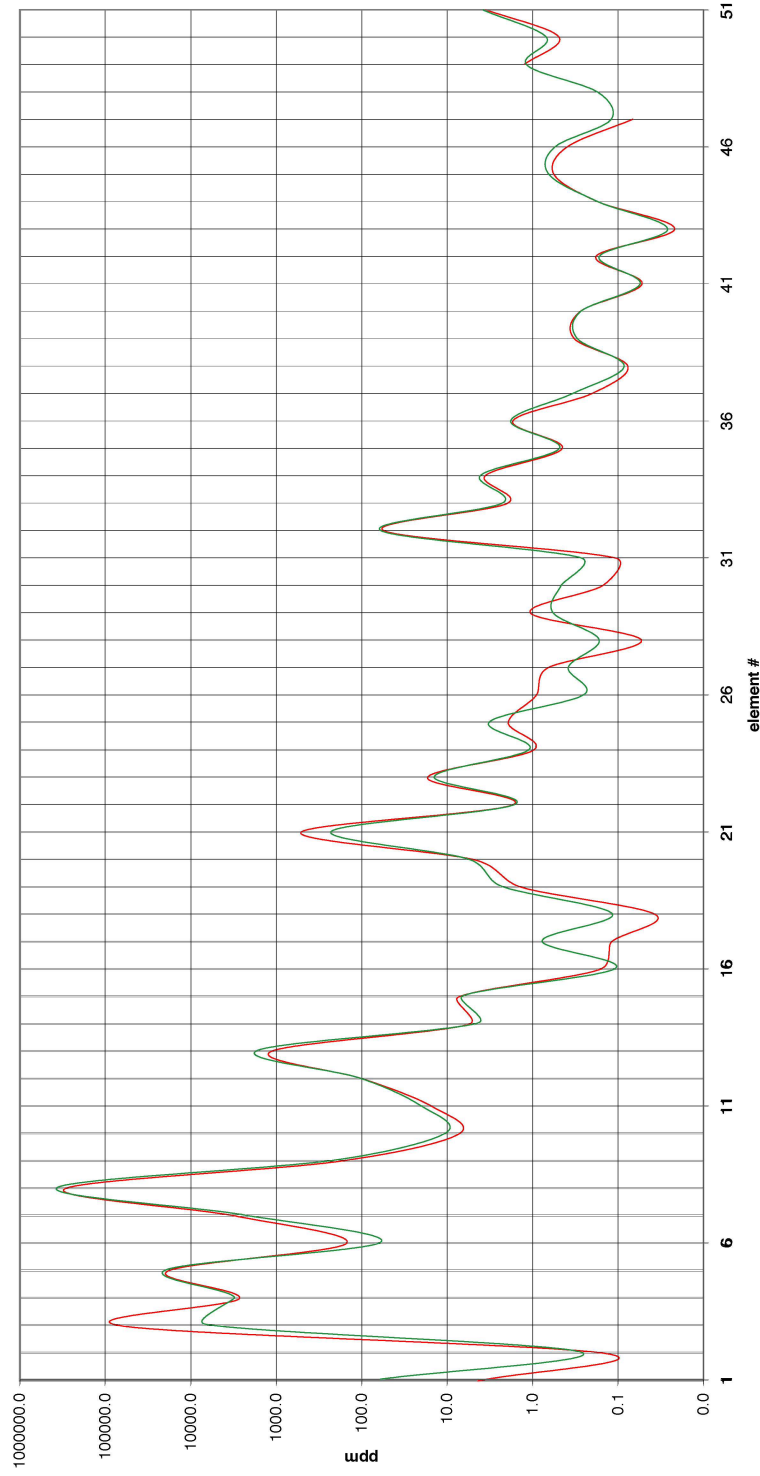
In this graph selected intervals, represented by individual lines, are overlain to illustrate the differences and similarities between the concentration in parts per million (ppm) and element number (#). The comparison of the lithology at 77.6 m in E53 with the lithology at 117 m in MC is shown in this graph (Bistran, 2009). For a detailed summary of the elements identified and specific concentrations please refer to Bistran (2009).

Overlain Geochemical Plots of E53 83 m and MC 117 m



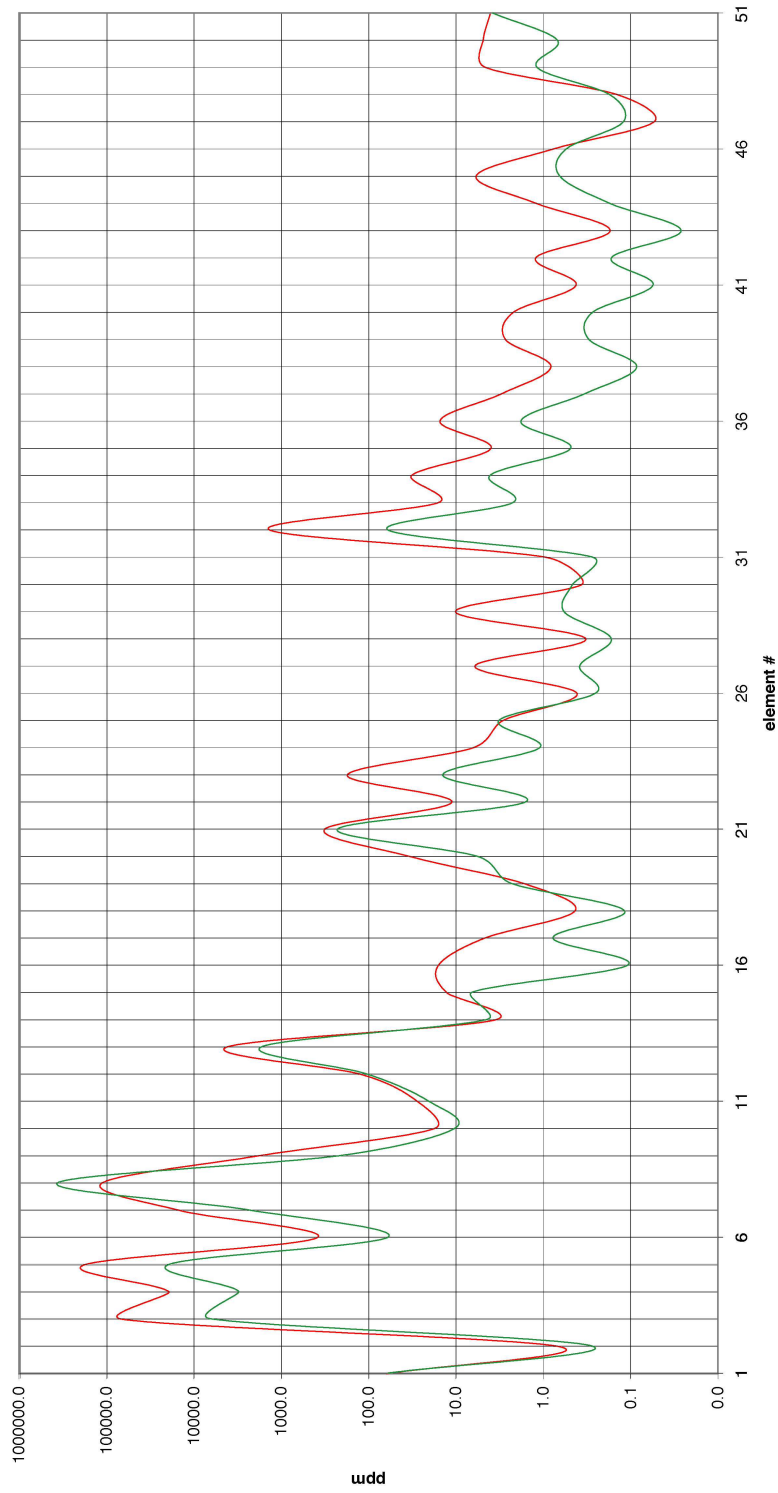
In this graph selected intervals, represented by individual lines, are overlain to illustrate the differences and similarities between the concentration in parts per million (ppm) and element number (#). The comparison of the lithology at 83 m in E53 with the lithology at 117 m in MC is shown in this graph (Bistran, 2009). For a detailed summary of the elements identified and specific concentrations please refer to Bistran (2009).

Overlay Geochemical Plots of E53 85 m and MC 117 m



In this graph selected intervals, represented by individual lines, are overlain to illustrate the differences and similarities between the concentration in parts per million (ppm) and element number (#). The comparison of the lithology at 85 m in E53 with the lithology at 117 m in MC is shown in this graph (Bistran, 2009). For a detailed summary of the elements identified and specific concentrations please refer to Bistran (2009).

Overlay Geochemical Plots of E53 90 m and MC 117 m



In this graph selected intervals, represented by individual lines, are overlain to illustrate the differences and similarities between the concentration in parts per million (ppm) and element number (#). The comparison of the lithology at 90 m in E53 with the lithology at 117 m in MC is shown in this graph (Bistran, 2009). For a detailed summary of the elements identified and specific concentrations please refer to Bistran (2009).